SYNTHESIS, CHARACTERIZATION AND REACTIVITY STUDY OF BIS(IMINO)-*N*-HETEROCYCLIC CARBENE TRANSITION METAL COMPLEXES

Jameel Al Thagfi

A DISSERTATION SUBMITTED TO

THE FACULTY OF GRADUATE STUDIES

IN PARTIAL FULFILLMENT OF THE REQUIREMENTS

FOR THE DEGREE OF

DOCTOR OF PHILOSOPHY

GRADUATE PROGRAM IN CHEMISTRY

YORK UNIVERSITY

TORONTO, ONTARIO

February 2014

Abstract

Three generations of the first 1,3-bis(imino) *N*-heterocyclic carbene (NHC) ligand precursors were synthesized, isolated and characterized. The synthetic methodologies of the ligand precursors were controlled by the iminic carbon substituents. The corresponding complexes of Cr(III), Fe(II), Co(II), Pd(II), and Zn(II) were prepared from the *in situ* deprotonation of the NHC ligand precursors or from the related Cu(I) or Ag(I) adducts. The NHC ring fragment and iminic carbon substituents had a significant impact on the solid-state structure of these complexes in which mono-, bi- and tridentate coordination modes were observed.

The catalytic activities of chromium, iron and cobalt complexes of 1,3-bis(imino) NHC ligands were evaluated in ethylene polymerization. The activities of chromium(III) complexes of imidazol-2-ylidene showed slightly enhanced activities with a relatively electron-poor phenyl group (compared to methyl) installed on the iminic carbons. These results suggest that a decrease in the electron-donating or an increase in the π-accepting capability of the ligand may produce more active olefin polymerization catalysts.

The ligand scaffold was then modified by introducing a benzimidazole moiety to reduce σ-electron donating and increase the π-accepting ability of the ligand and this may lead to a more electropositive metal center. Although these ligands were designed as a tridentate ligand, such coordination mode could not be achieved in the transition metal complexes of imidazole-2-ylidene and benzimidazol-2-ylidene. Steric and electronic parameters perhaps prevent them from adopting this coordination fashion. The five-membered ring of the carbene was then replaced by a six-membered ring of pyrimidin-2-ylidene to achieve a tridentate coordination mode.

DFT calculations were performed to assess the electronic properties of the bis(imino)-NHC ligands. The pyrimidin-2-ylidene and the benzimidazol-2-ylidene are predicted to be the best σ–donor and the best π-acceptor of these NHC ligands based on their energy of the highest occupied and the lowest unoccupied molecular orbitals, respectively.

Acknowledgments

I would like to express great thanks to my supervisor Professor Gino Lavoie for giving me the opportunity to pursue my Ph.D. study, and for his important guidance, invaluable suggestions and continued support during this work. I also thank the committee members Professor Michael Organ and Professor Dennis Stynes for helpful discussions and their guidance. I am also grateful to the examining committee members Professor Kevin Smith, Professor Pierre Potvin and Professor Gunho Sohn for their valuable discussions and suggestions. I wish to thank Professor A. B. P. Lever for his invaluable insights into DFT methods and calculations, Dr. Howard Hunter for his help in NMR spectroscopy, Dr. S. Dastgir for helpful discussions, Dr. Alan J. Lough of the University of Toronto (Toronto, Ontario), and Drs. James F. Britten and Hilary A. Jenkins of McMaster University (Hamilton, Ontario) for X-ray data acquisition and for their assistance in either solving or refining the molecular structures described in this thesis. I want to thank the members of the Lavoie group, past and present (Tim Larocque, Anna Badaj, Delwar Hossain, Barbara Skrela, Edwin Alvarado, Mike Harkness and Richard Morris) for their friendship.

I would like to express special thanks to my parents, my wife, my brothers and my sisters for their unlimited encouragement and support. The Government of the Kingdom of Saudi Arabia deserves great thanks for the scholarship.

Table of Contents

Abstract ii

Acknowledgments iv

Table of Contents v

List of Tables ix

List of Figures x

List of Schemes xii

List of Abbreviations xv

Chapter One 1

Introduction 1

1.1 Olefin polymerization 2

1.1.1 Nickel(II) and palladium(II) complexes of α-diimine ligands 2

1.1.2 Nickel (II) complexes of salicylaldimine ligands 5

1.1.3 Iron(II), cobalt(II) and chromium(III) complexes of tridentate 2,6-bis(imino)-pyridine ligands 6

1.2 Carbenes 12

1.2.1 *N*-heterocyclic carbenes (NHC) 15

1.3 Research objectives 26

Chapter Two.. 28

Synthesis, Characterization and Reactivity Study of Bis(imino)imidazol-2-ylidene Transition Metal Complexes.. 28

2.1 Synthesis of 1,3-bis(imino)ethyl/benzyl imidazolium salts 30

2.2 Attempts to isolate the free carbene 37

2.3 Synthesis of transition metal NHC complexes.. 38

2.3.1 Bis(imino)imidazol-2-ylidene silver(I) complexes.................................... 39

2.3.2 Bis(imino)imidazol-2-ylidene copper(I) complexes.................................. 41

2.3.3 Bis(imino)imidazol-2-ylidene iron(II) complex 45

2.3.4 Bis(imino)imidazol-2-ylidene cobalt(II) complex..................................... 47

2.3.5 Bis(imino)imidazol-2-ylidene chromium complexes 49

2.3.6 Bis(imino)imidazol-2-ylidene palladium complexes................................. 52

2.3.7 Bis(imino)imidazol-2-ylidene zinc complexes 56

2.4 Polymerization of ethylene... 58

2.5 Conclusions 60

2.6 Experimental procedures.. 61

Chapter Three.. 77

Synthesis, Characterization and Reactivity Study of Bis(imino)benzimidazol-2-ylidene Transition Metal Complexes.. 77

3.1 Synthesis of 1,3-bis(imino)ethyl/benzyl benzimidazolium salts....................... 79

3.2 Attempts of isolating the free carbene 81

3.3 Synthesis of NHC transition metal complexes 86

3.3.1 Bis(imino)benzimidazol-2-ylidene silver complex 86

3.3.2 Bis(imino)benzimidazol-2-ylidene copper and chromium complexes 87

3.3.3 Bis(imino)benzimidazol-2-ylidene iron and cobalt complexes 89

3.4 Polymerization of ethylene 91

3.5 Conclusions 91

3.6 Experimental procedures 92

Chapter Four 102

Synthesis, Characterization and Reactivity Study of Bis(imino) pyrimidin-2-ylidene Transition Metal Complexes 102

4.1 Synthesis of 1,3-bis[1-(2,6-dimethylphenylimino)ethyl]-4,5,6-trihydro pyrimidinium salt 104

4.2 Synthesis of NHC transition metal complexes 105

4.2.1 Bis(imino)pyrimidin-2-ylidene copper and chromium complexes 105

4.2.2 Bis(imino)pyrimidin-2-ylidene iron and cobalt complexes 109

4.3 Polymerization of ethylene 110

4.4 Conclusions 111

4.5 Experimental procedures 112

Chapter Five 119

Spectroscopic and Density Functional Theory Studies of Bis(imino)-*N*-Heterocyclic Carbene Iron(II) Complexes 119

5.1 Cyclic voltammetry of the imidazolium salt and the related NHC iron complexes 121

5.2 Density functional theory study of bis(imino)-NHC iron(II) complexes......... 125

5.3 Conclusions 133

5.4 Experimental procedures and computational details....................................... 134

References 136

Appendices.. 153

Appendix A: X-ray crystal structure data 153

Appendix B: DFT data for the optimized structures.. 254

List of Tables

Table of Contents v

Table 5.1. Cyclic voltammetry data for **2.7** and **2.17** 122

Table 5.2. Comparison of selected geometrical parameters of the complex **2.17** as quintet and triplet spin multiplicities with X-ray structural parameters. 128

Table 5.3. Percent contribution of fragments for alpha and beta spin orbitals for NHC Fe(II) complexes. 131

List of Figures

Figure 1.1. Linear and bent carbene and the nature of their frontier orbitals 12

Figure 1.2. Carbene electronic configuration 13

Figure 1.3. Substituents electronic effects for diamino-, phosphinosilyl-, and diboryl-carbenes... 14

Figure 1.4. (a) Covalent bonding in the Schrock triplet carbene, (b) donor-acceptor bonding in the Fischer carbene and (c) NHC bonding in transition metal complexes. 15

Figure 2.1. ORTEP of **2.7** 32

Figure 2.2. ORTEP of **2.10** 35

Figure 2.3. ORTEP of **2.15** 43

Figure 2.4. ORTEP of **2.16**. 45

Figure 2.5. ORTEP of **2.17** 47

Figure 2.6. ORTEP of **2.18**. 49

Figure 2.7. ORTEP of **2.20** 51

Figure 2.8. ORTEP of **2.21**. 55

Figure 2.9. ORTEP of **2.23** 58

Figure 3.1. ORTEP of **3.7** 82

Figure 3.2. ORTEP of **3.8** 85

Figure 4.1. ORTEP of **4.6** 108

Figure 5.1. Steric parameters (A_L and A_H) for NHC ligands... 120

Figure 5.2. Percent buried volume % V_{bur} for NHC ligands. 121

Figure 5.3. Cyclic voltammogram for the imidazolium salt **2.7**.................................... 123

Figure 5.4. Cyclic voltammogram for imidazol-2-ylidene iron(II) complex **2.17**.......... 123

Figure 5.5. Cyclic voltammogram for benzimidazol-2-ylidene iron(II) complex **3.13** .. 124

Figure 5.6. Cyclic voltammogram for pyrimidin-2-ylidene iron(II) complex **4.7**.......... 124

Figure 5.7. HOMO and LUMO representation and relative energy for imidazol-2-ylidene **1.55**, benzimidazol-2-ylidene **1.56** and pyrimidin-2-ylidene **1.57** generated at the B3LYP/DGDZVP level of calculation. 126

Figure 5.8. Alpha HOMO and LUMO representations and relative energies for NHC iron(II) complexes generated at the UB3LYP/TZVP level of calculation. 129

Figure 5.9. Beta HOMO and LUMO representations and relative energies for NHC iron(II) complexes generated at the UB3LYP/TZVP level of calculation. 130

Figure 5.10. Electrostatic potential maps of bis(imino) NHC ligand (top; B3LYP/TZVP) and their iron complexes (bottom; B3LYP/TZVP) 133

List of Schemes

Scheme 1.1. Mechanism for ethylene polymerization with Ni(II) and Pd(II) α-diimine complexes 4

Scheme 1.2. Chain propagation and transfer process. 9

Scheme 1.3. Attempt for isolating imidazolin-2-ylidene (**1.7**). 16

Scheme 1.4. Attempt for isolating imidazol-2-ylidene (**1.9**). 16

Scheme 1.5. Original complexes of NHC, Wanzlick's (**1.12**), Öfele's (**1.14**) and Lappert's complexes (**1.15**). 17

Scheme 1.6. Synthesis of imidazoline-2-thiones from imidazolium salts. 18

Scheme 1.7. Synthesis of the first stable NHC. 18

Scheme 1.8. Synthesis of imidazol-2-ylidene from imidazole-2(3H)-thions. 18

Scheme 1.9. Synthetic route of symmetrical/unsymmetrical substituted imidazolium salts. 19

Scheme 1.10. Synthetic routes of imidazolium salts. 19

Scheme 1.11. Synthesis of five-, six- and seven-membered saturated NHC ligand precursors. 20

Scheme 1.12. Synthesis of NHC ligands. 21

Scheme 1.13. Synthesis of free NHCs and their ligand precursors. 22

Scheme 1.14. Synthesis of NHC transition metal complexes via the reaction of a metal precursor with free carbene. 23

Scheme 1.15. Synthesis of NHC transition metal complexes via oxidative addition. 23

Scheme 1.16. Synthesis of NHC transition metal complexes via transmetalation reaction. 24

Scheme 1.17. Synthesis of NHC transition metals complexes via reaction of an imidazolium salt with a basic metal precursor. 24
Scheme 1.18. Synthesis of NHC transition metals complexes via thermolysis of tetraaminoethylene. 24
Scheme 2.1. Synthesis of 1-iminoimidazole **2.4**, **2.5** and **2.6**. 30
Scheme 2.2. Synthetic route toward **2.7**. 31
Scheme 2.3. Attempted synthesis of unsymmetrical imidazolium salts **2.8** and **2.9**. 33
Scheme 2.4. Proposed reaction mechanism for the formation of **2.7**. 34
Scheme 2.5. Synthesis of the imidazolium salt **2.10**. 34
Scheme 2.6. Decomposition of **2.10** in the presence of $^{n}Bu_4NCl$. 36
Scheme 2.7. Synthetic route toward **2.11**. 36
Scheme 2.8. Possible decomposition pathways for the imidazolium salts **2.7** and **2.10**. 37
Scheme 2.9. Synthesis of silver(I) NHC complex **2.12**. 40
Scheme 2.10. Synthesis of the NHC silver(I) complex **2.14**. 41
Scheme 2.11. Synthetic route to the NHC copper complexes **2.15** and **2.16**. 42
Scheme 2.12. Synthesis of the NHC iron(II) complex **2.17**. 46
Scheme 2.13. Synthesis of the NHC cobalt(II) complex **2.18**. 48
Scheme 2.14. Synthesis of the NHC chromium(III) complex **2.19**. 50
Scheme 2.15. Synthesis of the NHC chromium(III) complex **2.20**. 50
Scheme 2.16. Synthesis of the NHC palladium(II) complexes **2.21** and **2.22**. 53
Scheme 2.17. Proposed allyl group isomerization ($\sigma \rightarrow \pi$) in **2.21**. 54
Scheme 2.18. Synthesis of the NHC zinc(II) complex **2.23**. 57
Scheme 2.19. Synthesis of the NHC zinc(II) complex **2.24**. 57

Scheme 3.1. Synthesis of 1-iminoethylimidazole **3.3** and **3.4**. 79

Scheme 3.2. Synthesis of benzimidazolium salt **3.5**. 80

Scheme 3.3. Synthesis of benzimidazolium salt **3.6**. 81

Scheme 3.4. Reaction of benzimidazolium salt **3.6** with $KN(SiMe_3)_2$. 81

Scheme 3.5. Attempt for deprotonating benzimidazolium salt **3.6**.................................. 83

Scheme 3.6. Possible decomposition pathways for benzimidazolium salt **3.6**. 84

Scheme 3.7. The reaction of **3.4** with boron trifluoride-diethyl etherate adduct. 85

Scheme 3.8. Synthesis of the benzimidazol-2-ylidene silver(I) complex **3.9**.................. 87

Scheme 3.9. Synthesis of the benzimidazol-2-ylidene copper and chromium complexes **3.10** and **3.11**. 88

Scheme 3.10. Attempt to synthesize the benzimidazol-2-ylidene copper (I) complex **3.12**. 89

Scheme 3.11. Synthesis of the benzimidazol-2-ylidene iron(II) **3.13** and cobalt(II) **3.14** complexes. 90

Scheme 4.1. Synthesis of pyrimidinium chloride salt **4.2**.. 105

Scheme 4.2. Attempt to synthesize pyrimidinium tetrafluoroborate salt **4.4**................. 105

Scheme 4.3. Synthesis of pyrimidin-2-ylidene copper and chromium complexes **4.5** and **4.6**, respectively. 107

Scheme 4.4. Synthesis of pyrimidin-2-ylidene iron and cobalt complexes **4.7** and **4.8**. 110

List of Abbreviations

Å	Angstrom, (Å = 10^{-10} m)
Ad	Adamantyl
α	Alpha
Anal.	Analysis
Ar	Aryl
av	Average
β	Beta
bar	Unit of pressure
B3LYP	Becke 3-parameter Lee–Yang–Parr exchange-correlation functional
br	Broad
Bu	Butyl
°C	Degree Celsius
C_6D_6	Deuterated benzene
ca.	Approximate
CCDC	Cambridge crystallographic data center
CD_2Cl_2	Deuterated methylene chloride
CD_3CN	Deuterated acetonitrile
CH_2Cl_2	Methylene chloride
CH_3CN	Acetonitrile
calcd.	Calculated
COD	1,5-Cyclooctadiene
coe	Cyclooctene
Cp	Cyclopentadienyl
°	Degree
δ	NMR chemical shift, ppm
Δ	Difference

d	Doublet
DCM	Dichloromethane
DFT	Density functional theory
DGDZVP	Density Gauss Double-Zeta Valence with Polarization
DMSO	Dimethylsulfoxide
e.g.	For example, abbreviation of Latin ‘exempli gratia’
equiv	Equivalents
et al.	And others, abbreviation of Latin ‘et alii’
eV	Electron volt
Et_2O	Diethyl ether
Fc^+/Fc	Ferrocenium/ferrocene
g	Gram
h	Hour
HCl	Hydrochloric acid
i.e.	That is, abbreviation of Latin ‘id est’
*i*Pr	Isopropyl
IR	Infrared
IUPAC	International Union of Pure and Applied Chemistry
J	Coupling constant, Hz
kcal	Kilocalorie
kg	Kilogram
kJ	Kilojoule
KO^tBu	Potassium *tert*-butoxide
λ	Wavelength, lambda
M	Molar; mol L^{-1}
m	Multiplet
MAO	Methylaluminoxane
Me	Methyl

MeCN	Acetonitrile
MHz	Megahertz; 10^6 Hz
Mes	Mesityl
mg	Milligram
μL	Microliter
mL	Milliliter
mM	Millimolar
mmol	Millimol
μ_{eff}	Effective magnetic moment
MW	Molecular weight
NHC	*N*-heterocyclic carbene
NMR	Nuclear magnetic resonance
OAc^-	Acetate anion
ORTEP	Oak Ridge Thermal Ellipsoid Plot
Ph	Phenyl
π	Pi; pi bond
PE	Polyethylene
ppm	Parts per million
RT	Room temperature
σ	Sigma; sigma bond
s	Singlet
tert	Tertiary
THF	Tetrahydrofuran
TOF	Turnover frequencies
TON	Turnover number
t	Triplet
TZVP	Triple-Zeta Valence with Polarization
ν	Wavenumber; cm^{-1}

VT	Variable temperature
V	Volt
Xyl	2,6-C_6H_3-Me_2

Chapter One

Introduction

1.1 Olefin polymerization

The understanding of the nature of well-defined single-site organometallic catalysts for olefin polymerization has led to improve and control polymer properties.[1] The discovery of group 4 metallocenes[2] and half-sandwich titanium-amide (constrained-geometry) complexes[3] activated with methylaluminoxane (MAO) were breakthroughs in this field.[1] Early transition metal catalysts (titanium, zirconium, or chromium) can unfortunately be poisoned by functionalized olefins due to their high oxophilicity.[4] Academic and industrial researchers are striving to develop superior families of catalysts that tolerate functional groups and attend to the high demand of improved polymers properties.[1]

Late transition metals are low oxophilic catalysts that can be functional-group tolerant and copolymerize ethylene with polar comonomers under mild conditions.[4] Advances have been made due to the extraordinary discovery of the active (α-diimine)nickel catalysts that produce linear or highly branched polyethylene (PE), controlled by the ligand scaffold and reaction conditions.[5] Drent reported the first example of ethylene and methacrylate copolymerization reaction catalyzed by Pd(II)-based complex bearing a bidentate phosphino-sulfonate ligand, which I will not further mention.[6]

1.1.1 Nickel(II) and palladium(II) complexes of α-diimine ligands

The Pd(II) and Ni(II) catalysts of α-diimine ligands (**1.1**) were the first examples of late transition metal catalysts that can polymerize ethylene and α-olefins producing high molecular weight polymers possessing new properties.[1,7]

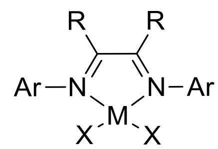

R = H, Me
Ar = 2,6-iPr$_2$C$_6$H$_3$
M = Ni, Pd

1.1

Exceptional ethylene polymerization activities of the diimine nickel catalysts were reported with a turnover frequency up to 3.9 x 10^5 h^{-1} (11,000 kg of PE mol^{-1} of Ni h^{-1}).[7] Highly linear to moderately branched polyethylenes were produced by these Ni(II) catalysts, where the degree of branching is dependent upon the reaction conditions and catalyst structure. Less branched, more linear and lower molecular weight polymers were obtained by reducing the steric bulk of the α-diimine ligand (*e.g.* replacing *o*-isopropyl groups with *o*-methyl groups).[7] The α-diimine palladium catalysts exhibited low polymerization activities for ethylene and α-olefins. Highly branched polyethylenes with high molecular weights were produced.[7] However, considerably lower polymerization rates for α-olefins than ethylene were reported for these Ni and Pd systems.[4]

The cationic active species is generated *in situ* by the reaction of the α-diimine metal halide complexes with methylaluminoxane (MAO) in the presence of olefins. Alternatively, the treatment of the complex with salts of non-coordinating anions affords cationic catalysts.[7] Ethylene coordinates to the cationic complex (**1.1a**) and this is followed by a migratory insertion of the metal alkyl into the coordinated olefin (**1.1b**). The energy barriers for insertions in nickel complexes are lower than that of palladium complexes by 4-5 kcal/mol and this explains the higher activities observed for Ni(II) compared to Pd(II) catalysts.[4,8] Successive to the migratory insertion step, β-agostic interactions were observed in the 14-electron alkyl complexes. Rapid coordination of ethylene forms **1.1a**. Otherwise, β-hydride elimination affords an olefin metal hydride complex **1.1c**. Rotation of the olefin and reinsertion can occur to form a branched alkyl group in **1.1f**. Ethylene coordination and insertion can take place, resulting in branched polyethylene (Scheme 1.1).[4,7] Associative displacement of olefin with a new monomer (ethylene), in **1.1c**, produces a new chain. The steric bulk of the diimine ligands reduces the rate of associative displacement. This is because of the bulky *ortho* substituents of the aryl rings block axial sites of the square planar complex. Therefore, high molecular weight polymers were formed, as a result of higher rates of chain propagation than that of chain transfer.[4,7]

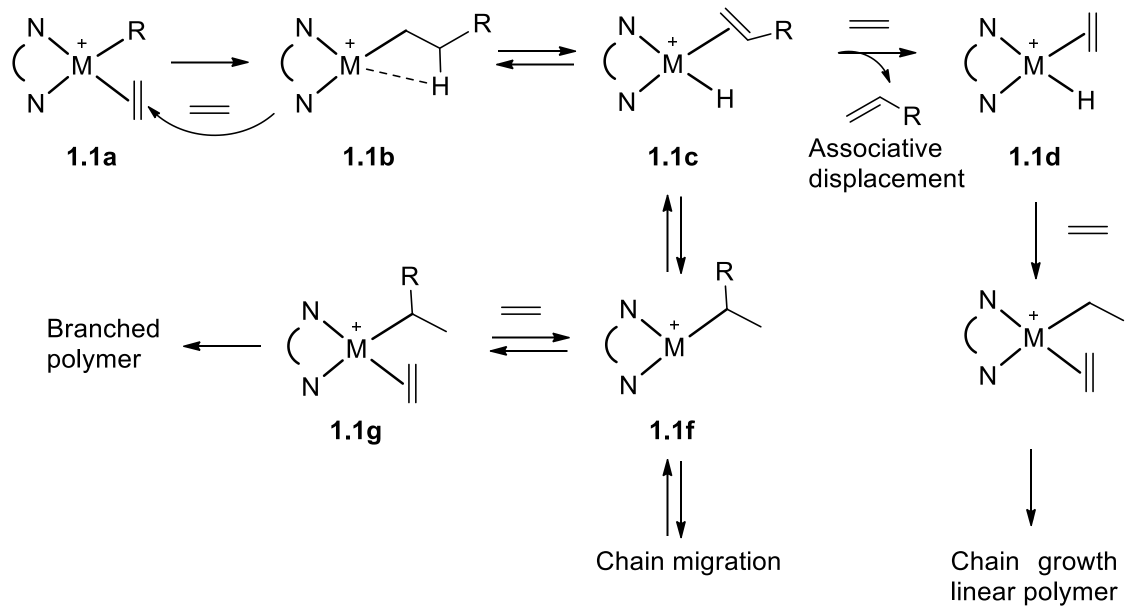

Scheme 1.1. Mechanism for ethylene polymerization with Ni(II) and Pd(II) α-diimine complexes.[4,7]

1.1.2 Nickel (II) complexes of salicylaldimine ligands

Salicylaldiminato Ni(II) complexes (**1.2**) are highly active catalysts for the polymerization of ethylene in the presence of a phosphine scavenger and they are able to act as single-component catalysts.[9] They are very versatile catalysts due to many substitution sites.[4] Also, the use of a neutral Ni(II) center and bulky ligand scaffold provide tolerance toward functionalized groups and prevent the catalyst deactivation process.[9b]

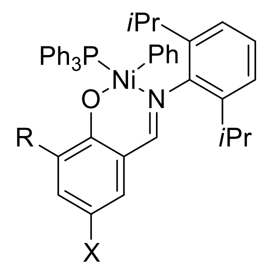

R = ^{t}Bu, X = H

1.2

Subsequent to the addition of a suitable phosphine scavenger ($Ni(COD)_2$ (COD = 1,5-cyclooctadiene) or $B(C_6F_5)_3$) to the reaction mixture of the catalyst, toluene and ethylene, a highly active ethylene polymerization catalyst was generated. The bulky aryl substituents are proposed to facilitate phosphine ligand dissociation and generate a vacant site for ethylene to coordinate,[9] as supported by theoretical calculations.[10] This bulkiness hampers the deactivation of the catalyst through the formation of a bis(salicylaldiminato) nickel complex.[5] The increased steric hindrance of the ketimine moiety[11] and the phenolic ring of these complexes protects the metal center by blocking the axial positions and reduces the rate of associative displacement of olefin with a new monomer (ethylene),[9b] as proposed for α-diimine Ni(II) and Pd(II) complexes.[7,12] The activity of these complexes was enhanced by incorporating an electron-withdrawing group. However, incorporating an electron-rich substituent at the 5-position of the salicylaldiminato ring reduces the activity.[9b] The (salicylaldiminato) nickel catalysts are tolerant to functional groups and stay active in aqueous media or in polar solvents.[13] The copolymerization of norbornenes and functionalized olefins by these nickel(II) complexes was also reported.[9a,13b,14]

1.1.3 Iron(II), cobalt(II) and chromium(III) complexes of tridentate 2,6-bis(imino)-pyridine ligands

The great success of Ni- and Pd-(α-diimine) catalytic systems toward ethylene polymerization and their functional group tolerance have motivated researchers to study other late transition metal systems that can catalytically polymerize α-olefins.[15] This was the initiative behind the synthesis of iron(II) and cobalt(II) complexes of 2,6-bis(arylimino)-pyridine (**1.3**).[15-16] The ligands were chosen with bulky substituents at the *ortho*-positions of the phenyl rings, as seen previously in the Ni- and Pd-(α-diimine) systems.[17]

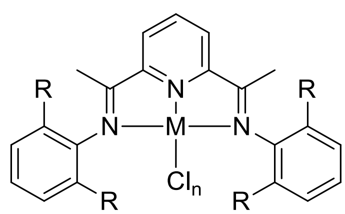

R = *i*Pr, n = 2, M = Fe, Co
R = *i*Pr, n = 2, 3, M = Cr

1.3

The iron and cobalt complexes of bis(arylimino)pyridine ligands exhibit extraordinary reactivity toward ethylene polymerization; in some cases, comparable to that of group 4 metallocenes.[15-16] The precatalysts were activated by methylaluminoxane (MAO) or modified methylaluminoxane (MMAO) in toluene under ethylene. Contrary to the Ni(II) and Pd(II) complexes of α-diimine ligands, highly linear polyethylene (PE), with T_m of 133–139 °C, was obtained using these catalysts.[13,14d]

The molecular weights of the polymer were dependent on several factors, including ligand structure and transition metal choice.[15,16d] The polymer molecular weights increase with increasing the steric bulk of the *ortho*-aryl substituents. For instance, the 2,6-bis[1-(2,6-diisopropylphenylimino)ethyl]pyridine iron(II) chloride catalyst produces polymer with peak MW of 71,000, whereas the analogous iron(II) complex with 2,6-dimethylphenyl substituents shows a peak MW of 33,000.[15,16d] Higher molecular weight polymers were produced by the iron catalysts than by the cobalt analogous.[15,16d]

An increase in ethylene concentration leads to high turnover frequencies (TOFs)[15] and therefore, this proposes that the rate of chain growth is dependent on ethylene pressure.[16d] However, a low dependence on ethylene pressure was observed for the analogous cobalt catalysts.[15,16d] The bis(arylimino)pyridine iron systems show extreme activities, whereas the related cobalt complexes show an order of magnitude lower activity.[15,16c,16d]

The highly active catalysts for oligomerization of ethylene were obtained by reducing the steric bulk of the bis(arylimino)pyridine iron complex, using a single *ortho*-substituent on each aryl ring.[15,16e] In general, turnover frequencies increased with ethylene pressure and temperature. The highest activity with turnover frequency of $1.0 \times 10^5\ h^{-1}$ at 25 °C and 1 atm was observed for the *ortho*- methyl-substituted bis(arylimino)pyridine iron complex. However, reduced activities were reported for sterically bulkier catalysts (ethyl-substituted) under similar conditions.[16e]

The proposed ethylene polymerization mechanism is shown in Scheme 1.2.[16c,18] The reaction of bis(arylimino)pyridine iron or cobalt halides with MAO *in situ* generates the active species proposed to be a methylated metal cation with a vacant site in which ethylene can coordinates forming an olefin complex intermediate.[16c,18]

The chain propagation pathway (path A) involves migratory insertion of the metal alkyl into the coordinated ethylene, in which the rate is first order with respect to ethylene pressure. Consecutive steps of ethylene coordination and migratory insertion continue until chain transfer takes place.[16c,18]

The chain transfer mechanism includes β-H transfer to the metal (path B), to the monomer (path C) or to aluminum (path D). The β-H transfer to the metal center is a unimolecular step that is independent of monomer concentration. It is followed by associative displacement of the polymer chain by the coordinated ethylene. The other possible process, which is a bimolecular step, is β-H transfer to monomer (path C) and it is first-order with respect to the monomer concentration. Only one unsaturated chain end (vinyl end group) per polymer chain is produced by β-H transfer reaction to the metal or to the monomer. The proposed chain transfer to aluminum (path D) is dependent on the alkyl aluminum concentration. This chain transfer process proceeds via an alkyl bridge between metals leading to exchange of the polymer chain for an alkyl group from aluminum to yield saturated polymer chains.[16c,18]

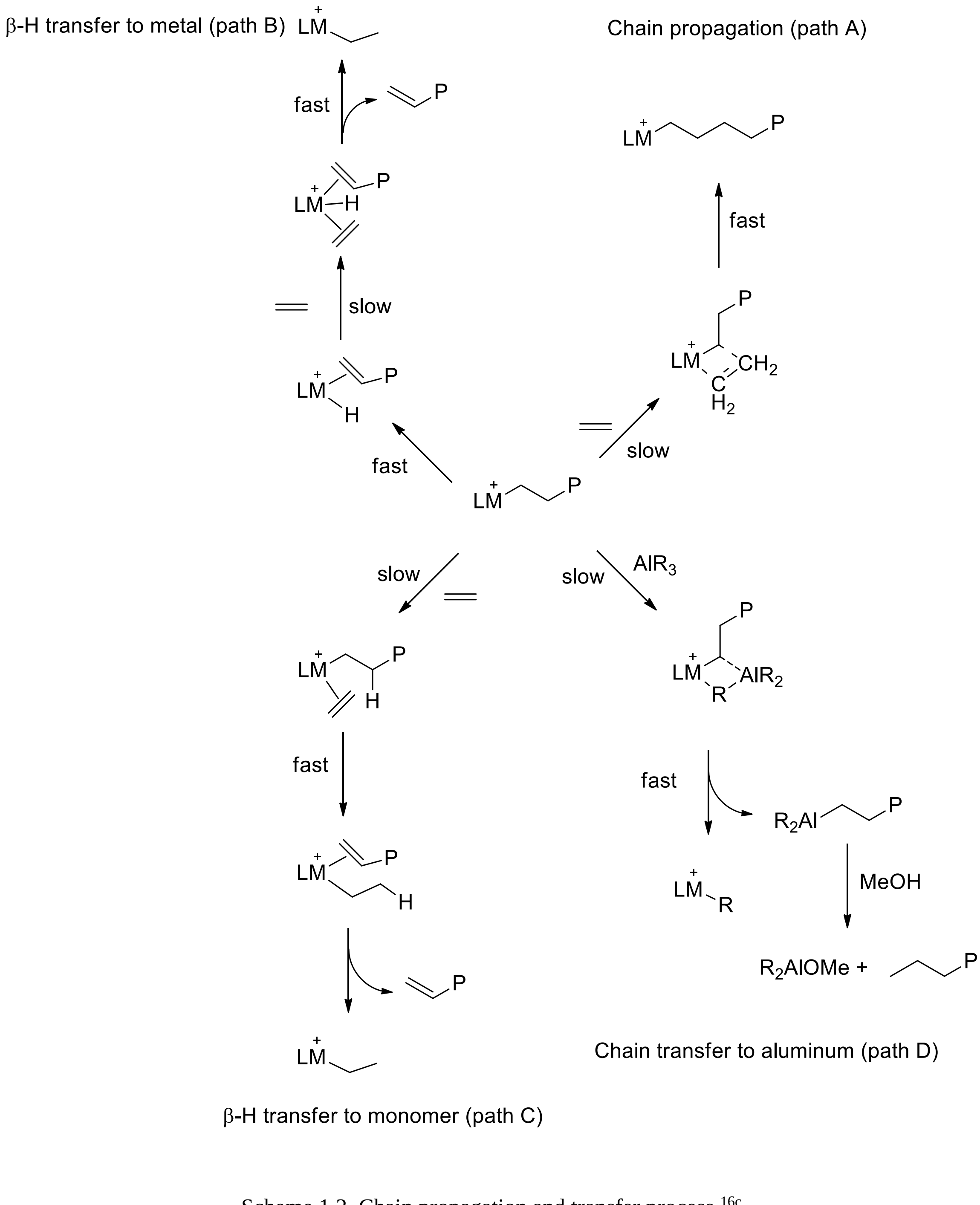

Scheme 1.2. Chain propagation and transfer process.[16c]

Despite excellent activities in ethylene polymerization, iron and cobalt complexes of the bis(arylimino)pyridine exhibit catalyst deactivation at elevated temperatures.[16c,19] This has been addressed by installing suitable aryl substituents that lead to more temperature-tolerant complexes.[19] For example, Fe(II) complexes of bis(imino)pyridine ligands functionalized with boryl substituents have longer lifetimes at high temperatures than the analogous complexes with 2-methylphenyl substituents.[19b]

The applications of the bis(arylimino)pyridine ligands in ethylene polymerization and oligomerization were extended to chromium complexes (**1.3**).[20] The catalytic activity and polyethylene molecular weight were in part affected by the substituents of the ligands. For example, the Cr(III) catalyst of this ligand that has the imino nitrogen substituted with cyclohexyl groups has a lower activity than the analogous arylimino substituents.[20c] An increase of the bulkiness in *ortho* substituents of aryl rings of these complexes from methyl groups to *tert*-butyl groups reduced their activity.[20b] As reported for iron(II) and cobalt(II) complexes of bis(arylimino)pyridine ligands,[15-16] the analogous chromium complexes containing bulkier *ortho* substituents in the aryl imino groups give higher molecular weights.[20b,20c]

Further applications of bis(arylimino)pyridine transition metal complexes toward catalytic transformations have since been extensively studied by modifying the ligand scaffold and establishing structure-activity relationships.[20b,21] Some of these catalytic transformations include hydrogenation of olefins, hydrosilylation of aldehydes and ketones, reduction of aldehydes and ketones, oxidation of alkanes, cyclopropanation of alkenes, electrocatalytic reduction of carbon dioxide, cross-coupling reactions, dinitrogen activation and cycloaddition of dienes.[21c-e,21h,21j,21k,22]

The modification of the bis(arylimino)pyridine ligands by replacing the bis(imino) moieties with 2,6-bis(NHC)pyridine ligands yielded the corresponding early and middle transition-metal complexes (**1.4**) evaluated in oligomerization/polymerization of ethylene.[23] The 2,6-bis(NHC)pyridine complexes of V(III) show higher activity (1,280 g $mmol^{-1}$ of V h^{-1} bar^{-1}) for ethylene polymerization than the related Ti(III) (791 g $mmol^{-1}$ of V h^{-1} bar^{-1}), upon activation with MAO.[23b] The 2,6-bis(NHC)pyridine Cr(III) complexes are very active in ethylene oligomerization with activities up to ca. 40,000 g $mmol^{-1}$ of Cr h^{-1} bar^{-1}, comparable to the ethylene oligomerization activities of bis(imino)pyridine iron(II) complexes.[24a,24b,16e,24] In contrast, 2,6-bis(NHC)pyridine complexes of Fe(II) and Co(II) are inactive.[23b]

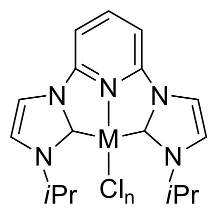

M = V, n = 3
M = Cr, n = 3
M = Fe, n = 2
M = Co, n = 2

1.4

In this thesis, further modifications of the bis(arylimino)pyridine ligands by incorporating an *N*-heterocyclic carbene (NHC) fragment into the ligand scaffold will be discussed and therefore the subject of carbene will be introduced.

1.2 Carbenes

Carbenes are neutral compounds containing a divalent carbon atom which has only six valence-shell electrons.[25] The carbene center can adopt a linear or a bent geometry. An *sp*-hybridized carbene center with two degenerate nonbonding orbitals (p_x and p_y) is the characteristic of linear carbenes. However, bent carbenes have an sp^2-hybridization carbene carbon atom. The p_x orbital is stabilized by gaining partial *s* character and therefore it is known as σ, whereas the p_y orbital (named as p_π) remains unaffected (Figure 1.1).[25-26]

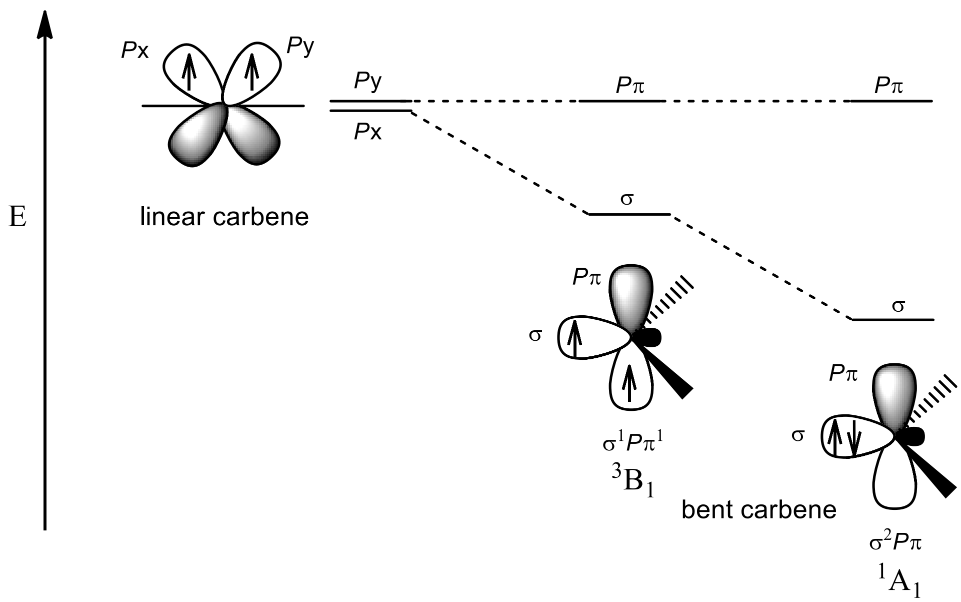

Figure 1.1. Linear and bent carbene and the nature of their frontier orbitals.[25-26]

The two nonbonding electrons of a carbene center can be unpaired with parallel spin resulting in a triplet state with $\sigma^1 p_\pi^1$ configuration (Figure 1.2). However, they can be paired in either σ or p_π orbital in which the σ^2 is more stable than the $p\pi^2$ and this forms singlet carbene state (Figure 1.2).[25-26] A $\sigma^1 p_\pi^1$ configuration can also be predicted for an excited singlet state.[25]

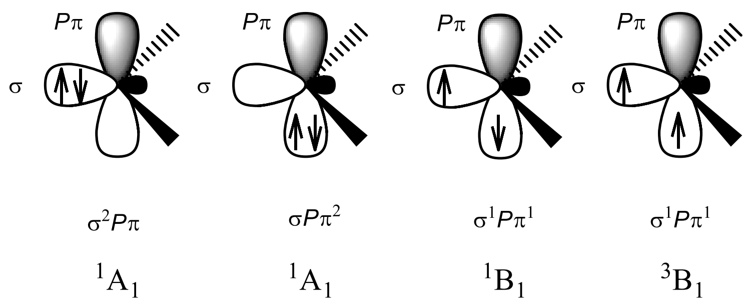

Figure 1.2. Carbene electronic configuration.[25]

The reactivity of carbenes can be predicted based on the ground-state spin multiplicity by the energy gap between σ and p_π orbitals. The singlet ground state is favored when the relative energy separation between σ and p_π orbitals is at least 2 eV, while one lower than 1.5 eV favors triplet state.[27] Singlet carbenes can be both electrophilic and nucleophilic species due to the presence of a filled σ and a vacant p_π orbital. In contrast, triplet carbenes are diradical species containing two partially occupied orbitals.[25-26]

The multiplicity of the ground state is influenced by electronic and steric effects of the substituents on the carbene center.[25-26] Electron-withdrawing substituents lower the relative energy of the σ orbital, whereas the energy level of the P_π remains unaffected. Therefore, the singlet ground state is stabilized.[28] On the other hand, electron donating substituents stabilize the triplet state by lowering the energy gap of σ and P_π orbital.[25-26] Mesomeric effects are important in determining the reactivity of carbenes.[29] For π electrons-donating substituents, the relative energy of the σ orbital is unchanged, while energy of the π orbital is increased by the π interaction. Consequently, the p_π–σ energy gap increases resulting in a bent singlet carbene (R_2N–C–NR_2, Figure 1.3).[26,30] A carbene is almost linear at the carbon atom when both a π-acceptor and a π-donor atom are the substituents on the carbene carbon (R_2P–C–SiR_3, Figure 1.3).[26] Though most carbenes with π-acceptor substituents are singlet, they are linear or nearly linear (R_2B–C–BR_2, Figure 1.3).[31]

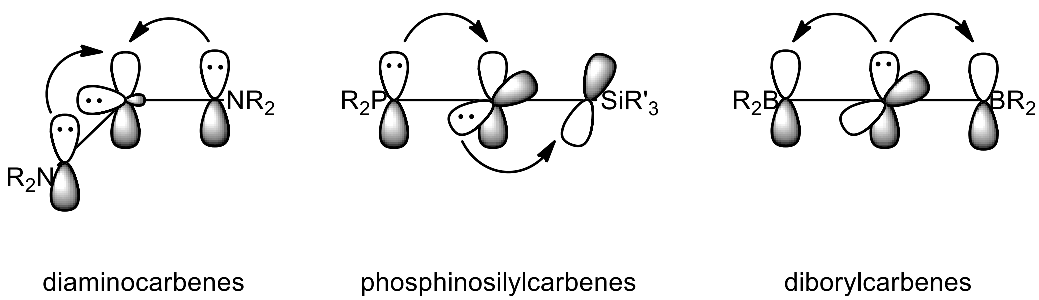

Figure 1.3. Substituents electronic effects for diamino-, phosphinosilyl-, and diboryl-carbenes.[25]

Carbenes are kinetically stabilized by bulky substituents. In addition, the ground-state spin multiplicity is highly dependent upon the steric effects in which minimal electronic effects are present.[25] Bulky substituents enlarge bond angle around the carbene center resulting in a more linear geometry and thereby the triplet state is preferred.[32] For example, the dimethylcarbene is a singlet with a bent bond angle[33] smaller than that for the triplet di(*tert*-butyl)-[34] and diadamantylcarbenes[35].

Fischer[36] and Schrock[37] carbenes have different binding natures in transition metal complexes (Figure 1.4).[38] In the Schrock carbene complexes, the interactions of a metal fragment with a triplet carbene form a covalent metal-carbene bond (Figure14.a). Whereas, a donor-acceptor bonding interaction with σ-donation by the carbene carbon to a metal and π-back donation to carbene are the characteristic of Fischer carbene complexes (Figure 1.4b).[25] *N*-heterocyclic carbenes (NHC) ligands coordinate to transition metals through σ bonding. However, π-back donation is weaker than that in the Fischer carbene complexes

(Figure 1.4c), due to the π donation of N atoms to the carbene p_π orbital resulting in partially filled orbital.[25,38]

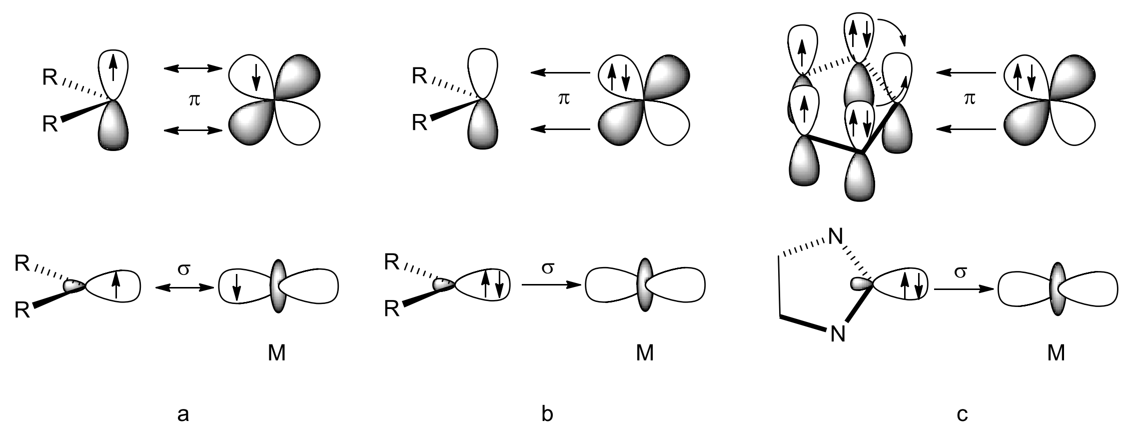

Figure 1.4. (a) Covalent bonding in the Schrock triplet carbene, (b) donor-acceptor bonding in the Fischer carbene and (c) NHC bonding in transition metal complexes.

1.2.1 *N*-heterocyclic carbenes (NHC)

The initial work by Wanzlick, in 1960, to isolate the postulated imidazolidin-2-ylidene (**1.7**) by α-elimination of chloroform led to the dimerized compound **1.6** (Scheme 1.3).[39] Wanzlick *et al.* noticed that the stability of unsaturated *N*-heterocyclic five-membered rings was partially due to aromatic resonance structures.[30] Further attempts toward isolating free carbenes using KO^{t}Bu to deprotonate tetraphenylimidazolium perchlorate (**1.8**) generated the corresponding carbene in solution (**1.9**). The free carbene could not be isolated, however it was trapped with phenylisothiocyanate (Scheme 1.4).[40]

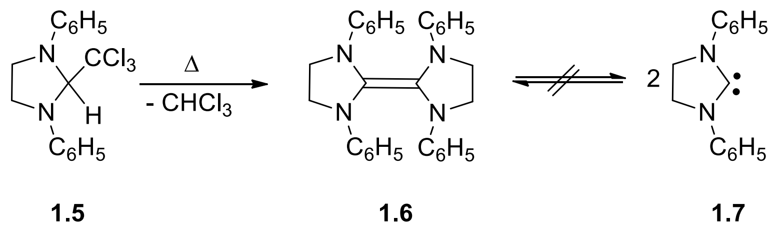

Scheme 1.3. Attempt for isolating imidazolin-2-ylidene (**1.7**).

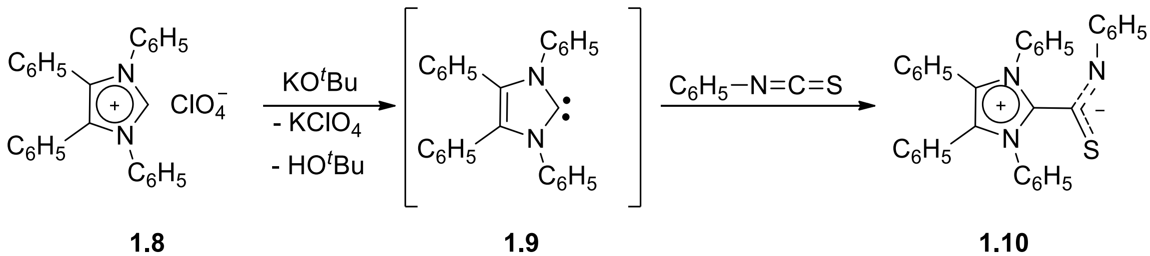

Scheme 1.4. Attempt for isolating imidazol-2-ylidene (**1.9**).

Transition metal complexes of NHC were independently reported by Wanzlick[41] and Öfele[42]. The treatment of basic metal precursors with the imidazolium salts afforded the related NHC complexes (Scheme 1.5). Shortly, Lappert *et al.* reported Pt(II) imidazolidin-2-ylidene complex afforded by the reaction of bis(1,3-diphenylimidazolidin-2-ylidene) (**1.6**) with di-μ-chlorodichlorobis(triethylphosphine)diplatinum(II) (Scheme 1.5).[43]

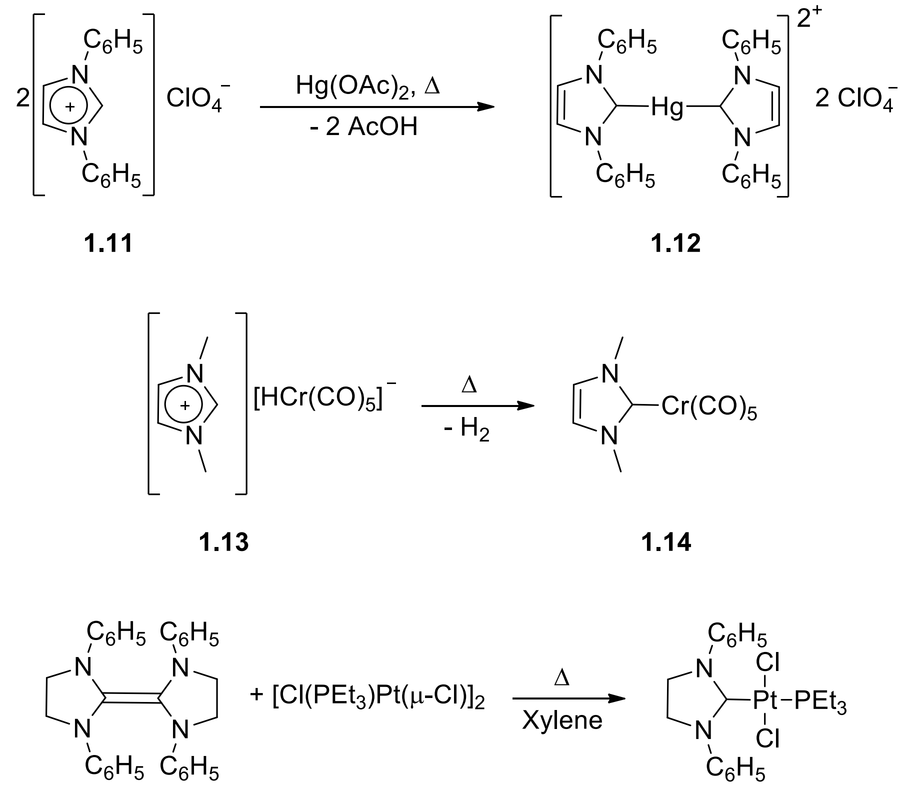

Scheme 1.5. Original complexes of NHC, Wanzlick's (**1.12**), Öfele's (**1.14**) and Lappert's complexes (**1.15**).

Arduengo *et al. in situ* deprotonated the imidazolium salts with NaOMe and subsequently treated them with elemental sulfur to prepare the imidazoline-2-thiones (**1.18**) (Scheme 1.6).[26,44] It was not until 1991 when Arduengo *et al.* isolated the first stable NHC (**1.20**) by careful deprotonation of the *N,N'*-diadamantyl imidazolium salt **1.19**, using sodium hydride as base and a catalytic amount of dimethylsulfoxide (Scheme 1.7). The carbene was crystallized from a concentrated THF solution as colorless crystals which were stable under inert conditions even at 240 °C. An X-ray diffraction analysis of the crystals definitively confirmed the first NHC structure.[45]

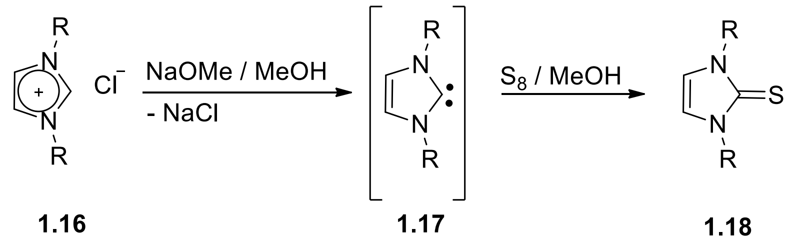

Scheme 1.6. Synthesis of imidazoline-2-thiones from imidazolium salts.

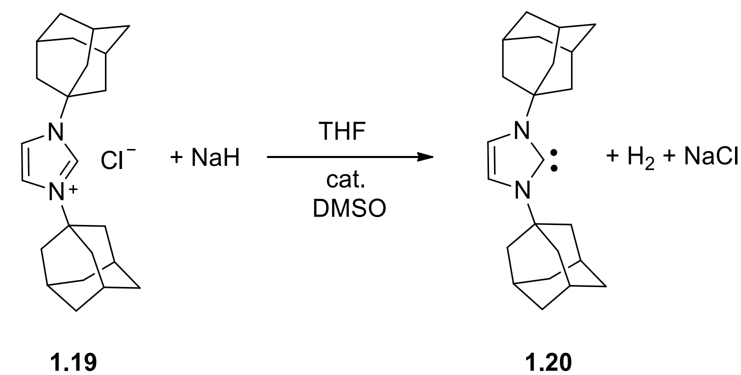

Scheme 1.7. Synthesis of the first stable NHC.

Alkyl-substituted NHCs were also accessible by the reaction of substituted imidazol-2(3H)-thione with potassium in boiling THF (Scheme 1.8), as reported by Kuhn *et al.*[46] The lone-pair electrons of the carbene center are stabilized by inductive effects of the more electronegative nitrogen atoms. Also, the lone-pair electrons of nitrogen atoms form a π-interaction with vacant p_π orbital of the carbene.[25,30]

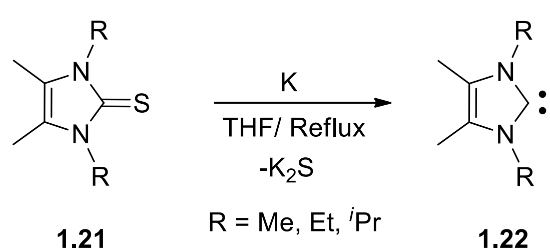

Scheme 1.8. Synthesis of imidazol-2-ylidene from imidazole-2(3H)-thions.

1.2.1.1 Synthesis of imidazolium salts

Imidazolium salts are usually afforded by either nucleophilic substitution on the azole ring or building up the heterocyclic compound containing the desired substituents.[47] The reaction of an imidazolide anion with alkyl-halides yields the substituted imidazole that is reacted with an additional alkyl-halides to afford imidazolium salts (Scheme 1.9).[48] Alternatively, an azole ring can be synthesized by reacting glyoxal, primary amine, ammonium chloride and formaldehyde to afford asymmetrical imidazolium salts (Scheme 1.10a), while symmetrical imidazolium salts can similarly be afforded by the reaction of glyoxal, primary amine and formaldehyde (Scheme 1.10b).[49] The 1,2-diamines react with triethoxymethane to produce aryl imidazolium salts (Scheme 1.10c).

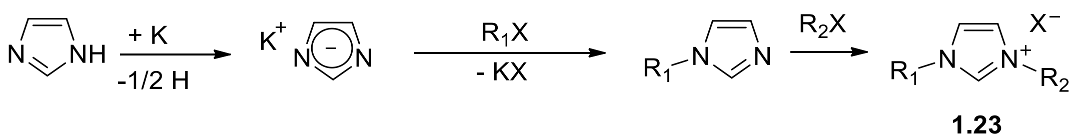

Scheme 1.9. Synthetic route of symmetrical/unsymmetrical substituted imidazolium salts.

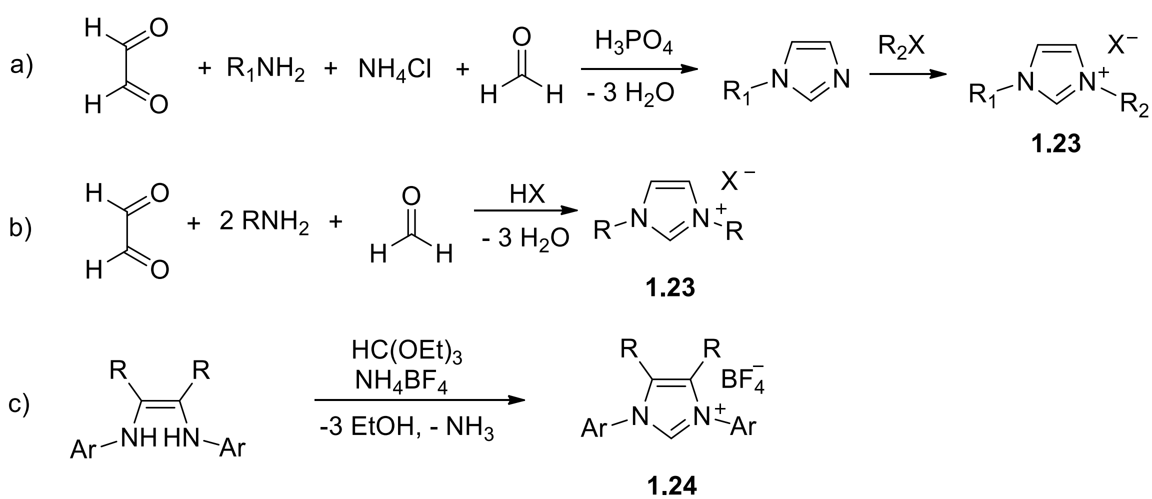

Scheme 1.10. Synthetic routes of imidazolium salts.

The related five-, six- and seven-membered rings of the amidinium salts can be afforded by the reaction of diamines with triethoxymethane[50] (Scheme 1.11a) or dihaloalkanes with formamidine[51] (Scheme 1.11b). They can also be synthesized by treating *N,N′*-diarylamidine with a dihaloalkane in the presence of potassium carbonate (Scheme 1.11c).[51b]

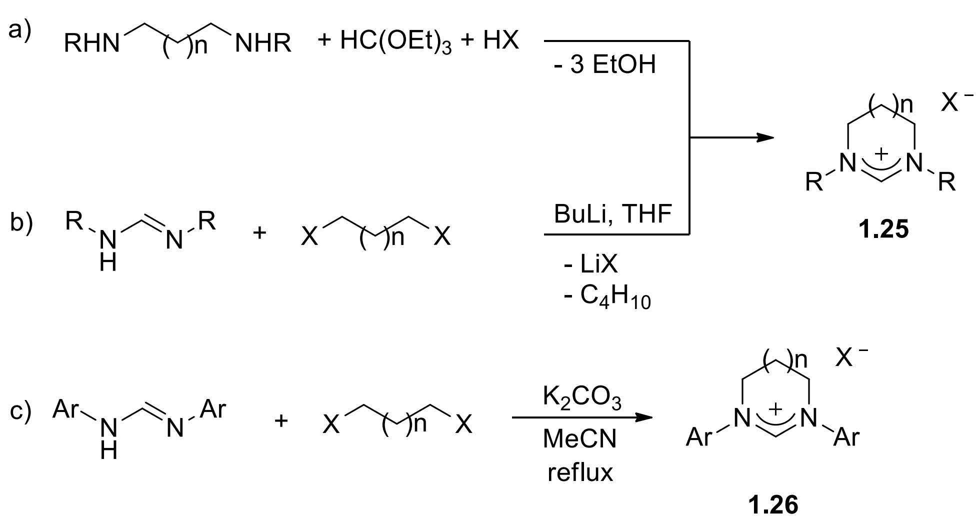

Scheme 1.11. Synthesis of five-, six- and seven-membered saturated NHC ligand precursors.

1.2.1.2 Synthesis of the NHC

The deprotonation of an imidazolium salt with a strong base, such as $MN(SiMe_3)_2$ (M = Li, Na, K) (Scheme 1.12a),[52] potassium/sodium hydride (Scheme 1.12b),[45,53] BuLi[54] (Scheme 1.12c) or potassium *tert*-butoxide[55] (Scheme 1.12d), yields a free NHC ligand. Sodium hydride in liquid ammonia can also be used to generate free carbenes from imidazolium salts (Scheme 1.12e).[56]

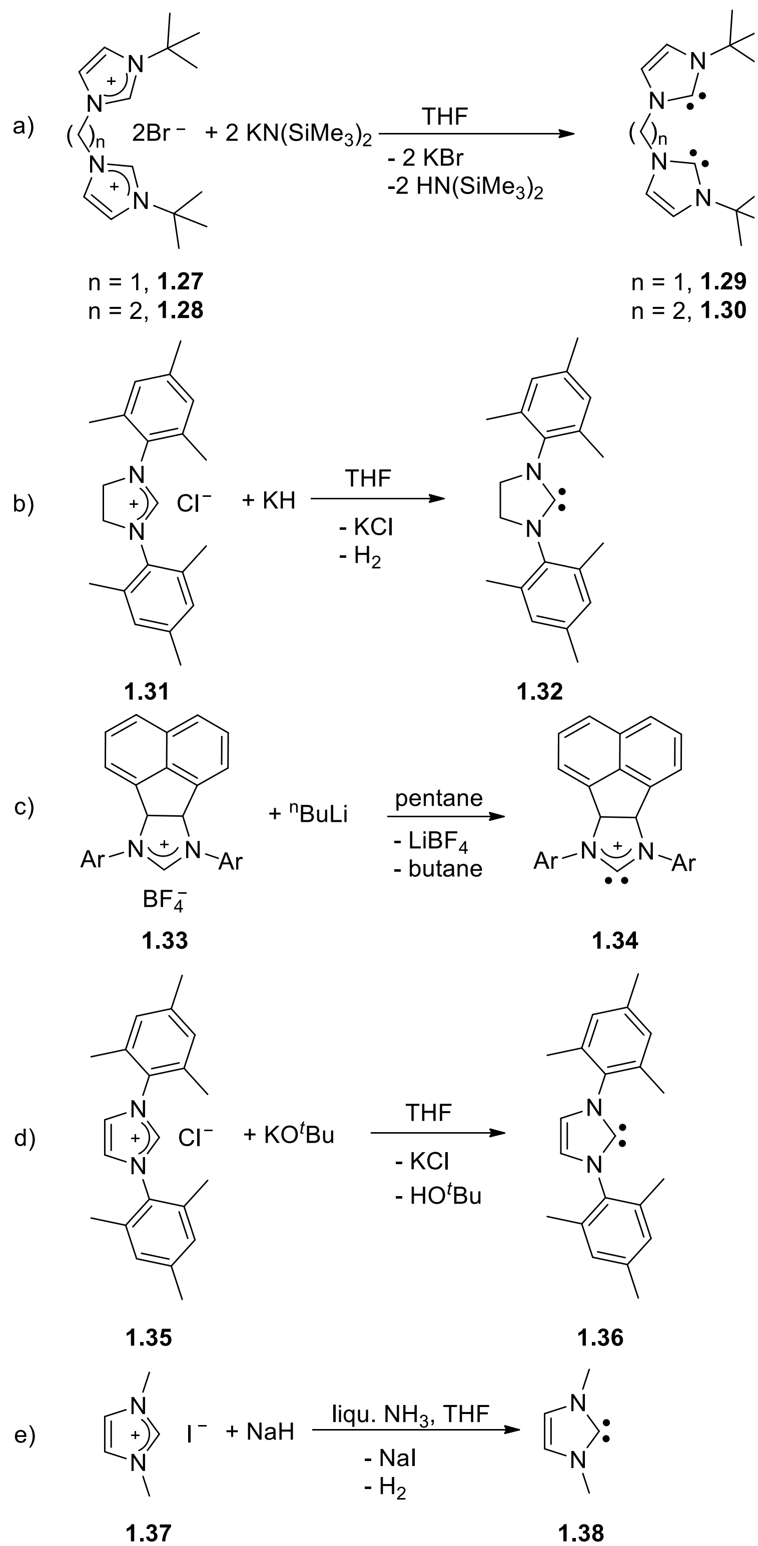

Scheme 1.12. Synthesis of NHC ligands.

The reaction of 1,3,4-triphenyl-1,2,4-triazolium perchlorate with sodium methoxide in methanol afforded 5-methoxy-1,3,4-triphenyl-4,5-dihydro-lH-1,2,4-triazole (**1.39**) that was heated at 80 °C to release methanol and to generate the corresponding carbene (Scheme 1.13).[57]

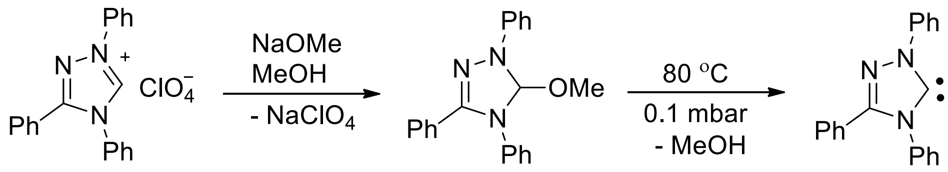

1.39 1.40

Scheme 1.13. Synthesis of free NHCs and their ligand precursors.

1.2.1.3 Synthesis of NHC transition metals complexes

Transition metal complexes of NHCs are commonly afforded by six different methods. Firstly, a transition metal complex can be treated with a free carbene. Neutral nucleophilic NHCs can displace other ligands, like carbon monoxide or acetonitrile, in a complex.[25,30] For instance, a carbon monoxide ligand in the complexes ($M(CO)_n$ M = W or Ni) is replaced with NHC (Scheme 1.14a).[58] Imidazolium salts can also be deprotonated in the presence of a metal salt to give the corresponding NHC complexes (Scheme 1.14b).[25,59] Secondly, a mononuclear carbene complex can be afforded by reacting a dimeric complex with NHCs (Scheme 1.14c).[25,56b] Thirdly, oxidative addition across the carbon-halide bond of the salt yields the related NHC complex (Scheme 1.15).[60] Fourthly, carbene transfer reactions, using silver[61] or copper[59] adducts as transmetalating reagents, afford the related NHC complexes (Scheme 1.16a,b).[25,48] Fifthly, the reaction of an imidazolium salt with a basic transition metal precursor[25,30,47] in which a basic anion or ligand (*e.g.* acetates[62] or amides[23d]) is *in situ* used to deprotonate the salt (Scheme 1.17). Sixthly, the NHC complexes are synthesized by the reaction of dimeric NHCs with a transition metal precursor. For example, the reaction of the electron-rich tetraaminoethylene with $Fe(CO)_5$ affords the corresponding NHC complex (Scheme 1.18).[25,47,63]

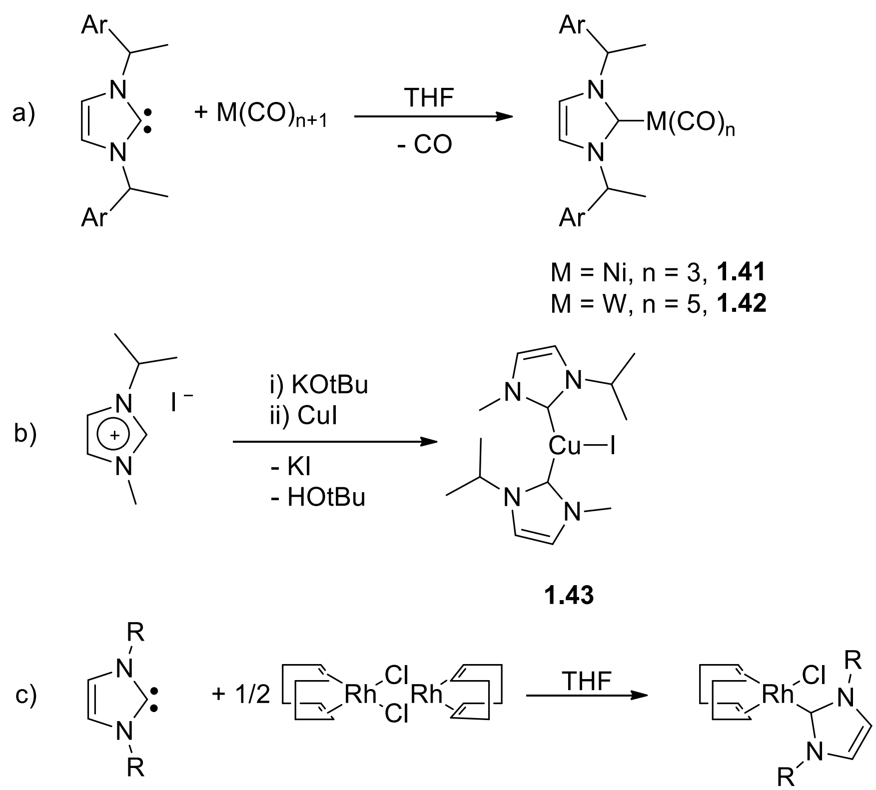

1.43

1.44

Scheme 1.14. Synthesis of NHC transition metal complexes via the reaction of a metal precursor with free carbene.

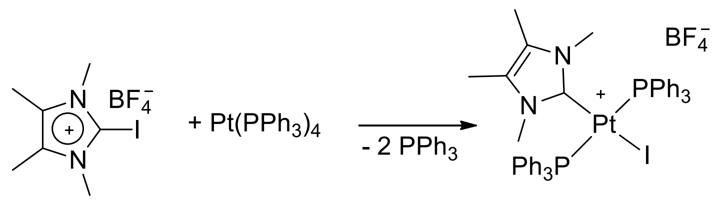

1.45

Scheme 1.15. Synthesis of NHC transition metal complexes via oxidative addition.

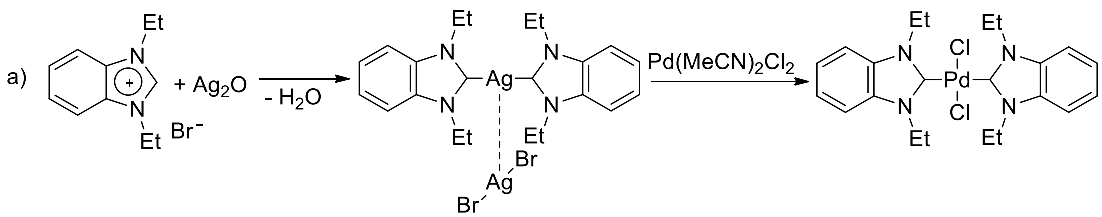

1.46 **1.47**

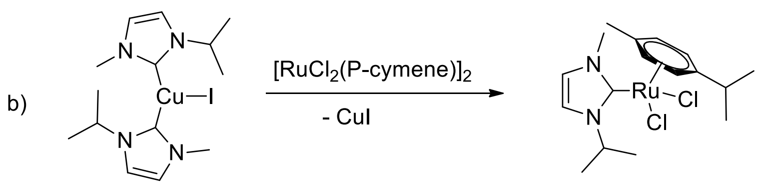

1.43 **1.48**

Scheme 1.16. Synthesis of NHC transition metal complexes via transmetalation reaction.

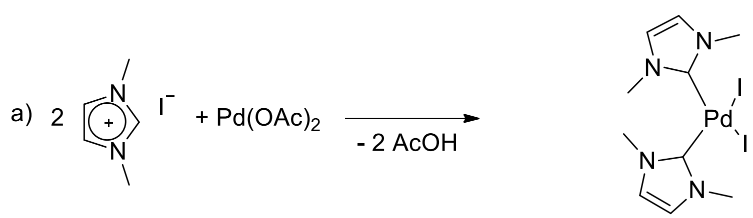

1.49

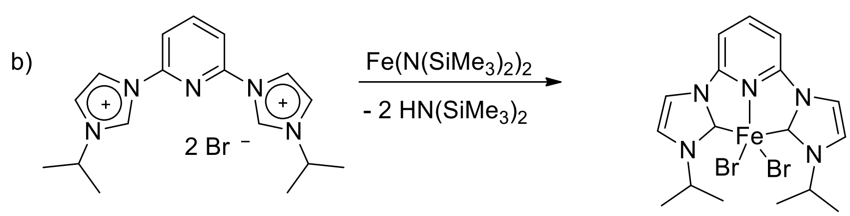

1.50

Scheme 1.17. Synthesis of NHC transition metal complexes via reaction of an imidazolium salt with a basic metal precursor.

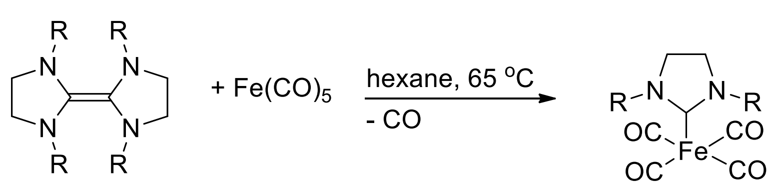

1.51

Scheme 1.18. Synthesis of NHC transition metal complexes via thermolysis of tetraaminoethylene.

1.2.1.4 NHC transition metal complexes as polymerization catalysts

NHC transition metal complexes are extensively implemented in catalytic transformations.[30,48,64] However, their use in oligomerization and polymerization of alkenes has been much less explored.[65] The use of NHC transition metal complexes in olefin polymerization was introduced in 1998.[66] As mentioned above, the early- to middle-transition metal complexes of the bis(NHC)pyridine (**1.4**) were tested for oligomerization/polymerization of ethylene. Although less active than bis(arylimino)pyridine complexes of Cr(III), Fe(II) and Co(II), some of the bis(NHC)pyridine complexes are excellent catalysts for the oligomerization of ethylene, with the highest performance realized for the chromium complex of the ligand bearing the 2,6-diisopropylphenyl group (40,000 kg mol^{-1} of Cr h^{-1} bar^{-1}).[23a-e] A lower activity of 70 kg mol^{-1} of Cr h^{-1} bar^{-1} was observed for the related chromium complex with the ligand containing adamantyl substituents. A decreased activity was observed after 30 min of reaction time and the catalysts were rapidly deactivated above 50 °C. However, the corresponding iron and cobalt 2,6-bis(NHC) complexes (**1.4**) were inactive.[23a-e] In other work, very low activities (> 2 kg mol^{-1} of M bar^{-1} h^{-1}) for the substituted imino(NHC) complexes of Cr(III) and Co(II) (**1.52**) were reported, whereas the related Fe(II) complex (**1.52**) was inactive upon activation with MAO.[67]

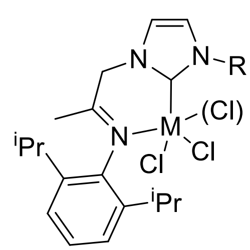

R = 2,4,6-$Me_3C_6H_2$, $iPr_2C_6H_3$, Me
M = Cr, Fe, Co

1.52

1.3 Research objectives

This research was dedicated to synthesize, isolate and characterize three new classes of bis(imino)-NHC ligands (**1.55**, **1.56** and **1.57**) and their corresponding transition metal complexes by replacing the pyridine moiety in the 2,6-bis(imino)pyridine ligand (**1.53**)[15-16] with an NHC fragment. Incorporation of an NHC ligand into transition metal complexes facilitates electronics and sterics tuning and improves their thermal stability.[26,30,64,68] Although bis(imino)pyridine complexes of iron(II) and cobalt(II) are highly active catalysts for ethylene polymerization, the rate of either homopolymerize or copolymerize α-olefins is stall very low.[16c,21l,24,69] The 5-membered bis(imino) NHC ligands (**1.55** and **1.56**) offer a more opened coordination environment than the analogous 6-membered 2,6-bis(imino)pyridine ligand (**1.53**), in which bulky substrates such as α-olefins may easily be coordinated to the metal center. The imine fragments enhance the π-accepting ability of the ligand and therefore a more electropositive metal center in predicted, in contrast to the 2,6-bis(NHC) pyridine ligand (**1.54**).[23a-c] The imino substituents play a significant role in the electronic properties, stability, coordination mode, and catalytic activities of the resulting complexes. Also, these potential bis(imino)-NHC ligands can coordinate in mono-, bi-, or tridentate fashion through the carbene carbon and one or both iminic fragments. The corresponding bis(imino)-NHC complexes of Cr(III), Fe(II) and Co(II) were also synthesized, characterized and their catalytic activities were evaluated in polymerization of ethylene to establish the structure-property relationships.

The synthesis of bis(imino) imidazol-2-ylidene ligands (**1.55**) and their corresponding complexes of Cr(III), Fe(II) and Co(II) will be presented in Chapter 2. The iminic substituents were changed to tune their electronic properties. The modification of ligands by replacing imidazol-2-ylidene with benzimidazol-2-ylidene ligand (**1.56**) to reduce σ-electron donation of the NHC fragment will be covered in Chapter 3. In addition, the corresponding benzimidazol-2-ylidene complexes of Cr(III), Fe(II) and Co(II) were synthesized and the effect of introducing the benzimidazol-2-ylidene moiety were studied in ethylene polymerization. The research was further extended by replacing the 5-membered NHC ring with the 6-membered (bis(imino)pyrimidin-2-ylidene) (**1.57**) to allow the new ligand to coordinate in a tridentate mode (Chapter 4). DFT calculations were carried out to shed light on the electronic properties of these three new bis(imino)-NHC ligands (Chapter 5). The highest occupied molecular orbital (HOMO) and the lowest unoccupied molecular orbital (LUMO) and the electron density mapping for the ligands and their related complexes were also studied.

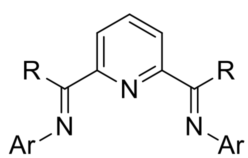

1.53

Brookhart/Gibson

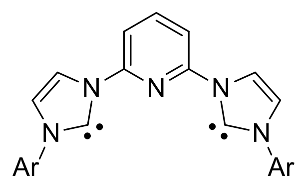

1.54

Danopoulos/Gibson

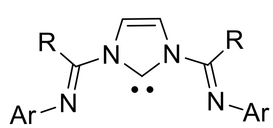

1.55

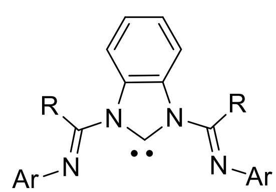

1.56

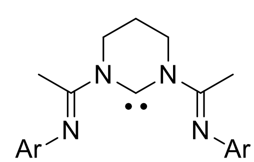

1.57

This work

Chapter Two

Synthesis, Characterization and Reactivity Study of Bis(imino)imidazol-2-ylidene Transition Metal Complexes

1st Generation

The potential of utilizing late transition metal catalysts that can polymerize α-olefins was enhanced by the outstanding activity and functional group tolerance of Ni- and Pd-(α-diimine) catalytic systems.[7,12a,15] This has led to the synthesis of the exceptional active iron(II) and cobalt(II) complexes of 2,6-bis(arylimino)pyridine[15-16] for ethylene polymerization. The modifications of the ligand structure alter the electronic and steric properties of the corresponding catalysts and thus structure–property relationships have been established.[16c,16e,18,70] The iron(II) and cobalt(II) complexes of 2,6-bis(arylimino)pyridine exhibited extraordinary activities in ethylene polymerization, however short lifetimes were observed at elevated temperatures.[16c,16d,69b,71] Although the low thermal stability of these complexes has been improved by modifying the ligand substitutions,[19,72] the homopolymerization or copolymerization rates of α-olefins are still low.[16c,21l,24,69]

Inspired by those results and the improved thermal stability of transition metal complexes bearing NHC,[26,30,68] we targeted the modification of the ligand framework by replacing the pyridine moiety with an NHC fragment. The five-membered imidazol-2-ylidene ligand affords a more opened coordination environment than that of the related six-membered pyridine ring of 2,6-bis(arylimino)pyridine[15-16] and 2,6-bis(NHC) pyridine,[23a-c,23e] and may hence ease the coordination of α-olefins. Moreover, the electropositive nature of the corresponding transition metal complexes are enhanced by the π-accepting capability of imine fragments and therefore may be more active than the related complexes of 2,6-bis(NHC) pyridine.[23a-c,23e]

Herein, a series of related imidazolium salts with chloride, iodide and tetrafluoroborate counter anions were prepared using different synthetic methodologies dictated by the iminic carbon substituents.[73] Both the iminic substituents and the counter ion play a significant role in the stability and reactivity of the resulting salts and the corresponding transition metal complexes.

The related imidazol-2-ylidene transition metal complexes were successfully synthesized by *in situ* deprotonation of the parent imidazolium salt or by transmetalation reaction of the corresponding silver or copper complexes.[73] The catalytic activities of imidazole-2-ylidene complexes of chromium, iron and cobalt toward ethylene polymerization at standard temperature and pressure with methylaluminoxane (MAO) as an activator were evaluated.

2.1 Synthesis of 1,3-bis(imino)ethyl/benzyl imidazolium salts

Related 1-iminoimidazole compounds **2.4**, **2.5** and **2.6** were prepared by reacting imidazole with the corresponding *N*-imidoyl chloride **2.1**, **2.2** and **2.3**, respectively, in excellent yields (Scheme 2.1).

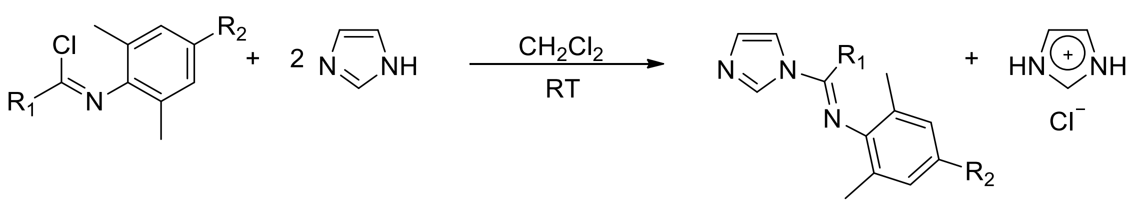

R_1= Me, R_2= H **2.1**
R_1= Ph, R_2= Me **2.2**
R_1= ^tBu, R_2= H **2.3**

R_1= Me, R_2= H **2.4**
R_1= Ph, R_2= Me **2.5**
R_1= ^tBu, R_2= H **2.6**

Scheme 2.1. Synthesis of 1-iminoimidazole **2.4**, **2.5** and **2.6**.

The 1,3-bis[1-(2,6-dimethylphenylimino)ethyl]imidazolium chloride (**2.7**) was synthesized by the reaction of 1-iminoethylimidazole (**2.4**) with *N*-(2,6-

dimethylphenyl)acetimidoyl chloride (**2.1**) in toluene (93% yield). The ^{1}H NMR ($CDCl_3$) spectrum of **2.7** displayed a characteristic downfield resonance for the imidazolium proton (-NC*H*N-) at δ 12.54, while the two equivalent protons on the backbone (-NC*H*C*H*N-) were observed at δ 8.39. 1D NOE NMR experiments revealed that the imine substituents in compound **2.7** adopted an *E*-conformation in solution.

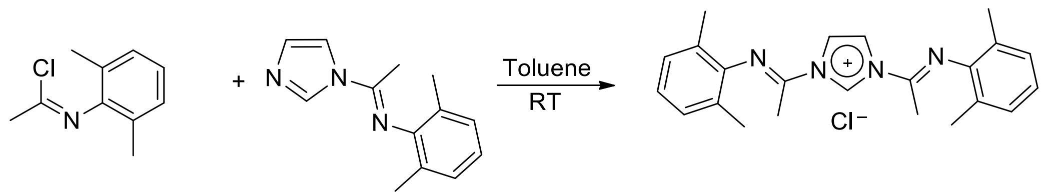

2.1 **2.4** **2.7**

Scheme 2.2. Synthetic route toward **2.7**.

X-ray-quality crystals were obtained by slow diffusion of pentane into a saturated acetonitrile solution at –40 °C. The molecule crystallized in the $P\bar{1}$ space group, and the solid-state molecular structure further confirmed the *E*-conformation for compound **2.7** (Figure 2.1). The N1–C1 (1.339(3) Å) and N2–C1 (1.335(3) Å) bond lengths are similar and they are shorter than N1–C2 (1.389(3) Å) and N2–C3 (1.392(3) Å), due to delocalization of electrons between the N1–C1–N2 atoms. The imine bonds N3–C4 (1.261(3) Å) and N4–C6 (1.258(3) Å) are within the range of N–C double bond length. The imine substituents and the imidazolium ring are in different planes, as revealed by the N3–C4–N1–C1 and N4–C6–N2–C1 torsion angles of 169.75º and 177.18º, respectively. As predicted, a single FTIR C=N stretching frequency was observed at 1698 cm^{-1} for **2.7**.

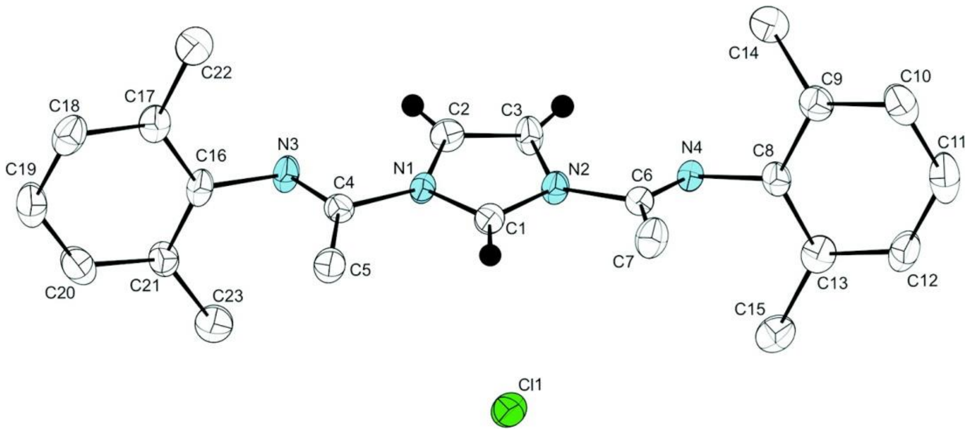

Figure 2.1. ORTEP of **2.7** (50% probability level). Hydrogen atoms are omitted for clarity. Selected bond lengths (Å) and angles (deg.): N1–C1 1.339(3), N2–C1 1.335(3), N1–C2 1.389(3), N2–C3 1.392(3), C2–C3 1.338(4), N3–C4 1.261(3), N4–C6 1.258(3), N1–C1–N2 107.3(2), C1–N1–C4 124.7(2), C1–N2–C6 126.5(2), N2–C6–N4 114.2(2), N3–C4–N1 114.9(2).

The synthesis of the analogous 1,3-bis[(2,6-dimethylphenylimino)neopentyl] imidazolium chloride salt was attempted by reacting *N*-(2,6-dimethylphenyl)pivalimidoyl chloride (**2.3**) with 1-(2,6-dimethylphenyl-imino)neopentylimidazole (**2.6**), however the steric bulk of the *tert*-butyl group may hinder nucleophilic attack on the iminic carbon. The reaction of *N*-(2,4,6-trimethylphenyl)phenyl imidoyl chloride (**2.2**) with the 1-(2,4,6-trimethylphenylimino)benzyl imidazole (**2.5**) was unsuccessful probably due to nucleophilic attack on iminic carbons substituted with phenyl groups by a chloride anion. Surprisingly, attempts to generate the unsymmetrical 1,3-disubstituted imidazolium salts **2.8** and **2.9** by reacting *N*-(2,6-dimethylphenyl)acetimidoyl chloride with mono-substituted imidazole (**2.6**) or (**2.5**) afforded the symmetrical imidazolium salt **2.7** as an off-white precipitate (Scheme 2.3). The proposed reaction mechanism for yielding the compound **2.7** (instead of **2.8** and **2.9**) is presented in Scheme 2.4.

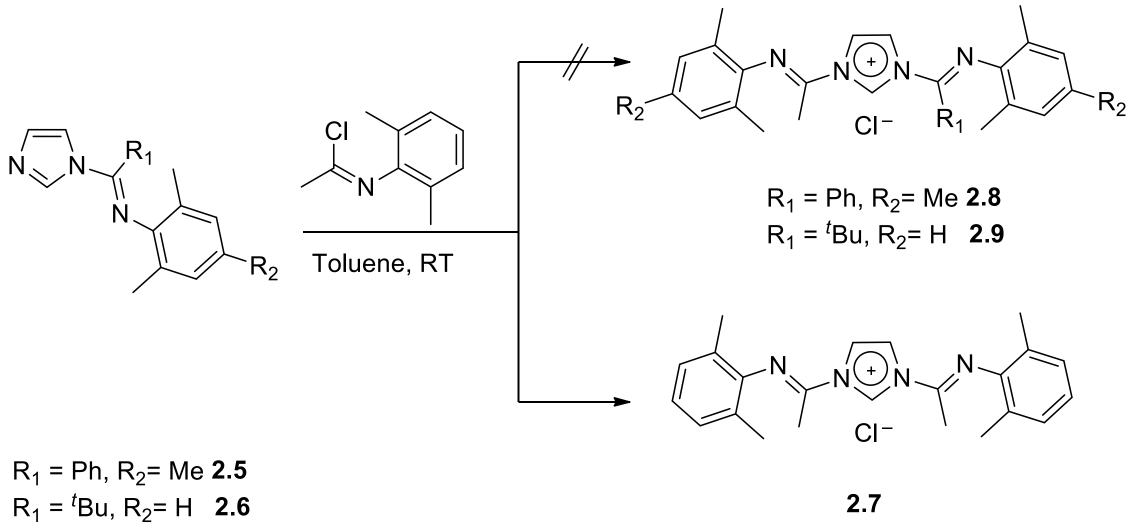

Scheme 2.3. Attempted synthesis of unsymmetrical imidazolium salts **2.8** and **2.9**.

The reaction of *N*-imidoyl chloride (**2.3**) with $NaBF_4$ to *in situ* generate the related nitrilium salt and the subsequent addition of 1-(2,6-dimethylphenylimino) neopentylimidazole (**2.6**) was unsuccessful**.** The analogous 1,3-bis[(2,4,6-trimethylphenylimino)benzyl]imidazolium tetrafluoroborate salt **2.10** was however synthesized, in 96% yield, by the reaction of the *in situ* generated nitrilium salt with mono-substituted imidazole (**2.5**) (Scheme 2.5). This modified procedure utilizes the more active nitrilium salt with a non-coordinating tetrafluoroborate anion. The imidazolium proton (-NC*H*N-) and the two equivalent backbone protons (-NC*H*C*H*N-) appeared at δ 9.22 and 7.90, as shown in ^{1}H NMR spectrum of **2.10**, respectively. The imine (*C*=N) and the backbone carbon (-N*C*H*C*HN-) atoms resonated at δ 148.2 and 120.9 in $^{13}C\{^1H\}$ spectrum, respectively.

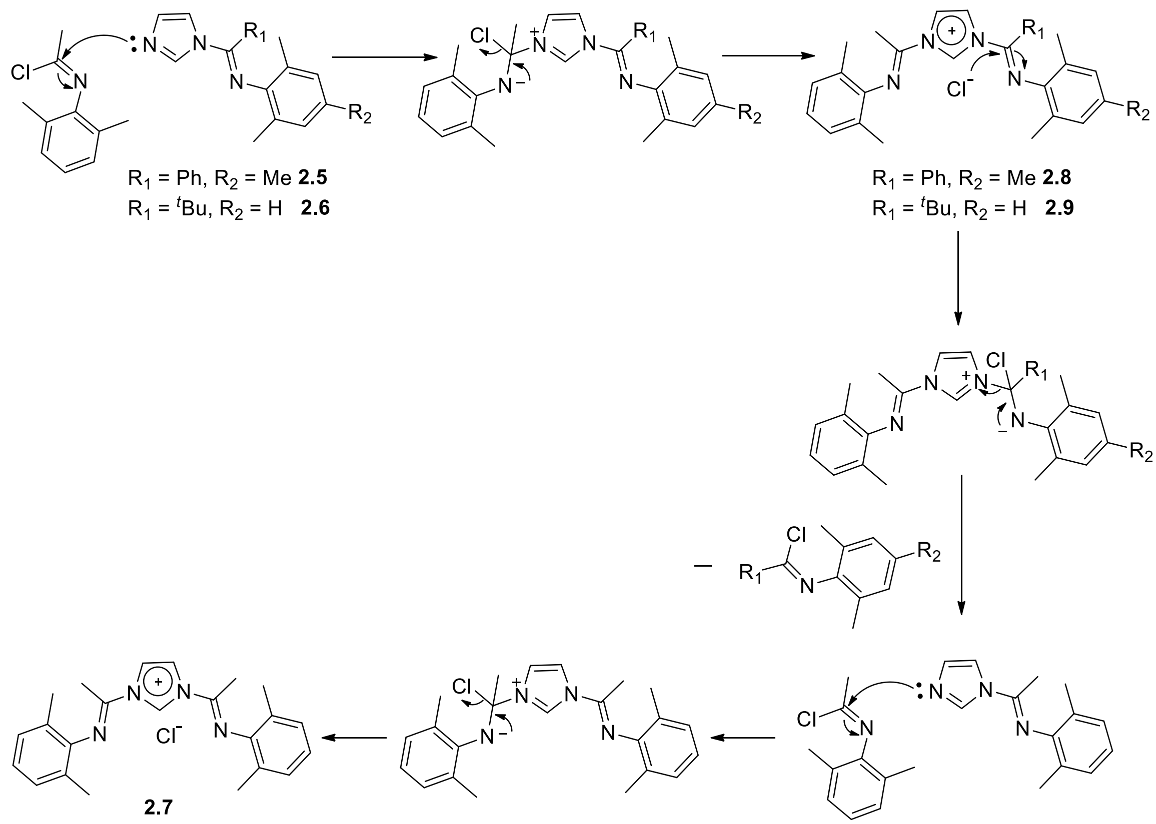

Scheme 2.4. Proposed reaction mechanism for the formation of **2.7**.

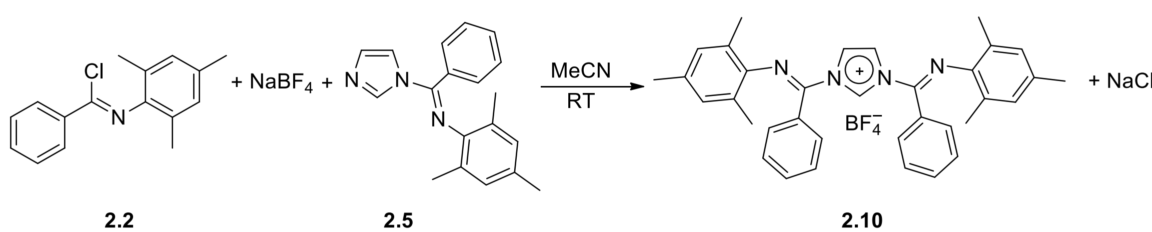

Scheme 2.5. Synthesis of the imidazolium salt **2.10**.

Suitable crystals for an X-ray diffraction study for **2.10** were obtained by slow vapor diffusion of pentane into a saturated dichloromethane solution at room temperature. The molecular structure of this compound is displayed in Figure 2.2 along with selected bond lengths and angles. The molecule crystallized in the $P2_1/m$ space group with both iminic groups adopting the *E*-conformation and only one-half of the molecular structure for **2.10** was in the asymmetric unit with a crystallographic mirror plane orthogonal to the imidazolium ring. The length of iminic double bond N2–C3 (1.273(3) Å) is comparable to that observed in **2.7**. As predicted, a single FTIR C=N stretching vibrational frequency was observed at 1676 cm^{-1}.

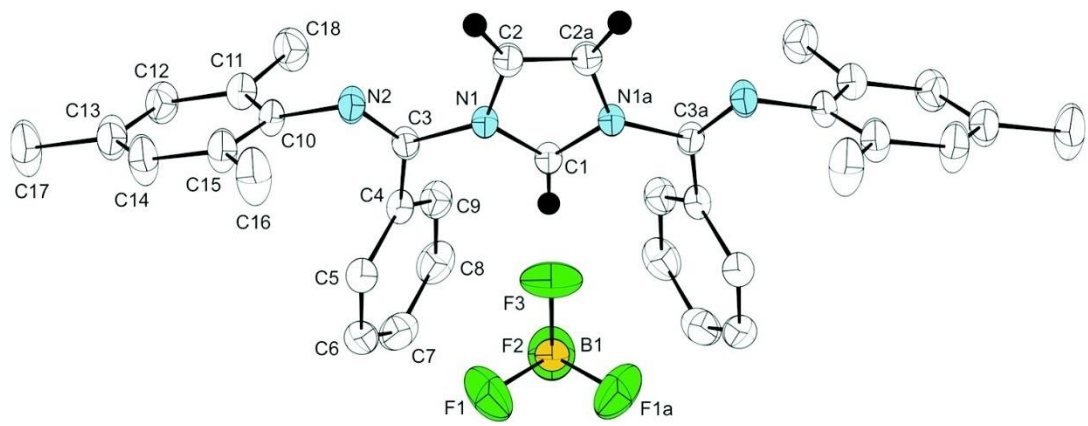

Figure 2.2. ORTEP of **2.10** (50% probability level). Hydrogen atoms are omitted for clarity. Selected bond lengths (Å) and angles (deg.): N1–C1 1.333(2), N1–C2 1.399(3), C2–C2a 1.348(4), N1–C3 1.446(2), N2–C3 1.273(3), N1–C1–N1a 108.9(3), C1–N1–C3 124.30(19), N1–C3–N2 115.43(19).

To obtain a better understanding of the formation of compound **2.7** rather than the unsymmetrical salts **2.8** and **2.9**, the stability of salt **2.10** was investigated. The addition of a chloride source ($^{n}Bu_4NCl$) to **2.10** led to decomposition of the salt to its starting materials (mono-substituted imidazole (**2.5**) and *N*-(2,4,6-trimethylphenyl)benzimidoyl chloride (**2.2**)) (Scheme 2.6). This demonstrates the ease of the N–C_{imino} bond cleavage and supports the inability of forming **2.8**, because the chloride anion attacks the iminic carbon. Similarly, N–C_{imino} bond cleavage was recently reported for the related 1,3-bis[1-(2,6-diisopropylphenylimino)ethyl]imidazolium chloride in either THF at room temperature or in toluene at elevated temperature, while the analogous salt with BF_4^- anion was stable due to the non-nucleophilic nature of this anion.[74]

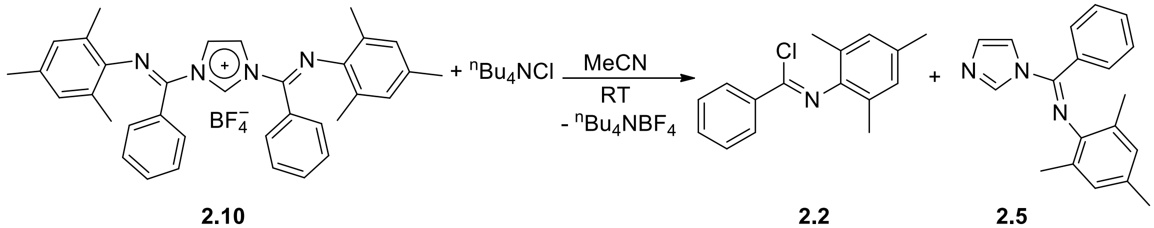

Scheme 2.6. Decomposition of **2.10** in the presence of $^{n}Bu_4NCl$.

The 1,3-bis[(2,4,6-trimethylphenylimino)benzyl]imidazolium iodide derivative **2.11** was synthesized (94% yield) by a similar route, in which NaI was used instead of $NaBF_4$. Alternatively, **2.11** could also be prepared by an ion exchange of compound **2.10** with NaI (Scheme 2.7). The ability of synthesise of **2.11** with iodide as counter anion and unsuccessful affording of **2.8** with chloride counter anion demonstrate that iodide is a poor nucleophile compared to chloride anion. Similar to **2.10**, the FTIR stretching frequency was observed at $\nu_{C=N}$ 1676 cm^{-1} for **2.11**.

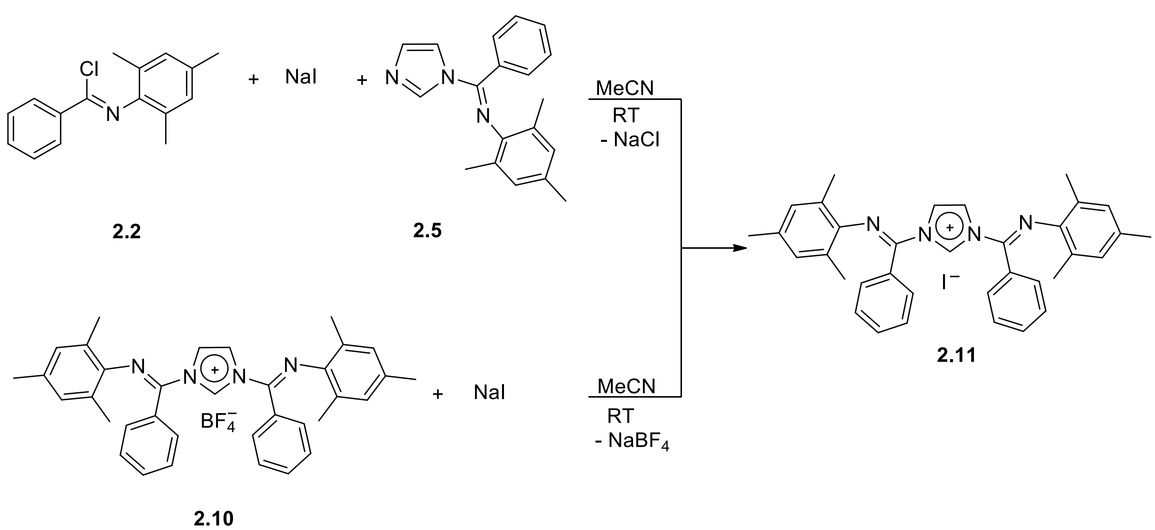

Scheme 2.7. Synthetic route toward **2.11**.

2.2 Attempts to isolate the free carbene

Efforts to generate the corresponding free NHC by using a range of bases were unsuccessful even at –78 °C. This can be attributed to either the decomposition of the imidazolium salts, or the high reactivity of the assumed carbene. One possible decomposition pathway is the 1,2-rearrangement of the azole ring substituents to the central carbene carbon.[75] Similarly, intramolecular rearrangements of substituents in the synthesis of the unsymmetrical tridentate dianionic NHCs were reported.[76]

The proposed decomposition pathways for imidazolium salts **2.7** and **2.10** are presented in Scheme 2.8. The reaction of bulky bases such as lithium mesityl and lithium 2,2,6,6-tetramethylpiperidide at –78 °C with **2.10** resulted in the deprotonation of the salt as evidenced by the disappearance of the most downfield central imidazolium proton resonance at δ 9.22 in the ^{1}H NMR spectrum. Unfortunately, the assumed carbene readily decomposed and could not be isolated.

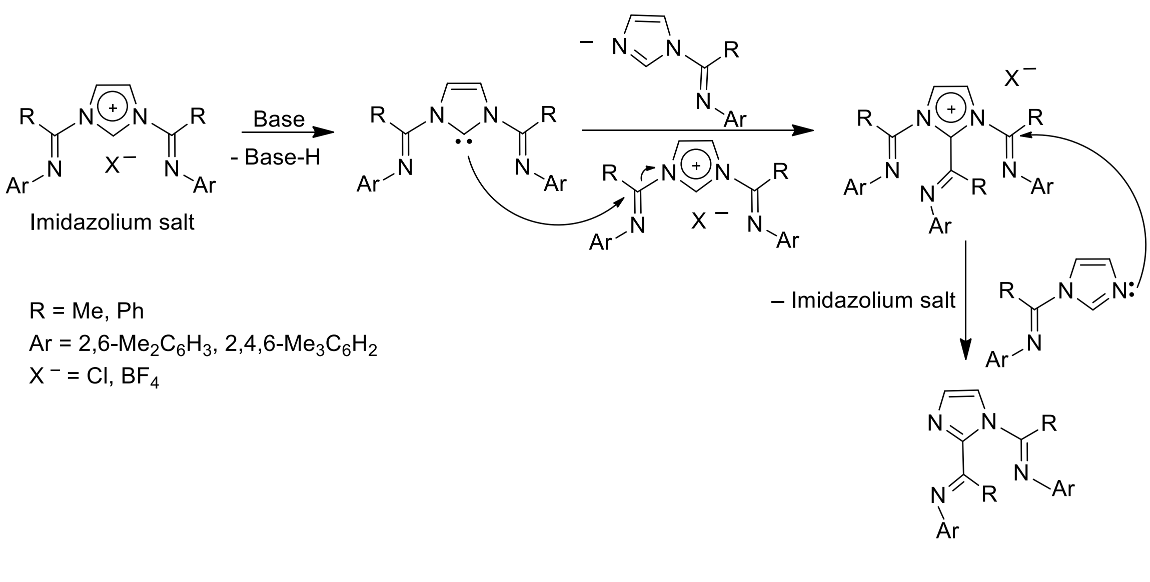

Scheme 2.8. Possible decomposition pathways for the imidazolium salts **2.7** and **2.10**.

The isolation of the related 1,3-bis[1-(2,6-diisopropylphenylimino)ethyl]imidazol-2-ylidene was just recently reported.[74] The deprotonation was performed at –78 °C in pentane for 12 h and the isolated carbene was only stable for 1 h in solution at room temperature.[74]

2.3 Synthesis of transition metal NHC complexes

Many experiments were attempted to synthesize the corresponding transition metal carbene complexes by reacting metal precursors with *in situ* deprotonated imidazolium salts, however the expected products could not be isolated. For instance, the synthesis of the related Y(III) and Zr(IV) complexes were attempted due to the diamagnetic nature of these complexes in which NMR spectroscopy can easily be used to investigate the reaction outcomes and establish a synthetic methodology. Therefore, this methodology can be extended to the related paramagnetic Cr(III), Fe(II) and Co(II) complexes. The reaction of **2.10** with NaH in C_6D_6 generated bubbles, assumed to be H_2, as indication of the deprotonation of the salt. Subsequent addition of $YCl_3{\cdot}3THF$ to the resulting mixture failed to afford the expected product, however a mixture of other compounds including benzimidoyl chloride (**2.2**) were produced. The reaction of the salt **2.10** with NaH and $ZrCl_4{\cdot}2THF$ gave similar results. This shows the ability of a chloride anion to attack the iminic carbon and lead to N–C_{imino} bond cleavage, as discussed above in section 2.1.

Despite all attempts to initially deprotonate and coordinate the ligand to a transition metal, the targeted complexes could not be isolated. Since the imidazolium salts were unstable in the presence of external bases, the use of a basic metal precursor as an alternative route toward the synthesis of the desired complexes of NHC was investigated. Initially, $Zr(NMe_2)_4$ was utilized under several reaction conditions to deprotonate compound **2.10** and coordinate to Zr. However, a mixture of compounds that could not be separated was formed. Unidentified compounds were also observed from the reaction of $KN(SiMe_3)_2$ with $[(coe)_2RhCl]_2$, at –37 °C and subsequent addition of **2.10**. A THF solution of $NaN(SiMe_3)_2$ was added to a suspension of $Pd(CNMe)_2Cl_2$, $Pd(COD)Cl_2$ or $YCl_3{\cdot}3THF$ at –37 °C in THF. The mixture was then filtrated and the filtrate was added to a suspension of salt **2.10** in THF. However, the corresponding benzimidoyl chloride (**2.2**) and an unknown mixture of other compounds were produced.

2.3.1 Bis(imino)imidazol-2-ylidene silver(I) complexes

Since the isolation of the free carbene was unsuccessful, silver carbene complexes can be used as transmetalating agents to afford the desired transition metal carbene complexes.[61,77] The imidazolium salts **2.7** or **2.10** were reacted with Ag_2O or Ag_2CO_3 in the presence of molecular sieves, however the corresponding anilides were observed, as a result of the ineffective removal of the water byproduct. A suitable procedure was then adopted to use a basic metal precursor that can be utilized in the synthesis of the desired NHC complexes. The *in situ* reaction of $NaN(SiMe_3)_2$ with $AgBF_4$ generated the silver amide ($AgN(SiMe_3)_2$) in toluene. A similar reaction was reported using $KN(SiMe_3)_2$ and AgOTf in lieu of $NaN(SiMe_3)_2$ and $AgBF_4$, respectively.[78] This synthetic procedure is much more convenient than the reported method.[79] The silver complex ($[C_{imi}({}^{\wedge}Imine_{Me})_2]AgCl$) **2.12** was synthesized in 67% yield by the addition of the filtrate containing the silver amide to a toluene suspension of **2.7** at low temperature (Scheme 2.9).[73b] The silver carbene complex (**2.12**) is a diamagnetic species that allows the using

NMR spectroscopy to explore the chemistry of the new class of the bis(imino) NHC transition metal complexes.

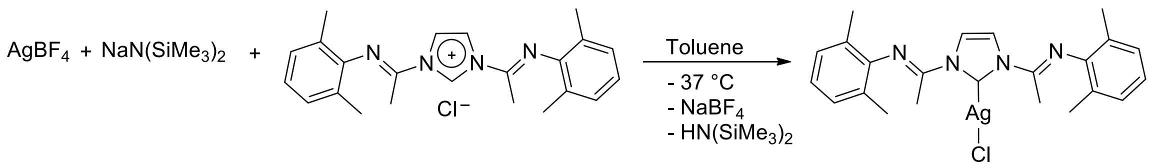

2.7 **2.12**

Scheme 2.9. Synthesis of silver(I) NHC complex **2.12**.

Upon coordination of the carbene to the silver, the ^{1}H NMR ($CDCl_3$) spectrum of **2.12** showed the disappearance of the most downfield resonance of the central imidazolium proton observed for the parent salt **2.7**. The protons for the azole ring (−NC*H*C*H*N−) resonated at δ 8.08, upfield with respect to that of the salt **2.7**. The ^{13}C resonance of the carbene central carbon was not observed due to the labile character of the silver-carbene bond,[61,80] long relaxation time of the carbene and low solubility. A monodentate coordination mode of the ligand through the carbene center is expected based on a single IR stretching frequency for the C=N bond at 1684 cm^{-1} for **2.12**.

Unfortunately, the reaction of $NaN(SiMe_3)_2$ with $AgBF_4$ and then with the salt **2.10** at –37 °C did not afford the desired silver NHC complex (**2.13**). On the other hand, the use of the analogous iodide imidazolium salt **2.11** generated the Ag(I) NHC complex **2.14** (Scheme 2.10). This can be attributed to the ability of a coordinated iodide anion to stabilize the desired silver complex. This procedure provides an additional route to prepare Ag(I) NHC complexes otherwise inaccessible using conventional approaches.

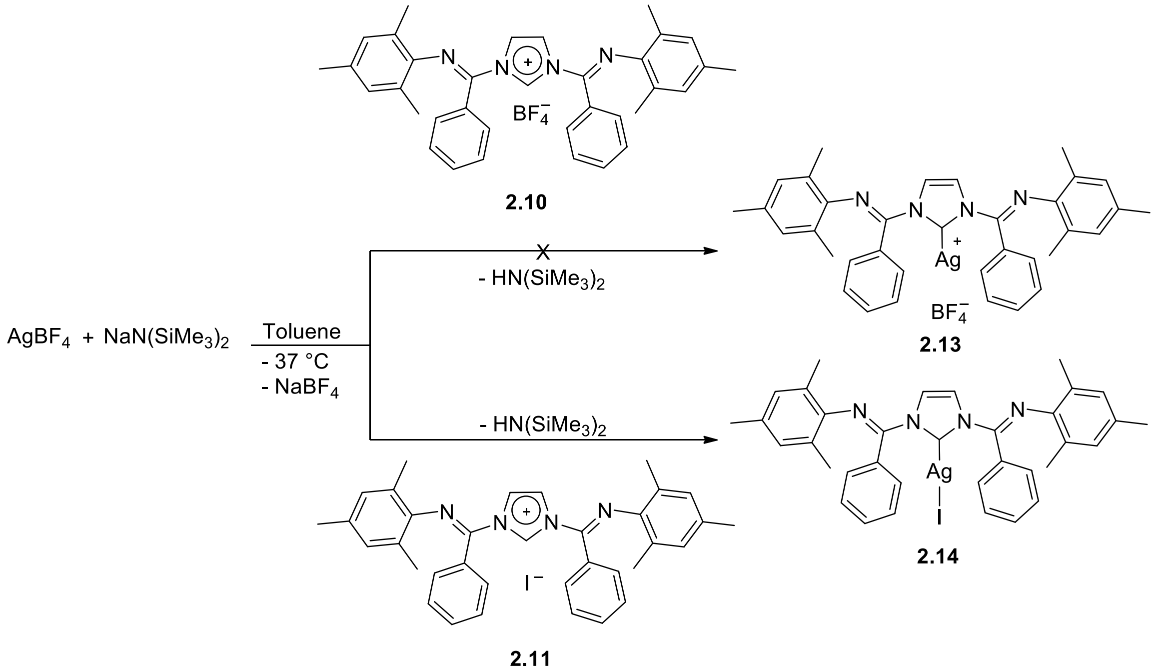

Scheme 2.10. Synthesis of the NHC silver(I) complex **2.14**.

2.3.2 Bis(imino)imidazol-2-ylidene copper(I) complexes

Recently, copper carbene complexes have been reported as transmetalating agents to late transition metals complexes and as an alternative of the commonly used silver carbene complexes.[59,81] Moreover, the NMR spectroscopy of the copper carbene complexes sheds light on the chemistry of other related paramagnetic complexes. The corresponding copper carbene complexes ([C_{imi}(^$Imine_{Me}$)$_2$]CuI) **2.15** and ([C_{imi}(^$Imine_{Ph}$)$_2$]CuI) **2.16** were successfully isolated in 77% and 61% yield, respectively [73a] (Scheme 2.11) by the reaction of *in situ* generated $CuN(SiMe_3)_2$ with the imidazolium salts **2.7** or **2.10**.

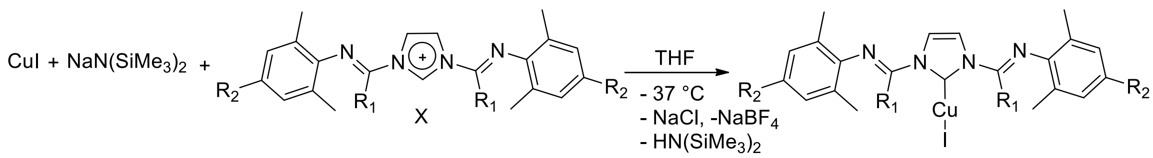

Scheme 2.11. Synthetic route to the NHC copper complexes **2.15** and **2.16**.

The proton resonances of the central carbon at δ 12.54 and 9.22 for **2.7** and **2.10**, respectively, were disappeared, as shown in ^{1}H NMR spectra for both NHC Cu(I) complexes **2.15** and **2.16.** The backbone protons moved upfield to δ 7.85 for the complex **2.15** with respect to that of the corresponding protons of the salt **2.7** (δ 8.39). In contrast, only a small change in chemical shift from δ 7.90 to 8.01 was observed for the backbone protons upon formation of **2.16**. The IR C=N vibrational stretching frequencies were observed at 1676 and 1653 cm^{-1} in **2.15** and **2.16**, respectively.

Crystals of complexes **2.15** and **2.16** suitable for X-ray diffraction studies were grown by slow vapor diffusion of pentane into a concentrated dichloromethane and THF solution, respectively, at room temperature. The molecule crystallized in the $P\bar{1}$ space group and adopted a distorted tetrahedral geometry at the metal center, as bimetallic structure for **2.15** with two bridging iodide ligands (Figure 2.3). The carbene ligand chelates to the metal center in a bidentate fashion with the carbene carbon and one iminic N atom. This is in contrast to the symmetric structure suggested from the ^{1}H and ^{13}C NMR spectra in solution.

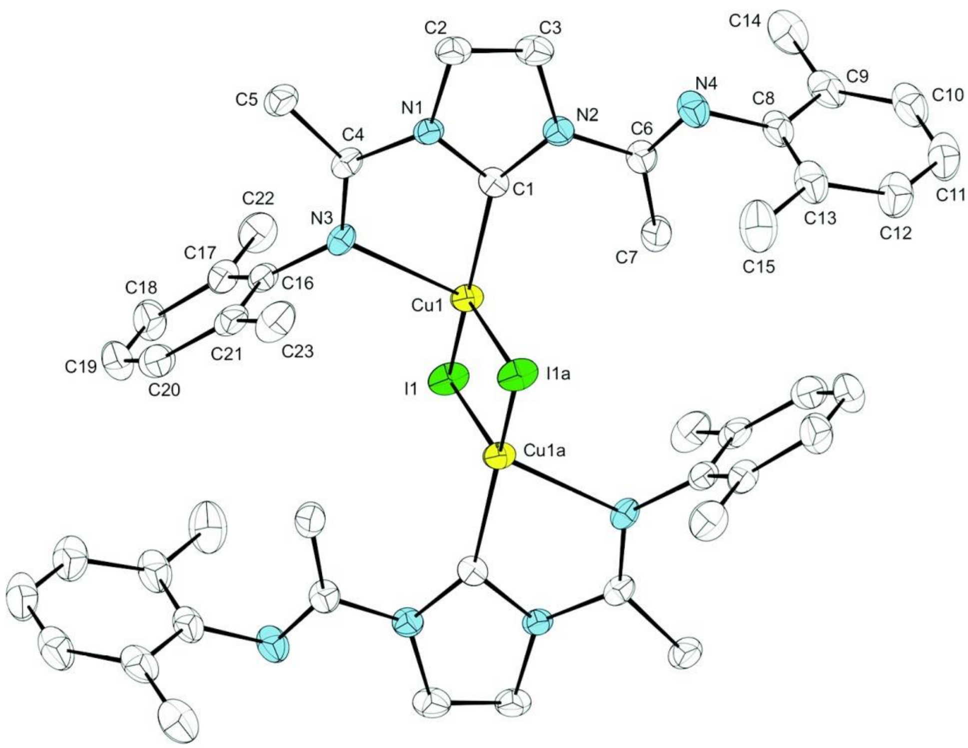

Figure 2.3. ORTEP of **2.15** (50% probability level). Hydrogen atoms and solvent molecule are omitted for clarity. Selected bond lengths (Å) and angles (deg.): Cu1–C1 1.945(4), Cu1–N3 2.292(3), Cu1–I1 2.6357(6), Cu1–I1a 2.5838(6), N1–C1 1.374(5), N1–C2 1.398(5), N1–C4 1.435(5), N2–C1 1.362(5), N2–C3 1.404(5), N2–C6 1.430(6), C2–C3 1.333(7), N3–C4 1.257(5), N4–C6 1.263(6), N3–Cu1–C1 77.86(15), N1–C1–N2 102.7(3), Cu1–C1–N1 115.3(3), C1–N1–C4 120.1(3), N1–C4–N3 115.6(4), Cu1–N3–C4 110.5(3), Cu1–C1–N2 141.3(3), C1–N2–C6 123.8(4), N2–C6–N4 115.1(4).

The Cu–Cu bond length in **2.15** (2.63657(10) Å) is shorter than that of the published data for the bimetallic NHC copper(I) bromide complex (2.707 Å).[82] The Cu1–C1 bond length of 1.945(4) Å is comparable to that of the reported value for the dimer Cu(I)Br NHC complex (1.905(4) Å).[82a] The Cu1–N3 bond length is 2.292(3) Å and it is smaller than the reported value for the 2-pyridyl-substituted NHC Cu(I)Br monomer complex by 0.1625 Å.[82b] The iminic bond lengths N3–C4 (1.257(5) Å) and N4–C6 (1.263(6) Å) are comparable to each other.

The angle between the 2,6-dimethylphenyl ring on N3 and the main plane of bidentate metalocycle is 6.08º with a C1–Cu1–N3 bite angle of 77.86(15)º. The short bond length of C1–N1 (1.374(5) Å) was observed compared to N1–C2 (1.398(5) Å) and N2–C3 (1.404(5) Å). The σ-bond character of the carbene center increased, as revealed by decrease of the bond angle of N1–C1–N2 (102.7(3)º) compared to that of the ligand precursor **2.7**.

An ORTEP view of **2.16** is depicted in Figure 2.4 along with selected bond lengths and angles. The molecule crystallized in the $P\bar{1}$ space group and the NHC ligand coordinated to the metal center in a monodentate manner forming a linear structure. The bond distances of Cu1–C1 (1.901(5) Å) and Cu1–I1 (2.3969(8) Å) are close to the published data of Cu–carbene (1.905(4) Å) and Cu–Br (2.4475(7) Å), respectively, for the dimer NHC Cu(I)Br complex.[82a] The smaller bond angle of N1–C1–N2 (103.4(4)º) and the longer bond lengths of N1–C1 (1.353(7) Å) and N2–C1 (1.375(7) Å) in the complex **2.16** than the corresponding bond angle of N1–C1–N1a (108.9(3)º and bond length of N1–C1(1.333(2) Å in the parent salt **2.10**, respectively, evidenced the increased σ-bond character of the carbene center. The double bond lengths, N3–C4 (1.269(7) Å) and N4–C11 (1.271(7) Å), are comparable to the related N2–C3 (1.273(3) Å) in the salt **2.10**, suggesting the absence of coordination of the iminic nitrogen atoms to the metal.

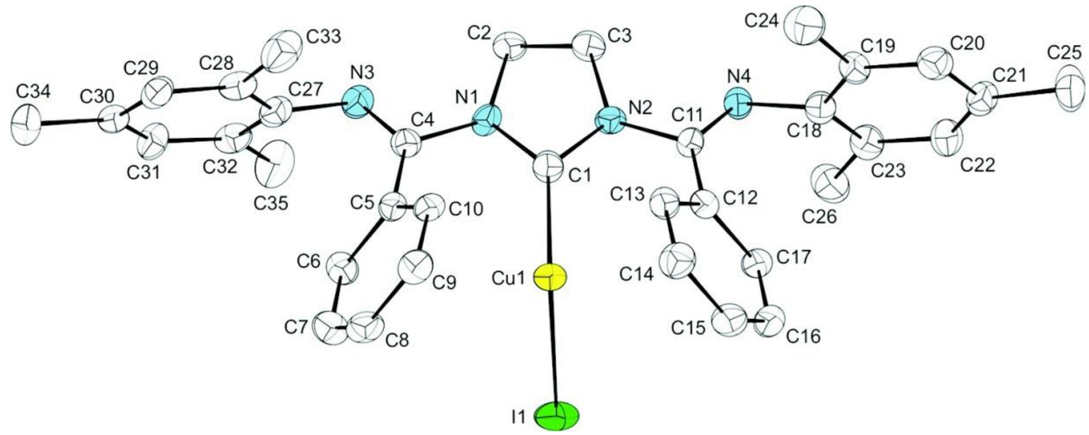

Figure 2.4. ORTEP of **2.16** (50% probability level). Hydrogen atoms are omitted for clarity. Selected bond lengths (Å) and angles (deg.): Cu1–C1 1.901(5), Cu1–I1 2.3969(8), N1–C1 1.353(7), N1–C2 1.407(7), N1–C4 1.445(7), N2–C1 1.357(7), N2–C3 1.396(7), N2–C11 1.435(7), C2–C3 1.343(8), N3–C4 1.269(7), N4–C11 1.271(7), C1–Cu1–I1 169.35(17), N1–C1–N2 103.4(4), N1–C1–Cu1 129.0(4), N2–C1–Cu1 126.3(4), C1–N1–C4 124.5(5), C1–N2–C11 125.0(5).

2.3.3 Bis(imino)imidazol-2-ylidene iron(II) complex

The iron(II) complex of bis(imino)imidazol-2-ylidene was synthesized to evaluate its performance toward ethylene polymerization. Transmetalating reactions of both NHC silver (**2.12**) and NHC copper (**2.15** or **2.16**) complexes to the related Fe(II) generated a mixture of products that could not be identified. Alternatively, the desired iron complex ([C_{imi}(^$Imine_{Me}$)$_2$]$FeCl_2$) **2.17** was afforded in good yield (84%) by the addition of a THF solution of $KN(SiMe_3)_2$ to a THF suspension of $FeCl_2$ at –37 ºC. The filtrate was then added to a THF suspended solution of the salt **2.7** at low temperature (Scheme 2.12).[73b] The magnetic susceptibility for **2.17** was 5.54 μB, as determined by the Evans method,[83] consistent with four unpaired electrons.

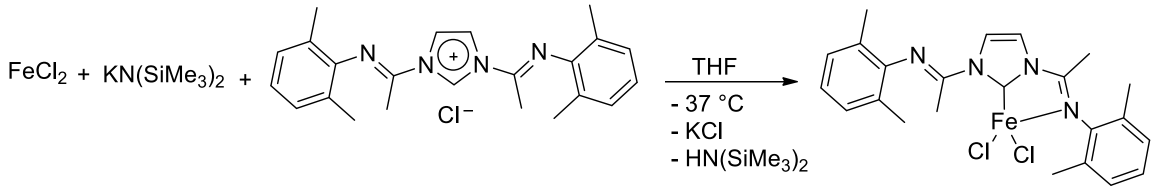

Scheme 2.12. Synthesis of the NHC iron(II) complex 2.17.

The slow diffusion of pentane into the concentrated dichloromethane solution of the complex **2.17** at –40 ºC afforded crystals suitable for an X-ray diffraction study. The molecule adopted a distorted tetrahedral geometry around the Fe center and crystallized in the $P2_1/C$ space group (Figure 2.5). The bite angle (N3–Fe1–C1) of 76.90(11)º is comparable to that of the reported value for the analogous 2,6-diisopropylphenyl bis(imino)imidazol-2-ylidene iron(II) of 77.1(1)º,[84] while it is smaller than the average bite angle of the reported[23d] pincer (C-N-C)$FeBr_2$ complex (72.43º). The Fe–C1 bond length is 2.091(3) Å, which is comparable to the reported range of Fe–carbene bond lengths of 2.085(2) to 2.193(10) Å.[23d,84] As observed for 2,6-diisopropylphenylbis(imino)imidazol-2-ylidene iron(II),[84] the ligand binds to the metal in a bidentate fashion in which N3–Fe1 is equal to 2.145(3) Å. The iminic bond length of N3–C4 (1.269(4) Å) for the coordinated nitrogen atom is longer than the corresponding bond of N4–C6 (1.256(4) Å). The N1–C1–N2 angle (103.5(3)º) is smaller than N1–C1–N2 of the ligand precursor **2.7** (107.3(2)º).

Two IR stretching frequencies were observed at 1695 and 1685 cm^{-1} suggesting a bidentate coordination mode of the ligand. A similar behavior has been reported for iron(II) complex of 2,6-diisopropylphenylbis(imino)imidazol-2-ylidene[84] and the five-membered ring of bis(imino)pyrrolyl ligands.[85] A methylene spacer was installed within the iminic arm to allow for a tridentate coordination of the 2,6-diisopropylphenylbis(imino)imidazol-2-ylidene, however the desired coordination mode was not achieved, probably due to a high σ-donation of the NHC.[84] The coordination of the second iminic nitrogen atom causes steric constrain as expected based on the large yaw distortion angle[86] observed in **2.17** (θ 16.5°). This steric strain and an electron-rich metal center forbid a tridentate coordination fashion of the ligand. Attempts to abstract the halide from the metal center to force the ligand to coordinate in a tridentate binding mode using different silver reagents were inconclusive.

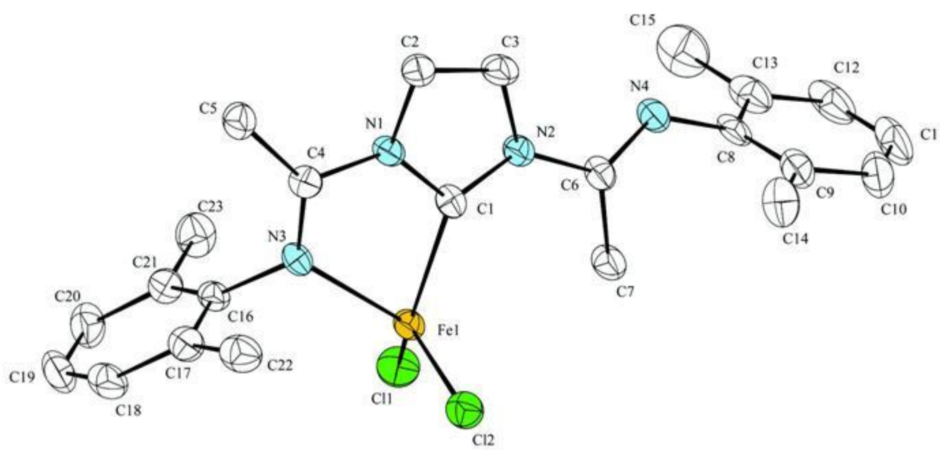

Figure 2.5. ORTEP of **2.17** (50% probability level). Hydrogen atoms are omitted for clarity. Selected bond lengths (Å) and angles (deg.). Fe1–C1 2.091(3), Fe1–N3 2.145(3), Fe1–Cl1 2.2404(9), Fe1–Cl2 2.2442(10), N1–C1 1.369(4), N2–C1 1.350(4), N3–C4 1.269(4), N4–C6 1.256(4), C1–Fe1–N3 76.90(11), C1–Fe1–Cl1 116.67(9), C1–N1–C2 111.5(3), C1–N2–C3 111.9(3), N2–C1–N1 103.5(3), N1–C4–N3 114.9(3), N2–C6–N4 116.0(3).

2.3.4 Bis(imino)imidazol-2-ylidene cobalt(II) complex

The cobalt(II) complex of bis(imino)imidazol-2-ylidene was afforded as a potential ethylene polymerization catalyst. This complex ($[C_{imi}(\text{^}Imine_{Me})_2]CoCl_2$) **2.18** was successfully synthesized in 87% yield[73b] (Scheme 2.13) by a similar procedure to the analogous iron complex (**2.17**). The magnetic susceptibility for **2.18** is 4.24 μB, as measured using the Evans method,[83] in agreement with three unpaired electrons.

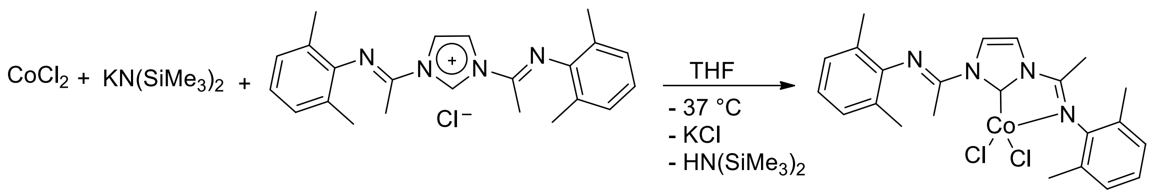

Scheme 2.13. Synthesis of the NHC cobalt(II) complex **2.18**.

X-ray-quality crystals were grown by cooling down a concentrated dichloromethane solution of **2.18** to –40 ºC. The solid-state molecular structure depicted a distorted tetrahedral geometry around the Co center, and the molecule crystallized in the $P2_1/C$ space group (Figure 2.6). The C1–Co1–Cl1 and C1–Co1–Cl2 bond angles are 117.57(10)º and 110.61(11)º, respectively. The C1–Co1 bond length is 2.030(3) Å, which is comparable to the published value of Co–carbene (1.942(6) Å) bond of [trans–Co(CNC)(κ^1–CF_3–SO_3)$_2$(py)].[23c] As observed in **2.17** and in cobalt complexes of a five-membered ring of bis(imino)pyrrolyl ligands,[85] the ligand coordinated in a bidentate fashion with a high yaw distortion angle of θ 17.8° in **2.18**. The bite angle C1–Co1–N3 is 79.99(12)º and bond length of Co1–N3 is equal to 2.077(3) Å. The iminic bond N3–C4 (1.273(4) Å) is longer than the corresponding bond of N4–C6 (1.253(4) Å) because of π-back donation to the coordinated iminic bond. The N1–C1–N2 angle (103.7(3)º) is smaller than N1–C1–N2 of the ligand precursor **2.7** (107.3(2)º). The stretching frequency ($\nu_{C=N}$) of the iminic bonds for the ligand precursor **2.7** is 1698 cm^{-1}, while those of the corresponding cobalt complex (**2.18**) are 1685, 1652 cm^{-1}, as expected for a bidentate coordination of the ligand.

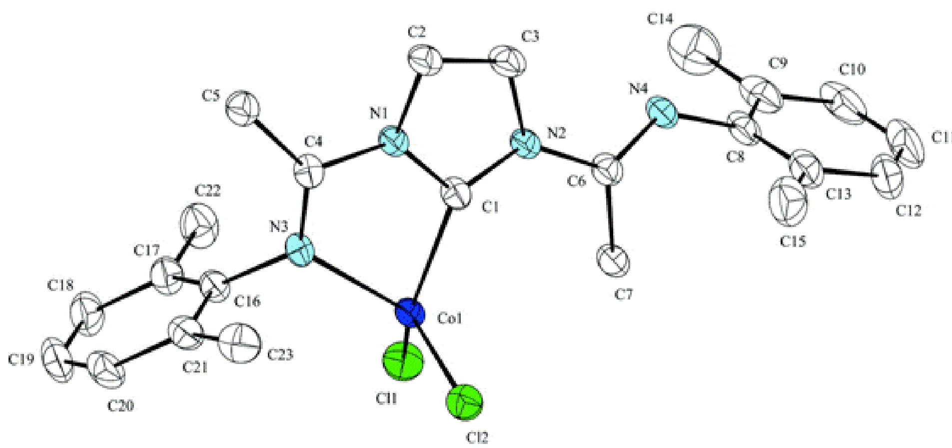

Figure 2.6. ORTEP of **2.18** (50% probability level). Hydrogen atoms are omitted for clarity. Selected bond lengths (Å) and angles (deg.). Co1–C1 2.030(3), Co1–N3 2.077(3), Co1–Cl1 2.2239(10), Co1–Cl2 2.2293(11), N1–C1 1.367(4), N2–C1 1.350(4), N3–C4 1.273(4), N4–C6 1.253(4), C1–Co1–N3 79.99(12), C1–Co1–Cl1 117.57(10), C1–Co1–Cl2 110.61(11), C1–N1–C2 111.5(3), C1–N2–C3 111.4(3), N2–C1–N1 103.7(3).

2.3.5 Bis(imino)imidazol-2-ylidene chromium complexes

Coordination of the bis(imino)imidazol-2-ylidene to the more electron-deficient Cr(III) metal center was investigated to explore the activity of early transition metal complexes in ethylene polymerization. Moreover, the more electropositive metal offers a better chance for the ligand to bind in a tridentate fashion, something that had failed to this point. Although the imidazol-2-ylidene complexes of silver (**2.12**) or copper (**2.15** and **2.16**) could not be utilized as transmetalating agents to afford the related iron (**2.17**) or cobalt (**2.18**) complexes, the transmetalation reaction of the silver complex (**2.12)** with $CrCl_3\cdot 3THF$ gave $[C_{imi}(^{\wedge}Imine_{Me})_2]CrCl_3$ (**2.19**) in 58% yield (Scheme 2.14).[73b] Similarly, $[C_{imi}(^{\wedge}Imine_{Ph})_2]CrCl_3$ (**2.20**) was synthesized in 71% yield by the transmetalation reaction with the Cu(I) complex (**2.16**) (Scheme 2.15).[73b] This transmetalation reaction using **2.16** to afford early transition metal complexes is the first to be reported. Therefore, the copper carbene complex can efficiently be used as an alternative agent to the frequently used silver complexes in carbene transmetalation reactions.

The magnetic susceptibilities for **2.19** and **2.20** were 4.84 and 4.57 μB,[83] respectively, in agreement with three unpaired electrons.[87] The FTIR stretching frequency for the iminic groups in **2.19** and **2.20** showed two bands: one at 1687 and 1653 cm^{-1}, respectively, and one at 1618 cm^{-1}. These results suggest coordination of the ligand in a bidentate mode.

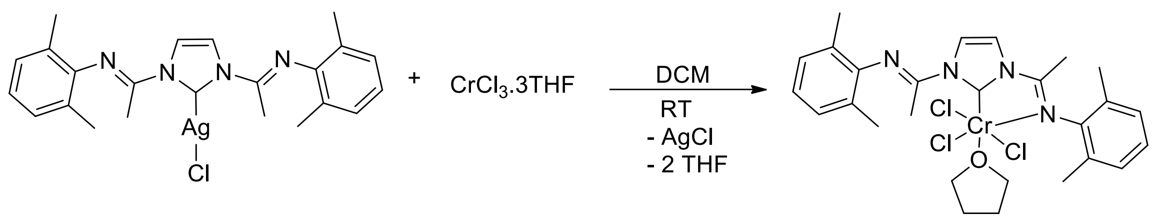

2.12 **2.19**

Scheme 2.14. Synthesis of the NHC chromium(III) complex **2.19**.

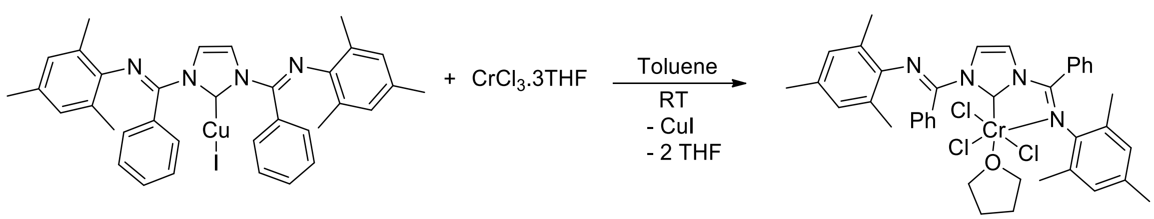

2.16 **2.20**

Scheme 2.15. Synthesis of the NHC chromium(III) complex **2.20**.

X-ray-quality crystals were grown by vapor diffusion of pentane into a saturated THF solution of complex **2.20** at room temperature. The chromium–carbene bond length is 2.048(3) Å, which is shorter than the corresponding reported value of bis(carbene)$CrCl_3$(THF) complex[88] (2.134(5) and 2.109(5) Å). The molecule crystallized in the $P\bar{1}$ space group and adopted a distorted octahedral geometry around chromium (Figure 2.7), in which a THF molecule coordinated to the metal center. The Cr1−O1 bond length (2.080(2) Å) is shorter than that of the reported value for (C^Imine)$CrCl_3$(THF) (2.100(3) Å)[89] and even shorter than that of the bis(carbene)$CrCl_3$(THF) complex (2.163(3) Å).[88] The ligand binds to the metal in a bidentate fashion and forms a 5-member metallocycle ring in which the C1–Cr1–N3 bite angle is 76.90(11)º with a Cr1–N3 bond length of 2.164(3) Å. The O1–Cr1–C1 angle of 166.44(11)° is smaller than those in the (C^Imine)$CrCl_3$(THF) 168.84(15)[89] and for bis(carbene)$CrCl_3$(THF) complex (179.30(19)°).[88]

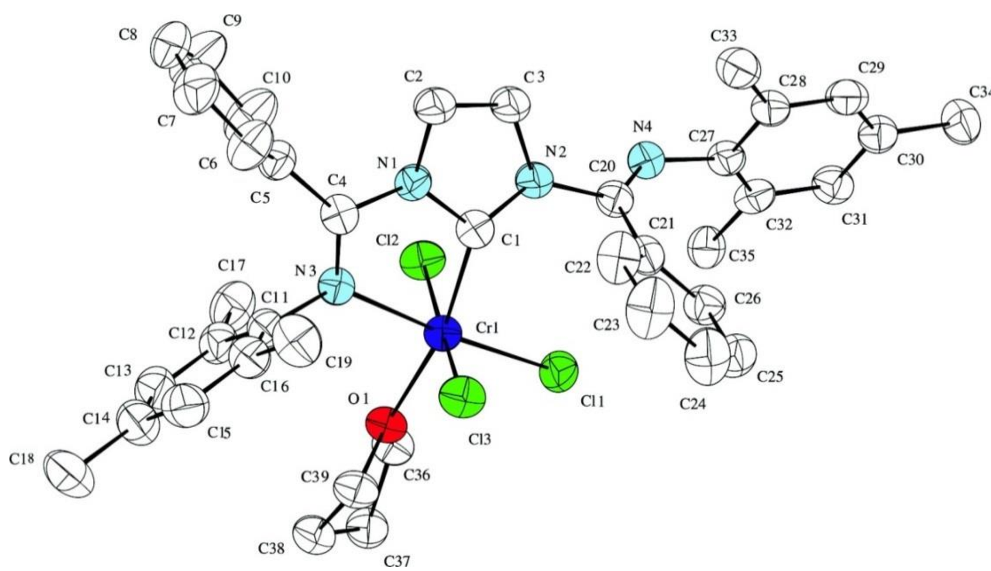

Figure 2.7. ORTEP of **2.20** (50% probability level). Hydrogen atoms are omitted for clarity. Selected bond lengths (Å) and angles (deg.). Cr1–C1 2.048(3), Cr1–N3 2.164(3), Cr1–Cl1 2.2880(10), Cr1–Cl2 2.2426(8), Cr1–Cl3 2.2959(9), Cr1–O1 2.080(2), N1–C1 1.377(4), N2–C1 1.346(4), N3–C4 1.294(4), N4–C20 1.261(4), N1–C1–N2 103.7(3), N3–Cr1–Cl1 175.03(7), N3–Cr1–Cl2 88.28(6), N3–Cr1–Cl3 89.22(6), N1–C4–N3 114.6(3), N2–C6–C20 113.7(3), C1–Cr1–N3 76.90(11), C1–Cr1–O1 166.44(11), C1–Cr1–Cl1 98.20(9), C1–Cr1–Cl2 82.05(8), C1–Cr1–Cl3 94.62(8).

The bond lengths and bond angles for **2.20** are more comparable to those of the reported (C^Imine)$CrCl_3$(THF)[89] than to those of the bis(carbene)$CrCl_3$(THF),[88] due to the latter being less electropositive and lacking an imine π-acceptor. The bond length of N3–C4 (1.294(4) Å) is longer than that of N4–C20 (1.261(4) Å) and this can be attributed to π-back donation to the coordinated iminic bond. The N1–C1–N2 angle (103.7(3)°) is smaller than the corresponding N1–C1–N1a of the ligand precursor **2.10** (108.9(3)°).

2.3.6 Bis(imino)imidazol-2-ylidene palladium complexes

The desired bis(imino)imidazol-2-ylidene palladium complexes were synthesized to enhance a tridentate coordination mode of the ligand and also due to the diamagnetic nature of these complexes. The palladium complex ([C_{imi}(^$Imine_{Me}$)$_2$]Pd(allyl)Cl) (**2.21**) was successfully synthesized by the transmetalation reaction with the silver NHC complex **2.12** (76% yield). Complex **2.21** can also be obtained by the reaction of [Pd(allyl)Cl]$_2$ with $NaN(SiMe_3)_2$ at –37 °C, and subsequent addition of the filtrate to the imidazolium salts **2.7** (Scheme 2.16). A pincer type ligand can coordinate to a palladium center in a tridentate fashion forming η^1-allyl complex.[90] Therefore, the chloride was abstracted from **2.21** by its reaction with $AgBF_4$ to afford the related cationic NHC palladium complex ([C_{imi}(^$Imine_{Me}$)$_2$]Pd(allyl)BF_4) (**2.22**) (Scheme 2.16).

The ^{1}H NMR spectrum shows broad resonances for the allyl protons as an indication of a fluxional process at room temperature. Therefore, a variable-temperature NMR study was performed at –50 ºC and resonances corresponding to the allyl protons were resolved. This process may be attributed to isomerization between η^3-allyl and η^1-allyl palladium complex.[54a,80] The trans effect for the carbene ligand compared to the chloride ligand, and the possibility of coordination of an iminic nitrogen to Pd may facilitate the allyl isomerization process (Scheme 2.17).

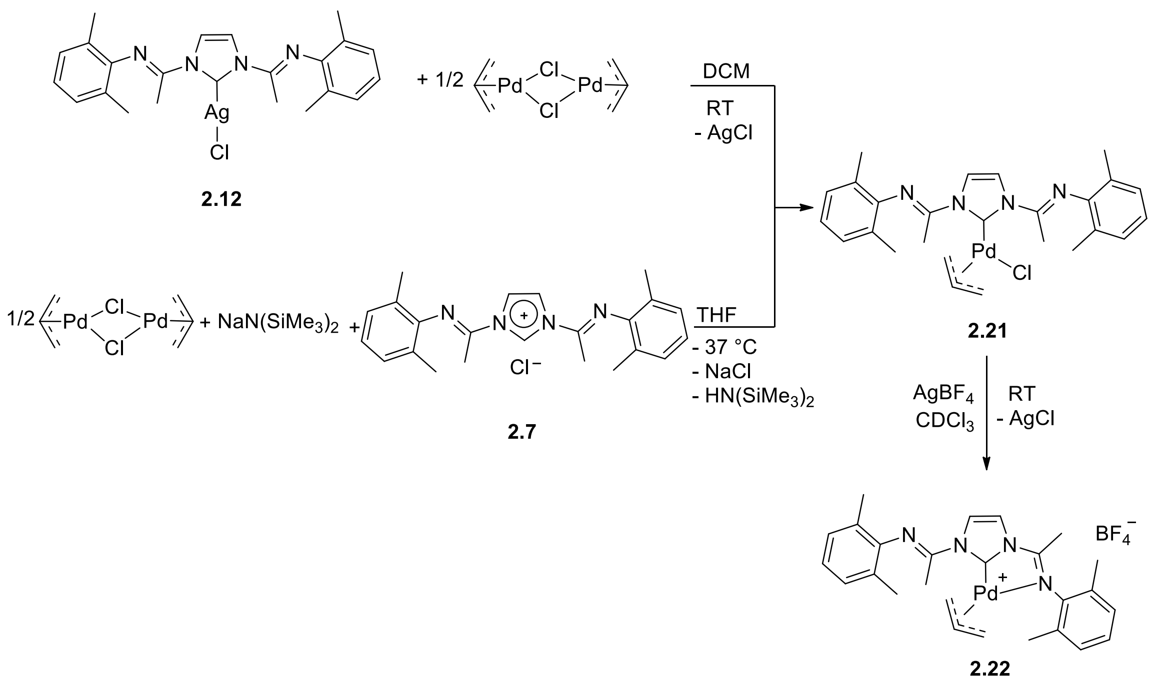

Scheme 2.16. Synthesis of the NHC palladium(II) complexes **2.21** and **2.22**.

The protons for the azole ring were observed at δ 8.38, in **2.21** and at δ 8.08 and 8.00 in the complex **2.22**, while the corresponding protons in the silver-carbene complex **2.12** appeared at **δ** 8.08. The ^{13}C NMR for the carbene resonances in **2.21** and **2.22** appeared at δ 180.9 and 180.0, respectively. The iminic carbon resonances appeared at δ 165.2 and 153.7 in the complex **2.22**, while the iminic carbon resonance in **2.21** (δ 157.8) presented a downfield shift to compared to that in the silver–carbene complex **2.12**.

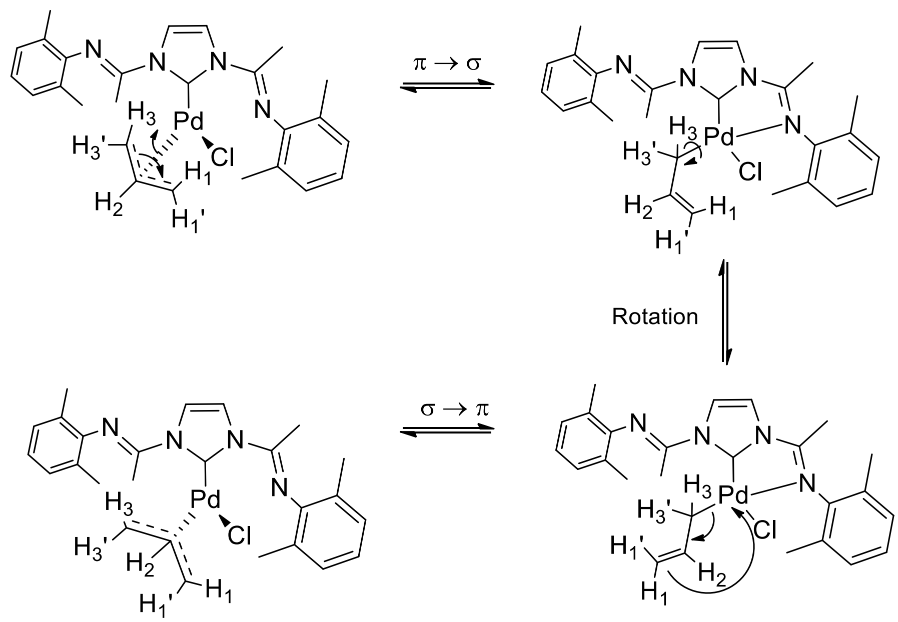

Scheme 2.17. Proposed allyl group isomerization (σ→ π) in **2.21**.

Two C=N vibrational frequencies at 1676 and 1653 cm^{-1} were observed for **2.21** lower than that of the corresponding silver-carbene complex **2.12 (**1684 cm^{-1}). This suggested two different iminic bonds due to isomerization between η^3-allyl and η^1-allyl palladium complex. A bidentate chelating fashion is suggested by IR stretching frequency observed at 1685 and 1655 cm^{-1} for **2.22**.

Suitable crystals for an X-ray diffraction study for **2.21** were grown by slow vapor diffusion of pentane into a concentrated dichloromethane solution at room temperature (Figure 2.8) and the molecule crystallized in the $P\bar{1}$ space group. The ligand binds to the metal center in a monodentate coordination mode and the molecule adopts square planar geometry around the Pd(II) center. The bond distance of Pd1–C1 (2.031(5) Å) is within the range of the reported Pd–carbene bond of (2.003(17)–2.072(2) Å).[80,82,91] The increase of σ-bond character of C1, after coordination, is revealed by the observed long bond lengths of N1–C1 (1.362(6) Å) and N2–C1 (1.404(7) Å) in **2.21** compared to those in the corresponding imidazolium salt **2.7**, as well as by the decrease of the bond angle N1–C1–N2 of the salt from 107.3(2)º to 103.2(4)º in the complex **2.21**. The angle between the best plane of the azole ring and the coordination plane is 71.62°, deviated from the perpendicular, and this may be due to steric effects between the η^3-allyl group and the phenyl rings. The Pd–C26 (2.115(6) Å) bond length is shorter than the Pd–C24 (2.178(6)Å), because of the stronger trans effect of the NHC compared to chloride ligand, similar to the reported values in palladium-allyl chloride complexes containing benzimidazol-2-ylidene.[80]

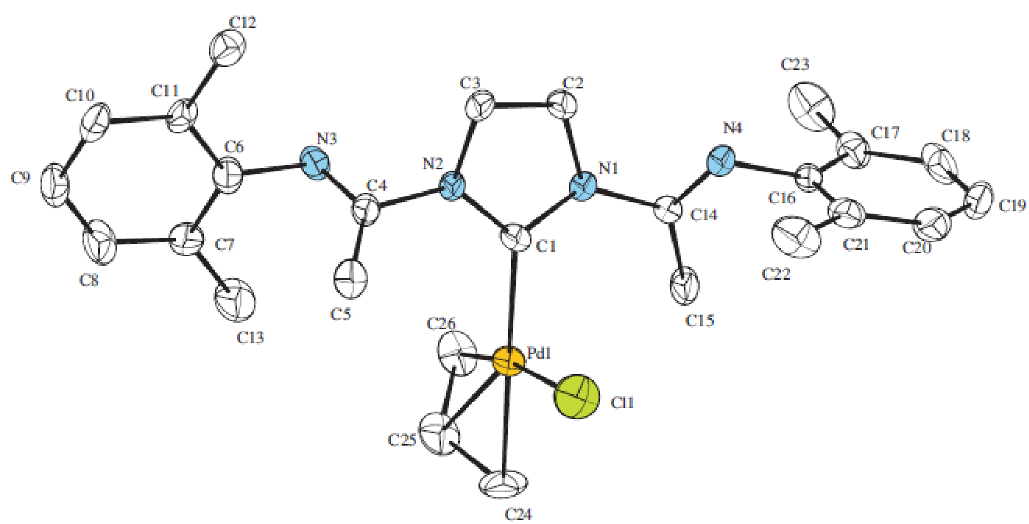

Figure 2.8. ORTEP of **2.21** (50% probability level). Hydrogen atoms are omitted for clarity. Selected bond lengths (Å) and angles (deg.). Pd1–C1 2.031(5), Pd1–Cl1 2.3671(16), Pd1–C24 2.178(6), Pd1–C25 2.130(6), Pd1–C26 2.115(6), N1–C1 1.362(6), N1–C2 1.404(7), N2–C1 1.362(6), N2–C3 1.383(7), C2–C3 1.333(7), N3–C4 1.260(7), N4–C14 1.257(6), C1–Pd1–C24 166.7(2), C1–Pd1–Cl1 92.89(16), C1–N1–C2 111.6(4), C1–N2–C3 111.6(4), N2–C1–N1 103.2(4).

The Pd–Cl1 bond length is 2.3671(16) Å in the range of the published results of Pd–Cl (2.326(5)–2.419(8) Å).[80,91-92] The C=N bond lengths, N3–C4 (1.260(7) Å) and N4–C14 (1.257(6) Å) are comparable to the related N3–C4 (1.261(3) Å) in the salt, due to the absence of coordination of the iminic nitrogen atoms to the metal.

2.3.7 Bis(imino)imidazol-2-ylidene zinc complexes

The analogous Zn(II) carbene complex ($[C_{imi}(\text{^}Imine_{Me})_2]ZnCl_2$) (**2.23**) was synthesized to explore the reactivity of a diamagnetic complex which was isostructural to Fe(II) (**2.17**) and Co(II) (**2.18**) complexes. This complex was afforded either by using the silver carbene complex (**2.12**) as a transmetalating agent, or by reacting the *in situ* generated zinc amide complex with imidazolium salt **2.7** (Scheme 2.18). The latter procedure was used with $ZnCl_2$, $NaN(SiMe_3)_2$ and the salt **2.10**. However, it failed to provide the desired complex and instead the decomposed benzimidoyl chloride was detected by ^1H NMR. This also demonstrates the role of chloride anion in the decomposition of the salt **2.10**. The use of ZnI_2 in lieu of $ZnCl_2$ afforded the desired NHC complex **2.24** ($[C_{imi}(\text{^}Imine_{Ph})_2]ZnI_2$) in 62% yield under similar reaction conditions (Scheme 2.19).

The resonance for the azole ring protons shifted upfield to δ 8.05 and 7.68 for the complexes **2.23** and **2.24**, respectively, compared to the ligand precursors **2.7** (δ 8.39) and **2.10** (δ 7.90). The carbene resonance for **2.23** appeared at δ 179.0 and δ 181.8 for the complex **2.22**. The iminic carbon resonances for complexes **2.23** and **2.24** experienced a downfield shift to δ 142.4 and 153.9, respectively. The IR C=N frequencies were observed at 1689 and 1660 cm^{-1} for **2.23** and at 1668 and 1653 cm^{-1} for **2.24** as an indication of a bidentate coordination fashion.

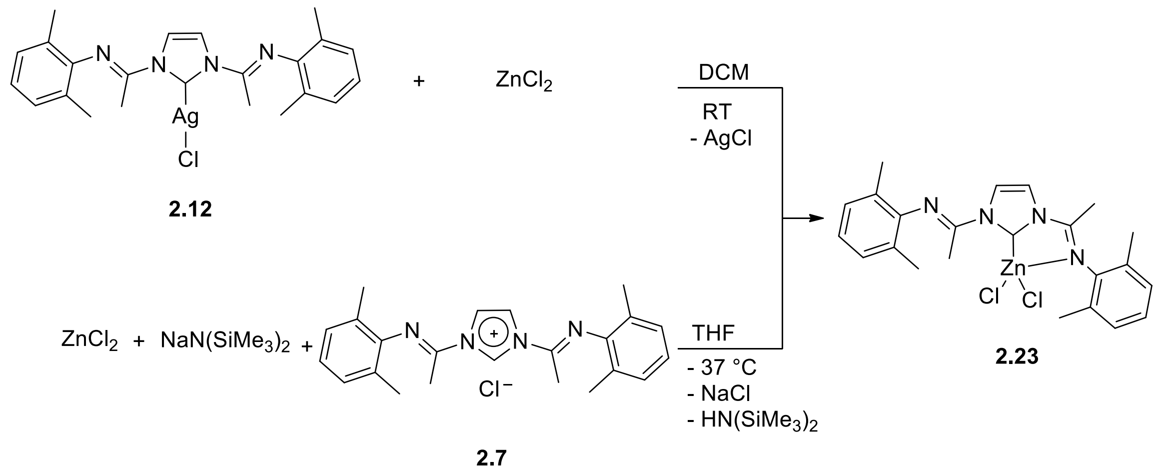

Scheme 2.18. Synthesis of the NHC zinc(II) complex **2.23**.

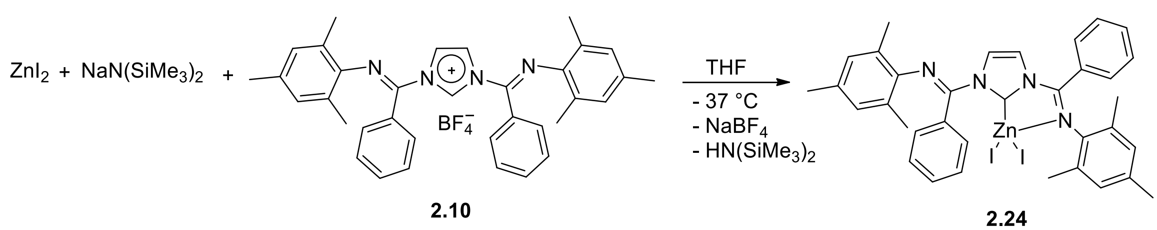

Scheme 2.19. Synthesis of the NHC zinc(II) complex **2.24**.

X-ray-quality crystals were grown by slow vapor diffusion of pentane into a dichloromethane concentrated solution of **2.23** (Figure 2.9). The zinc–carbene bond length is 2.031(4) Å, which is comparable to those of the reported value of 2.049(6) and 2.048 Å for bis pyridyl-substituted NHC Zn(II) iodide complex[93] and the chiral bidentate NHC Zn(II) complex,[94] respectively. The molecule crystallized in the $P2_1/C$ space group and adopted a distorted tetrahedral geometry at the zinc center. The Cl1–Zn1–Cl2 angle is

116.46(5)º, with C1–Zn1–N3 bite angle of 78.91(15)º. The ligand binds to the metal center in a bidentate mode and forms 5-membered metallocycle. The N3–C4 bond length of 1.273(5) Å is similar to that of N4–C14 (1.263(5) Å). The N1–C1–N2 angle (104.3(3)º) is smaller than that in the ligand precursor (107.3(2)º) and the sum of all angles around the carbene center is 359.9º, as expected for an sp^2-hybridized carbon atom.

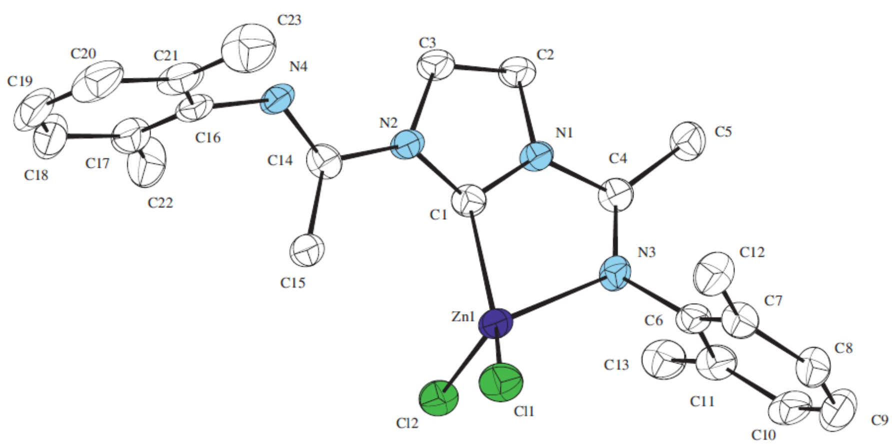

Figure 2.9. ORTEP of **2.23** (50% probability level). Hydrogen atoms are omitted for clarity. Selected bond lengths (Å) and angles (deg.): Zn1–C1 2.031(4), Zn1–N3 2.139(3), Zn1–Cl1 2.2152(13), Zn1–Cl2 2.2234(13), N1–C1 1.365(5), N1–C2 1.403(5), N2–C1 1.345(5), N3–C4 1.273(5), N4–C14 1.263(5), C1–Zn1–N3 78.91(15), C1–Zn1–Cl1 119.31(13), N3–Zn1–Cl1 109.16(10), Cl1–Zn1–Cl2 116.46(5), C1–N1–C2 111.5(3), C1–N2–C3 111.3(3), N2–C1–N1 104.3(3), N2–C1–Zn1 144.3(3), N1–C1–Zn1 111.2(3), N3–C4–N1 114.8(4).

2.4 Polymerization of ethylene

Complexes **2.17, 2.18, 2.19** and **2.20** were tested for ethylene polymerization at room temperature with 1 atm of C_2H_4 and 1000 equivalents of methylaluminoxane (MAO). The MAO, as a cocatalyst, alkylates the precatalyst and creates a free site. The chromium complexes $[C_{imi}(\text{^}Imine_{Me})_2]CrCl_3$ (**2.19**) and $[C_{imi}(\text{^}Imine_{Ph})_2]CrCl_3$ (**2.20**) gave activities of 21 and 34 kg of PE mol^{-1} of Cr h^{-1}, respectively. These results are higher than the activities for the neutral bis(NHC) complexes of chromium(III) by about 2 orders of magnitude.[88] However, these activities are lower than those reported by Gibson for his bis(NHC) chromium(III) complexes by about 3 orders of magnitude.[23a,23b] Substituting the methyl groups in **2.19** with relatively electron-poor phenyl rings in **2.20** increased the activity. This suggests that the catalytic activities can be further improved by reducing electron donation to the metal center or increasing the π-accepting ability of the ligand. The melting points determined by differential scanning calorimetry for the polymer produced by **2.19** and **2.20** were 134−135 °C, suggesting a linear polymer.

Unfortunately, the iron (**2.17**) and the cobalt (**2.18**) complexes exhibited no activity under similar reaction conditions. Similarly, iron and cobalt complexes of the chelating bis(NHC) ligand were not active, however the related complexes of titanium, vanadium, and chromium showed activity.[23a,23b] This could be due to the tendency of late transition metal complexes containing NHC ligands to decompose through reductive elimination of the alkylimidazolium compound.[95]

To obtain more insight into activation of the bis(imino) NHC complexes with MAO and the possible decomposition pathway of the activated complex, the iron complex (**2.17**) was treated with 5 equivalents of trimethylaluminum ($AlMe_3$). The reaction led to a black precipitate and unfortunately the NMR spectrum of the reaction outcome was featureless, due to very broad resonances. It is hypothesized that a methyl iron complex may initially form, however reductive elimination reaction affords Fe(0) and the alkylimidazolium salt.

2.5 Conclusions

The new class of 1,3-bis(imino)imidazol-2-ylidene ligand precursors have been synthesized and characterized. The substituents on the iminic carbon affect the procedures for synthesizing the imidazolium salts and also the preparation of the related transition metal complexes. The imidazol-2-ylidene complexes of silver(I), copper(I), iron(II), cobalt(II), chromium(III), palladium(II) and zinc(II) were isolated and characterized. Those complexes were synthesized via *in situ* deprotonation of the parent imidazolium salts, or using either silver or copper complexes as transmetalating agents. The substituents on the iminic carbon play an important role on the solid-state structure of the resulting copper complexes, in which both a mono- and bidentate coordination modes were observed. As determined by X-ray crystallography, the ligand coordinated to iron, cobalt, chromium and zinc in a bidentate mode through the carbene carbon and one iminic nitrogen atoms. A monodentate coordination mode for the imidazol-2-ylidene complex of palladium was revealed by X-ray structure determination study.

The catalytic activity of carbene complexes of iron(II), cobalt(II) and chromium(III) were tested for ethylene polymerization. Although the iron and cobalt complexes were inactive, chromium complexes showed moderate activities. The activity of these complexes was slightly enhanced by replacing the methyl substituents on the iminic carbon with a relatively electron-poor phenyl groups. An increase in the π-accepting ability or a decrease in the electron-donating ability of the ligand is predicted to generate more active catalysts for olefin polymerization.

As mentioned above, the reactivity of the imidazol-2-ylidene complexes of Cr(III) (1^{st} generation) was slightly improved by reducing the electron density on the metal center. Although the bis(imino)imidazol-2-ylidene was designed as tridentate ligand, all attempts to achieve such coordination mode were unsuccessful even with relatively electron-deficient Cr(III) metal. Therefore, these issues will be dealt in the next chapter by tuning the electronic properties of the NHC ligand.

2.6 Experimental procedures

All experiments were performed under a dinitrogen atmosphere in a drybox or using standard Schlenk techniques. Solvents used in the preparation of air- and/or moisture-sensitive compounds were dried by using an MBraun Solvent Purification System fitted with alumina columns and stored over molecular sieves under a positive pressure of dinitrogen (pentane, toluene, and THF) or dried by refluxing and then distilling from sodium (toluene) under a positive pressure of dinitrogen. Deuterated solvents were degassed using three freeze-pump-thaw cycles. C_6D_6 was vacuum-distilled from sodium, and $CDCl_3$ and CD_3CN were vacuum-distilled from CaH_2. NMR spectra were recorded on a Bruker AV 400 (^1H at 400 MHz, ^{13}C at 100 MHz) or Bruker AV 300 spectrometer (^1H at 300 MHz, ^{13}C at 75.5 MHz) at room temperature unless otherwise stated. The spectra were internally referenced relative to the residual protio solvent (^1H) and solvent (^{13}C) resonances, and chemical shifts were reported with respect to δ 0 for tetramethylsilane. Solution magnetic susceptibilities were measured using the Evans method.[83] Elemental composition was determined by ANALEST of the Department of Chemistry, University of Toronto or by Guelph Chemical Laboratories Ltd.

Benzoyl chloride and 2,4,6-trimethylaniline were purchased from Sigma-Aldrich. *N*-(2,6-Dimethylphenyl)acetamide was purchased from Sigma-Aldrich or Alfa Aesar and used without further purification. Copper(I) iodide was purchased from Riedel-de Haën and was dried overnight in a vacuum oven at 80 °C. Iron(II) chloride, cobalt(II) chloride, sodium iodide, sodium and potassium bis(trimethylsilyl)amide were purchased from Sigma-Aldrich. Chromium(III) chloride was purchased from Strem Chemicals. *N*-(2,6-Dimethylphenyl)acetimidoyl chloride,[96] *N*-(2,4,6-trimethylphenyl)phenylimidoyl chloride,[96] *N*-(2,6-dimethylphenyl)pivalimidoyl chloride[96] and $CrCl_3 \cdot 3THF$[97] were synthesized using the published procedures. Deuterated NMR solvents were purchased from Cambridge Isotope Laboratories. MAO was graciously donated by Albemarle Corp.

1-[(2,6-Dimethylphenylimino)ethyl]imidazole (2.4).

N-(2,6-Dimethylphenyl)acetimidoyl chloride (**2.1**) (2.55 g, 14.0 mmol) was dissolved in dichloromethane (10 mL) and added to a dichloromethane (30 mL) solution of imidazole (1.92 g, 28.1 mmol) at room temperature. A white precipitate was immediately formed. The reaction mixture was stirred for 5 h. Water was added to the mixture and the organic product was extracted with dichloromethane. The combined dichloromethane layers were dried over Na_2SO_4. The solvent was removed under vacuum to give **2.4** as a brown solid (2.85 g, 13.4 mmol, 95%). ^{1}H NMR (300 MHz, $CDCl_3$): δ 8.23 (s, 1H, NC*H*N), 7.72 (s, 1H, NC*H*CHN), 7.16 (s, 1H, NCHC*H*N), 7.05 (d, ^3J = 7.5 Hz, 2H, *m*-C$H_{(Xyl)}$), 6.96 (t, ^3J = 6.8 Hz, 1H, *p*-C$H_{(Xyl)}$), 2.16 (s, 3H, C$H_{3(imine)}$), 2.05 (s, 6H, *o*-C$H_{3(Xyl)}$); ^{13}C{^{1}H} NMR (75.5 MHz, $CDCl_3$): δ 149.0 (*C*=N), 144.6 ($C_{ipso(Xyl)}$), 135.2 (N*C*N), 129.9 (NC*C*N), 127.8

(m-CH$_{(Xyl)}$), 126.3 (o-CCH$_{3(Xyl)}$), 123.4 (p-CH$_{(Xyl)}$), 116.0 (NCCN), 17.7 (o-CH$_{3(Xyl)}$), 15.4 (CH$_{3(imine)}$); FTIR (neat) $\nu_{C=N}$ 1680 cm^{-1}; M.P. 57.0–58.0 ºC.

1-[(2,4,6-Trimethylphenylimino)benzyl]imidazole (2.5).

N-(2,4,6-Trimethylphenyl)benzimidoyl chloride (**2.2**) (5.47 g, 21.2 mmol) was dissolved in dichloromethane (15 mL) and added to a dichloromethane (100 mL) solution of imidazole (2.96 g, 43.4 mmol) at room temperature. Immediately, a white precipitate formed. The reaction mixture was stirred for 3.5 h. Water was added to the mixture and the organic product was extracted with dichloromethane. The combined dichloromethane washings were dried over Na_2SO_4. The solvent was removed under vacuum to give **2.5** as a yellow oil (5.97 g, 20.6, 97%). ^{1}H NMR (400 MHz, $CDCl_3$): δ 7.91 (s, 1H, NCHN), 7.57 (s, 1H, NCHCHN), 7.38 (t, ^{3}J = 7.1 Hz, 1H, p-C$H_{(phenyl)}$), 7.30 (t, ^{3}J = 7.1 Hz, 2H, m-C$H_{(phenyl)}$), 7.22 (d, ^{3}J = 7.1 Hz, 2H, o-C$H_{(phenyl)}$), 7.15 (s, 1H, NCHCHN), 2.17 (s, 3H, p-C$H_{3(mesityl)}$), 2.01 (s, 6H, o-C$H_{3(mesityl)}$); ^{13}C{^{1}H} NMR (100 MHz, $CDCl_3$): δ 150.0 (C=N), 142.2 ($C_{ipso(mesityl)}$), 137.4 (NCN), 132.8 (p-CCH$_{3(mesityl)}$), 131.2 ($C_{ipso(phenyl)}$), 130.9 (p-CH$_{(phenyl)}$), 130.1 (NCCN), 128.6 (o-CH$_{(phenyl)}$ + m-CH$_{(phenyl)}$), 128.5 (m-CH$_{(mesityl)}$), 126.4 (o-CCH$_{3(mesityl)}$), 118.0 (NCCN), 20.7 (p-CH$_{3(mesityl)}$), 18.4 (o-CH$_{3(mesityl)}$). FTIR (neat) $\nu_{C=N}$ 1655 cm^{-1}. M.P. 78.0–79.0 ºC.

1-[(2,6-Dimethylphenylimino)neopentyl]imidazole (2.6).

N-(2,6-Dimethylphenyl)pivalimidoyl chloride (**2.3**) (944 mg, 4.22 mmol) was dissolved in dichloromethane (20 mL) and added to a dichloromethane (10 mL) solution of imidazole (580 mg, 8.52 mmol) at room temperature. A white precipitate was immediately formed. The reaction mixture was stirred for 3.5 h. Water was added to the mixture and the organic product was extracted with dichloromethane. The combined dichloromethane layers were dried over Na_2SO_4. The solvent was removed under vacuum to give **2.6** as a colorless oil (1.07 g, 4.19 mmol, 99%). ^{1}H NMR (400 MHz, CD_2Cl_2): δ 7.23 (s, 1H, NC*H*N), 6.92 (d, ^3J = 7.6 Hz, 2H, *m*-C$H_{(Xyl)}$), 6.82-6.85 (m, 3H, NC*H*CHN, NCHC*H*N, *p*-C$H_{(Xyl)}$), 2.03 (s, 6H, *o*-C$H_{3(Xyl)}$), 1.41 (s, 9H, (CH_3)$_{3(imine)}$); ^{13}C{^{1}H} NMR (100 MHz, CD_2Cl_2): δ 158.5 (*C*=N), 144.8 ($C_{ipso(Xyl)}$), 135.3 (N*C*N), 128.0 (N*C*CN), 127.9 (*m*-*C*$H_{(Xyl)}$), 125.3 (*o*-*C*$CH_{3(Xyl)}$), 123.5 (NC*C*N), 39.9 (*C*(CH_3)$_3$), 28.3 (C(*C*H_3)$_3$), 17.8 (*o*-*C*$H_{3(Xyl)}$).

1,3-Bis[1-(2,6-dimethylphenylimino)ethyl]imidazolium chloride (2.7).

N-(2,6-Dimethylphenyl)acetimidoyl chloride (**2.1**) (2.00 g, 11.0 mmol) was dissolved in a minimal amount of toluene and added to a solution of 1-(2,6-dimethylphenylimino)ethylimidazole (**2.4**) (2.35 g, 11.0 mmol) in toluene (15 mL) at room temperature. A white precipitate formed within minutes. The reaction mixture was stirred for 42 h and filtered. The white solid was washed with toluene and pentane, and dried under vacuum (4.06 g, 93%). Crystals suitable for X-ray diffraction studies were grown at –40 ºC by slow diffusion of pentane into a saturated acetonitrile solution. ^{1}H NMR (300 MHz, $CDCl_3$): δ 12.54 (s, 1H, NC*H*N), 8.39 (s, 2H, NC*H*C*H*N), 7.10(d, ^3J = 6.4 Hz, 4H, *m*-C$H_{(Xyl)}$), 7.05 (t, ^3J = 6.0 Hz, 2H, *p*-C$H_{(Xyl)}$), 2.87 (s, 6H, C$H_{3(imine)}$), 2.05 (s, 12H, *o*-C$H_{3(Xyl)}$); ^{13}C{^{1}H} NMR (75.5 MHz, $CDCl_3$): δ 150.1 (*C*=N), 143.2 ($C_{ipso(Xyl)}$), 138.9 (N*C*N), 128.6 (*m*-*C*$H_{(Xyl)}$), 126.2 (*o*-*C*$CH_{3(Xyl)}$), 125.3 (*p*-*C*$H_{(Xyl)}$), 118.3 (N*C*CN), 18.2 (*o*-*C*$H_{3(Xyl)}$), 17.6 (*C*$H_{3(imine)}$). FTIR (neat) $\nu_{C=N}$ 1698 cm^{-1}. Anal. Calcd. For $C_{23}H_{27}ClN_4$(%):

C, 69.95; H, 6.89 ; N, 14.19. Found (%): C, 69.61; H, 6.85; N, 14.47. M.P. 168.0–171.0 ºC.

1,3-Bis[(2,4,6-trimethylphenylimino)benzyl]imidazolium tetrafluoroborate (2.10).

N-(2,4,6-Trimethylphenyl)phenyl imidoyl chloride (**2.2**) (3.33 g, 12.9 mmol) was dissolved in acetonitrile (5 mL) and added to an acetonitrile (30 mL) suspension of sodium tetrafluoroborate (1.57 g, 14.3 mmol) at room temperature. The reaction mixture was stirred for 24 h. A solution of 1-(2,6-dimethylphenylimino)benzylimidazole (**2.5**) in acetonitrile (20 mL) was then added to the reaction mixture. The mixture was stirred for 23 h at room temperature and filtered. The filtrate was collected and the volatiles were removed under vacuum. The yellow solid was washed with toluene and pentane to give (7.41 g, 96%) of the expected product. Crystals suitable for X-ray diffraction studies were grown at room temperature under nitrogen by vapor diffusion of pentane into a saturated dichloromethane solution. ^{1}H NMR (300 MHz, $CDCl_3$): δ 9.22 (s, 1H, NC*H*N), 7.90 (s, 2H, NC*H*C*H*N), 7.53 (d, ^{3}J = 6.8 Hz, 4H, *o*-C$H_{(phenyl)}$), 7.37–7.46 (m, 6H, *m*-C$H_{(phenyl)}$ + *p*-C$H_{(phenyl)}$), 6.74 (s, 4H, *o*-C$H_{3(mesityl)}$), 2.19 (s, 6H, *p*-C$H_{3(mesityl)}$), 2.03 (s, 12H, *o*-C$H_{3(mesityl)}$); ^{13}C{^{1}H} NMR (75.5 MHz, $CDCl_3$): δ 148.2 (*C*=N), 140.7 ($C_{ipso(mesityl)}$), 134.7 ($C_{ipso(phenyl)}$), 134.5 (N*C*N), 132.6 (*p*-*C*$H_{(mesityl)}$), 129.5 (*m*-*C*$H_{(mesityl)}$), 129.3 (*m*-*C*$H_{(phenyl)}$), 129.0 (*o*-*C*$H_{(phenyl)}$), 127.7 (*p*-*C*C$H_{3(mesityl)}$), 126.7 (*o*-*C*C$H_{3(mesityl)}$), 120.9 (NC*C*N), 20.9 (*p*-*C*$H_{3(mesityl)}$), 18.4 (*o*-*C*$H_{3(mesityl)}$); ^{19}F NMR (282 MHz, $CDCl_3$): δ –152.6. FTIR (neat) $\nu_{C=N}$ 1676 cm^{-1}. Anal. Calcd. For $C_{35}H_{35}BF_4N_4$ (%): C, 70.24; H, 5.89; N, 9.36. Found (%): C, 69.97; H, 6.01; N, 9.60. M.P. 184.0–188.0 ºC

1,3-Bis[(2,4,6-trimethylphenylimino)benzyl]imidazolium iodide (2.11).

An acetonitrile (3 mL) solution of sodium iodide (40.2 g, 0.268 mmol) was added to a solution of *N*-(2,4,6-trimethylphenyl)phenyl imidoyl chloride (**2.2**) (68.5 mg, 0.266 mmol) in acetonitrile (3 mL) at room temperature. The reaction mixture was stirred for 1 h. A solution of 1-(2,4,6-trimethylphenylimino)benzylimidazole (**2.5**) (74.5 mg, 0.257 mmol) in acetonitrile (3 mL) was then added to the reaction mixture. The mixture was stirred for 24 h at room temperature and filtered. The filtrate was collected and the volatiles were removed under vacuum. The yellow solid was washed with toluene and pentane to give **2.11** (152.3 mg, 94%). ^{1}H NMR (300 MHz, $CDCl_3$): δ 9.53 (s, 1H, NC*H*N), 7.83 (d, ^{3}J = 7.4 Hz, 4H, *o*-C$H_{(phenyl)}$), 7.79 (s, 2H, NC*H*C*H*N), 7.45 (t, ^{3}J = 6.8 Hz, 2H, *p*-C$H_{(phenyl)}$), 7.40 (d, ^{3}J = 7.5 Hz, 4H, *m*-C$H_{(phenyl)}$), 6.74 (s, 4H, *o*-C$H_{(mesityl)}$), 2.18 (s, 6H, *p*-C$H_{3(mesityl)}$), 2.08 (s, 12H, *o*-C$H_{3(mesityl)}$); ^{13}C{^{1}H} NMR (75.5 MHz, $CDCl_3$): δ 148.0 (*C*=N), 140.8 ($C_{ipso(mesityl)}$), 135.5 (N*C*N), 134.5 ($C_{ipso(phenyl)}$), 132.5 (*p*-*C*$H_{(phenyl)}$), 129.8 (*o*-*C*$H_{(phenyl)}$), 129.3 (*m*-*C*$H_{(phenyl)}$), 129.0 (*m*-*C*$H_{(mesityl)}$), 127.7 (*p*-*C*C$H_{3(mesityl)}$), 126.7 (*o*-*C*C$H_{3(mesityl)}$), 120.8 (NC*C*N), 20.8 (*p*-*C*$H_{3(mesityl)}$), 19.1 (*o*-*C*$H_{3(mesityl)}$). FTIR (neat): $\nu_{C=N}$ 1676 cm^{-1}.

1,3-Bis[1-(2,6-dimethylphenylimino)ethyl]imidazol-2-ylidene silver(I) chloride (2.12).

Sodium bis(trimethylsilyl)amide (36.9 mg, 0.201 mmol) was dissolved in toluene (10 mL) and added dropwise to a toluene (7 mL) suspension of $AgBF_4$ (38.0 mg, 0.195 mmol) at −37 °C. The reaction mixture was slowly warmed to room temperature and subsequently stirred for 50 min. The mixture was then filtered, and the filtrate was added dropwise to a toluene (3 mL) suspension of 1,3-bis[1-(2,6-dimethylphenylimino)ethyl]- imidazolium chloride (**2.7**) (61.3 mg, 0.155 mmol) at −37 °C. The reaction mixture was slowly warmed to room temperature and stirred for an additional 3.5 h. The mixture was filtered, and the brown solid product was washed with 15 mL of pentane. Yield: 65.2 mg, 0.130 mmol, 67%. ^{1}H NMR (300 MHz, $CDCl_3$): δ 8.08 (s, 2H, NC*H*C*H*N), 7.09 (d, ^3J = 6.8 Hz, 4H, *m*-C$H_{(Xyl)}$), 7.01 (t, ^3J = 6.8 Hz, 2H, *p*-C$H_{(Xyl)}$), 2.55 (s, 6H, C$H_{3(imine)}$), 2.09 (s, 12H, *o*-C$H_{3(Xyl)}$). ^{13}C{^{1}H} NMR (75.5 MHz, $CDCl_3$): δ 152.5 (*C*=N), 144.3 ($C_{ipso(Xyl)}$), 128.5 (*m*-*C*$H_{(Xyl)}$), 126.3 (*o*-$C_{(Xyl)}$), 124.6 (*p*-*C*$H_{(Xyl)}$), 119.6 (N*CC*N), 18.4 (*o*-*C*$H_{3(Xyl)}$), 17.7 (*C*$H_{3(imine)}$). FTIR (neat): $\nu_{C=N}$ 1684 cm^{-1}. Anal. Calcd. for $C_{23}H_{26}AgClN_4$ (%): C, 55.05; H, 5.22; N, 11.17. Found (%): C, 55.25; H, 4.99; N, 10.93.

1,3-Bis[(2,4,6-trimethylphenylimino)benzyl]imidazol-2-ylidene silver(I) iodide (2.14).

Sodium bis(trimethylsilyl)amide (45.4 mg, 0.248 mmol) was dissolved in toluene (5 mL) and added dropwise to a toluene (3 mL) suspension of silver tetrafluoroborate (47.1 mg, 0.242 mmol) at –37 °C. The reaction mixture was slowly warmed to room temperature and subsequently stirred for 1h. It was then filtered and added dropwise to a toluene (5 mL) suspension of 1,3-bis[(2,4,6-trimethylphenylimino)benzyl]imidazolium iodide **(2.11**) (80.2 mg, 0.145 mmol) at –37 °C. The reaction mixture was slowly warmed to room temperature and stirred for 7 h. The mixture was filtered and the volatiles were removed under vacuum. The brown solid product was further washed with pentane and dried under vacuum. Yield: 61.2 mg, 76%. ^{1}H NMR (300 MHz, C_6D_6): 8.19 (s, 2H, NC*H*C*H*N), 7.09–7.11 (b,10H, *o*-C$H_{(phenyl)}$ + *m*-C$H_{(phenyl)}$ + *p*-C$H_{(phenyl)}$), 6.72 (s, 4H, *o*-C$H_{(mesityl)}$), 2.14 (s, 12H, *o*-C$H_{3(mesityl)}$), 2.13 (s, 6H, *p*-C$H_{3(mesityl)}$); ^{13}C{^{1}H} NMR (75.5 MHz, C_6D_6): δ 153.7 (*C*=N), 142.7 ($C_{ipso(mesityl)}$), 133.3 ($C_{ipso(phenyl)}$), 132.5 (*o*-*C*$H_{(phenyl)}$), 130.2 (*p*-*C*C$H_{3(mesityl)}$), 129.4 (m-CH$_{(phenyl)}$ + p-CH$_{(phenyl)}$), 129.2 (m-CH$_{(mesityl)}$), 126.3 (o-CCH$_{3(mesityl)}$), 120.4 (NCCN), 20.7 (p-CH$_{3(mesityl)}$), 18.8 (o-CH$_{3(mesityl)}$). FTIR (neat): $\nu_{C=N}$ 1653 cm^{-1}. Anal. Calcd. for $C_{35}H_{34}AgIN_4$ (%): C, 56.39; H, 4.60; N, 7.52. Found (%): C, 56.64; H, 4.72; N, 7.29.

1,3-Bis[1-(2,6-dimethylphenylimino)ethyl]imidazol-2-ylidene copper(I) iodide (2.15).

Sodium bis(trimethylsilyl)amide (125 mg, 0.679 mmol) was dissolved in THF (3 mL) and added dropwise to a THF (3 mL) suspension of copper(I) iodide (125 mg, 0.656 mmol) at –37 °C. The reaction mixture was slowly warmed to room temperature and subsequently stirred for 1 h. It was then added dropwise to a THF (3 mL) suspension of 1,3-bis[1-(2,6-dimethylphenylimino)ethyl]imidazolium chloride (**2.7**) (259 mg, 0.656 mmol) at –37 °C. The reaction mixture was slowly warmed to room temperature and stirred for 7 h. The mixture was then filtered and the orange solid product was further washed with toluene and pentane. Yield: 279 mg, 77%. Crystals suitable for X-ray diffraction studies were grown at room temperature under nitrogen by vapor diffusion of pentane into a saturated dichloromethane solution. ^{1}H NMR (400 MHz, $CDCl_3$): δ 7.85 (s, 2H, NCHCHN), 6.97 (d, ^{3}J = 7.1 Hz, 4H, m-C$H_{(Xyl)}$), 6.81 (t, ^{3}J = 7.1 Hz, 2H, p-C$H_{(Xyl)}$), 2.38 (s, 6H, C$H_{3(imine)}$), 2.08 (s, 12H, o-C$H_{3(Xyl)}$); ^{13}C{^{1}H} NMR (100 MHz, $CDCl_3$): δ 154.0 (C=N), 144.9 ($C_{ipso(Xyl)}$), 128.2 (m-CH$_{(Xyl)}$), 127.2 (o-$C_{(Xyl)}$), 124.0 (p-CH$_{(Xyl)}$), 117.9 (NCCN), 18.8 (o-CH$_{3(Xyl)}$), 16.9 (CH$_{3(imine)}$). FTIR (neat) $\nu_{C=N}$ 1676 cm^{-1}. Anal. Calcd. For $C_{23}H_{26}N_4CuI$ (%): C, 50.32; H, 4.77; N, 10.21. Found (%): C, 50.31; H, 4.86; N, 10.25.

1,3-Bis[(2,4,6-trimethylphenylimino)benzyl]imidazol-2-ylidene copper(I) iodide (2.16).

Sodium bis(trimethylsilyl)amide (142 mg, 0.774 mmol) was dissolved in a THF (3 mL) and drop wise added to a THF (3 mL) suspension of copper(I) iodide (143 mg, 0.751) at –37°C. The reaction mixture was slowly warmed to room temperature and it was stirred for 1 h. It was then added dropwise to a THF (3 mL) suspension of 1,3-bis[(2,4,6-trimethylphenylimino)benzyl]imidazolium tetrafluoroborate (**2.10**) (449 mg, 0.751 mmol) at –37 °C. The reaction mixture was brought to room temperature and stirred for 7 h. The mixture was filtered and the filtrate was concentrated to about 1 mL. Pentane was added to precipitate a reddish-yellow solid that was further washed with toluene and pentane to give the desired product as a light-yellow solid (323 mg, 61%). Crystals suitable for X-ray diffraction study were grown at room temperature under nitrogen by slow liquid diffusion of pentane into a saturated THF solution. ^{1}H NMR (400 MHz, $CDCl_3$): δ 8.01 (s, 2H, NC*H*C*H*N), 7.31 (t, 2H, ^3J = 8.1 Hz, *p*-C$H_{3(\text{phenyl})}$), 7.29 (t, ^3J = 7.1 Hz, 4H, *m*-C$H_{(\text{phenyl})}$), 7.53 (d, ^3J = 7.1 Hz, 4H, *o*-C$H_{3(\text{phenyl})}$), 6.73 (s, 4H, *o*-C$H_{(\text{mesityl})}$), 2.19 (s, 6H, *p*-C$H_{3(\text{mesityl})}$), 2.03 (s, 12H, *o*-C$H_{3(\text{mesityl})}$); ^{13}C{^{1}H} NMR (75.5 MHz, $CDCl_3$): δ 185.6 (N*C*N), 152.7 (*C*=N), 141.9 ($C_{\text{ipso(mesityl)}}$), 133.5 (*p*-*C*$H_{3(\text{mesityl})}$), 132.3 (*p*-*C*$H_{(\text{phenyl})}$), 130.3 ($C_{\text{ipso(phenyl)}}$), 129.4 (*m*-*C*$H_{(\text{mesityl})}$), 129.1 (*o*-*C*$H_{(\text{phenyl})}$), 128.9 (*m*-$C_{(\text{mesityl})}$), 126.3 (*o*-*C*$H_{3(\text{mesityl})}$), 120.0 (N*CC*N), 20.8 (*p*-*C*$H_{3(\text{mesityl})}$), 18.7 (*o*-*C*$H_{3(\text{mesityl})}$). FTIR (neat) $\nu_{C=N}$ 1653 cm^{-1}. Anal. Calcd. For $C_{35}H_{34}N_4CuI$ (%): C, 59.96; H, 4.89; N, 7.99. Found (%): C, 59.55; H, 5.30; N, 7.87.

1,3-Bis[1-(2,6-dimethylphenylimino)ethyl]imidazol-2-ylidene iron(II) chloride (2.17).

Potassium bis(trimethylsilyl) amide (161 mg, 0.807 mmol) was dissolved in THF (6 mL) and added dropwise to a THF (4 mL) suspension of iron(II) chloride (100 mg, 0.790 mmol) at −37 °C. The reaction mixture was kept at −37 °C for 20 h and agitated occasionally. It was then filtered, and the filtrate was added dropwise to a THF (9 mL) suspension of 1,3-bis[1-(2,6-dimethylphenylimino)ethyl]imidazolium chloride (**2.7**) (297 mg, 0.752 mmol) at −37 °C. The reaction mixture was slowly warmed to room temperature and stirred for an additional 20 h. The mixture was then concentrated, and pentane was added to precipitate a yellow solid. The solid was dissolved in dichloromethane and then filtered. The volatile was removed under vacuum to give the product in 84% yield (244 mg, 0.503 mmol). Crystals suitable for X-ray diffraction studies were grown at −40 °C under nitrogen by slow diffusion of pentane into a saturated dichloromethane solution. FTIR (neat):$\nu_{C=N}$ 1695, 1685 cm^{-1}. Anal. Calcd. for $C_{23}H_{26}Cl_2FeN_4$ (%): C, 56.93; H, 5.40; N, 11.55. Found (%): C, 56.68; H, 5.62; N, 11.49.

1,3-Bis[1-(2,6-dimethylphenylimino)ethyl]imidazol-2-ylidene cobalt(II) chloride (2.18).

Potassium bis(trimethylsilyl) amide (67.6 mg, 0.340 mmol) was dissolved in THF (5 mL) and added dropwise to a THF (3 mL) suspension of cobalt(II) chloride (42.2 mg, 0.325 mmol) at −37 °C. The reaction mixture was kept at −37 °C for 22 h and agitated occasionally. It was then filtered, and the filtrate was added dropwise to a THF (3 mL) suspension of 1,3-bis[1-(2,6- dimethylphenylimino)ethyl]imidazolium chloride (**2.7**) (122 mg, 0.308 mmol) at −37 °C. The reaction mixture was slowly warmed to room temperature and stirred for an additional 22 h. It was then concentrated, and pentane was added to precipitate the product as a green solid (131 mg, 0.269 mmol, 87% yield). Crystals suitable for X-ray diffraction studies were grown at −40 °C under nitrogen from a saturated dichloromethane solution. FTIR (neat): $\nu_{C=N}$ 1685, 1652 cm^{-1}. Anal. Calcd. for $C_{23}H_{26}Cl_2CoN_4$ (%): C, 56.57; H, 5.37; N, 11.47. Found (%): C, 56.31; H, 5.48; N, 11.17.

1,3-Bis[1-(2,6-dimethylphenylimino)ethyl]imidazol-2-ylidene chromium(III) chloride (2.19).

A dichloromethane solution of $CrCl_3\cdot3THF$ (37.2 mg, 0.0993 mmol) was added, at room temperature, to a dichloromethane suspension of 1,3-bis[1-(2,6-dimethylphenylimino)ethyl]imidazol-2-ylidene silver(I) chloride (**2.12**) (49.8 mg, 0.0992 mmol). The reaction mixture was stirred overnight and subsequently filtered. The filtrate was collected, and the solvent was removed under vacuum. The residue was extracted with toluene, and the product was recovered as a light-olive green solid by removing the volatiles under reduced pressure. Yield: 29.6 mg, 0.0573 mmol, 58% yield. FTIR (neat): $\nu_{C=N}$ 1687, 1618 cm^{-1}. Anal. Calcd. for $C_{23}H_{26}Cl_3CrN_4$ (%): C, 53.17; H, 4.91; N, 11.11. Found (%): C, 53.45; H, 5.07; N, 10.84.

1,3-Bis[(2,4,6-trimethylphenylimino)benzyl]imidazol-2-ylidene chromium(III) chloride (2.20).

To a mixture of 1,3-bis[(2,4,6-trimethylphenylimino)benzyl]imidazol-2-ylidene copper(I) iodide (**2.16**) (160 mg, 0.229 mmol) and $CrCl_3\cdot3THF$ (86.3 mg, 0.230 mmol) was added 18 mL of toluene at room temperature, and the mixture was stirred for 44 h. The mixture was then filtered, and the solvent was removed under vacuum to give **2.20** as a light green solid (109 mg, 0.163 mmol, 71% yield). Crystals suitable for X-ray diffraction studies were grown under nitrogen by vapor diffusion of pentane into a saturated THF solution. FTIR (neat): $\nu_{C=N}$ 1653, 1617 cm^{-1}. Anal. Calcd. for $C_{35}H_{34}CrCl_3N_4$ (%): C, 62.83; H, 5.12; N, 8.37. Found (%): C, 62.59; H, 4.78; N, 8.51.

1,3-Bis[1-(2,6-dimethylphenylimino)ethyl]imidazol-2-ylidene palladium(II) allyl chloride (2.21).

Allyl palladium(II) chloride dimer (20.0 mg, 0.0547 mmol) was dissolved in a dichloromethane (5 mL) and added to a dichloromethane (8 mL) suspension of 1,3-bis[1-(2,6-dimethylphenylimino)ethyl]imidazol-2-ylidene silver(I) chloride (**2.12**) (55.0 mg, 0.110 mmol). The reaction mixture was stirred for 20 h in absence of light. The mixture was filtered and the volatiles were removed under vacuum. The brown solid product was further washed with pentane and dried under vacuum. Yield: 279 mg, 77%. ^{1}H NMR (400 MHz, $CDCl_3$) T = –50 °C: δ 8.38 (s, 2H, NC*H*C*H*N), 7.08 (d, ^3J = 2.6 Hz, 4H, *m*-C$H_{(Xyl)}$), 7.03 (t, ^3J = 7.4 Hz, 2H, *p*-C$H_{(Xyl)}$), 5.53 (m, ^3J = 6.2 Hz, 1H, C$H_{(allyl)}$), 3.73 (d, ^3J = 5.8 Hz, 1H, C$H_{(allyl\text{-}syn\ (trans\text{-}C))}$), 3.59 (d, ^3J = 6.8 Hz, 1H, C$H_{(allyl\text{-}syn\ (trans\text{-}Cl))}$), 3.34 (d, ^3J = 13.7 Hz, 1H, C$H_{(allyl\text{-}anti\ (trans\text{-}Cl))}$), 2.75 (d, ^3J = 12.2 Hz, 1H, C$H_{(allyl\text{-}anti\ (trans\text{-}C))}$), 2.65 (s, 6H, C$H_{3(imine)}$), 2.09 (s, 6H, *o*-C$H_{3(Xyl)}$), 2.04 (s, 6H, *o*-C$H_{3(Xyl)}$); ^{13}C{^{1}H} NMR (100 MHz, $CDCl_3$): δ 180.9 (N*C*N), 157.8 (*C*=N), 144.4 ($C_{ipso(Xyl)}$), 128.4 (*o*-$C_{(Xyl)}$), 126.5 (*m*-C$H_{(Xyl)}$), 125.2 (*p*-C$H_{(Xyl)}$), 121.4 (N*CC*N), 118.8 (*C*$H_{(allyl)}$), 74.2 (*C*$H_{2(allyl\text{-}trans\text{-}Cl)}$), 61.3 *C*$H_{2(allyl\text{-}trans\text{-}C)}$), 18.4 (*o*-*C*$H_{3(Xyl)}$), 18.3 (*C*$H_{3(imine)}$). FTIR (neat): $\nu_{C=N}$ 1676, 1653 cm^{-1}. Anal. Calcd. for $C_{26}H_{31}PdClN_4$ (%): C, 57.68; H, 5.77; N, 10.35. Found (%): C, 57.34; H, 5.90; N, 10.10.

1,3-Bis[1-(2,6-dimethylphenylimino)ethyl]imidazol-2-ylidene palladium(II) allyl tetrafluoroborate (2.22).

Silver tetrafluoroborate (22.7 mg, 0.0516 mmol) was added to a deuterated chloroform (0.6 mL) solution of 1,3-bis[1-(2,6-dimethylphenylimino)ethyl]imidazol-2-ylidene palladium(II) allyl chloride (**2.21**) (10.0 mg, 0.0513 mmol). The reaction mixture was stirred for 2 h in absence of light. The mixture was filtered to give a yellow solution. ^{1}H NMR (300 MHz, $CDCl_3$): δ 8.08 (d, ^{3}J = 2.0 Hz, 1H, NC*H*CN), 8.00 (d, ^{3}J = 2.1 Hz, 1H, NCC*H*N), 7.03–7.11 (m, 4H, *m*-C$H_{(Xyl)}$ + 1H, *p*-C$H_{(Xyl)}$,), 7.01 (t, ^{3}J = 1.2 Hz, 1H, *p*-C$H_{(Xyl)}$), 5.60 (m, ^{3}J = 6.5 Hz, 1H, C$H_{(allyl)}$), 3.85 (d, ^{3}J = 6.8 Hz, 1H, C$H_{(allyl\text{-}syn\ (trans\text{-}C))}$), 3.34 (d, ^{3}J = 10.0 Hz, 1H, C$H_{(allyl\text{-}anti\ (trans\text{-}N))}$), 3.31 (d, ^{3}J = 4.2 Hz, 1H, C$H_{(allyl\text{-}syn\ (trans\text{-}N))}$), 2.95 (d, ^{3}J = 12.3 Hz, 1H, C$H_{(allyl\text{-}anti\ (trans\text{-}C))}$), 2.52 (s, 3H, C$H_{3(imine)}$), 2.43 (s, 3H, C$H_{3(imine)}$), 2.28 (s, 3H, *o*-C$H_{3(Xyl)}$), 2.13 (s, 3H, *o*-C$H_{3(Xyl)}$), 2.07 (s, 6H, *o*-C$H_{3(Xyl)}$); ^{13}C{^{1}H} NMR (100 MHz, $CDCl_3$): δ 180.0 (N*C*N), 165.2 (*C*=N), 153.7 (*C*=N), 145.3 (*o*-$C_{(Xyl)}$), 144.5 (*o*-$C_{(Xyl)}$), 129.1 (*m*-*C*$H_{(Xyl)}$), 128.9 (*m*-*C*$H_{(Xyl)}$), 128.8 ($C_{ipso(Xyl)}$), 128.6 (*m*-*C*$H_{(Xyl)}$), 127.3 (*o*-$C_{(Xyl)}$), 125.7 ($C_{ipso(Xyl)}$) 124.7 (*p*-*C*$H_{(Xyl)}$), 122.1 (NC*C*N), 120.93 (*C*$H_{(allyl)}$), 120.3 (N*C*CN), 74.8 (*C*$H_{2(allyl\text{-}trans\text{-}N)}$), 56.1 *C*$H_{2(allyl\text{-}trans\text{-}C)}$), 19.2 (*o*-*C*$H_{3(Xyl)}$), 18.36 (*o*-*C*$H_{3(Xyl)}$), 18.12 (*o*-*C*$H_{3(Xyl)}$), 14.8 (*C*$H_{3(imine)}$). ^{19}F NMR (282 MHz, $CDCl_3$): δ –152.0. FTIR (neat): $\nu_{C=N}$ 1685, 1655 cm^{-1}. Anal. Calcd. for $C_{26}H_{31}BF_4N_4Pd$ (%). C, 52.68; H, 5.27; N, 9.45. Found (%) C, 52.41; H, 4.98; N, 9.30.

1,3-Bis[1-(2,6-dimethylphenylimino)ethyl]imidazol-2-ylidene zinc(II) chloride (2.23).

Sodium bis(trimethylsilyl)amide (125 mg, 0.682 mmol) was dissolved in THF (3 mL) and added dropwise to a THF (3 mL) suspension of zinc(II) chloride (121 mg, 0.662 mmol) at –37 °C. The reaction mixture was slowly warmed to room temperature and subsequently stirred for 80 minutes. It was then filtered and added dropwise to a THF (4 mL) suspension of 1,3-bis[1-(2,6-dimethylphenylimino)ethyl]imidazolium chloride (**2.7**) (261 mg, 0.662 mmol) at –37 °C. The reaction mixture was slowly warmed to room temperature and stirred for 3 h. The solvent was removed in vacuum to give light yellow solid product that was further washed with 12 mL of toluene and 12 mL of pentane. Yield: 249 mg, 76%. Crystals suitable for X-ray diffraction studies were grown at room temperature under nitrogen by vapor diffusion of pentane into a saturated dichloromethane solution. ^{1}H NMR (400 MHz, $CDCl_3$): δ 8.05 (s, 2H, NC*H*C*H*N), 7.11 (d, ^{3}J = 1.2 Hz, 4H, *m*-C$H_{(Xyl)}$), 7.08 (t, ^{3}J = 9.2 Hz, 2H, *p*-C$H_{(Xyl)}$), 2.49 (s, 6H, C$H_{3(imine)}$), 2.17 (s, 12H, *o*-C$H_{3(Xyl)}$); ^{13}C{^{1}H} NMR (100 MHz, $CDCl_3$): δ 179.0 (N*C*N), 155.2 (*C*=N), 142.4 ($C_{ipso(Xyl)}$), 128.4 (*m*-*C*$H_{(Xyl)}$), 128.0 (*o*-$C_{(Xyl)}$), 126.0 (*p*-*C*$H_{(Xyl)}$), 119.7 (N*CC*N), 18.5 (*o*-*C*$H_{3(Xyl)}$), 16.2 (*C*$H_{3(imine)}$). FTIR (neat) $\nu_{C=N}$ 1689, 1660 cm^{-1}. Anal. Calcd. for $C_{23}H_{26}ZnCl_2N_4$ (%): C, 55.83; H, 5.30; N, 11.32. Found (%): C, 56.02; H, 5.11; N, 11.51.

1,3-Bis[(2,4,6-trimethylphenylimino)benzyl]imidazol-2-ylidene zinc(II) iodide (2.24).

Sodium bis(trimethylsilyl)amide (17 mg, 0.092 mmol) was dissolved in a THF (3 mL) and dropwise added to a THF (3 mL) suspension of zinc(II) iodide (29 mg, 0.075) at –37°C. The reaction mixture was slowly warmed to room temperature and stirred for 1 h. It was then added dropwise to a THF (3 mL) suspension of 1,3-bis[(2,4,6-trimethylphenylimino)benzyl]imidazolium tetrafluoroborate (**2.10**) (52 mg, 0.087 mmol) at –37 °C. The reaction mixture was brought to room temperature and stirred for 3.5 h. The mixture was filtered and the solvent was removed in vacuum to give a yellow solid that was washed with toluene and pentane to give the desired product (45.5 mg, 62%). ^{1}H NMR (400 MHz, $CDCl_3$): δ 7.68 (s, 2H, NC*H*C*H*N), 7.51 (t, 2H, ^{3}J = 7.0 Hz, *p*-C$H_{(phenyl)}$), 7.43 (t, ^{3}J = 7.6 Hz, 4H, *m*-C$H_{(phenyl)}$), 7.37 (d, ^{3}J = 7.4 Hz, 4H, *o*-C$H_{(phenyl)}$), 6.72 (s, 4H, *o*-C$H_{(mesityl)}$), 2.18 (s, 18H, *p*-C$H_{3(mesityl)}$ + *o*-C$H_{3(mesityl)}$); ^{13}C{^{1}H} NMR (100 MHz, $CDCl_3$): δ 181.8 (N*C*N), 153.9 (*C*=N), 140.1 (*p*-*C*$H_{(mesityl)}$), 132.4 (*p*-*C*$H_{(phenyl)}$), 129.6 (*o*-*C*$H_{(phenyl)}$), 129.2 (*o*-*C*$H_{3(phenyl)}$), 129.1 (*m*-*C*$H_{(mesityl)}$), 128.4 (*o*-$C_{(mesityl)}$), 127.7 ($C_{ipso(phenyl)}$), 125.4 ($C_{ipso(mesityl)}$), 121.1 (N*CC*N), 20.9 (*p*-*C*$H_{3(mesityl)}$), 18.5 (*o*-*C*$H_{3(mesityl)}$). FTIR (neat) $\nu_{C=N}$ 1667, 1653 cm^{-1}. Anal. Calcd. for $C_{35}H_{34}ZnI_2N_4$ (%): C, 50.66; H, 4.13; N, 6.75. Found (%): C, 50.39; H, 4.09; N, 6.86.

General Procedure for Ethylene Polymerization

Ethylene polymerization was performed at atmospheric pressure and room temperature in a 500 mL Schlenk flask containing a magnetic stir bar. The flask was conditioned in an oven at 130 °C for at least 18 h prior to use. The hot flask was brought to room temperature under a dynamic vacuum and backfilled with ethylene. Under an atmosphere of ethylene, the flask was charged with 20 mL of dry toluene and 1000 equivalents of MAO with respect to the catalyst (7.5−8.7 μmol). The solution was stirred for 10−15 min before a solution of the catalyst in either toluene or dichloromethane was introduced into the flask via a syringe. The reaction mixture was vigorously stirred for 10 min after the addition of the catalyst and subsequently quenched with a 1:1 mixture of concentrated hydrochloric acid and methanol. The resulting mixture was filtered, and any solid collected was washed with distilled water. Solids collected were dried under vacuum at approximately 50 °C for 24 h. The chromium complexes **2.19** and **2.20** gave respectively 28 mg (3.5 kg of PE mol^{-1} of

Cr; 21 kg of PE mol^{-1} of Cr h^{-1}) and 46 mg (5.7 kg of PE mol^{-1} of Cr; 34 kg of PE mol^{-1} of Cr h^{-1}) of polyethylene, as averages of two 10 min runs.

X-ray crystallographic data for **2.7**, **2.10**, **2.15**, **2.16**, **2.17**, **2.18**, **2.20**, **2.21** and **2.23** were collected at the University of Toronto on a Bruker-Nonius Kappa-CCD diffractometer using monochromated Mo Kα radiation (λ = 0.71073 Å) at 150 K and were measured using a combination of ϕ scans and ω scans with κ offsets, to fill the Ewald sphere. Intensity data were processed using the Denzo-SMN package.[98] Absorption corrections were carried out using SORTAV.[99] The structures were solved and refined using a combination of Superflip,[100] SHELXS-97 (for **2.21**),[101] SIR-92 (for **2.10**),[102] and SHELXTL V6.1 (for **2.7**, **2.15**, **2.16**, **2.17**, **2.18**, **2.20**, **2.23**)[103] for full-matrix least squares refinement based on F^2. All H atoms were included in calculated positions and allowed to refine in riding-motion approximation with U_{iso} tied to the carrier atom.

Chapter Three

Synthesis, Characterization and Reactivity Study of Bis(imino)benzimidazol-2-ylidene Transition Metal Complexes

2nd Generation

The variations of steric and electronic properties of iron and cobalt complexes containing 2,6-bis(imino)pyridine ligands led to important structure-property relationships in oligomerization and polymerization of ethylene.[16c,16e,18,21a,70a,70b,104] For example, the nature of the nitrogen substituents in these ligands controls the activity of the corresponding catalysts and the resulting polymer properties.[70b]

In the previous chapter, the synthesis of a new family of first generation of 1,3-bis(imino)imidazol-2-ylidene ligand precursors with different counter anions and substituents on the iminic carbon, and the corresponding transition metal complexes were described.[73] The stability and reactivity of the ligand precursors and the resulting complexes were affected by a counter anion and iminic substituents. These first generation complexes[73] demonstrated ligands coordinated to Cr(III), Fe(II), Co(II), Pd(II) and Cu(I) in either a mono- or bidentate coordination fashion, as determined by X-ray diffraction studies. The catalytic ethylene polymerization activity of these chromium(III) complexes showed that the catalyst with electron-poor substituents (phenyl groups) on the iminic carbon was more active than the related methyl analogous.[73b] This suggests that improved activities may be achieved in olefin polymerization by enhancing the π-accepting or decreasing the electron-donating ability of the ligand.

The ligand scaffold was then further modified by introducing benzimidazole moiety considered as a less σ-electron donating[105] and a better π-accepting ligand[106] than its counterpart. Moreover, the π-acidic character of the imine fragments increases the electropositive nature of the resulting transition metal complexes and therefore this may lead to a higher activity than that of the complexes of 2,6-bis(NHC)pyridine.[23a-c,23e] The more opened coordination sphere provided by the new 5-membered ring of this ligand than that of the related 6-membered ring of 2,6-bis(imino)pyridine[15,16d] and 2,6-bis(NHC)pyridine[23a-c,23e] ligands could potentially facilitate the coordination of α-olefins.

In this chapter, the synthesis, characterization and coordination of the first bis(imino)benzimidazol-2-ylidene ligands and their corresponding transition metal complexes will be discussed. The targeted tridentate coordination mode of the benzimidazol-2-ylidene ligand to a metal center could possibly be favored by increasing the steric bulk of the fused benzene ring. Moreover, the less σ-electron donating[105] and better π-accepting ability of this ligand[106] than the imidazol-2-ylidene ligand may lead to a less electron-rich metal center and may favor a tridentate coordination mode. The catalytic polymerization activity of the analogous complexes of Cr(III), Fe(II) and Co(II) bearing benzimidazol-2-ylidene ligand will also be presented.

3.1 Synthesis of 1,3-bis(imino)ethyl/benzyl benzimidazolium salts

The 1-iminoethylbenzimidazole compounds **3.3** and **3.4** were prepared by the reaction of benzimidazole with the corresponding *N*-imidoyl chloride (**3.1** and **3.2**, respectively) in excellent yields (Scheme 3.1).

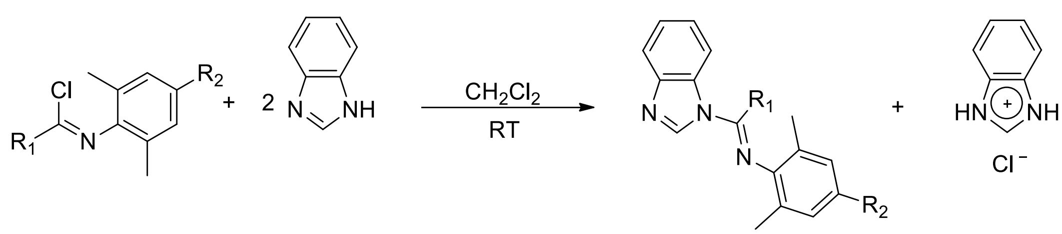

R_1=Me, R_2=H **3.1**
R_1=Ph, R_2=Me **3.2**

R_1=Me, R_2=H **3.3**
R_1=Ph, R_2=Me **3.4**

Scheme 3.1. Synthesis of 1-iminoethylimidazole **3.3** and **3.4**.

The 1,3-bis[1-(2,6-dimethylphenylimino)ethyl]benzimidazolium chloride (**3.5**) was synthesized in 80% yield by the reaction of the 1-iminoethylbenzimidazole (**3.3**) and *N*-(2,6-dimethylphenyl)acetimidoyl chloride (**3.1**) in toluene (Scheme 3.2). A single $\nu_{C=N}$ stretching frequency at 1690 cm^{-1} was identified, similar to that of the analogous compound **2.7**. The ^{1}H NMR ($CDCl_3$) spectrum of **3.5** showed both *E,Z*- and *E,E*-isomers. The benzimidazolium proton (–NC*H*N–) of the minor *E,E*-isomer displayed a resonance at the most downfield position of δ 12.27. The backbone protons resonated at δ 9.02 (–NCC*H*CH–) and δ 7.75 (–NCCHC*H*–) with the corresponding ^{13}C resonances identified at δ 118.9 (–NC*C*HCH–) and δ 129.2 (–NCCH*C*H–). The ^{13}C resonances for central benzimidazolium and iminic carbon appeared at δ 126.1 and 153.2, respectively.

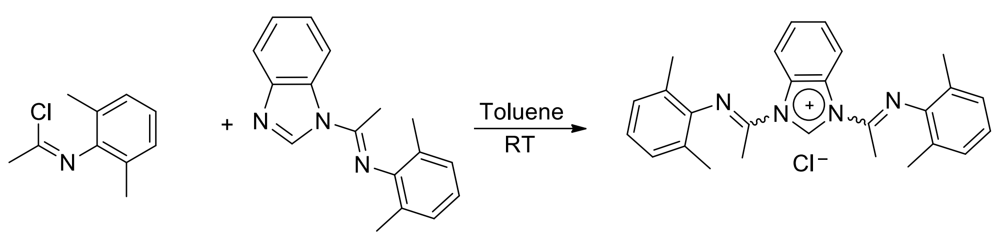

3.1 **3.3** **3.5**

Scheme 3.2. Synthesis of benzimidazolium salt **3.5**.

The analogous 1,3-bis[(2,4,6-trimethylphenylimino)benzyl]benzimidazolium tetrafluoroborate **3.6** was synthesized by the reaction of the *in situ* generated nitrilium salt with mono-substituted benzimidazole **3.4** in 92% yield (Scheme 3.3). Compound **3.6** is an NHC ligand precursor with a reduced σ-electron donating ability (e.g. replacing imidazole-2-ylidene with benzimidazol-2-ylidene) and electron-poor substituents (phenyl group) on the iminic carbons. The benzimidazolium proton (–NC*H*N–) resonance appeared at δ 9.59, as shown in the ^{1}H NMR ($CDCl_3$) spectrum of **3.6**. The iminic (*C*=N) and the central

(N*C*N) carbon atoms resonated at δ 149.4 and 142.8, respectively. The FTIR $\nu_{C=N}$ stretching frequency was observed at 1674 cm^{-1} for **3.6** lower by 16 cm^{-1} than in the analogous **3.5**.

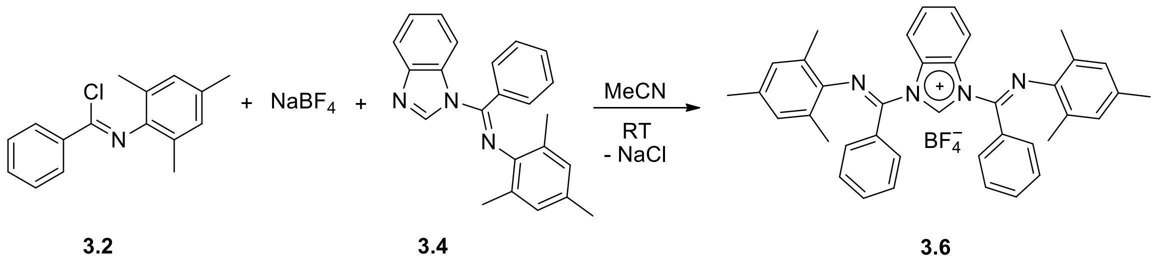

Scheme 3.3. Synthesis of benzimidazolium salt **3.6**.

3.2 Attempts of isolating the free carbene

Attempts to deprotonate the benzimidazolium salt **3.6** using either NaH, KH, $NaOC(CH_3)_3$ or lithium mesityl led to decomposition of the salt. In contrast, the reaction of potassium bis(trimethylsilyl)amide with the benzimidazolium salt (**3.6**) afforded a mixture of undefined compounds. However, the precipitation of the concentrated solution of this mixture led to the amine adduct (**3.7**), the corresponding anilide and unknown byproducts (Scheme 3.4). The anilide was probably formed from the hydrolysis of the parent salt (**3.6**) or the amine adduct (**3.7**).

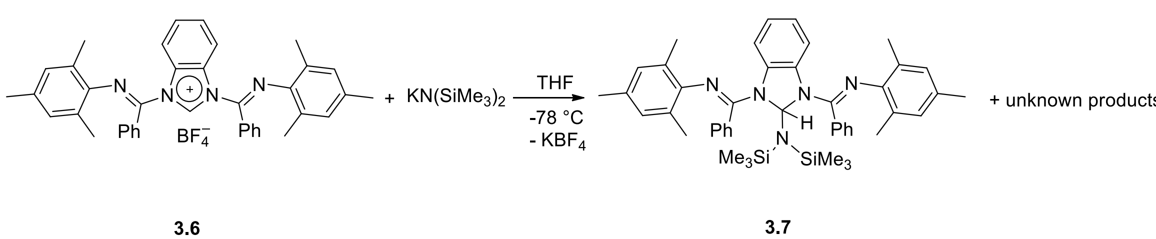

Scheme 3.4. Reaction of benzimidazolium salt **3.6** with $KN(SiMe_3)_2$.

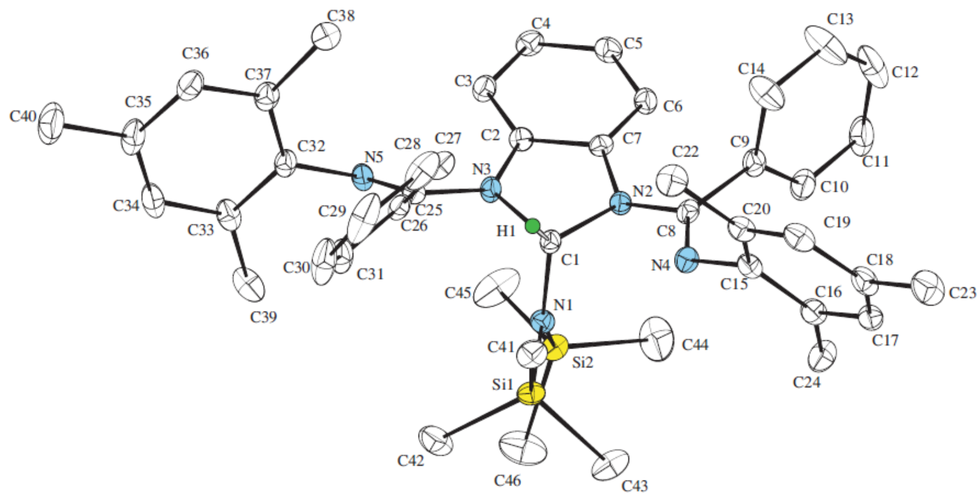

Figure 3.1. ORTEP of **3.7** (50% probability level). Hydrogen atoms are omitted for clarity. Selected bond lengths (Å) and angles (deg.). N1–C1 1.451(3), N2–C1 1.486(3), N3–C1 1.487(3), N2–C7 1.425(3), N3–C2 1.397(3), C2–C7 1.398(3), N4–C8 1.284(3), N5-C25 1.281(3), N2–C1–N3 100.27(17), N2–C1–N1 114.49(18), N3–C1–N1 114.28(18), C1–N2–C7 110.53(17), C1–N3–C2 111.08(18), C1–N3–C25 123.45(18), C1–N2–C8 118.03(18).

Crystals of **3.7** suitable for an X-ray diffraction study were obtained from a saturated benzene solution at room temperature. The molecule crystallized in the $P2_1/n$ space group with a distorted tetrahedral geometry around the central carbon (C1), as shown in Figure 3.1. The bond angles N3–C1–N1 and N2–C1–N1 are 114.28(18)^o and 114.49(18)^o, respectively. The N1–C1 bond length is 1.451(3) Å. The bond lengths of N2–C1 and N3–C1 are 1.486(3) and 1.487(3) Å, respectively, and they are longer than that of the reported value of the central carbon-nitrogen bond of the benzimidazolium ring of 1,3-dibenzyl-2,3-dihydro-1-H-benzimidazol-2-ylacetonitrile adduct (1.367(2) Å).[107] Due to the absence of π-electron delocalization in the benzimidazole ring, these bonds are relatively elongated compared to N2–C7 (1.425(3) Å) and N3–C2 (1.397(3) Å). The length of iminic bond N4–C8 (1.284(3) Å) is comparable to that of N5–C25 (1.281(3) Å). The bond angle N2–C1–

N3 (100.27(17)º) is smaller than that of the central benzimidazolium bond angle (N–C–N) (106.37(19)º) for the reported structure of benzimidazol-2-ylacetonitrile adduct.[107] The angle C1–N3–C25 (123.45(18)º) is wider than the angle C1–N2–C8 (118.03(18)º) in which N4 is pointed toward N1.

The attempted deprotonation of the benzimidazolium salt **3.6** with lithium mesityl led to a mixture of unknown products (Scheme 3.5). After precipitation from the concentrated benzene solution of this mixture, the decomposed compound **3.8**, the corresponding anilide and multiple byproducts were observed. The compound **3.8** may be generated by the reaction of the assumed reactive free carbene with the benzimidazolium salt. Then, the hydrolysis reaction led to the corresponding anilide (proposed mechanism A, Scheme 3.6). On the other hand, the benzimidazolium salt could be hydrolyzed and then the mono-substituted benzimidazole could have reacted with the counter ion (BF_4^-) to generate compound **3.8** (proposed mechanism B, Scheme 3.6). Compound **3.8** was also independently synthesized by the reaction of mono-substituted benzimidazole **3.4** with boron trifluoride-diethyl etherate adduct in toluene (Scheme 3.7) (76% yield).

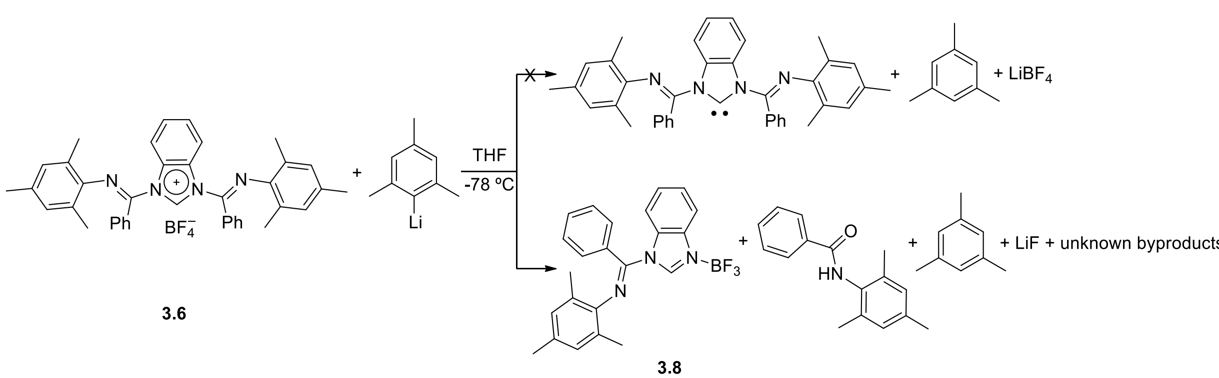

Scheme 3.5. Attempt for deprotonating benzimidazolium salt **3.6**.

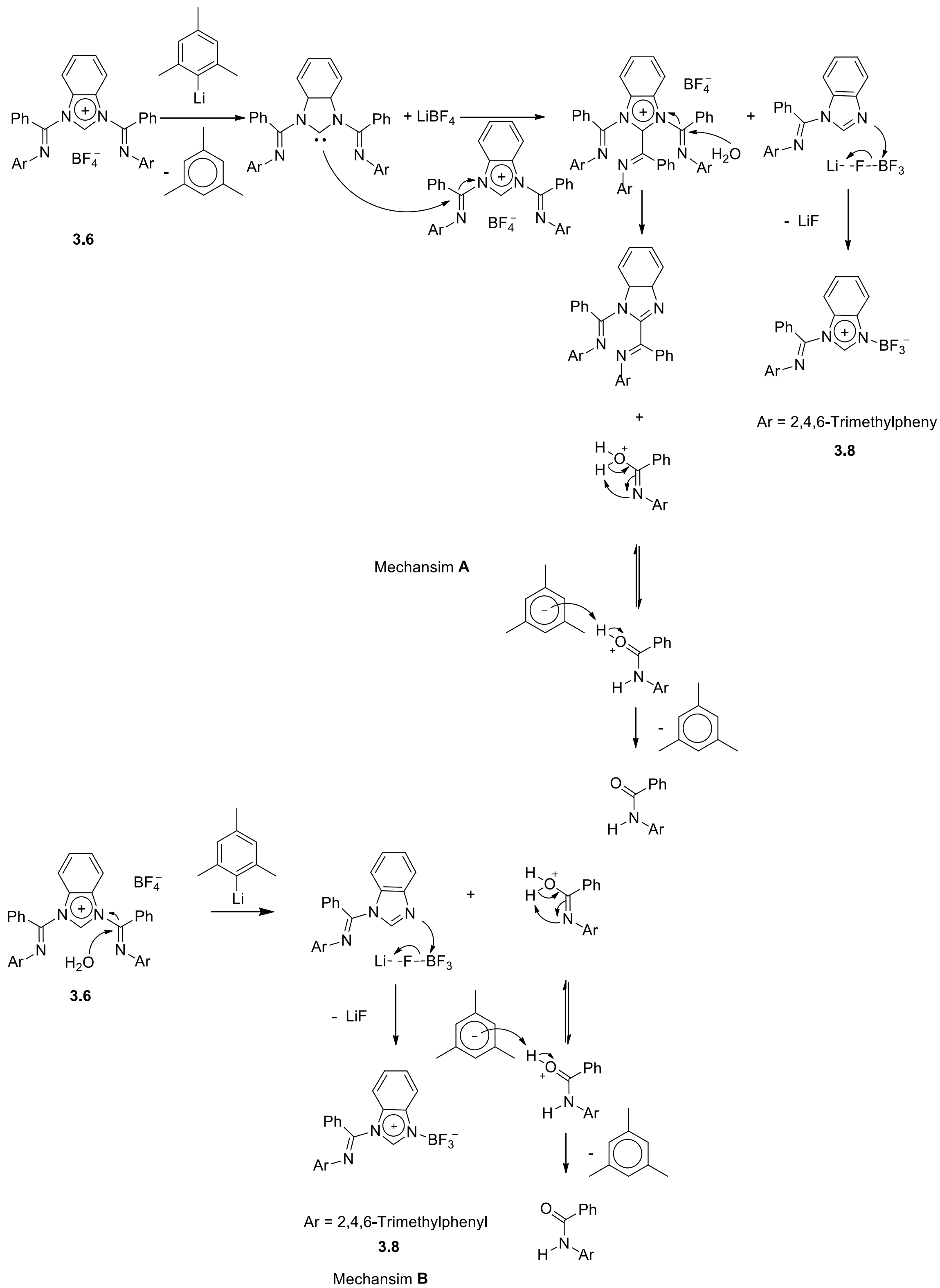

Scheme 3.6. Possible decomposition pathways for benzimidazolium salt **3.6**.

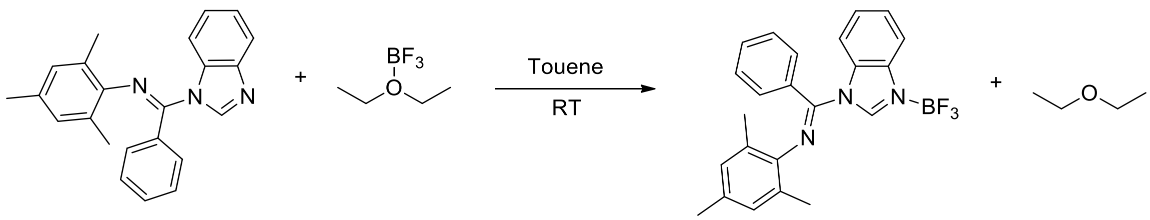

Scheme 3.7. The reaction of **3.4** with boron trifluoride-diethyl etherate adduct.

X-ray-quality crystals of **3.8** were grown from a concentrated benzene solution of the reaction outcome and the molecule crystallized in the $P2_1/a$ space group (Figure 3.2). The bond lengths of N1–C1 (1.313(3) Å), and N2–C1 (1.353(3), Å) are shorter than the single nitrogen–carbon bond of bis(NBF_3) adduct (1,3-dimethyl-1,3-diazolidine).[108] Also, the bond angle N1–C1–N2 (107.4(2)°) is comparable to the reported value of N–C–N (107.6(12)°) for bis(NBF_3).[108] The bond length of N1–B1 (1.588(4) Å) is shorter than the average distance of the published value of nitrogen–boron bonds of bis(NBF_3) adduct.[108]

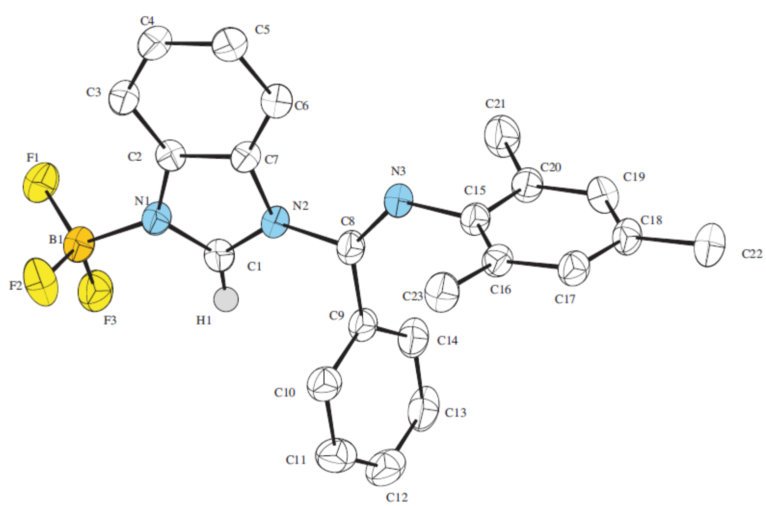

Figure 3.2. ORTEP of **3.8** (50% probability level). Selected bond lengths (Å) and angles (deg). N1–C1 1.313(3), N2–C1 1.353(3), C2–C7 1.398(3), N1–C2 1.403(3), N2–C7 1.415(3), N1–B1 1.588(4), N2–C8 1.434(3), N3–C8 1.271(3), N1–C1–N2 107.4(2), C1–N1–B1 124.9(2), N2–C8–N3 115.8(2).

3.3 Synthesis of NHC transition metal complexes

3.3.1 Bis(imino)benzimidazol-2-ylidene silver complex

Since the isolation of the free carbene was not possible, the corresponding silver carbene complex can be used as a transmetalating agent to afford the related carbene transition metal complexes.[61,77] The procedures utilized in Chapter 2 for the synthesis of the first generation of bis(imino) imidazole-2-ylidene transition metal complexes[73] were also used to afford the related the bis(imino) benzimidazole-2-ylidene transition metal complexes. The filtrate of *in situ* generated silver amide $Ag[N(SiMe_3)_2]$ was added to a toluene suspension of the benzimidazolium salt (**3.5**) at low temperature and the desired silver adduct ($[C_{benz}(\text{^}Imine_{Me})_2]AgCl$) (**3.9**) was afforded as precipitate in 49% yield (Scheme 3.8).

After coordination, the central benzimidazolium proton observed for the parent salt **3.5** disappeared and a single isomer was shown in the ^{1}H NMR ($CDCl_3$) spectrum of **3.9**. The backbone protons (−NCC*H*CH−) and (−NCCHC*H*−) resonances appeared at δ 8.37 and 7.55, respectively, upfield with respect to those of the salt **3.5**. In the $^{13}C\{^1H\}$ NMR spectrum, the iminic carbon (*C*=N) nucleus resonated at δ 155.0, a higher frequency than that of **3.5**. Similar to $[C_{imi}(\text{^}Imine_{Me})_2]AgCl$ **2.12**, the carbene resonance was not observed due to the labile character of the silver-carbene bond,[61,80] long relaxation time and low solubility. As in $[C_{imi}(\text{^}Imine_{Me})_2]AgCl$ **2.12**, a monodentate coordination fashion of the ligand through the carbene center is expected based on a single IR stretching frequency for the C=N bond at 1675 cm^{-1} for **3.9**.

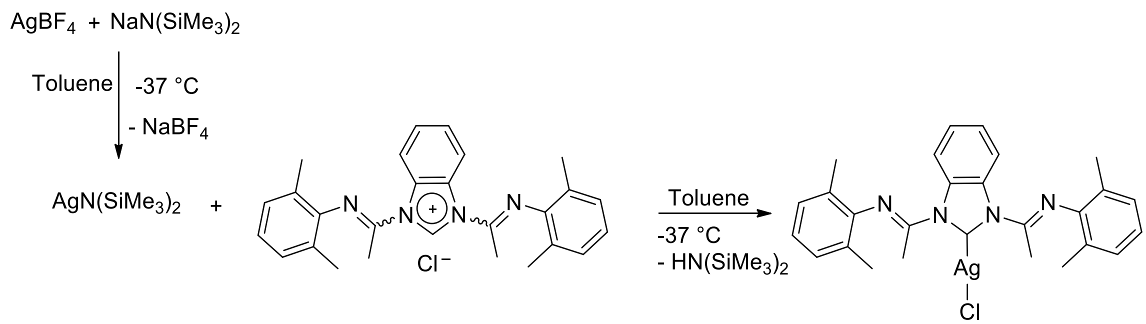

3.5

3.9

Scheme 3.8. Synthesis of the benzimidazol-2-ylidene silver(I) complex **3.9**.

3.3.2 Bis(imino)benzimidazol-2-ylidene copper and chromium complexes

The copper complex ([C_{benz}(^$Imine_{Me}$)$_2$]CuI) (**3.10**) was used as a transmetalating agent to the related carbene transition metal complexes and it was afforded by the analogous procedure of synthesizing [C_{imi}(^$Imine_{Me}$)$_2$]CuI (**2.15**).[109] The reaction of the *in situ* generated copper amide with the salt **3.5** give complex **3.10** in 28% yield, as an orange solid (Scheme 3.9). Two IR stretching frequency bands at 1668 and 1653 cm^{-1} were observed for **3.10**. This suggests that a bidentate coordination fashion of the ligand to each metal center of the dimeric complex with bridging iodides. The benzimidazol-2-ylidene backbone proton resonances shifted upfield to δ 8.44 (−NCC*H*CH−) and δ 7.41 (−NCCHC*H*−) compared to the parent salt **3.5**. The corresponding ^{13}C{^{1}H} NMR resonances presented lower chemical shifts at δ 116.3 (−NC*C*HCH−) and δ 125.3 (−NCCH*C*H−) than those in **3.5**. A higher chemical shift for the iminic carbon resonance was observed at δ 156.6 than those of the related bis(imino)-imidazol-2-ylidene copper(I) iodide complexes (**2.15** and **2.16**).[73a] The low solubility of the complex and long relaxation times of the carbene carbon (−N*C*N−) prevent the observation of its resonance in ^{13}C spectrum of **3.10**.

Synthesis of the more electropositive Cr(III) complex with the benzimidazol-2-ylidene ligand was investigated to test its activity toward ethylene polymerization and to force the ligand in a tridentate coordination fashion. The reaction of complex **3.10** with $CrCl_3{\cdot}3THF$ gave $[C_{benz}(\wedge Imine_{Me})_2]CrCl_3$ (**3.11**) in 71% yield (Scheme 3.9).[109] Complex **3.11** is a paramagnetic species with magnetic susceptibility of 3.75 μB, as measured by the Evans method,[83] is consistent with reported values for similar Cr(III) complexes[87-88,110] and with the predicted value (μ_{eff} = 3.87 μB) for three unpaired electrons. A bidentate coordination mode for the ligand is predicted in **3.11** based on the two IR stretching frequency bands observed for the iminic groups at 1683 and 1622 cm^{-1}.

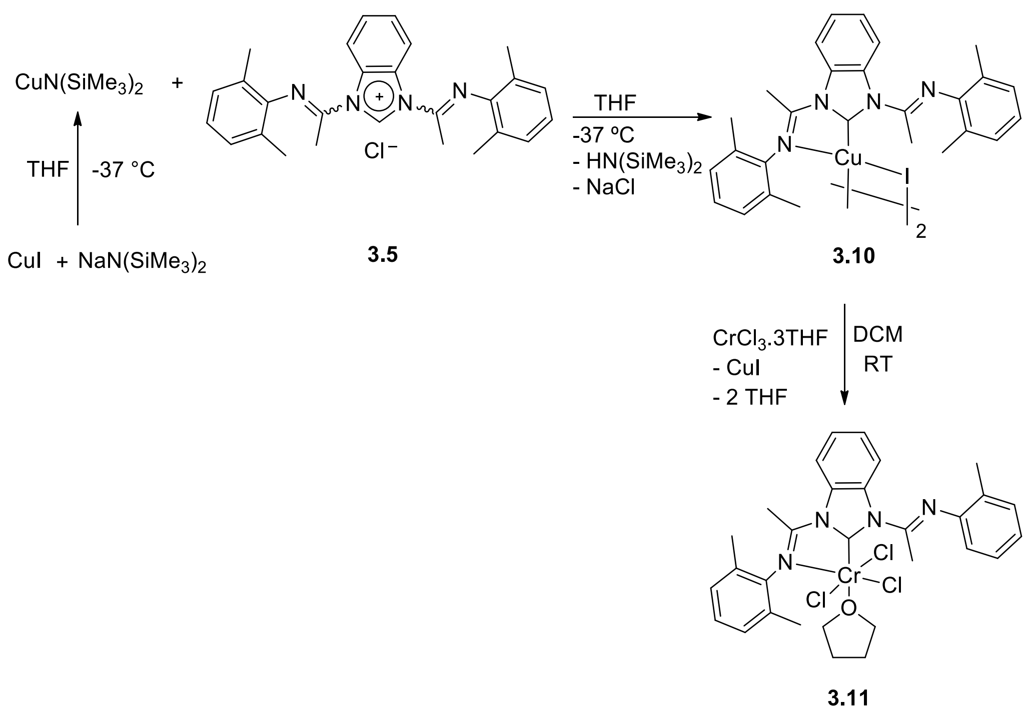

Scheme 3.9. Synthesis of the benzimidazol-2-ylidene copper and chromium complexes **3.10** and **3.11**.

The reaction of the *in situ* generated $CuN(SiMe_3)_2$ with a benzimidazolium tetrafluoroborate salt **3.6** at –37 °C was attempted (Scheme 3.10), however analysis of the crude reaction mixture by ^{1}H NMR spectroscopy displayed broad resonances. The reaction of the expected complex **3.12** with $CrCl_3{\cdot}3THF$ led to the decomposition of the complex to undefined compounds and to the corresponding benzimidoyl chloride (Scheme 3.10), as evidenced by the ^{1}H NMR spectrum. The decomposition of **3.12** may be due to reducing the overall electron density by incorporating benzimidazol-2-ylidene with phenyl group substituents and coordinating the ligand to electron-deficient metal (Cr(III)). This resulted in the more electropositive iminic carbon atoms which could easily be attracted by a chloride anion and therefore led to decomposition of the expected complex.

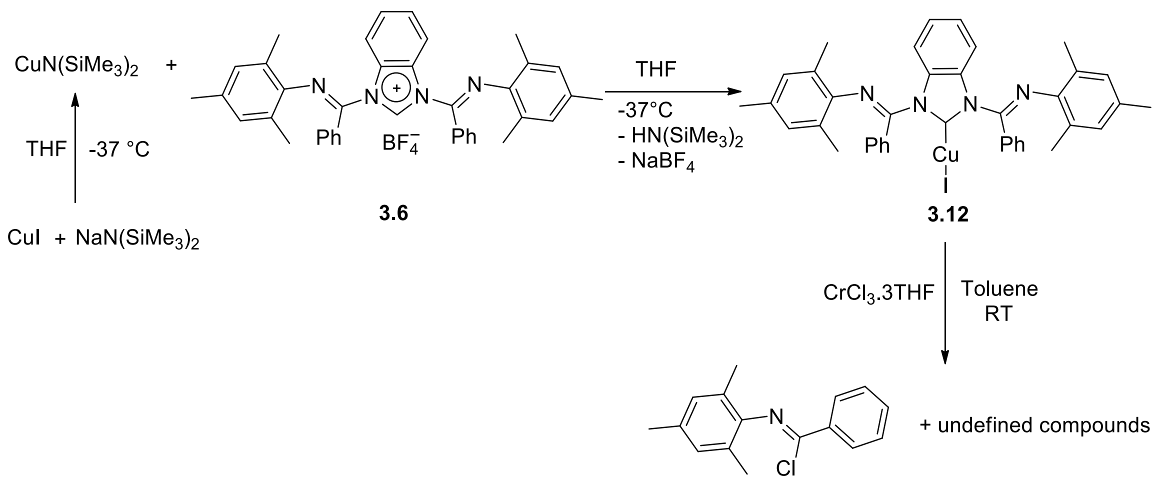

Scheme 3.10. Attempt to synthesize the benzimidazol-2-ylidene copper (I) complex **3.12**.

3.3.3 Bis(imino)benzimidazol-2-ylidene iron and cobalt complexes

The benzimidazol-2-ylidene iron and cobalt complexes were synthesized for evaluating their activity in ethylene polymerization. Using the procedure previously used in Chapter 2 for the synthesis of the related imidazol-2-ylidene transition metal complexes,[73b] the iron

([C_{benz}(^$Imine_{Me}$)$_2$]$FeCl_2$) **3.13** and cobalt ([C_{benz}(^$Imine_{Me}$)$_2$]$CoCl_2$) (**3.14**) complexes were synthesized by adding FeCl[N($SiMe_3$)$_2$] or CoCl[N($SiMe_3$)$_2$], generated *in situ* by reaction of KN($SiMe_3$)$_2$ with MCl_2, to a THF suspension of the benzimidazolium salt **3.5** at −37 °C in 71% and 62% yields,[109] respectively (Scheme 3.11). The magnetic susceptibility of the paramagnetic high-spin complexes **3.13** and **3.14** were 5.86 and 4.27 μB, respectively, as measured using the Evans method.[83] These values are in agreement with the predicted four and three unpaired electrons for the iron and cobalt complexes, respectively. They are also consistent with those reported for related iron[15,16c,73b,84,111] and cobalt[16c,73b,112] complexes. As previously observed in the first generation of carbene iron and cobalt complexes (Chapter 2), a bidentate coordination of the ligand to the metal center is predicted based on the two IR stretching frequency bands for the iminic bonds in **3.13** (1683 and 1629 cm^{-1}) and **3.14** (1683 and 1607 cm^{-1}).[73b]

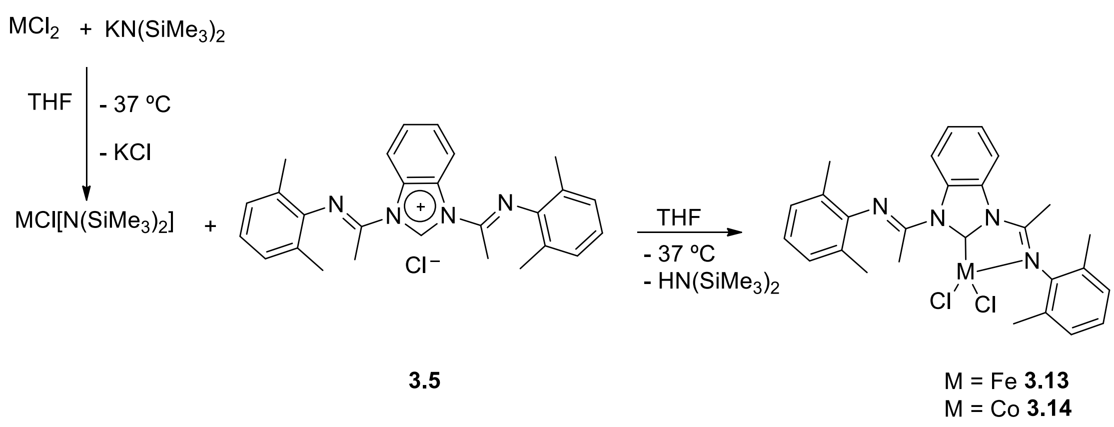

Scheme 3.11. Synthesis of the benzimidazol-2-ylidene iron(II) **3.13** and cobalt(II) **3.14** complexes.

3.4 Polymerization of ethylene

The catalytic activity of complexes **3.11, 3.13** and **3.14** toward ethylene polymerization was evaluated with 1000 equivalents of methylaluminoxane as a cocatalyst under ambient conditions. The activity for these complexes are comparable to that observed for the related first generation complexes.[73b] The chromium complex $[C_{benz}(^\wedge Imine_{Me})_2]CrCl_3$ (**3.11**) gave activities of 23 kg of PE mol^{-1} of Cr h^{-1}. Surprisingly, incorporating a lesser σ-electron donating NHC ligand (e.g. benzimidazole-2-ylidene) into the ligand scaffold did not greatly enhance the reactivity compared to that of imidazole-2-ylidene chromium complex $[C_{imi}(^\wedge Imine_{Me})_2]CrCl_3$ (**2.19**) of 21 kg of PE mol^{-1} of Cr h^{-1}. After 30 min, a 1.6-fold increase in polyethylene was observed for **3.11**. This is less than the three-fold increase in the polyethylene anticipated for a stable catalyst, and therefore the activated catalyst has a short lifetime. However, the analogous iron (**3.13**) and the cobalt (**3.14**) complexes exhibited no reactivity attributed to reductive elimination of the alkylbenzimidazolium salt upon activation with MAO.[95]

3.5 Conclusions

The first 1,3-bis(imino)benzimidazol-2-ylidene ligand precursors have been synthesized and characterized. The substituents on the iminic carbon play an important role in the synthetic methodology toward the salts, and the overall stability of their related transition metal complexes. The corresponding benzimidazol-2-ylidene complexes of silver(I), copper(I), iron(II), cobalt(II) and chromium(III) were also isolated and characterized. As suggested by FTIR stretching frequencies, the benzimidazol-2-ylidene ligand coordinated to silver in monodentate mode. In contrast, the ligand chelated to copper, iron, cobalt and chromium in a bidentate fashion through the carbene carbon and an iminic nitrogen atom.

As observed in Chapter 2, the iron and cobalt complexes of benzimidazol-2-ylidene showed no activity toward ethylene polymerization. Although incorporating a less σ-electron donating and a better π-accepting ligand (benzimidazol-2-ylidene), the chromium complex (**3.11**) exhibited moderate activities, similar that of the related imidzol-2-ylidene complex of chromium (**2.19**). All attempts to force the five-membered ring containing benzimidzol-2-ylidene ligands to chelate to a metal center in a tridentate coordination mode were unsuccessful, even using an electron-deficient Cr(III) transition metal. The synthesis of a related bis(imino) six-membered NHC ligand and their corresponding transition metal complexes will be discussed in the following chapter. This ligand is predicted to coordinate to a metal center in a tridentate mode.

3.6 Experimental procedures

All experiments were performed under a dinitrogen atmosphere in a drybox or using standard Schlenk techniques. Solvents used in the preparation of air- and/or moisture-sensitive compounds were dried by using an MBraun Solvent Purification System fitted with alumina columns and stored over molecular sieves under a positive pressure of dinitrogen (pentane, toluene, and THF) or dried by refluxing and then distilling from sodium (toluene) under a positive pressure of dinitrogen. Deuterated solvents were degassed using three freeze-pump-thaw cycles. C_6D_6 was vacuum-distilled from sodium, and $CDCl_3$ and CD_3CN were vacuum-distilled from CaH_2. NMR spectra were recorded on a Bruker AV 400 (^{1}H at 400 MHz, ^{13}C at 100 MHz) or Bruker AV 300 spectrometer (^{1}H at 300 MHz, ^{13}C at 75.5 MHz) at room temperature unless otherwise stated. The spectra were internally referenced relative to the residual protio solvent (^{1}H) and solvent (^{13}C) resonances, and chemical shifts were reported with respect to δ 0 for tetramethylsilane. Solution magnetic susceptibilities were measured using the Evans method.[83] Elemental composition was determined by the Guelph Chemical Laboratories Ltd.

Benzoyl chloride and 2,4,6-trimethylaniline were purchased from Sigma-Aldrich. *N*-(2,6-Dimethylphenyl)acetamide was purchased from Sigma-Aldrich or Alfa Aesar and used without further purification. Benzimidazole was purchased from Alfa Aesar. Copper(I) iodide was purchased from Riedel-de Haën and was dried overnight in a vacuum oven at 80 °C. Iron(II) chloride, cobalt(II) chloride, sodium and potassium bis(trimethylsilyl)amide were purchased from Sigma-Aldrich. Chromium(III) chloride was purchased from Strem Chemicals. *N*-(2,6-Dimethylphenyl)acetimidoyl chloride,[96] *N*-(2,4,6-trimethylphenyl)phenylimidoyl chloride[96] and $CrCl_3\cdot 3THF$[97] were synthesized using the published procedures. Deuterated NMR solvents were purchased from Cambridge Isotope Laboratories. MAO was graciously donated by Albemarle Corp.

1-[(2,6-Dimethylphenylimino)ethyl)]benzimidazole (3.3).

N-(2,6-Dimethylphenyl)acetimidoyl chloride (**3.1**; 2.26 g, 12.5 mmol) was dissolved in dichloromethane (30 mL) and added to a dichloromethane solution (30 mL) of benzimidazole (2.94 g, 24.9 mmol) at room temperature. The reaction mixture was stirred for 18 h. Water was added to the mixture, and the organic product was extracted with dichloromethane. The combined dichloromethane layers were dried over Na_2SO_4 and subsequently filtered. The solvent was removed under vacuum to give the product as a light-yellow solid (2.83 g, 10.8 mmol, 86%). ^{1}H NMR (300 MHz, $CDCl_3$): δ 8.58 (m, 1H, CNCC*H*), 8.41 (s, 1H, NC*H*N), 7.86 (m, 1H, NCC*H*), 7.30−7.40 (m, 2H, CNCCHC*H*, NCCHC*H*), 7.10 (d, ^3J = 7.5 Hz, 2H, *m*-C$H_{(Xyl)}$), 6.98 (t, ^3J = 7.2 Hz, 1H, *p*-C$H_{(Xyl)}$), 2.33 (s, 3H, C$H_{3(imine)}$), 2.10 (s, 6H, *o*-C$H_{3(Xyl)}$). ^{13}C{^{1}H} NMR (75.5 MHz, $CDCl_3$): δ 150.6 (*C*=N), 145.5 ($C_{ipso(Xyl)}$), 143.9 (N*C*CH), 141.3 (N*C*N), 132.4 (N*C*CH), 128.3 (*m*-*C*$H_{(Xyl)}$), 126.7 (*o*-$C_{(Xyl)}$), 125.2 (NCCH*C*H), 124.4 (NCCH*C*H),123.7 (*p*-*C*$H_{(Xyl)}$), 120.2 (CNC*C*H), 116.8 (NC*C*H), 18.4 (*o*-*C*$H_{3(Xyl)}$). 16.7 (*C*$H_{3(imine)}$).

1-[(2,4,6-Trimethylphenylimino)benzyl]benzimidazole (3.4)

N-(2,4,6-Trimethylphenyl)phenyl imidoyl chloride (**3.2**; 3.70 g, 14.4 mmol) was dissolved in dichloromethane (30 mL) and added to a dichloromethane solution (70 mL) of benzimidazole (3.40 g, 28.8 mmol) at room temperature. The reaction mixture was stirred for 18 h and it was then filtered. Water was added to the filtrate, and the organic product was extracted with dichloromethane. The combined dichloromethane layers were dried over Na_2SO_4 and subsequently filtered. The solvent was removed under vacuum to give the product as a yellow solid (4.57 g, 13.5 mmol, 94%). ^{1}H NMR (300 MHz, $CDCl_3$): δ 8.12 (s, 1H, NC*H*N), 8.08 (d, ^3J = 8.0 Hz, 1H, CNCC*H*), 7.90 (d, ^3J = 7.6 Hz, 1H, NCC*H*), 7.42 (t, ^3J = 5.8 Hz, 1H, *p*-C$H_{(phenyl)}$), 7.35–7.39 (m, 4H, *m*-C$H_{(phenyl)}$), CNCCHC*H*, NCCHC*H*), 7.29 (d, ^3J = 7.5 Hz, 2H, *o*-C$H_{(phenyl)}$), 6.79 (s, 4H, *o*-C$H_{(mesityl)}$), 2.24 (s, 3H, *p*-C$H_{3(mesityl)}$), 2.11 (s, 6H, *o*-C$H_{3(mesityl)}$); ^{13}C{^{1}H} NMR (75 MHz, $CDCl_3$): δ 151.0 (*C*=N), 144.5 (N*C*CH), 143.0 (N*C*N), 142.6 ($C_{ipso(mesityl)}$), 132.9 (N*C*CH), 132.5 ($C_{ipso(phenyl)}$), 131.7 (*p*-*C*$CH_{3(mesityl)}$), 130.8 (*p*-*C*$H_{(phenyl)}$), 128.6 (*m*-*C*$H_{(mesityl)}$), 128.5 (*m*-*C*$H_{(phenyl)}$, *o*-

CH$_{(phenyl)}$), 126.3 (o-CCH$_{3(mesityl)}$), 124.5 (NCC), 123.9 (NCC), 120.4 (CNC), 115.5 (CNC), 20.6 (p-CH$_{3(mesityl)}$), 18.5 (o-CH$_{3(mesityl)}$).

1,3-Bis[1-(2,6-dimethylphenylimino)ethyl]benzimidazolium chloride (3.5).

N-(2,6-Dimethylphenyl)acetimidoyl chloride (**3.1**; 1.73 g, 9.55 mmol) was dissolved in 20 mL of toluene and added to a solution of 1-(2,6-dimethylphenylimino)benzimidazole (**3.3**) (2.51 g, 9.55 mmol) in toluene (20 mL) at room temperature. The reaction mixture was stirred for 24 h to give an off-white precipitate. The off-white solid was washed with toluene and pentane and dried under vacuum (3.42 g, 7.70 mmol, 80%). ^{1}H NMR (400 MHz, CDCl$_3$): major isomer (*E,Z* isomer) δ 9.41 (s, 1H, NCHN), 8.65 (m, 1H, NCCHCH), 7.92 (m, 1H, NCCHCH), 7.46 (m, 2H, NCCHCH), 7.12 (d, ^3J = 7.6 Hz, 2H, m-C$H_{(Xyl)}$), ca. 7.05 (2H, m-C$H_{(Xyl)}$; obstructed by resonances from the minor isomer), ca. 6.98 (2H, p-CH$_{(Xyl)}$; overlapping magnetically inequivalent nuclei), 2.63 (s, 3H, C$H_{3(imine)}$), 2.43 (s, 3H, C$H_{3(imine)}$), 2.11 (s, 6H, o-C$H_{3(Xyl)}$), 2.08 (s, 6H, o-C$H_{3(Xyl)}$); minor isomer (*E,E* isomer) δ 12.27 (s, 1H, NCHN), 9.02 (m, 2H, NCCHCH), 7.75 (m, 2H, NCCHCH), 7.14 (d, ^3J = 7.6 Hz, 4H, m-C$H_{(Xyl)}$), ca. 7.05 (2H, p-C$H_{(Xyl)}$; obstructed by resonances from the major isomer), 3.11 (s, 6H, C$H_{3(imine)}$), 2.16 (s, 12H, o-C$H_{3(Xyl)}$). ^{13}C{^{1}H} NMR (100 MHz, CDCl$_3$): major isomer (*E,Z* isomer) δ 151.0, 145.8, 145.2, 145.0, 141.6, 131.8, 127.9, 126.6, 126.5, 125.9, 125.4, 125.1, 124.3, 123.9, 119.2, 117.2, 29.2, 18.3, 17.9, 17.0; minor isomer (*E*,*E* isomer): δ 153.2 (C=N), 144.1 ($C_{ipso(Xyl)}$), 131.8 (NCCH), 129.2 (NCCHCH), 128.5 (m-CH$_{(Xyl)}$), 128.3 (o-$C_{(Xyl)}$), 126.1 (NCHN), 124.9 (p-CH$_{(Xyl)}$), 118.9 (NCCHCH), 19.0 (CH$_{3(imine)}$), 18.5 (o-CH$_{3(Xyl)}$). FTIR (neat): νC=N 1690 cm^{-1}.

1,3-Bis[(2,4,6-trimethylphenylimino)benzyl]benzimidazolium tetrafluoroborate (3.6).

Sodium tetrafluoroborate (0.57 g, 5.1 mmol) was added to an acetonitrile solution (5 mL) of *N*-(2,4,6-trimethylphenyl)phenyl imidoyl chloride (**3.2**; 1.33 g, 5.14 mmol) at room temperature. The reaction mixture was stirred for 1 h. A solution of 1-[(2,4,6-trimethylphenylimino)benzyl]benzimidazole (**3.4**) in acetonitrile (12 mL) was then added to the reaction mixture. The mixture was stirred for 20 h at room temperature and filtered. The filtrate was collected and the volatiles were removed under vacuum. The yellow solid was washed with toluene and pentane to give (3.30 g, 92%) of the expected product. ^{1}H NMR (300 MHz, $CDCl_3$): δ 9.59 (s, 1H, NC*H*N), 7.48–7.55 (m, 10H, *m*-C$H_{(\text{phenyl})}$ + *p*-C$H_{(\text{phenyl})}$ + NCC*H* + NCCC*H*), 7.42 (d, ^{3}J = 7.1 Hz, 4H, *o*-C$H_{(\text{phenyl})}$), 6.78 (s, 4H, *o*-C$H_{(\text{mesityl})}$), 2.23 (s, 6H, *p*-C$H_{3(\text{mesityl})}$), 2.10 (s, 12H, *o*-C$H_{3(\text{mesityl})}$); ^{13}C{^{1}H} NMR (100 MHz, $CDCl_3$): δ 149.4 (*C*=N), 142.8 (N*C*N), 141.1 ($C_{\text{ipso(mesityl)}}$), 134.5 ($C_{\text{ipso(phenyl)}}$), 132.6 (NCC*C*), 131.3 (CN*C*), 129.5 (*o*-*C*$H_{(\text{phenyl})}$), 129.4 (*o*-*C*$H_{(\text{phenyl})}$), 129.1 (*o*-*C*C$H_{3(\text{mesityl})}$), 128.9 (*o*-*C*C$H_{3(\text{mesityl})}$), 128.3 (*p*-*C*$H_{(\text{phenyl})}$),126.7 (*p*-*C*C$H_{3(\text{mesityl})}$), 117.1 (NC*C*), 20.8 (*p*-*C*$H_{3(\text{mesityl})}$), 18.5 (*o*-*C*$H_{3(\text{mesityl})}$). FTIR (neat): νC=N 1674 cm^{-1}.

1-Borontrifluoride-3-[2,4,6-trimethylphenylimino)benzyl]benzimidazole (3.8).

Boron trifluoride diethyl etherate (3.1) (80.0 μl, 0.637 mmol) was added to a toluene solution (6 mL) of 1-[(2,4,6-trimethylphenylimino)benzyl]benzimidazole (**3.4**; 214 mg, 0.631 mmol) at room temperature. The reaction mixture was stirred for 1 h to give a yellow solution. The solvent was removed under vacuum and the solid was washed with benzene (0.6 ml). The solvent was removed under vacuum to give a light-yellow solid (195 mg, 0.479 mmol, 76%). ^{1}H NMR (400 MHz, CDCl$_3$): δ 8.67 (s, 1H, NC*H*N), 8.13 (d, ^3J = 8.2 Hz, 1H, CNCC*H*), 8.04 (d, ^3J = 8.3 Hz, 1H, NCC*H*), 7.59 (t, ^3J = 7.5 Hz, 1H, *p*-C*H*$_{(phenyl)}$), 7.51 (m, 2H, CNCCHC*H*, NCCHC*H*), 7.41 (t, ^3J = 7.6 Hz, 2H, *m*-C*H*$_{(phenyl)}$), 7.25 (d, ^3J = 6.4 Hz, 2H, *o*-C*H*$_{(phenyl)}$), 6.80 (s, 4H, *o*-C*H*$_{(mesityl)}$), 2.23 (s, 3H, *p*-C*H*$_{3(mesityl)}$), 2.05 (s, 6H, *o*-C*H*$_{3(mesityl)}$); ^{13}C{^{1}H} NMR (100 MHz, CDCl$_3$): δ 149.8 (*C*=N), 141.4 (*C*$_{ipso(mesityl)}$), 141.0 (N*C*N), 134.5 (N*C*CH), 133.9 (*p*-*C*CH$_{3(mesityl)}$), 132.2 (*o*-*C*CH$_{3(mesityl)}$), 131.5 (N*C*CH), 129.6 (*C*$_{ipso(phenyl)}$), 129.4 (*m*-*C*H$_{(mesityl)}$), 128.9 (*m*-*C*H$_{(phenyl)}$), 128.4 (*o*-*C*H$_{(phenyl)}$), 127.2 (CN*C*), 126.9 (CN*C*), 125.9 (*p*-*C*H$_{(phenyl)}$), 117.9 (NC*C*), 116.2 (NC*C*), 20.7 (*p*-*C*H$_{3(mesityl)}$), 18.4 (*o*-*C*H$_{3(mesityl)}$).

1,3-Bis[1-(2,6-dimethylphenylimino)ethyl]benzimidazol-2-ylidene silver(I) chloride (3.9).

Sodium bis(trimethylsilyl)amide (47.7 mg, 0.260 mmol) was dissolved in toluene (8 mL) and added dropwise to a toluene (7 mL) suspension of AgBF$_4$ (50.2 mg, 0.258 mmol) at –37 °C. The reaction mixture was slowly warmed to room temperature and subsequently stirred for 40 min. The mixture was then filtered and the filtrate was added dropwise to a toluene suspension (3 mL) of 1,3-bis[1-(2,6-dimethylphenylimino)ethyl]-benzimidazolium chloride (**3.5**) (114 mg, 0.256 mmol) at –37 °C. The reaction mixture was slowly warmed to room temperature and stirred for overnight to give a brown solid suspension. The supernatant was removed and the brown solid was dried in vacuum. Yield: 69.4 mg, 0.126 mmol, 49%. ^{1}H NMR (400 MHz, CDCl$_3$): δ 8.37 (m, 2H, NCC*H*CH), 7.55 (m, 2H, NCCHC*H*), 7.15 (d, ^3J = 7.6 Hz, 4H, *m*-C*H*$_{(Xyl)}$), 7.03 (t, ^3J = 7.6 Hz, 2H, *p*-C*H*$_{(Xyl)}$), 2.70 (s, 6H, C*H*$_{3(imine)}$), 2.24 (s, 12H, *o*-C*H*$_{3(Xyl)}$); ^{13}C{^{1}H} NMR (100 MHz,

$CDCl_3$): δ 155.0 (*C*=N), 145.0 ($C_{ipso(Xyl)}$), 133.1 (N*C*CH), 128.7 (*m*-$CH_{(Xyl)}$), 126.4 (NCCH*C*H), 125.7 (*o*-$C_{(Xyl)}$), 124.7 (*p*-$CH_{(Xyl)}$), 115.9 (NC*C*HCH), 20.9 ($CH_{3(imine)}$),18.9 (*o*-$CH_{3(Xyl)}$). FTIR (neat): $\nu_{C=N}$ 1675 cm^{-1}. Anal. Calcd. for $C_{27}H_{28}AgClN_4$ (%): C, 58.76; H, 5.11; N, 10.15. Found (%): C, 58.54; H, 4.91; N, 9.83.

1,3-Bis[1-(2,6-dimethylphenylimino)ethyl]benzimidazol-2-ylidene] copper(I) iodide (3.10).

Sodium bis(trimethylsilyl)amide (116 mg, 0.630 mmol) was dissolved in THF (4 mL) and added dropwise to a THF (5 mL) suspension of copper(I) iodide (119 mg, 0.622 mmol) at −37 °C. The reaction mixture was slowly warmed to room temperature and stirred for 1 h. It was then added dropwise to a THF (5 mL) suspension of 1,3-bis[1-(2,6-dimethylphenylimino)ethyl]benzimidazolium chloride (**3.5**; 277 mg, 0.622 mmol) at −37 °C. The reaction mixture was slowly warmed to room temperature and stirred for an additional 20 h. The volatile was removed under vacuum to give an orange solid (105 mg, 0.175 mmol, 28%). ^{1}H NMR (400 MHz, $CDCl_3$): δ 8.44 (m, 2H, NCC*H*CH), 7.41 (m, 2H, NCCHC*H*), 7.00 (d, ^3J = 7.5 Hz, 4H, *m*-C$H_{(Xyl)}$), 6.84 (t, ^3J = 7.5 Hz, 2H, *p*-C$H_{(Xyl)}$), 2.69 (s, 6H, C$H_{3(imine)}$), 2.17 (s, 12H, *o*-C$H_{3(Xyl)}$). ^{13}C{^{1}H} NMR (100 MHz, $CDCl_3$): δ 156.6 (*C*=N), 145.3 ($C_{ipso(Xyl)}$), 133.8 (N*C*CH), 128.3 (*m*-$CH_{(Xyl)}$), 127.1 (*o*-$C_{(Xyl)}$), 125.3 (NCCH*C*H), 123.9 (*p*-$CH_{(Xyl)}$), 116.3 (NC*C*HCH), 19.5 ($CH_{3(imine)}$), 19.1 (*o*-$CH_{3(Xyl)}$). FTIR (neat) $\nu_{C=N}$ 1668, 1653 cm^{-1}. Anal. Calcd. for $C_{27}H_{28}CuIN_4$ (%): C, 54.14; H, 4.71; N, 9.35. Found (%): C, 53.97; H, 4.54; N, 9.08.

1,3-Bis[1-(2,6-dimethylphenylimino)ethyl]benzimidazol-2-ylidene] chromium(III) chloride (3.11).

To a mixture of $CrCl_3$·3THF (39.4 mg, 0.105 mmol) and 1,3-bis[1-(2,6-dimethylphenylimino)ethyl]benzimidazol-2-ylidene copper(I) iodide (**3.10**; 62.9 mg, 0.105 mmol) was added 10 mL of dichloromethane at room temperature. The reaction mixture was stirred overnight and subsequently filtered. The solvent was removed under vacuum. The solid was then dissolved in toluene and filtered. The filtrate was collected, and the solvent was removed under vacuum to give a blue-green solid in 71% yield (42.5 mg, 0.0750 mmol). FTIR (neat): $\nu_{C=N}$ 1683, 1622 cm^{-1}. μ_{eff} = 3.75 μB. Anal. Calcd. for $C_{27}H_{28}CrCl_3N_4$ (%): C, 57.20; H, 4.98; N, 9.88. Found (%): C, 56.94; H, 4.98; N, 10.10.

1,3-Bis[1-(2,6-dimethylphenylimino)ethyl]benzimidazol-2-ylidene] iron(II) chloride (3.13).

Potassium bis(trimethylsilyl)amide (65.6 mg, 0.329 mmol) was dissolved in THF (4 mL) and added dropwise to a THF (8 mL) suspension of iron(II) chloride (41.4 mg, 0.327 mmol) at −37 °C. The reaction mixture was slowly warmed to room temperature and stirred for 40 min, filtered, and added dropwise to a THF (5 mL) suspension of 1,3-bis[1-(2,6-dimethylphenylimino)ethyl]benzimidazolium chloride (**3.5**; 144 mg, 0.323 mmol) at −37 °C. The reaction mixture was slowly warmed to room temperature and stirred for an additional 22 h. The reaction mixture was filtered, and the solution was concentrated to about 1 mL. Pentane was added to precipitate a yellow solid. The supernatant was removed, and the residual solid was dried to give the product in 71% yield (122 mg, 0.228 mmol).

FTIR (neat): $\nu_{C=N}$ 1683, 1629 cm^{-1}. μ_{eff} = 5.86 μB. Anal. Calcd. for $C_{27}H_{28}FeCl_2N_4$ (%): C, 60.58; H, 5.27; N, 10.47. Found (%): C, 60.30; H, 5.02; N, 10.15.

1,3-Bis[1-(2,6-dimethylphenylimino)ethyl]benzimidazol-2-ylidene] cobalt(II) chloride (3.14).

Potassium bis(trimethylsilyl)amide (70.2 mg, 0.352 mmol) was dissolved in THF (4 mL) and added dropwise to a THF (8 mL) suspension of cobalt(II) chloride (45.5 mg, 0.350 mmol) at −37 °C. The reaction mixture was stirred for 40 min at room temperature. It was then filtered, and the filtrate was added dropwise to a THF (5 mL) suspension of 1,3-bis[1-(2,6- dimethylphenylimino)ethyl]benzimidazolium chloride (**3.5**; 153 mg, 0.344 mmol) at −37 °C. The reaction mixture was slowly warmed to room temperature and stirred for an additional 22 h. It was filtered, and the solution was concentrated to about 1 mL. Pentane was added to precipitate the product as a green solid in 62% yield (115 mg, 0.344 mmol). FTIR (neat): $\nu_{C=N}$ 1683, 1607 cm^{-1}. μ_{eff} = 4.27 μB. Anal. Calcd. for $C_{27}H_{28}CoCl_2N_4$ (%): C, 60.23; H, 5.24; N, 10.41. Found (%): C, 60.50; H, 5.02; N, 10.18.

General Procedure for Ethylene Polymerization

Ethylene polymerization was performed at atmospheric pressure and room temperature in a 500 mL Schlenk flask containing a magnetic stir bar. The flask was conditioned in an oven at 130 °C for at least 18 h prior to use. The hot flask was brought to room temperature under a dynamic vacuum and backfilled with ethylene. Under an atmosphere of ethylene, the flask was charged with 20 mL of dry toluene and 1000 equivalents of MAO with respect to the catalyst (7.6 μmol). The solution was stirred for 10−15 min before a solution of the catalyst in either toluene or dichloromethane was introduced into the flask via a syringe. The reaction mixture was vigorously stirred for either 10 or 30 min after the addition of the catalyst and subsequently quenched with a 1:1 mixture of concentrated hydrochloric acid and methanol. The resulting mixture was filtered, and any solid collected was washed with distilled water. Solids collected were dried under vacuum at approximately 50 °C for 24 h. The chromium complex **3.11** gave 29 mg (3.8 kg of PE mol^{-1} of Cr; 23 kg of PE mol^{-1} of Cr h^{-1}) of polyethylene, as averages of three 10 min runs. In contrast, the complex **3.11** gave 45 mg (5.9 kg of PE mol^{-1} of Cr; 12 kg of PE mol^{-1} of Cr^{-1} h^{-1}) of polyethylene, as averages of two 30 min runs.

Chapter Four

Synthesis, Characterization and Reactivity Study of Bis(imino) pyrimidin-2-ylidene Transition Metal Complexes

3rd Generation

The 2,6-bis(imino)pyridine ligands chelated to chromium(III), iron(II) and cobalt(II) complexes in a tridentate fashion.[15,16d,20b] The variations at the central donor of 2,6-bis(imino)pyridine[15,16d] from the 6-membered ring to the 5-membered bis(arylimino)pyrrole led to a different ligand coordinating behavior.[21a,85b] As shown in structure **A**, a wide exocyclic angle α allows the ligand to bind in a tridentate mode, however a bidentate coordination mode is predicted for small α angles.[85b] The bis(imino)pyrrolato ligands feature a more opened coordination sphere, in which a bidentate coordination is favored.[85b]

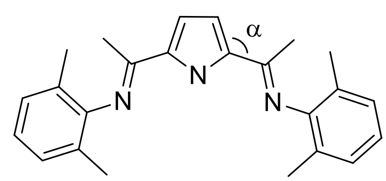

A

In the previous chapter, the first 1,3-bis(imino)benzimidazol-2-ylidene ligand precursors and the corresponding complexes of silver(I), copper(I), iron(II), cobalt(II) and chromium(III) were synthesized and characterized. Similar to the imidazol-2-ylidene ligand, the benzimidazol-2-ylidene ligand coordinated to the metal center in either a mono- or bidentate fashion.[73] Although increasing the steric bulk, reducing σ-electron donating and enhancing π-accepting ability of the ligand by replacing the imidazol-2-ylidene with benzimidazol-2-ylidene, the desired tridentate coordination mode was not achieved. Coordination of the second iminic nitrogen to form a symmetric complex would induce steric constraints preventing the ligand from chelating in a tridentate mode. Therefore, modifying the ligand scaffold by replacing the five-membered NHC with a six-membered NHC (a ring-extended carbene), such as pyrimidin-2-ylidene, will alleviate this strain and may allow the ligand to bind in a tridentate fashion. Such coordination is expected to enhance the stability of the resulting transition metal complexes.

In this chapter, the synthesis of the new 1,3-bis(imino)pyrimidinium salt, and the corresponding pyrimidin-2-ylidene complexes of copper(I), iron(II), cobalt(II) and chromium(III) will be presented. The catalytic activities of these iron(II), cobalt(II) and chromium(III) complexes in ethylene polymerization will also be demonstrated.

4.1 Synthesis of 1,3-bis[1-(2,6-dimethylphenylimino)ethyl]-4,5,6-trihydro pyrimidinium salt

The (1-(2,6-dimethylphenylimino)ethyl)pyrimidine (**4.1**) was synthesized by reacting *N*-(2,6-dimethylphenyl) acetimidoyl chloride with 1,4,5,6-tetrahydropyrimidine in toluene, as a light-yellow oil in 87% yield (Scheme 4.1). The subsequent reaction of **4.1** with an additional equivalent of *N*-(2,6-dimethylphenyl)acetimidoyl chloride afforded the pyrimidinium salt **4.2** in benzene, as a white solid (57% yield). As expected, the IR stretching frequency for the iminic groups in compound **4.2** showed only one band at 1628 cm^{-1}. In the ^{1}H NMR ($CDCl_3$) spectrum, the most characteristic downfield resonance for the central pyrimidinium proton (NC*H*N) was identified at δ 9.93. The backbone methylene protons ($NCH_2CH_2CH_2N$, with the first and last H italic: NC*H*$_2$CH$_2$C*H*$_2$N) and (NCH$_2$C*H*$_2$CH$_2$N) were observed at δ 4.34 and 2.47, respectively, while the corresponding ^{13}C resonances resonated at δ 42.2 (N*C*H$_2$CH$_2$*C*H$_2$N) and δ 18.7 (NCH$_2$*C*H$_2$CH$_2$N). The central carbon (N*C*N) and the iminic carbon (*C*=N) nuclei appeared at δ 154.1 and 153.7, respectively.

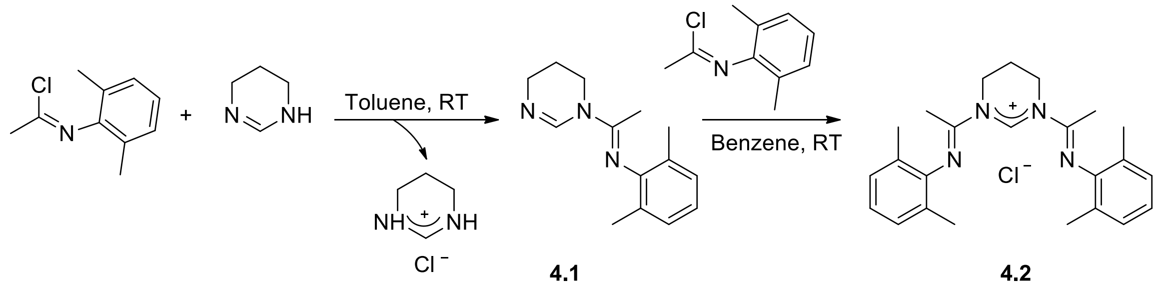

Scheme 4.1. Synthesis of pyrimidinium chloride salt **4.2**.

The attempted synthesis of bis[(2,6-dimethylphenylimino)benzyl]pyrimidinium tetrafluoroborate salt (**4.4**), aimed to reduce electron density on the metal center by replacing the methyl groups on the iminic carbon with a relatively electron-poor phenyl groups, was unsuccessful (Scheme 4.2).

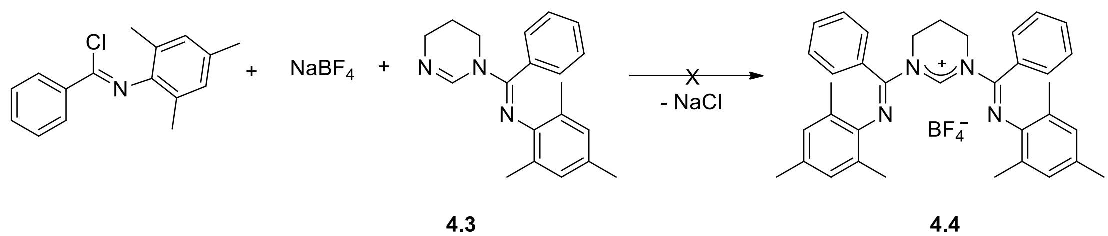

Scheme 4.2. Attempt to synthesize pyrimidinium tetrafluoroborate salt **4.4**.

4.2 Synthesis of NHC transition metal complexes

4.2.1 Bis(imino)pyrimidin-2-ylidene copper and chromium complexes

The pyrimidin-2-ylidene copper complex was afforded as a transmetalating agent to the related carbene transition metal complexes. This complex [C_{pyr}(^ImineMe)$_2$]CuI (**4.5**) was synthesized in 76% yield using analogous procedures to the synthesis of **2.15** and **2.16** (Scheme 4.3). The ^{1}H NMR (CD_3CN) spectrum of **4.5** showed the disappearance of the central pyrimidinium proton observed for the parent salt **4.2**, as an indication of carbene-copper bond formation. The backbone protons ($NCH_2CH_2CH_2N$) and ($NCH_2CH_2CH_2N$) resonated at δ 3.69 and 2.27, respectively and shifted upfield compared to that of the salt **4.2**., The ^{13}C resonances for the carbene center (N*C*N) and the iminic carbon (*C*=N) appeared at 162.3 δ and 146.1, respectively.

The FTIR spectrum for **4.5** displayed only one band for the imine group at 1635 cm^{-1}. This C=N stretching frequency is comparable to that of **4.2** and suggests a monodentate coordination fashion through the carbene center, as observed in the first generation for the analogous copper complex (**2.16**) (with phenyl substituents on the iminic carbene).[73a]

The synthesis of the more electropositive pyrimidin-2-ylidene Cr(III) complex was investigated to force the ligand binding in a tridentate fashion and to evaluate its reactivity in polymerization of ethylene. The transmetalation reaction of $[C_{pyr}(\wedge Imine_{Me})_2]CuI$ (**4.7**) and $CrCl_3 \cdot 3THF$ gave $[C_{pyr}(\wedge Imine_{Me})_2]CrCl_3$ complex (**4.6**) in 86% yield (Scheme 4.3). The magnetic susceptibility for **4.6** of 4.14 μ_B[83] was consistent with that observed for **2.19**, **2.20**, **3.11** and with other related reported values for Cr(III) complexes, and also was in agreement with the expected value of three unpaired electrons**.**[87] Only one $\upsilon_{C=N}$ band in the FTIR spectrum of **4.6** was observed for the imine fragments at 1623 cm^{-1}, lower than that for **4**.**2**. This observation is due to π-back donation to the iminic bonds from metal and it suggests coordination of both iminic nitrogen atoms of the ligand to the metal center.

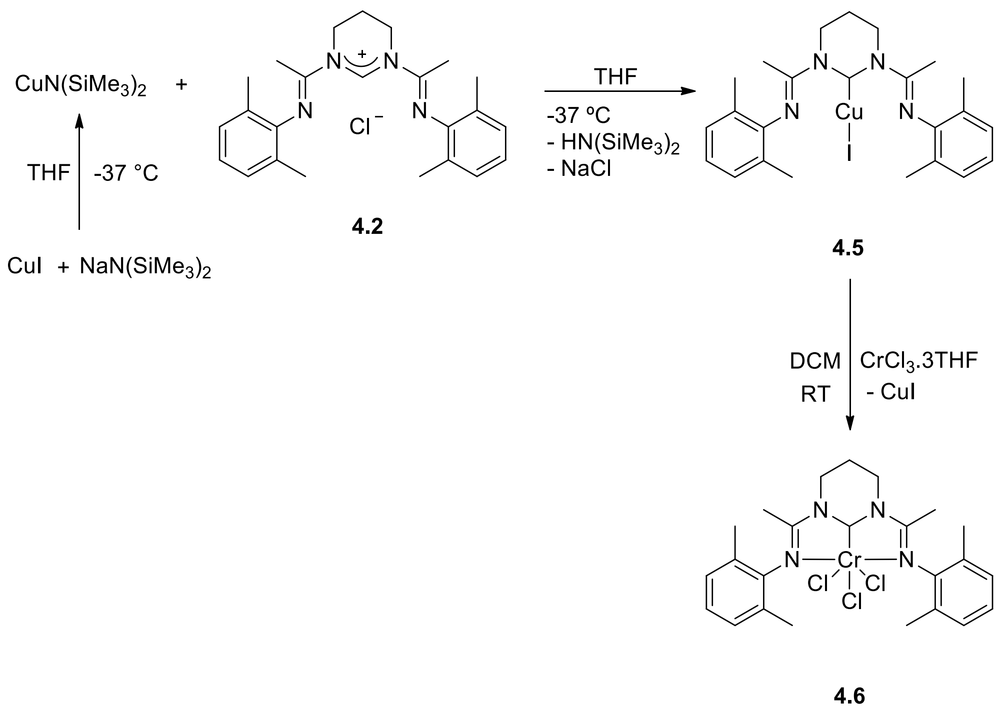

Scheme 4.3. Synthesis of pyrimidin-2-ylidene copper and chromium complexes **4.5** and **4.6**, respectively.

X-ray-quality crystals were obtained by slow evaporation of a saturated dichloromethane solution of the pyrimidin-2-ylidene Cr(III) complex **4.6**. The molecular structure of **4.6** showed that the molecule adopted a distorted octahedral geometry and it crystallized in the $P2_1/n$ space group (Figure 4.1). In contrast to the observed bidentate coordination mode in the first-generation of bis(imino) imidazol-2-ylidene chromium complex **2.20**, X-ray diffraction analysis of **4.6** demonstrated, for the first time, the ability of bis(imino)-NHC ligands to coordinate to a chromium metal in a tridentate fashion.

The C1−N1−C5 (114.0(2)°) and C1−N2−C15 (114.3(2)°) bond angles in **4.6** are similar to those of the reported for the analogous [2,6-bis(1-(2,6-dimethylphenylimino)ethyl)pyridine] $CrCl_3$ (113.1(3), 113.7(3)°),[20b] however they are notably smaller than the related angles in the $[C_{imi}(^\wedge Imine_{Me})_2]CrCl_3$ (**2.20**) (118.9(3), 119.6(3)°).[73b] The N3−Cr1−N4 bond angle in **4.6** 150.59(9)° is smaller than that of the reported 2,6-bis(1-(2,6-dimethylphenylimino)ethyl)pyridine (153.36(10)°).[20b] The C1−Cr1−N3 (75.65(10)°) and C1−Cr1−N4 (75.49(10)°) bite angles are comparable to the corresponding angles in the reported Cr(III) complex of bis(imino)pyridine of 75.75(11) and 77.24(11)°,[20b] in the Cr(III) complex of bis(NHC)pyridine of 76.3(2) and 75.68(9)°[23a] and in the $[C_{imi}(^\wedge Imine_{Ph})_2]CrCl_3$ (**2.20**) (76.90(11)°).[73b]

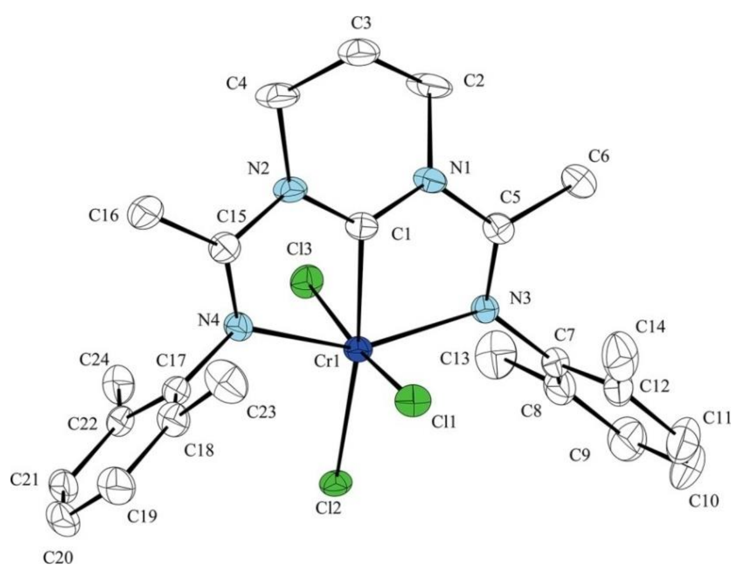

Figure 4.1. ORTEP of **4.6** (50% probability level). Hydrogen atoms and dichloromethane solvent molecule are omitted for clarity. Selected bond lengths (Å) and angles (deg.): Cr1−C1 1.989(3), Cr1−N3 2.133(2), Cr1−N4 2.142(2), Cr1−Cl1 2.2945(8), Cr1−Cl2 2.3293(7), Cr1−Cl3 2.3479(8), N1−C1 1.335(4), N2−C1 1.329(4), N3−C5 1.286(4), N4−C15 1.289(4); N1−C1−N2 121.6(2), C1−N1−C5 114.0(2), C1−N2−C15 114.3(2), C1−Cr1−N3 75.65(10), C1−Cr1−N4 75.49(10), C1−Cr1−Cl1 96.90(8), C1−Cr1−Cl2 167.85(8), C1−Cr1−Cl3 76.91(8), Cl1−Cr1−Cl3 173.67(3), N3−Cr1−N4 150.59(9).

A significantly shorter bond length of Cr1−C1 (1.989(3) Å) was observed than the related Cr−C1 bonds in the reported bis(NHC)pyridine chromium complex[23a] (2.087(6) and 2.1206(6) Å) and in the $[C_{imi}(^\wedge Imine_{Ph})_2]CrCl_3$[73b] (**2.20**) (2.048(3) Å). The Cr−C1 is similar to the Cr−$N_{pyridine}$ bond (1.993(3) Å) in the bis(imino)pyridine chromium complex,[20b] whereas it is shorter than the Cr−N bond in the bis(NHC)pyridine complex of $CrCl_3$ (2.049(4) Å).[23a] Although the bond lengths of $Cr-N_{imine}$ in **4.6** (2.133(2) and 2.142(2) Å) are closer to that of $Cr-N_{imine}$ bonds in the bis(imino)pyridine chromium complex (2.123(3) and 2.140(3) Å),[20b] they are shorter than the related $Cr-N_{imine}$ bond length in the $[C_{imi}(\wedge Imine_{Ph})_2]CrCl_3$ (**2.20**) (2.164(3) Å).[73b] The iminic bond lengths N3−C5 (1.286(4) Å) and N4−C15 (1.289(4) Å) are equivalent and they are comparable to the reported value for the coordinated iminic fragments of the $[C_{imi}(\wedge Imine_{Ph})_2]CrCl_3$ (**2.20**) (1.294(4) Å)[73b] and of bis(imino)pyridine complex of $CrCl_3$ (1.291(4) and 1.297(4) Å).[20b] The structural parameters of the 1,3-bis(imino)pyrimidin-2-ylidene complex of chromium (**4.6**) are comparable to the corresponding parameters of the chromium complexes of 2,6-bis(imino)pyridine[20b] and 2,6-bis(carbene)pyridine ligands,[23a] though their electronic properties are very distinguishable.

4.2.2 Bis(imino)pyrimidin-2-ylidene iron and cobalt complexes

The bis(imino)pyrimidin-2-ylidene iron and cobalt complexes were synthesized as potential catalysts for ethylene polymerization. These complexes $[C_{pyr}(\wedge Imine_{Me})_2]FeCl_2$ (**4.7**) and $[C_{pyr}(\wedge Imine_{Me})_2]CoCl_2$ (**4.8**) were synthesized in 81% and 74% yields, respectively, by a procedure analogous to that used for the synthesis of **2.17** and **2.18** (Scheme 4.4). The magnetic susceptibility of complexes **4.7** and **4.8** were 5.80 and 4.35 μB,[83] respectively, consistent with four and three unpaired electrons and similar to those reported for the related complexes.[15,16c,73b,84,111-112] Two IR stretching frequency bands were identified for the iminic groups in **4.7**: 1638, 1617 cm^{-1} and similarly in **4.8:** 1635, 1612 cm^{-1}. These values suggest a bidentate coordination mode for the pyrimidin-2-ylidene ligand to the metal center. Although the preferred angles of the six-membered bis(imino)pyrimidin-2-ylidene ligand, a tridentate coordination mode was not yet achieved. The higher electron density of the metal center in Fe(II) (**4.7**) and Co(II) (**4.8**) complexes and their lower oxidation state (+2) than the related complex of Cr(III) may forbid the desired tridentate coordination mode.

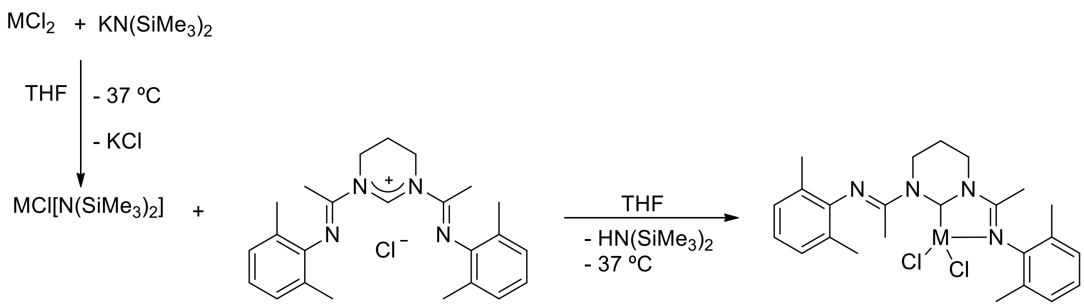

4.2

M = Fe, **4.7**
M = Co, **4.8**

Scheme 4.4. Synthesis of pyrimidin-2-ylidene iron and cobalt complexes **4.7** and **4.8**.

X-ray-quality crystals could not be grown to definitely determine the molecular structures of complexes **4.7** and **4.8**. However, crystals for the reported analogous complex (1,3-bis[1-(2,6-diisopropylphenylimino)-ethyl]pyrimidin-2-ylidene] iron chloride) were hardly obtained from a mixture of saturated solution of dichloromethane, diethyl ether and THF.[84] Its solid-state molecular structure showed a tridentate chelation of the ligand.[84]

4.3 Polymerization of ethylene

The catalytic activity of complexes **4.6**, **4.7** and **4.8** toward ethylene polymerization with 1000 equivalents of methylaluminoxane as cocatalyst were evaluated under ambient conditions. The results for these complexes are similar to those for the first generation of imidazol-2-ylidene complexes and the second generation of benzimidazol-2-ylidene complexes.[73]

The activity of chromium complex $[C_{pyr}(\text{^}Imine_{Me})_2]CrCl_3$ (**4.6**) was 31 kg of PE mol^{-1} of Cr h^{-1} (5.1 kg of PE mol^{-1} of Cr). Surprisingly, incorporating a stronger σ-electron donating NHC ligand (e.g. pyrimidin-2-ylidene) did not reduce the activity of **4.6** over those of $[C_{imi}(\text{^}Imine_{Me})_2]CrCl_3$ (**2.19**) (21 kg of PE mol^{-1} of Cr h^{-1}) or $[C_{benz}(\text{^}Imine_{Me})_2]CrCl_3$ (**3.11**) (23 kg of PE mol^{-1} of Cr h^{-1}). This may be due to the coordination of both iminic nitrogen atoms in **4.6** reducing the electron density at the metal center through π-back donation compared to coordination of only one iminic nitrogen in **2.19** and **3.11**. After 30 min, only a 1.4-fold increase in polyethylene (7.3 kg of PE mol^{-1} of Cr; 15 kg of PE mol^{-1} of Cr h^{-1}) was observed for **4.6**. This is less than the predicted three-fold increase in product for the stable catalyst and this suggests that the catalyst has a short lifetime. The iron (**4.7**) and cobalt (**4.8**) complexes exhibited no reactivity possibly attributed to reductive elimination of the alkylpyrimidinium salt upon activation with the MAO cocatalyst.[95]

4.4 Conclusions

The first 1,3-bis(imino) pyrimidinium salt has been synthesized and characterized. The pyrimidin-2-ylidene complexes of copper(I), iron(II), cobalt(II) and chromium(III) were also isolated and characterized. Based on FTIR stretching frequency, a monodentate coordination mode through the carbene center is expected for pyrimidin-2-ylidene ligand in the copper complex (**4.5**), while the ligand may coordinate to iron (**4.7**) and cobalt (**4.8**) in a bidentate fashion through the carbene carbon and one iminic nitrogen atom. The solid-state molecular structure of the pyrimidin-2-ylidene chromium complex (**4.6**) confirmed a tridentate coordination mode for the ligand to the metal center. The observed coordination mode is due to the six-membered central ring that removes steric constraints and a highly electropositive Cr(III) metal center. This demonstrates that the coordination mode of the bis(imino)-NHC ligands is dependent on both the metal nature and the structure of the ligand.

The iron (**4.7**) and cobalt (**4.8**) complexes of pyrimidin-2-ylidene showed no activity toward ethylene polymerization. The chromium complex (**4.6**) exhibited moderate activities, however a short catalyst life was observed.

4.5 Experimental procedures

All experiments were performed under a dinitrogen atmosphere in a drybox or using standard Schlenk techniques. Solvents used in the preparation of air- and/or moisture-sensitive compounds were dried by using an MBraun Solvent Purification System fitted with alumina columns and stored over molecular sieves under a positive pressure of dinitrogen (pentane, toluene, and THF) or dried by refluxing and then distilling from sodium (toluene) under a positive pressure of dinitrogen. Deuterated solvents were degassed using three freeze-pump-thaw cycles. C_6D_6 was vacuum-distilled from sodium, and $CDCl_3$ and CD_3CN were vacuum-distilled from CaH_2. NMR spectra were recorded on a Bruker AV 400 (^1H at 400 MHz, ^{13}C at 100 MHz) or Bruker AV 300 spectrometer (^1H at 300 MHz, ^{13}C at 75.5 MHz) at room temperature unless otherwise stated. The spectra were internally referenced relative to the residual protio solvent (^1H) and solvent (^{13}C) resonances, and chemical shifts were reported with respect to δ 0 for tetramethylsilane.

Solution magnetic susceptibilities were measured using the Evans method.[83] Elemental composition was determined by the Guelph Chemical Laboratories Ltd.

Benzoyl chloride and 2,4,6-trimethylaniline were purchased from Sigma-Aldrich. *N*-(2,6-Dimethylphenyl)acetamide was purchased from Sigma-Aldrich or Alfa Aesar and used without further purification. Copper(I) iodide was purchased from Riedel-de Haën and was dried overnight in a vacuum oven at 80 °C. Iron(II) chloride, cobalt(II) chloride, and 1,4,5,6-tetrahydropyrimidine, sodium and potassium bis(trimethylsilyl)amide were purchased from Sigma-Aldrich. Chromium(III) chloride was purchased from Strem Chemicals. *N*-(2,6-Dimethylphenyl)acetimidoyl chloride,[96] *N*-(2,4,6-trimethylphenyl) phenylimidoyl chloride[96] and $CrCl_3 \cdot 3THF$[97] were synthesized using the published procedures. Deuterated NMR solvents were purchased from Cambridge Isotope Laboratories. MAO was graciously donated by Albemarle Corp.

1-[(2,6-Dimethylphenylimino)ethyl]-4,5,6-trihydropyrimidine (4.1).

N-(2,6-Dimethylphenyl)acetimidoyl chloride (100 mg, 0.554 mmol) was dissolved in toluene (3 mL) and added to a toluene solution (3 mL) of 1,4,5,6-tetrahydropyrimidine (90.6 mg, 1.10 mmol) at room temperature. The reaction mixture was stirred for 16 h. The mixture was filtered, and the solvent was removed under vacuum to give the product as a light-yellow oil (111 mg, 87%). ^{1}H NMR (300 MHz, $CDCl_3$): δ 7.89 (s, 1H, NC*H*N), 7.03 (d, ^3J= 7.4 Hz, 2H, *m*- C$H_{(Xyl)}$), 6.88 (t, ^3J = 7.4 Hz, 1H, *p*-C$H_{(Xyl)}$), 3.88 (t, ^3J = 6.0 Hz, 2H, CNCH_2CH$_2$), 3.49 (t, ^3J = 6.0 Hz, 2H, C=NCH_2CH$_2$), 2.02 (s, 6H, *o*-C$H_{3(Xyl)}$), 1.96 (m, 2H, NCH$_2$CH_2), 1.88 (s, 3H, C$H_{3(imine)}$). ^{13}C{^{1}H} NMR (75.5 MHz, $CDCl_3$): δ 152.4 (*C*=N), 146.7 ($C_{ipso(Xyl)}$), 143.8 (N*C*N), 127.7 (*m*-*C*H$_{(Xyl)}$), 127.2 (*o*-$C_{(Xyl)}$), 122.3 (*p*-

CH$_{(Xyl)}$), 44.3 (C=NCH$_2$CH$_2$), 41.0 (NCH$_2$CH$_2$), 20.9 (NCH$_2$$CH_2$), 18.0 ($o$-$CH_{3(Xyl)}$), 14.2 ($CH_{3(imine)}$).

1,3-Bis[1-(2,6-dimethylphenylimino)ethyl]-4,5,6-trihydropyrimidinium chloride (4.2).

N-(2,6-Dimethylphenyl)acetimidoyl chloride (462 mg, 2.54 mmol) was dissolved in 8 mL of benzene and added to a solution of (1-(2,6-dimethylphenylimino)ethyl)-4,5,6-trihydropyrimidine (**4.1**; 583 mg, 2.54 mmol) in benzene (10 mL) at room temperature. The reaction mixture was stirred for 20 h. The white solid was washed with toluene and pentane and dried under vacuum (594 mg, 1.45 mmol, 57%). ^{1}H NMR (400 MHz, CDCl$_3$): δ 9.93 (s, ^{1}H, NCHN), 7.07 (d, ^{3}J = 7.5 Hz, 4H, m-C$H_{(Xyl)}$), 6.98 (t, ^{3}J = 7.5 Hz, 2H, p-C$H_{(Xyl)}$), 4.34 (t, ^{3}J = 5.7 Hz, 4H, NCH_2CH$_2$), 2.59 (s, 6H, C$H_{3(imine)}$), 2.47 (p, ^{3}J = 5.7 Hz, 2H, NCH$_2$CH_2), 2.07 (s, 12H, o-C$H_{3(Xyl)}$). ^{13}C{^{1}H} NMR (100 MHz, CDCl$_3$): δ 154.1 (NCN), 153.7 (C=N), 144.5 ($C_{ipso(Xyl)}$), 128.4 (m-CH$_{(Xyl)}$), 126.5 (o-$C_{(Xyl)}$), 124.5 (p-CH$_{(Xyl)}$), 42.2 (NCH$_2$CH$_2$), 18.7 (NCH$_2$$CH_2$), 18.5 ($o$-$CH_{3(Xyl)}$), 15.9 ($CH_{3(imine)}$). FTIR (neat) $\nu_{C=N}$ 1628 cm^{-1}.

1,3-Bis[1-(2,6-dimethylphenylimino)ethyl]-4,5,6-trihydropyrimidin-2-ylidene copper(I) iodide (4.5).

Sodium bis(trimethylsilyl)amide (50.7 mg, 0.276 mmol) was dissolved in THF (4 mL) and added dropwise to a THF (4 mL) suspension of copper iodide (52.1 mg, 0.274 mmol) at −37 °C. The reaction mixture was stirred for 30 min, and it was then added dropwise to a THF (5 mL) suspension of 1,3-bis[1-(2,6-dimethylphenylimino)ethyl]-4,5,6-

trihydropyrimidinium chloride (**4.2**; 112 mg, 0.273 mmol) at −37 °C. The reaction mixture was slowly warmed to room temperature and stirred for an additional 4 h. Pentane was added to precipitate a brown solid, and the supernatant was removed. The volatiles were removed under vacuum to give the product in 76% yield (118 mg, 0.208 mmol). ^{1}H NMR (400 MHz, CD_3CN): δ 7.09 (d, ^{3}J = 7.7 Hz, 4H, *m*-C$H_{(Xyl)}$), 6.97 (t, ^{3}J = 7.7 Hz, 2H, *p*-C$H_{(Xyl)}$), 3.69 (t, ^{3}J = 6.5 Hz, 4H, NCH_2CH$_2$), 2.28 (s, 12H, *o*-C$H_{3(Xyl)}$), 2.27 (m, ^{3}J = 6.5 Hz, 2H, NCH$_2$CH_2), 1.99 (s, 6H, C$H_{3(imine)}$). ^{13}C{^{1}H} NMR (100 MHz, CD_3CN): δ 162.3 (N*C*N), 146.1 (*C*=N), 130.3 (*o*-$C_{(Xyl)}$), 128.9 (*m*-*C*$H_{(Xyl)}$), 128.8 ($C_{ipso(Xyl)}$), 125.2 (*p*-*C*$H_{(Xyl)}$), 46.1 (N*C*H$_2$CH$_2$), 23.3 (NCH$_2$*C*H$_2$), 20.0 (*o*-*C*$H_{3(Xyl)}$), 16.8 (*C*$H_{3(imine)}$). FTIR (neat) $\nu_{C=N}$ 1635 cm^{-1}. Anal. Calcd. for $C_{24}H_{30}CuIN_4$ (%): C, 51.02; H, 5.35; N, 9.92. Found (%): C, 50.87; H, 5.16; N, 9.65.

1,3-Bis[1-(2,6-dimethylphenylimino)ethyl]-4,5,6-trihydropyrimidin-2-ylidene chromium(III) chloride (4.6).

A dichloromethane solution of $CrCl_3$·3THF (37.5 mg, 0.100 mmol) was added, at room temperature, to a dichloromethane suspension of 1,3-bis[1-(2,6-dimethylphenylimino)ethyl]-4,5,6-trihydropyrimidin-2-ylidene copper(I) iodide (**4.5**; 56.7 mg, 0.100 mmol). The reaction mixture was stirred for 20 h and subsequently filtered. The filtrate was collected, and the solvent was removed under vacuum to give a light-blue green solid. Yield: 45.9 mg, 0.0861 mmol, 86%. X-ray-quality crystals were grown from a concentrated dichloromethane solution of **4.6** by slow evaporation of the solvent. FTIR (neat): $\nu_{C=N}$ 1623 cm^{-1}. μ_{eff} = 4.14 μB. Anal. Calcd. for $C_{24}H_{30}CrCl_3N_4$ (%): C, 54.09; H, 5.67; N, 10.51. Found (%): C, 54.57; H, 5.81; N, 9.96.

1,3-Bis[1-(2,6-dimethylphenylimino)ethyl]-4,5,6-trihydropyrimidin-2-ylidene iron(II) chloride (4.7).

Potassium bis(trimethylsilyl)amide (51.6 mg, 0.259 mmol) was dissolved in THF (4 mL) and added dropwise to a THF (4 mL) suspension of iron(II) chloride (32.5 mg, 0.256 mmol) at −37 °C. The reaction mixture was kept at −37 °C for 3 h and agitated occasionally. It was then filtered, and the filtrate was added dropwise to a THF (4 mL) suspension of 1,3-bis[1-(2,6-dimethylphenylimino)ethyl]-4,5,6-trihydropyrimidinium chloride (**4.2**; 101 mg, 0.245 mmol) at −37 °C. The reaction mixture was slowly warmed to room temperature and stirred for an additional 20 h. The mixture was then concentrated, and pentane was added to precipitate a reddish solid. The solid was dissolved in dichloromethane and then filtered. The volatiles were removed under vacuum to give the product in 81% yield (123 mg, 0.245 mmol). FTIR (neat): $\nu_{C=N}$ 1638, 1617 cm^{-1}. μ_{eff} = 5.80 μB. Anal. Calcd. for $C_{24}H_{30}FeCl_2N_4$ (%): C, 57.50; H, 6.03; N, 11.18. Found (%): C, 57.21; H, 5.75; N, 10.89.

1,3-Bis[1-(2,6-dimethylphenylimino)ethyl]-4,5,6-trihydropyrimidin-2-ylidene cobalt(II) chloride (4.8).

Potassium bis(trimethylsilyl)amide (46.6 mg, 0.234 mmol) was dissolved in THF (4 mL) and added dropwise to a THF (4 mL) suspension of cobalt chloride (30.4 mg, 0.232 mmol) at −37 °C. The reaction mixture was kept at −37 °C for 3 h and agitated occasionally. It was then filtered, and the filtrate was added dropwise to a THF (4 mL) suspension of 1,3-bis[1-(2,6-dimethylphenylimino)ethyl]-4,5,6-trihydropyrimidinium chloride (**4.2**; 90.0 mg, 0.219 mmol) at −37 °C. The reaction mixture was slowly warmed to room temperature and stirred for an additional 20 h. The mixture was then concentrated, and pentane was added to precipitate a green solid. The solid was dissolved in dichloromethane and then filtered. The volatiles were removed under vacuum to give the product in 74% yield (81.8 mg, 0.162 mmol). FTIR (neat): $\nu_{C=N}$ 1635, 1612 cm^{-1}. μ_{eff} = 4.35 μB. Anal. Calcd. for $C_{24}H_{30}CoCl_2N_4$ (%): C, 57.15; H, 6.00; N, 11.11. Found (%): C, 56.88; H, 5.72; N, 10.94.

General Procedure for Ethylene Polymerization.

Ethylene polymerization was performed at room temperature and at atmospheric pressure in a 500 mL Schlenk flask containing a magnetic stir bar. The flask was kept in an oven at 130 °C for at least 18 h prior to use. The hot flask was brought to room temperature under a dynamic vacuum and back-filled with ethylene. Under an atmosphere of ethylene, the flask was charged with 20 mL of dry toluene and 1000 equiv of MAO with respect to the complex (7.6 μmol). The solution was stirred for 10−15 min before a solution of the catalyst in either toluene or dichloromethane was introduced into the flask via a syringe. The reaction mixture was stirred for either 10 or 30 min after the addition of the catalyst and subsequently quenched with a 1:1 mixture of concentrated hydrochloric acid and methanol. The resulting mixture was filtered. Any solid collected was washed with distilled water and dried under vacuum at approximately 50 °C for 24 h. Complex **4.6** gave 39 mg (5.1 kg of PE mol^{-1} of Cr; 31 kg of PE mol^{-1} of Cr h^{-1}) of polyethylene, as averages of three 10 min runs. In contrast, complex **4.6** gave 55 mg (7.3 kg of PE mol^{-1} of Cr; 15 kg of PE mol^{-1} of Cr h^{-1}) of polyethylene, as averages of two 30 min runs.

X-ray crystallographic data for compound **4.6** were collected at the University of Toronto on a Bruker Kappa APEX-DUO diffractometer using a copper ImuS tube with multilayer optics and were measured using a combination of ϕ scans and ω scans. The data were processed using APEX2 and SAINT.[113] Absorption corrections were carried out using SADABS.[113] The structure was solved and refined using OLEX2 (v. 1.2)[114] with SHELXS-97[101] for full-matrix least-squares refinement that was based on F^2. All H atoms were included in calculated positions and allowed to refine in riding-motion approximation with U_{iso} tied to the carrier atom.

Chapter Five

Spectroscopic and Density Functional Theory Studies of Bis(imino)-*N*-Heterocyclic Carbene Iron(II) Complexes

Many transformations that are catalyzed by transition metal complexes have been significantly improved by incorporating NHC ligands[48,115] due to the capability of tuning their electronic and steric properties.[68,105b] Nolan proposed a model to measure the steric bulk of NHCs using the length parameter A_L and the height parameter A_H (Figure 5.1).[116] A modified model to measure the NHCs steric bulk was proposed by Nolan and Cavallo. This model (percent buried volume, % V_{bur}) represents the volume percent of a sphere occupied by a ligand (Figure 5.2).[117]

The electronic properties of NHC ligands have been investigated and their Tolman electronic parameters[118] (TEP) were introduced by Crabtree[119] and Nolan[120]. The studies included IR vibrational frequencies of CO ligands in $M(CO)_2Cl(NHC)$ (M = Rh, Ir) and $[Ni(CO)_3(NHC)]$ complexes.[119-121] The effects of substitutes and ring size of NHCs on TEP were examined using DFT calculations to study their steric hindrance and electron-donor properties.[105b] The electron donating capabilities of carbene ligands were also quantified by the chemical shifts of ^{13}C of NHC palladium(II) complexes.[122] Moreover, chemical shifts of ^{31}P and ^{77}Se of carbene-phosphinidene and carbene-selenium adducts, respectively, were used to assess the π-accepting ability of NHC.[106,123] On the other hand, the electron donating properties of NHC ligands were studied using oxidation-reduction process of metal-carbene complexes.[68,124]

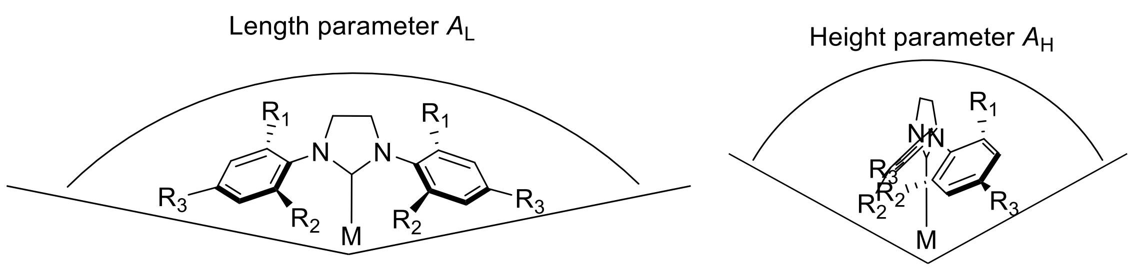

Figure 5.1. Steric parameters (A_L and A_H) for NHC ligands.

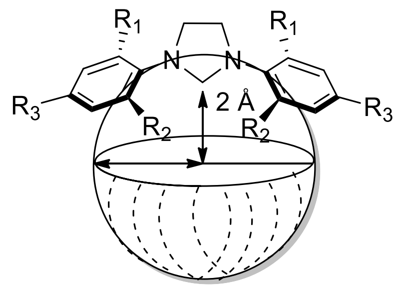

Figure 5.2. Percent buried volume % V_{bur} for NHC ligands.

In this chapter, cyclic voltammetry experiments were carried out to investigate the redox behavior of the three generations of bis(imino)-NHC iron(II) complexes described in the preceding chapters. In addition, DFT calculations were performed to further explore the π-accepting and σ-donating abilities of the bis(imino)-NHC ligands. The relative energy levels, the composition of the highest occupied molecular orbital (HOMO) and the lowest unoccupied molecular orbitals (LUMO), and the electron density mapping of the optimized structures are presented.

5.1 Cyclic voltammetry of the imidazolium salt and the related NHC iron complexes

The cyclic voltammograms for the imidazolium salt **2.7** and the related iron complex $[C_{imi}(\text{^}Imine_{Me})_2]FeCl_2$ (**2.17**) are respectively shown in Figure 5.3 and 5.4 and their results are illustrated in Table 5.1. An irreversible process was observed for **2.7** in which the anodic (E_{pa}) (829 and 1597 mV) and the cathodic (E_{pc}) (–746 mV) peaks are not related. For complex **2.17**, a reversible redox cycle is observed with a half-potential of –596 mV which it can be attributed to one-electron transfer for the Fe(II)-Fe(I). A reversible one-electron reduction process (Fe(II)-Fe(I)) of 1-[6-(cyclohexylethanimidoyl)-2-pyridinyl]ethylidene-2,6-dimethylaniline]iron dichloride was reported at –1150 mV in dichloromethane.[125] Irreversible processes were observed at 708 and 1148 mV for the cathodic and anodic peaks, respectively. An irreversible anodic (E_{pa}) potential peak was also identified at more positive potential (1338 mV). Gibson reported the cyclic voltammograms for the bis(imino)pyridine iron(II) complex in dichloromethane in which a single reversible cycle assigned for Fe(II)-Fe(III) with a half potential of 512 mV was observed.[126] However, different electrochemical data was reported for the same complex in acetonitrile in which reversible cycle for Fe(II)-Fe(III) at $E_{1/2}$ of 41 mV, irreversible cycles at ($E_{1/2}$) (–707 and –496 mV) and quasi-reversible cycle at $E_{1/2}$ of 566 mV were observed.[84]

Table 5.1. Cyclic voltammetry data for **2.7** and **2.17**.

Compound / complex	$E_{pa}1$ (mV)	$E_{pc}1$ (mV)	Δ_1^* (mV)	$E_{1/2}$ (mV)	$E_{pa}2$ (mV)	$E_{pc}2$ (mV)	Δ_2^* (mV)	$E_{1/2}$ (mV)	$E_{pa}3$
2.7	829	–746	---	---	1597	---	---	---	---
2.17	– 522	–614	92	–568	1148	708	---	---	1338

* $\Delta_1 = (E_{pa}1 - E_{pc}1)$, $\Delta_2 = (E_{pa2} - E_{pc2})$

Cyclic voltammograms for the related iron(II) complexes $[C_{benz}(\text{^}Imine_{Me})_2]FeCl_2$ (**3.13**) and $[C_{pyr}(\text{^}Imine_{Me})_2]FeCl_2$ (**4.7**) displayed very broad peaks that could not be utilized (Figure 5.5 and 5.6, respectively). Although starting with reduction or oxidation potential, using different number of scans or solution concentrations, the cyclic voltammograms were not improved. The cyclic voltammograms for the complex (**4.7**) is different from that reported for the related 1,3-bis[1-(2,6-diisopropylphenylimino)-ethyl]pyrimidin-2-ylidene]iron chloride complex.[84]

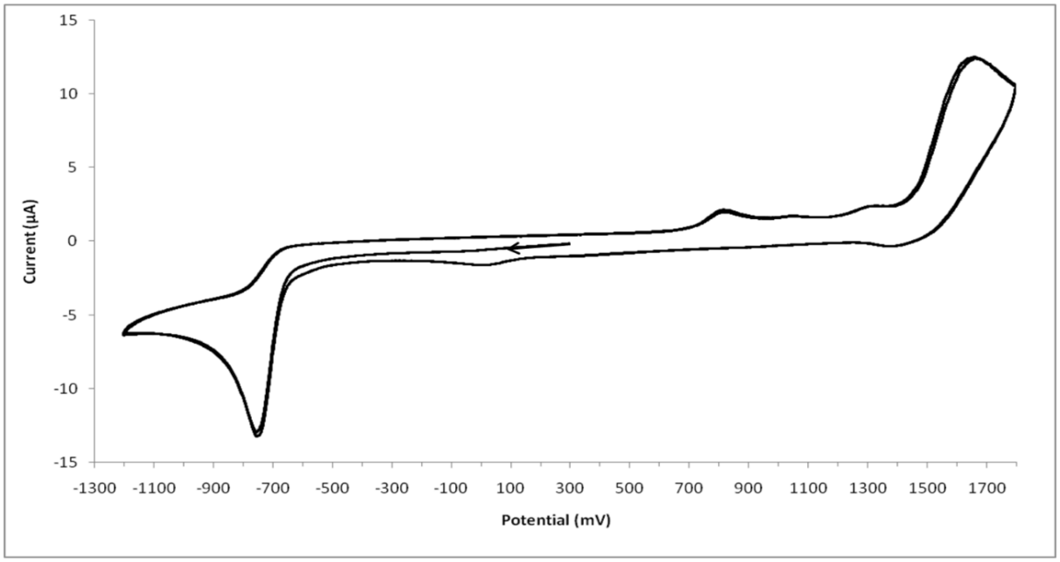

Figure 5.3. Cyclic voltammogram for the imidazolium salt **2.7,** 0.002 M in acetonitrile.

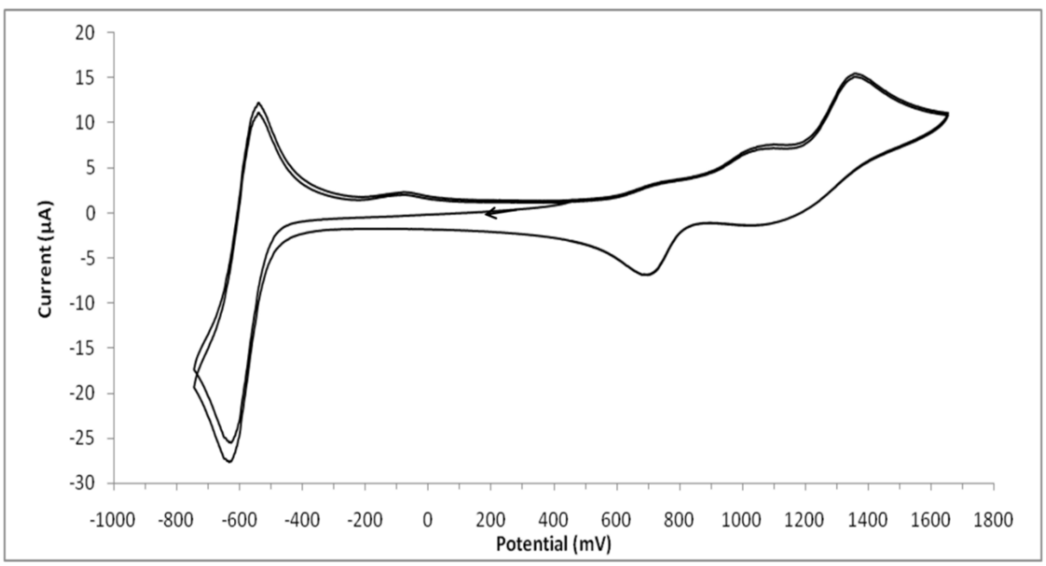

Figure 5.4. Cyclic voltammogram for imidazol-2-ylidene iron(II) complex **2.17,** 0.002 M in acetonitrile.

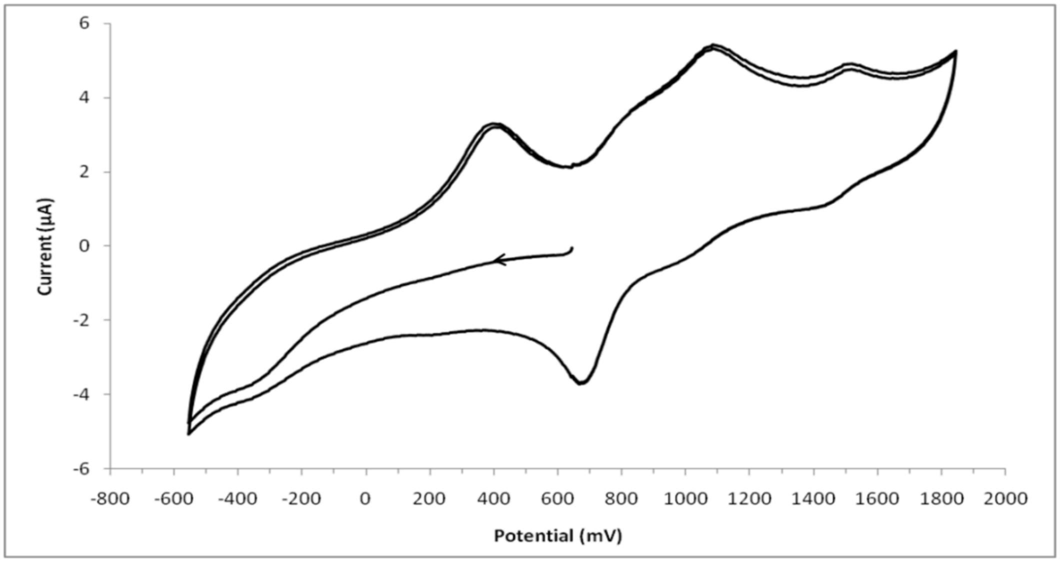

Figure 5.5. Cyclic voltammogram for benzimidazol-2-ylidene iron(II) complex **3.13,** 0.002 M in acetonitrile.

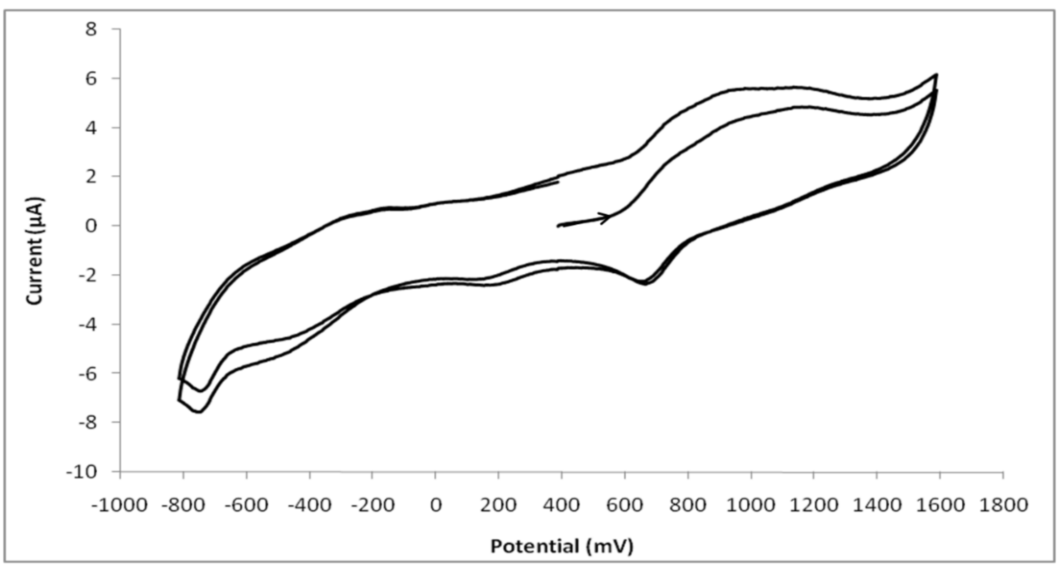

Figure 5.6. Cyclic voltammogram for pyrimidin-2-ylidene iron(II) complex **4.7,** 0.002 M in acetonitrile.

5.2 Density functional theory study of bis(imino)-NHC iron(II) complexes

DFT calculations were carried out to shed light on the electronic properties of the new family of bis(imino) NHC ligands. The B3LYP/DGDZVP[127] level of calculation was used to optimize the structure of the imidazolium salt **2.7**. The geometrical parameters in **2.7** were in good agreement with those in the X-ray structure of **2.7**, with root-mean-square deviation (RMSD) for all non-hydrogen atoms (counterion omitted) of bond lengths (0.011 Å) and of bond angles (0.065º).[128] Therefore, the structures of the related NHC ligands **1.55-1.57**, previously mentioned in Chapter 1, were optimized using the B3LYP/DGDZVP level of calculation.

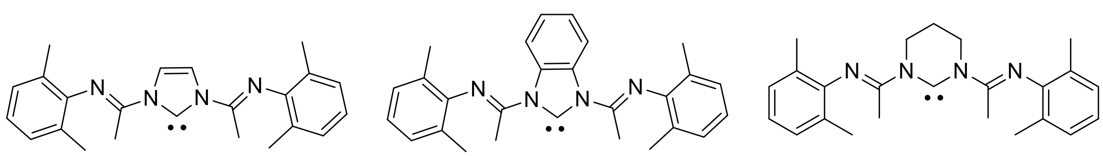

1.55 **1.56** **1.57**

A high contribution of the carbene carbon was observed in the HOMO for all three NHC ligands (**1.55-1.57**) (Figure 5.7). This is required for σ-bond formation in NHC transition metal complexes and also in agreement with published results.[129] Moreover, the carbene unhybridized p-orbital is notably contributing to the LUMO of the NHC ligands and this is essential for metal π-back donation to the ligand. The energy gaps of HOMO–LUMO were observed in the sequence of pyrimidin-2-ylidene (**1.57**) (4.80 eV), imidazol-2-ylidene (**1.55**) (4.77 eV) and benzimidazol-2-ylidene (**1.56**) (4.65 eV). The σ-electron donating and π-accepting character of a series of NHC ligands were evaluated based on the energy levels of HOMO and LUMO, respectively.[130] The greatest σ-electron donating ability is predicted for pyrimidin-2-ylidene (**1.57**) according to its highest energy of the HOMO of –5.86 eV compared to those of the NHC ligand **1.55** and **1.56**. However, the best π-accepting capability is expected for benzimidazol-2-ylidene (**1.56**) due to its lowest energy level of the LUMO (–1.40 eV) among those of other carbenes (**1.55** and **1.57**).[128]

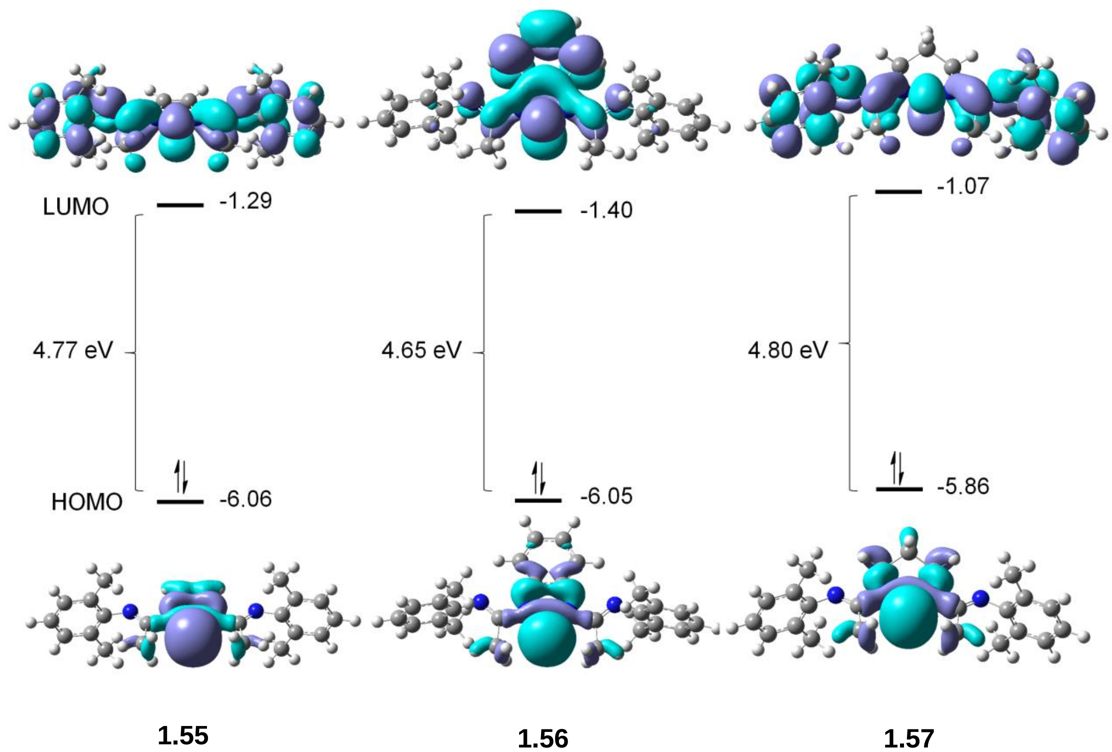

Figure 5.7. HOMO and LUMO representation and relative energy for imidazol-2-ylidene **1.55**, benzimidazol-2-ylidene **1.56** and pyrimidin-2-ylidene **1.57** generated at the B3LYP/DGDZVP level of calculation.

The reactivity of the related NHC Fe(II) complexes and their HOMO and LUMO nature were also computationally investigated. A more accurate level of calculations is essential for modeling transition metal complexes than that used for small organic molecules.[131] Due to the paramagnetic nature of the Fe(II) complexes (**2.17**, **3.13** and **4.7**), the unrestricted open-shell model UB3LYP/TZVP,[127a,127c,132] was used to calculate the electronic structures and energies of these complexes.

The X-ray molecular structure of **2.17** (as shown in Chapter 2, Figure 2.5) illustrates that the molecule adopts a distorted tetrahedral geometry at the metal center and therefore triplet (low-spin) and quintet (high-spin) multiplicities are predicted with two and four unpaired electrons, respectively. The optimized geometrical parameters of **2.17** as quintet multiplicity (high-spin) are more comparable to the X-ray data than those calculated as triplet multiplicity (low-spin) (Table 5.2). A lower ground state energy was also observed for its optimized structure as quintet multiplicity than that of the related triplet multiplicity by 0.0313 hartrees (82.4 kJ/mol).[128] The measured magnetic susceptibility of the complex of 5.54 μB, consistent with the predicted value for four unpaired electrons,[73b] (as mentioned in Chapter 2, section 2.3.3) further supports the favored high-spin configuration (quintet multiplicity).

Good agreements were observed between the bond lengths of the optimized structure and those of the crystallographic data of **2.17**, with RMSD for all non-hydrogen atoms of 0.024 Å. This value is better than the RMSD (heavy atoms) of 0.28 Å reported for bond lengths of the optimized structure of hydroxamate Zr(IV) complex in solution at the B3LYP/DGDZVP level of calculation.[133] The RMSD of lengths of the four coordinated bonds to the iron center in the optimized structure as quintet multiplicity (0.062 Å) is lower than that as triplet multiplicity (0.12 Å), consistent with the favored quintet multiplicity. A disagreement between some calculated bond angles and the corresponding angles in X-ray data of **2.17** was observed with RMSD for all non-hydrogen atoms of 2.1° in which the main disagreement was between the iron center and its four coordinated atoms.[128]

Table 5.2. Comparison of selected geometrical parameters of the complex **2.17** as quintet and triplet spin multiplicities with X-ray structural parameters.

X-ray data[73b]			UB3LYP/ TZVP (quintet state)		UB3LYP/ TZVP (triplet state)	
Atom 1	Atom 2	Length (Å)	Length (Å)	Δ^{a}	Length (Å)	Δ^{a}
C1	Fe1	2.091(3)	2.1469	–0.056	1.8499	0.241
N3	Fe1	2.145(3)	2.2545	–0.110	2.1477	–0.003
Cl1	Fe1	2.2404(9)	2.2586	–0.018	2.2480	–0.008
Cl2	Fe1	2.2442(10)	2.2597	–0.016	2.2469	–0.003
C1	N1	1.369(4)	1.3669	0.002	1.3833	–0.014
C1	N2	1.350(4)	1.3511	–0.001	1.3658	–0.016
C2	C3	1.340(5)	1.3440	–0.004	1.3406	–0.001
C2	N1	1.398(4)	1.4003	–0.002	1.3995	–0.002
C3	N2	1.401(4)	1.4001	0.001	1.4044	–0.003
C4	N3	1.269(4)	1.2715	–0.003	1.2815	–0.013
C6	N4	1.256(4)	1.2612	–0.005	1.2639	–0.008

[a] Δ = bond length determined experimentally by X-ray diffraction analysis – bond length determined computationally

A high electron density is expected in **4.7** according to its highest relative energies of the HOMO (–6.05 and –5.36 eV for the alpha- and beta-spin manifolds, respectively) compared to those for the related complexes **2.17** and **3.13** (Figures 5.8 and 5.9). Conversely, the calculated LUMO energies for the complex **3.13** (–2.46 and –2.86 eV for the alpha- and beta-spin manifolds, respectively) were the lowest in these complexes and therefore a low electron density was suggested in **3.13**. The energy of HOMO in the reported NHC iridium(III) complexes was decreased by 0.24 eV as a result of electron-withdrawing fluorinated substituents of phenyl rings on the ligands.[134] The energy gaps of HOMO-LUMO in **4.7** (3.92 and 2.86 eV for the alpha- and beta-spin manifolds, respectively) were the highest with respect to those observed in **2.17** and **3.13**. The HOMO-

LUMO energy gaps of the alpha-spin manifold (3.80–3.92 eV) were higher than those of the beta-spin manifold of 2.64–2.86 eV, as observed in the iron complexes **2.17**, **3.13** and **4.7**.[128]

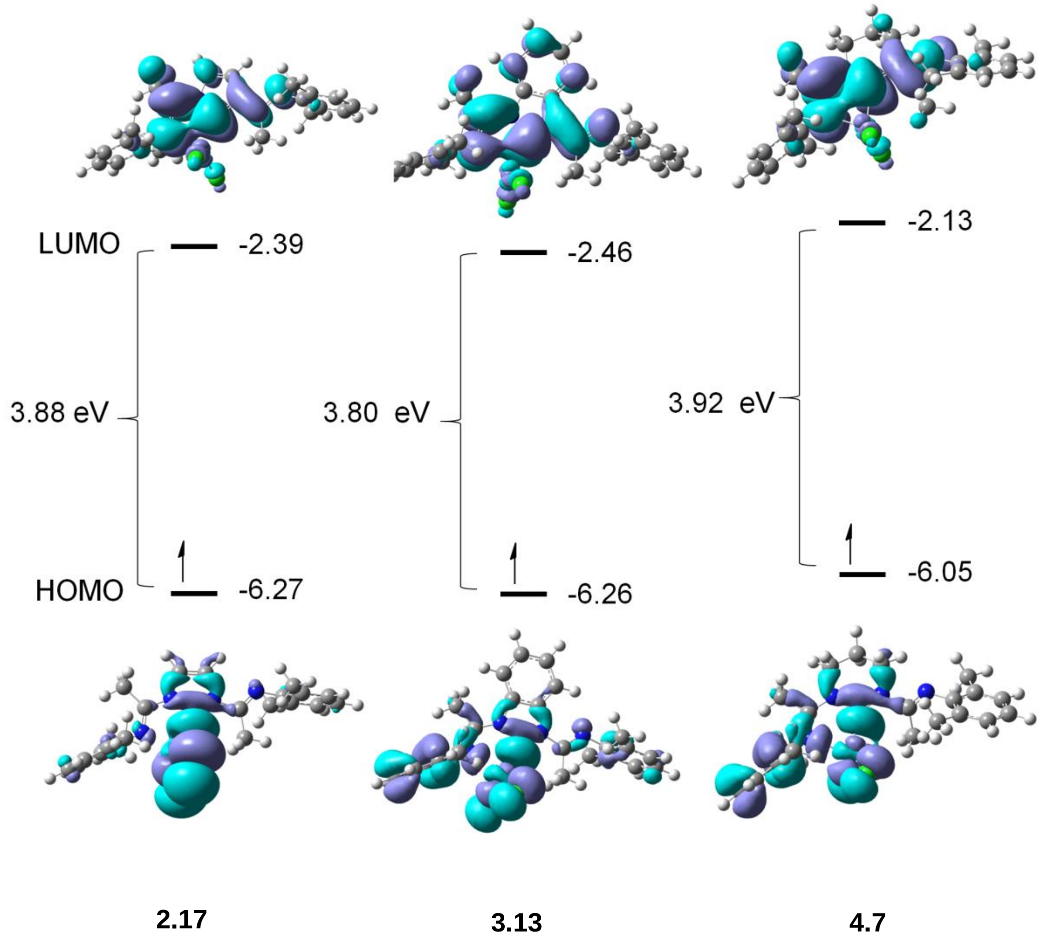

Figure 5.8. Alpha HOMO and LUMO representations and relative energies for NHC iron(II) complexes generated at the UB3LYP/TZVP level of calculation.

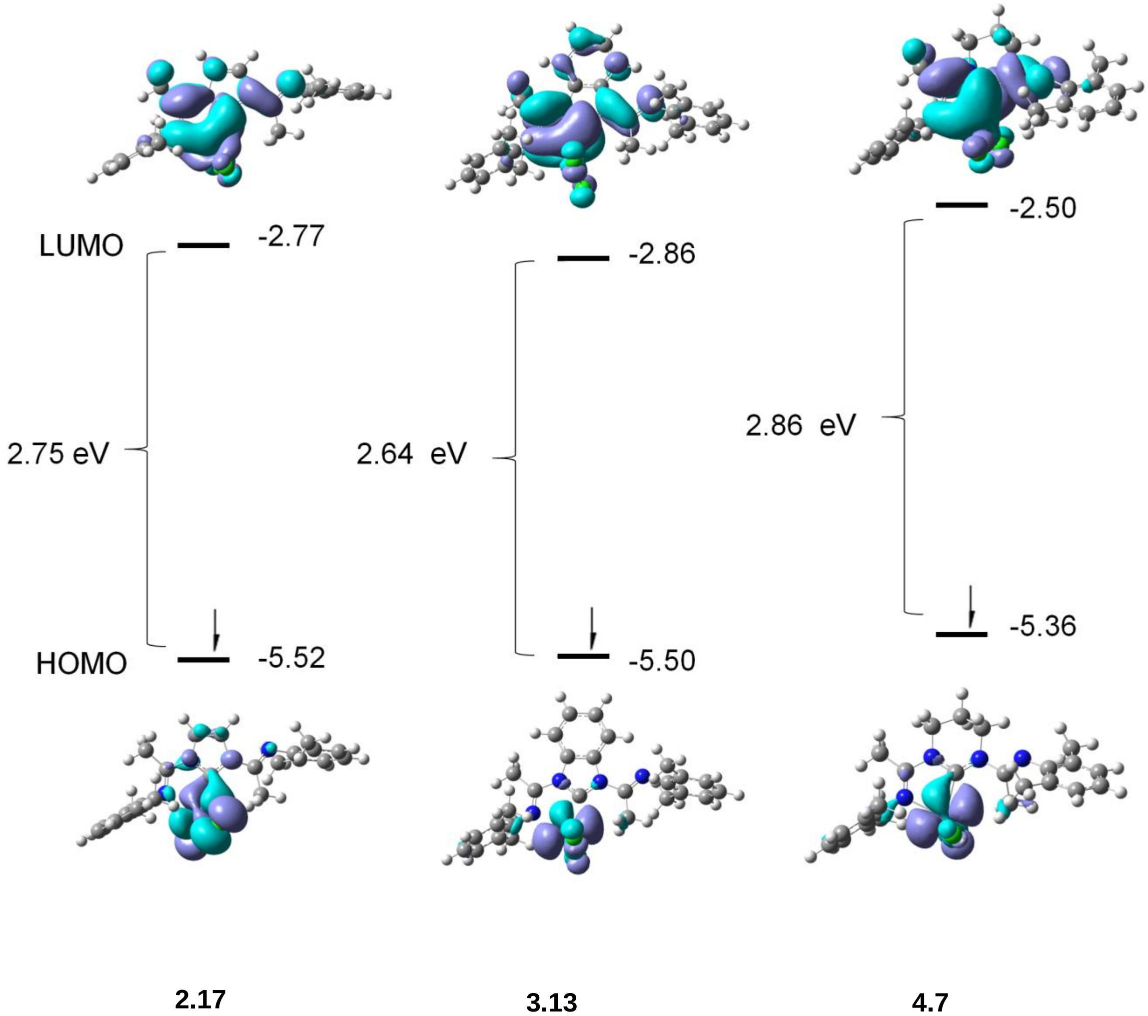

Figure 5.9. Beta HOMO and LUMO representations and relative energies for NHC iron(II) complexes generated at the UB3LYP/TZVP level of calculation.

The compositions of frontier molecular orbitals were studies by the AOMix program.[135] The molecules of **2.17**, **3.13** and **4.7** were individually treated as three fragments of Fe, $2Cl^{-}$ and NHC to evaluate their contribution to HOMO and LUMO. Good orbital mixing was observed in the HOMO of the alpha-spin manifold of the complex **2.17** in which each fragment contributes to the molecular orbital (NHC, 40.2%; Fe, 28.0%; $2Cl^{-}$, 31.9%) (Table 5.3). The highest percent contribution of the three fragments in the LUMO of alpha-spin was observed for the NHC fragment of 96.6%, while the iron center was the main contributor (92.3%) to the beta-spin HOMO. The NHC fragment has a significant contribution of 79.7% to the LUMO of beta-spin manifold.[128] Percent contributions of fragments for alpha and beta spin orbitals for the Fe(II) complexes **3.13** and **4.7** were similar to those observed for **2.17** (Table 5.3).

Table 5.3. Percent contribution of fragments for alpha and beta spin orbitals for NHC Fe(II) complexes.

Complex	Spin	Molecular orbital	%(Fe)	%($2Cl^-$)	%(NHC)	E (eV)
2.17	alpha	LUMO	2.0	1.4	96.6	–2.39
		HOMO	28.0	31.9	40.2	–6.27
	beta	LUMO	17.0	3.2	79.7	–2.77
		HOMO	92.3	3.5	4.2	–5.52
3.13	alpha	LUMO	2.3	1.6	96.1	–2.46
		HOMO	25.7	21.9	52.4	–6.26
	beta	LUMO	16.8	3.3	79.9	–2.86
		HOMO	91.8	3.6	4.7	–5.50
4.7	alpha	LUMO	2.1	1.3	96.5	–2.13
		HOMO	26.5	17.7	55.8	–6.05
	beta	LUMO	20.3	2.9	76.8	–2.50
		HOMO	90.5	3.9	5.6	–5.36

The molecular orbitals calculations for all of these complexes showed that the relative energies of alpha-spin manifolds, metal contributions (25.7–28.0%), were lower than those of the related the beta-spin HOMO, metal contributions (90.5–92.3%). Conversely, the relative energies of LUMO of alpha-spin manifolds, metal contributions (≈ 2%), were higher than those of the related beta-spin, metal contributions (16.8–20.3%). Higher percent contributions were calculated for the NHC fragments in HOMO for the alpha-spin manifold (40.2–55.8%) than those of the beta-spin (4.2–5.6%). Likewise, the percent contributions of NHC fragments in LUMO for the alpha-spin (≈ 96%) were higher than those observed for the beta-spin of 76.8–79.9% (Table 5.3).[128]

The electron donation and back-donation for the fragments of the iron complexes were investigated by the charge decomposition analysis (CDA)[136] method using the AOmix program[135]. The CDA results showed that electron donation of the NHC ligands to the iron center in **4.7**, **2.17** and **3.13** were 0.69, 0.67 and 0.64 a.u., respectively. However the differences between these results are minor, they suggest that the ranking of the electron donation for the NHCs is pyrimidin-2-ylidene (**1.57**) > imidazol-2-ylidene (**1.55**) > benzimidazol-2-ylidene (**1.56**).[128] This result is in agreement with that obtained from the relative energy levels of HOMO for the ligands (*vide supra*) and with the reported results.[105b,106,123] In contrast, the estimated back-donation to NHC from the iron center is 0.02 a.u. in all of these complexes in which no difference was calculated in π-accepting capability for the NHC ligands. The electron donation and back-donation calculated in NHC transition metal complexes using CDA were also not reliable.[137]

Minor differences were observed in the electron densities for the NHC ligands as shown in their electrostatic potential maps (Figure 5.10). Probably due to π-electrons in the benzene ring, a slightly high electron density appeared on the benzimidazol-2-ylidene (**1.56**) backbone compared to the corresponding ligands **1.55** and **1.57**. The electrostatic potential maps of the NHC iron(II) complexes show the lowest electron density resides on the NHC ligand fragment of complex **4.7**. The electron density on the NHC fragment of the complex **2.17** is lower than that of the complex **3.13**. These results further corroborate the greater electron donating ability of pyrimidin-2-ylidene (**1.57**) compared to imidazol-2-ylidene (**1.55**) and benzimidazol-2-ylidene (**1.56**). The electrostatic potential maps of NHC iron complexes show that the lowest electron density resides on the iminic carbon of the N–C_{imino} fragment that is coordinated to the Fe(II) center.[128] This explains the tendency towards nucleophilic attack at this iminic carbon in which the complex decomposes through N–C_{imino} cleavage (as stated in Chapter 2, section 2.1). A similar decomposition pathway was reported for the related bis(imino) NHC ligand.[74]

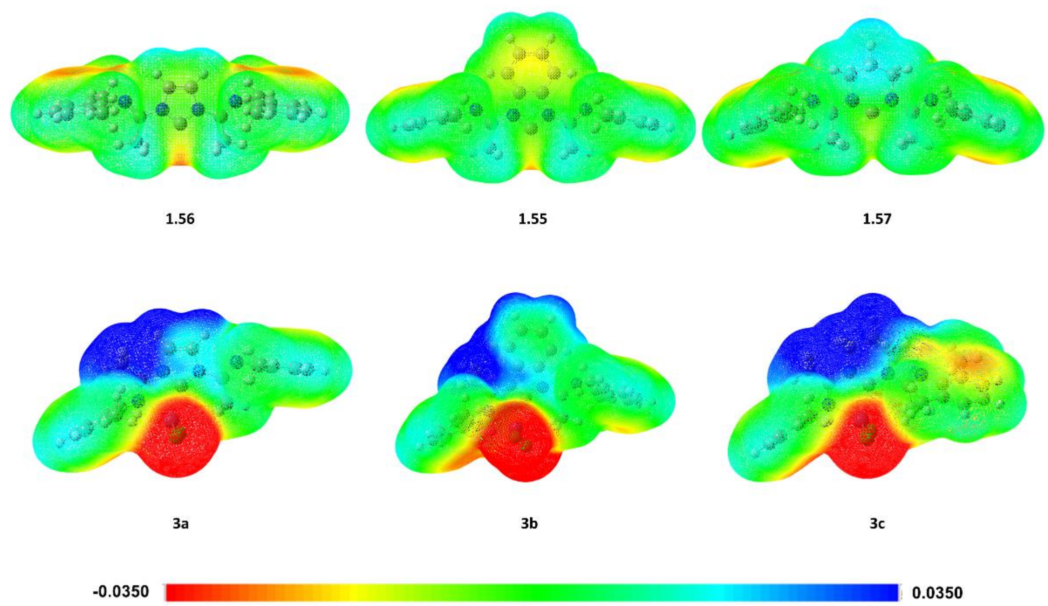

Figure 5.10. Electrostatic potential maps of bis(imino) NHC ligand (top; B3LYP/TZVP) and their iron complexes (bottom; B3LYP/TZVP). The color code is in the range of −0.0350 (deepest red) to (deepest blue) 0.0350 e/bohr^3.

5.3 Conclusions

The cyclic voltammetry experiments were carried out to investigate the redox behavior of the three generations of bis(imino)-NHC iron(II) complexes. While the voltammograms for the salt **2.7** and complex **2.17** can be interpreted, the voltammograms for the related complexes **3.13** and **4.7** cannot be explained.

The calculated bond lengths and angles for **2.17** using the UB3LYP/TZVP level of theory in quintet spin multiplicity are in better agreement with those of the X-ray structural data than those in triplet spin multiplicity. Furthermore, lower relative energy was calculated for the complex **2.17** in the quintet spin multiplicity than that in the triplet spin multiplicity by 82.4 kJ/mol, in accord with the measured magnetic susceptibility (Chapter 2, section 2.3.3).

The greater σ-electron donating ability is predicted for pyrimidin-2-ylidene (**1.57**), whereas the benzimidazol-2-ylidene (**1.56**) in the best π-accepting ligand among the studied NHCs, based on the molecular orbital calculations. Therefore, a higher electron density for the metal center is predicted in **4.7** than that in **2.17** and **3.13**. This was supported by the high relative energy of its HOMO, compared to that of the corresponding **2.17** and **3.13**. The CDA suggests that the ranking of the σ-electron donation is pyrimidin-2-ylidene (**1.57**) > imidazol-2-ylidene (**1.55**) > benzimidazol-2-ylidene (**1.56**). The reactivity of these complexes was also studied by their electron density maps.

5.4 Experimental procedures and computational details

The electrochemical measurements were performed using a BASi-Epsilon potentiostat, at a scan rate of 100 mV/s under N_2 at room temperature. Five scan cycles were performed and the direction of scans did not affect the cyclic voltammograms. The compound $[^{n}Bu_4N][PF_6]$ (0.1 M in CH_3CN) was used as a supporting electrolyte and the sample solution was approximately 2 mM in concentration. A platinum disk, platinum wire and $Ag/Ag^{+}Cl^{-}$ were used as working, counter and reference electrodes, respectively. Prior to measurements, the blank cyclic voltammograms were acquired in an acetonitrile solution of $^{n}Bu_4NPF_6$. The potentials were calibrated with respect to ferrocene/ferrocenium ion (Fc/Fc^{+}) as an internal standard as recommended by IUPAC.[138]

The DFT calculations were performed at the B3LYP and UB3LYP[127a,127c] levels of theory combined with the DGDZVP[127b] or TZVP[132] basis set, respectively. Gaussian 03[139] and Gaussian 09[140] programs were used for the calculations, whereas the GaussView 03[141] program was utilized for the molecular visualization. The calculations were carried out on the Shared Hierarchical Academic Research Computing Network (SHARCNET: www.sharcnet.ca) or on a personal computer. The closed shell model B3LYP/DGDZVP was used to perform the calculations on the diamagnetic compounds (**2.7**, **1.55**, **1.56** and **1.57**), whereas the structural properties and energies for the related paramagnetic Fe(II) complexes (**2.17**, **3.13** and **4.7**) were calculated using the unrestricted open-shell model UB3LYP/TZVP. Relative energies, percent contributions of fragments in HOMO and LOMO and CDA in the NHC iron(II) complexes were calculated by the AOMix program.[135] The GaussView 03[141] was used to generate the molecular orbitals and the electrostatic potential maps.

References

1. Britovsek, G. J. P.; Gibson, V. C.; Wass, D. F. *Angew. Chem. Int. Ed.* **1999**, *38*, 428-447.
2. (a) Sinn, H.; Kaminsky, W.; Vollmer, H.-J.; Woldt, R. *Angew. Chem. Int. Ed. Engl.* **1980**, *19*, 390-392; (b) Kaminsky, W. *Macromol. Chem. Phys.* **1996**, *197*, 3907-3945.
3. (a) Canich, J. A. M.; Turner, H. W. Constrained-geometry Catalysts. WO-A 92/12162, (Exxon), **1992**; (b) Chen, Y.-X.; Marks, T. J. *Organometallics* **1997**, *16*, 3649-3657.
4. Ittel, S. D.; Johnson, L. K.; Brookhart, M. *Chem. Rev.* **2000**, *100*, 1169-1204.
5. Gibson, V. C.; Spitzmesser, S. K. *Chem. Rev.* **2003**, *103*, 283-316.
6. Drent, E.; van Dijk, R.; van Ginkel, R.; van Oort, B.; Pugh, R. I. *Chem. Commun.* **2002**, 744-745.
7. Johnson, L. K.; Killian, C. M.; Brookhart, M. *J. Am. Chem. Soc.* **1995**, *117*, 6414-6415.
8. Svejda, S. A.; Johnson, L. K.; Brookhart, M. *J. Am. Chem. Soc.* **1999**, *121*, 10634-10635.
9. (a) Younkin, T. R.; Connor, E. F.; Henderson, J. I.; Friedrich, S. K.; Grubbs, R. H.; Bansleben, D. A. *Science* **2000**, *287*, 460-462; (b) Wang, C.; Friedrich, S.; Younkin, T. R.; Li, R. T.; Grubbs, R. H.; Bansleben, D. A.; Day, M. W. *Organometallics* **1998**, *17*, 3149-3151.
10. Chan, M. S. W.; Deng, L.; Ziegler, T. *Organometallics* **2000**, *19*, 2741-2750.
11. Klein, H.-F.; Bickelhaupt, A. *Inorg. Chim. Acta* **1996**, *248*, 111-114.

12. (a) Johnson, L. K.; Mecking, S.; Brookhart, M. *J. Am. Chem. Soc.* **1996**, *118*, 267-268; (b) Mecking, S.; Johnson, L. K.; Wang, L.; Brookhart, M. *J. Am. Chem. Soc.* **1998**, *120*, 888-899; (c) Killian, C. M.; Tempel, D. J.; Johnson, L. K.; Brookhart, M. *J. Am. Chem. Soc.* **1996**, *118*, 11664-11665.

13. (a) Bauers, F. M.; Mecking, S. *Angew. Chem. Int. Ed.* **2001**, *40*, 3020-3022; (b) Bauers, F. M.; Mecking, S. *Macromolecules* **2001**, *34*, 1165-1171.

14. Connor, E. F.; Younkin, T. R.; Henderson, J. I.; Hwang, S.; Grubbs, R. H.; Roberts, W. P.; Litzau, J. J. *J. Polym. Sci., Part A: Polym. Chem.* **2002**, *40*, 2842-2854.

15. Britovsek, G. J. P.; Gibson, V. C.; McTavish, S. J.; Solan, G. A.; White, A. J. P.; Williams, D. J.; Britovsek, G. J. P.; Kimberley, B. S.; Maddox, P. J. *Chem. Commun.* **1998**, 849-850.

16. (a) Bennett, A. M. A. Polymerization of Ethylene with Specific Iron or Cobalt Complexes, Novel Pyridinebis(imines) and Novel Complexes of Pyridinebis(imines) with Iron and Cobalt. WO 98/27124, (Dupont), **1998**; (b) Bennett, A. M. A. Polymerization of Olefins WO 9856832, **1998**; (c) Britovsek, G. J. P.; Bruce, M.; Gibson, V. C.; Kimberley, B. S.; Maddox, P. J.; Mastroianni, S.; McTavish, S. J.; Redshaw, C.; Solan, G. A.; Strömberg, S.; White, A. J. P.; Williams, D. J. *J. Am. Chem. Soc.* **1999**, *121*, 8728-8740; (d) Small, B. L.; Brookhart, M.; Bennett, A. M. A. *J. Am. Chem. Soc.* **1998**, *120*, 4049-4050; (e) Small, B. L.; Brookhart, M. *J. Am. Chem. Soc.* **1998**, *120*, 7143-7144.

17. Alyea, E. C.; Merrell, P. H. *Synth. React. Inorg. Met.-Org. Chem.* **1974**, *4*, 535-544.

18. Gibson, V.; Solan, G., Iron-Based and Cobalt-Based Olefin Polymerisation Catalysts. In *Metal Catalysts in Olefin Polymerization*, Guan, Z., Ed. Springer Berlin Heidelberg: **2009**, *26*, 107-158.

19. (a) Ionkin, A. S.; Marshall, W. J.; Adelman, D. J.; Bobik Fones, B.; Fish, B. M.; Schiffhauer, M. F.; Spence, R. E.; Xie, T. *Organometallics* **2008**, *27*, 1147-1156; (b) Ionkin, A. S.; Marshall, W. J.; Adelman, D. J.; Fones, B. B.; Fish, B. M.; Schiffhauer, M. F. *Organometallics* **2008**, *27*, 1902-1911; (c) Ionkin, A. S.; Marshall, W. J.; Adelman, D. J.; Fones, B. B.; Fish, B. M.; Schiffhauer, M. F.; Soper, P. D.; Waterland, R. L.; Spence, R. E.; Xie, T. *J. Polym. Sci., Part A: Polym. Chem.* **2007**, *46*, 585-611.

20. (a) Devore, D. F., S. S.; Frazier, K. A.; Patton, J. T. Transition Metal Complexes and Olefin Polymerization Process. WO 0069923, (Dow Chemical) **2000**; (b) Small, B. L.; Carney, M. J.; Holman, D. M.; O'Rourke, C. E.; Halfen, J. A. *Macromolecules* **2004**, *37*, 4375-4386; (c) Esteruelas, M. A.; López, A. M.; Méndez, L.; Oliván, M.; Oñate, E. *Organometallics* **2003**, *22*, 395-406; (d) Vidyaratne, I.; Scott, J.; Gambarotta, S.; Duchateau, R. *Organometallics* **2007**, *26*, 3201-3211.

21. (a) Gibson, V. C.; Redshaw, C.; Solan, G. A. *Chem. Rev.* **2007**, *107*, 1745-1776; (b) Sylvester, K. T.; Chirik, P. J. *J. Am. Chem. Soc.* **2009**, *131*, 8772-8774; (c) Trovitch, R. J.; Lobkovsky, E.; Bill, E.; Chirik, P. J. *Organometallics* **2008**, *27*, 1470-1478; (d) Bouwkamp, M. W.; Bowman, A. C.; Lobkovsky, E.; Chirik, P. J. *J. Am. Chem. Soc.* **2006**, *128*, 13340-13341; (e) Tondreau, A. M.; Lobkovsky, E.; Chirik, P. J. *Org. Lett.* **2008**, *10*, 2789-2792; (f) Tondreau, A. M.; Milsmann, C.;

Patrick, A. D.; Hoyt, H. M.; Lobkovsky, E.; Wieghardt, K.; Chirik, P. J. *J. Am. Chem. Soc.* **2010**, *132*, 15046-15059; (g) Archer, A. M.; Bouwkamp, M. W.; Cortez, M.-P.; Lobkovsky, E.; Chirik, P. J. *Organometallics* **2006**, *25*, 4269-4278; (h) Liu, P.; Zhou, L.; Li, X.; He, R. *J. Organomet. Chem.* **2009**, *694*, 2290-2294; (i) Yoon, H. J.; Heo, J.; Mirkin, C. A. *J. Am. Chem. Soc.* **2007**, *129*, 14182-14183; (j) Dayan, O.; Çetinkaya, B. *J. Mol. Catal. A: Chem.* **2007**, *271*, 134-141; (k) Britovsek, G. J. P.; England, J.; Spitzmesser, S. K.; White, A. J. P.; Williams, D. J. *Dalton Trans.* **2005**, 945-955; (l) Small, B. L. *Organometallics* **2003**, *22*, 3178-3183.

22. (a) Bart, S. C.; Lobkovsky, E.; Chirik, P. J. *J. Am. Chem. Soc.* **2004**, *126*, 13794-13807; (b) Tang, W.; Hu, X.; Zhang, X. *Tetrahedron Lett.* **2002**, *43*, 3075-3078; (c) Dias, E. L.; Brookhart, M.; White, P. S. *Chem. Commun.* **2001**, 423-424; (d) Chiericato Jr, G.; Arana, C. R.; Casado, C.; Cuadrado, I.; Abruña, H. D. *Inorg. Chim. Acta* **2000**, *300–302*, 32-42; (e) Scott, J.; Vidyaratne, I.; Korobkov, I.; Gambarotta, S.; Budzelaar, P. H. M. *Inorg. Chem.* **2008**, *47*, 896-911; (f) Liu, P.; Yan, M.; He, R. *Appl. Organomet. Chem.* **2010**, *24*, 131-134.

23. (a) McGuinness, D. S.; Gibson, V. C.; Wass, D. F.; Steed, J. W. *J. Am. Chem. Soc.* **2003**, *125*, 12716-12717; (b) McGuinness, D. S.; Gibson, V. C.; Steed, J. W. *Organometallics* **2004**, *23*, 6288-6292; (c) Danopoulos, A. A.; Wright, J. A.; Motherwell, W. B.; Ellwood, S. *Organometallics* **2004**, *23*, 4807-4810; (d) Danopoulos, A. A.; Tsoureas, N.; Wright, J. A.; Light, M. E. *Organometallics* **2004**, *23*, 166-168; (e) McGuinness, D. S.; Suttil, J. A.; Gardiner, M. G.; Davies,

N. W. *Organometallics* **2008**, *27*, 4238-4247; (f) Danopoulos, A. A.; Winston, S.; Motherwell, W. B. *Chem. Commun.* **2002**, 1376-1377.

24. Britovsek, G. J. P.; Mastroianni, S.; Solan, G. A.; Baugh, S. P. D.; Redshaw, C.; Gibson, V. C.; White, A. J. P.; Williams, D. J.; Elsegood, M. R. J. *Chem. Eur. J.* **2000**, *6*, 2221-2231.

25. Bourissou, D.; Guerret, O.; Gabbaï, F. P.; Bertrand, G. *Chem. Rev.* **2000**, *100*, 39-92.

26. Hahn, F. E.; Jahnke, M. C. *Angew. Chem. Int. Ed.* **2008**, *47*, 3122-3172.

27. Gleiter, R.; Hoffmann, R. *J. Am. Chem. Soc.* **1968**, *90*, 5457-5460.

28. (a) Harrison, J. F.; Liedtke, R. C.; Liebman, J. F. *J. Am. Chem. Soc.* **1979**, *101*, 7162-7168; (b) Feller, D.; Thatcher Borden, W.; Davidson, E. R. *Chem. Phys. Lett.* **1980**, *71*, 22-26.

29. (a) Hoffmann, R.; Zeiss, G. D.; Van Dine, G. W. *J. Am. Chem. Soc.* **1968**, *90*, 1485-1499; (b) Baird, N. C.; Taylor, K. F. *J. Am. Chem. Soc.* **1978**, *100*, 1333-1338.

30. Herrmann, W. A.; Köcher, C. *Angew. Chem. Int. Ed. Engl.* **1997**, *36*, 2162-2187.

31. (a) Schoeller, W. W. *J. Chem. Soc., Chem. Commun.* **1980**, 124-125; (b) Pauling, L. *J. Chem. Soc., Chem. Commun.* **1980**, 688-689.

32. Gilbert, B. C.; Griller, D.; Nazran, A. S. *J. Org. Chem.* **1985**, *50*, 4738-4742.

33. (a) Modarelli, D. A.; Morgan, S.; Platz, M. S. *J. Am. Chem. Soc.* **1992**, *114*, 7034-7041; (b) Richards, C. A.; Kim, S.-J.; Yamaguchi, Y.; Schaefer, H. F. *J. Am. Chem. Soc.* **1995**, *117*, 10104-10107.

34. Myers, D. R.; Senthilnathan, V. P.; Platz, M. S.; Jones, M. *J. Am. Chem. Soc.* **1986**, *108*, 4232-4233.

35. Gano, J. E.; Wettach, R. H.; Platz, M. S.; Senthilnathan, V. P. *J. Am. Chem. Soc.* **1982**, *104*, 2326-2327.

36. (a) Noller, H.; Hantsche, H.; Andréu, P. *Angew. Chem.* **1964**, *76*, 645-646; (b) Fischer, E. O. *Angew. Chem.* **1974**, *86*, 651-663; (c) Herndon, J. W. *Coord. Chem. Rev.* **2000**, *206–207*, 237-262.

37. (a) Schrock, R. R. *J. Am. Chem. Soc.* **1974**, *96*, 6796-6797; (b) Schrock, R. R. *Acc. Chem. Res.* **1979**, *12*, 98-104.

38. Kühl, O., The Nature of N-Heterocyclic Carbenes. In *Functionalised N-Heterocyclic Carbene Complexes*, John Wiley & Sons, Ltd: **2010**, 7-37.

39. (a) Wanzlick, H. W.; Schikora, E. *Angew. Chem.* **1960**, *72*, 494; (b) Wanzlick, H. W.; Kleiner, H. J. *Angew. Chem.* **1961**, *73*, 493; (c) Wanzlick, H. W. *Angew. Chem.* **1962**, *74*, 129-134.

40. Schönherr, H.-J.; Wanzlick, H.-W. *Justus Liebigs Ann. Chem.* **1970**, *731*, 176-179.

41. Wanzlick, H. W.; Schonher.Hj *Angew. Chem.* **1968**, *7*, 141.

42. Öfele, K.; Herberhold, M. *Angew. Chem. Int. Ed. Engl.* **1970**, *9*, 739-740.

43. (a) Cardin, D. J.; Cetinkaya, B.; Lappert, M. F.; Manojlovic-Muir, L.; Muir, K. W. *J. Chem. Soc. D* **1971**, 400-401; (b) Lappert, M. F. *J. Organomet. Chem.* **2005**, *690*, 5467-5473.

44. Arduengo, A. J.; Krafczyk, R. *Chem. unserer Zeit* **1998**, *32*, 6-14.

45. Arduengo, A. J.; Harlow, R. L.; Kline, M. *J. Am. Chem. Soc.* **1991**, *113*, 361-363.

46. N. Kuhn, T. K. *Synthesis* **1993**, 561-562.

47. Weskamp, T.; Böhm, V. P. W.; Herrmann, W. A. *J. Organomet. Chem.* **2000**, *600*, 12-22.

48. Herrmann, W. A. *Angew. Chem. Int. Ed.* **2002**, *41*, 1290-1309.

49. Gridnev, A. A.; Mihaltseva, I. M. *Synth. Commun.* **1994**, *24*, 1547-1555.

50. Özdemir, I.; Gürbüz, N.; Gök, Y.; Çetinkaya, B. *Heteroat. Chem* **2008**, *19*, 82-86.

51. (a) Jazzar, R.; Liang, H.; Donnadieu, B.; Bertrand, G. *J. Organomet. Chem.* **2006**, *691*, 3201-3205; (b) Iglesias, M.; Beetstra, D. J.; Knight, J. C.; Ooi, L.-L.; Stasch, A.; Coles, S.; Male, L.; Hursthouse, M. B.; Cavell, K. J.; Dervisi, A.; Fallis, I. A. *Organometallics* **2008**, *27*, 3279-3289.

52. (a) Douthwaite, R. E.; Haüssinger, D.; Green, M. L. H.; Silcock, P. J.; Gomes, P. T.; Martins, A. M.; Danopoulos, A. A. *Organometallics* **1999**, *18*, 4584-4590; (b) Dastgir, S.; Coleman, K. S.; Cowley, A. R.; Green, M. L. H. *Organometallics* **2005**, *25*, 300-306.

53. Arduengo, A. J.; Goerlich, J. R.; Marshall, W. J. *J. Am. Chem. Soc.* **1995**, *117*, 11027-11028.

54. (a) Dastgir, S.; Coleman, K. S.; Cowley, A. R.; Green, M. L. H. *Organometallics* **2010**, *29*, 4858-4870; (b) Arnold, P. L.; Mungur, S. A.; Blake, A. J.; Wilson, C. *Angew. Chem. Int. Ed.* **2003**, *42*, 5981-5984.

55. Arduengo, A. J.; Dias, H. V. R.; Harlow, R. L.; Kline, M. *J. Am. Chem. Soc.* **1992**, *114*, 5530-5534.

56. (a) Herrmann, W. A.; Elison, M.; Fischer, J.; Köcher, C.; Artus, G. R. J. *Chem. Eur. J.* **1996**, *2*, 772-780; (b) Herrmann, W. A.; Köcher, C.; Gooßen, L. J.; Artus, G. R. J. *Chem. Eur. J.* **1996**, *2*, 1627-1636.

57. Enders, D.; Breuer, K.; Raabe, G.; Runsink, J.; Teles, J. H.; Melder, J.-P.; Ebel, K.; Brode, S. *Angew. Chem. Int. Ed. Engl.* **1995**, *34*, 1021-1023.

58. Herrmann, W. A.; Goossen, L. J.; Artus, G. R. J.; Köcher, C. *Organometallics* **1997**, *16*, 2472-2477.

59. Venkatachalam, G.; Heckenroth, M.; Neels, A.; Albrecht, M. *Helv. Chim. Acta* **2009**, *92*, 1034-1045.

60. (a) Díez-González, S.; Nolan, S. P. *Ann. Rep. Prog. Chem. Sect. B* **2005**, *101*, 171; (b) McGuinness, D. S.; Cavell, K. J.; Yates, B. F. *Chem. Commun.* **2001**, 355-356.

61. Wang, H. M. J.; Lin, I. J. B. *Organometallics* **1998**, *17*, 972-975.

62. Herrmann, W. A.; Elison, M.; Fischer, J.; Köcher, C.; Artus, G. R. J. *Angew. Chem. Int. Ed. Engl.* **1995**, *34*, 2371-2374.

63. Lappert, M. F.; Pye, P. L. *J. Chem. Soc., Dalton Trans.* **1977**, 2172-2180.

64. Bantreil, X.; Broggi, J.; Nolan, S. P. *Ann. Rep. Prog. Chem. Sect. B* **2009**, *105*, 232-263.

65. (a) McGuinness, D. *Dalton Trans.* **2009**, 6915-6923; (b) Budagumpi, S.; Kim, K.-H.; Kim, I. *Coord. Chem. Rev.* **2011**, *255*, 2785-2809.

66. Jens, K. J. T., M.; Voges, M. H.; Blom, R.; Froseth, M. Catalyst for Polymerization of Olefins. WO 00/01739, **2000**.

67. Tilset, M. A., O.; Dhindsa, A.; Froseth, M. Metal Complex Catalysts for Polymerization of Ethylene. WO 02/49758, (Borealis Technology), **2002**.

68. Leuthäußer, S.; Schwarz, D.; Plenio, H. *Chem. Eur. J.* **2007**, *13*, 7195-7203.

69. (a) Small, B. L.; Brookhart, M. *Macromolecules* **1999**, *32*, 2120-2130; (b) Souane, R.; Isel, F.; Peruch, F.; Lutz, P. J. *C.R. Chim.* **2002**, *5*, 43-48; (c) Pellecchia, C.; Mazzeo, M.; Pappalardo, D. *Macromol. Rapid Commun.* **1998**, *19*, 651-655; (d)

Moniz Santos, J.; Ribeiro, M. R.; Portela, M. F.; Cramail, H.; Deffieux, A. *Macromol. Chem. Phys.* **2001**, *202*, 3043-3048.

70. (a) Britovsek, George J. P.; Gibson, Vernon C.; Mastroianni, S.; Oakes, Daniel C. H.; Redshaw, C.; Solan, Gregory A.; White, Andrew J. P.; Williams, David J. *Eur. J. Inorg. Chem.* **2001**, 431-437; (b) Britovsek, G. J. P.; Gibson, V. C.; Kimberley, B. S.; Mastroianni, S.; Redshaw, C.; Solan, G. A.; White, A. J. P.; Williams, D. J. *J. Chem. Soc., Dalton Trans.* **2001**, 1639-1644; (c) Tenza, K.; Hanton, M. J.; Slawin, A. M. Z. *Organometallics* **2009**, *28*, 4852-4867.

71. (a) Paulino, I. S.; Schuchardt, U. *J. Mol. Catal. A: Chem.* **2004**, *211*, 55-58; (b) Yu, J.; Liu, H.; Zhang, W.; Hao, X.; Sun, W.-H. *Chem. Commun.* **2011**, *47*, 3257-3259; (c) Semikolenova, N. V.; Zakharov, V. A.; Echevskaja, L. G.; Matsko, M. A.; Bryliakov, K. P.; Talsi, E. P. *Catal. Today* **2009**, *144*, 334-340; (d) Zohuri, G.; Seyedi, S.; Sandaroos, R.; Damavandi, S.; Mohammadi, A. *Catal. Lett.* **2010**, *140*, 160-166; (e) Guo, L.-h.; Gao, H.-y.; Zhang, L.; Zhu, F.-m.; Wu, Q. *Organometallics* **2010**, *29*, 2118-2125.

72. (a) Cao, X.; He, F.; Zhao, W.; Cai, Z.; Hao, X.; Shiono, T.; Redshaw, C.; Sun, W.-H. *Polymer* **2012**, *53*, 1870-1880; (b) Sun, W.-H.; Zhao, W.; Yu, J.; Zhang, W.; Hao, X.; Redshaw, C. *Macromol. Chem. Phys.* **2012**, *213*, 1266-1273; (c) Zhao, W.; Yu, J.; Song, S.; Yang, W.; Liu, H.; Hao, X.; Redshaw, C.; Sun, W.-H. *Polymer* **2012**, *53*, 130-137.

73. (a) Al Thagfi, J.; Dastgir, S.; Lough, A. J.; Lavoie, G. G. *Organometallics* **2010**, *29*, 3133-3138; (b) Al Thagfi, J.; Lavoie, G. G. *Organometallics* **2012**, *31*, 2463-2469.

74. Liu, P.; Wesolek, M.; Danopoulos, A. A.; Braunstein, P. *Organometallics* **2013**, *32*, 6286-6297.

75. (a) Bohler, C.; Stein, D.; Donati, N.; Grutzmacher, H. *New J. Chem.* **2002**, *26*, 1291-1295; (b) Amyes, T. L.; Diver, S. T.; Richard, J. P.; Rivas, F. M.; Toth, K. *J. Am. Chem. Soc.* **2004**, *126*, 4366-4374; (c) Steiner, G.; Kopacka, H.; Ongania, K.-H.; Wurst, K.; Preishuber-Pflügl, P.; Bildstein, B. *Eur. J. Inorg. Chem.* **2005**, 1325-1333; (d) Steiner, G.; Krajete, A.; Kopacka, H.; Ongania, K.-H.; Wurst, K.; Preishuber-Pflügl, P.; Bildstein, B. *Eur. J. Inorg. Chem.* **2004**, 2827-2836; (e) McGibbon, G. A.; Heinemann, C.; Lavorato, D. J.; Schwarz, H. *Angew. Chem. Int. Ed. Engl.* **1997**, *36*, 1478-1481; (f) Solé, S.; Gornitzka, H.; Guerret, O.; Bertrand, G. *J. Am. Chem. Soc.* **1998**, *120*, 9100-9101; (g) Aihara, H.; Matsuo, T.; Kawaguchi, H. *Chem. Commun.* **2003**, 2204-2205.

76. Despagnet-Ayoub, E.; Miqueu, K.; Sotiropoulos, J.-M.; Henling, L. M.; Day, M. W.; Labinger, J. A.; Bercaw, J. E. *Chem. Sci.* **2013**, *4*, 2117-2121.

77. (a) Garrison, J. C.; Youngs, W. J. *Chem. Rev.* **2005**, *105*, 3978-4008; (b) Lin, I. J. B.; Vasam, C. S. *Coord. Chem. Rev.* **2007**, *251*, 642-670.

78. Yamashita, Y.; Guo, X.-X.; Takashita, R.; Kobayashi, S. *J. Am. Chem. Soc.* **2010**, *132*, 3262-3263.

79. Hitchcock, P. B.; Lappert, M. F.; Pierssens, L. J. M. *Chem. Commun.* **1996**, 1189-1190.

80. Simpson, P. V.; Skelton, B. W.; Brown, D. H.; Baker, M. V. *Eur. J. Inorg. Chem.* **2011**, 1937-1952.

81. (a) Badaj, A. C.; Lavoie, G. G. *Organometallics* **2012**, *31*, 1103-1111; (b) Furst, M. R. L.; Cazin, C. S. J. *Chem. Commun.* **2010**, *46*, 6924-6925; (c) Chen, C.; Qiu, H.; Chen, W. *J. Organomet. Chem.* **2012**, *696*, 4166-4172.

82. (a) Schneider, N.; César, V.; Bellemin-Laponnaz, S.; Gade, L. H. *J. Organomet. Chem.* **2005**, *690*, 5556-5561; (b) Tulloch, A. A. D.; Danopoulos, A. A.; Kleinhenz, S.; Light, M. E.; Hursthouse, M. B.; Eastham, G. *Organometallics* **2001**, *20*, 2027-2031.

83. (a) Evans, D. F. *J. Chem. Soc.* **1959**, 2003-2005; (b) Sur, S. K. *J. Magn. Reson.* **1989**, *82*, 169-173; (c) Bain, G. A.; Berry, J. F. *J. Chem. Educ.* **2008**, *85*, 532-536.

84. Kaplan, H. Z.; Li, B.; Byers, J. A. *Organometallics* **2012**, *31*, 7343-7350.

85. (a) Mashima, K.; Tsurugi, H. *J. Organomet. Chem.* **2005**, *690*, 4414-4423; (b) Dawson, D. M.; Walker, D. A.; Thornton-Pett, M.; Bochmann, M. *J. Chem. Soc., Dalton Trans.* **2000**, 459-466.

86. Leung, C. H.; Incarvito, C. D.; Crabtree, R. H. *Organometallics* **2006**, *25*, 6099-6107.

87. Wang, D.; Liu, S.; Zeng, Y.; Sun, W.-H.; Redshaw, C. *Organometallics* **2011**, *30*, 3001-3009.

88. Kreisel, K. A.; Yap, G. P. A.; Theopold, K. H. *Organometallics* **2006**, *25*, 4670-4679.

89. Larocque, T. G.; Badaj, A. C.; Dastgir, S.; Lavoie, G. G. *Dalton Trans.* **2011**, *40*, 12705-12712.

90. (a) Crociani, B.; Antonaroli, S.; Burattini, M.; Paoli, P.; Rossi, P. *Dalton Trans.* **2010**, *39*, 3665-3672; (b) Barloy, L.; Ramdeehul, S.; Osborn, John A.; Carlotti, C.;

Taulelle, F.; De Cian, A.; Fischer, J. *Eur. J. Inorg. Chem.* **2000**, 2523-2532; (c) Canovese, L.; Visentin, F.; Uguagliati, P.; Lucchini, V.; Bandoli, G. *Inorg. Chim. Acta* **1998**, *277*, 247-252.

91. Clavier, H.; Correa, A.; Cavallo, L.; Escudero-Adán, E. C.; Benet-Buchholz, J.; Slawin, A. M. Z.; Nolan, S. P. *Eur. J. Inorg. Chem.* **2009**, 1767-1773.

92. Viciu, M. S.; Navarro, O.; Germaneau, R. F.; Kelly, R. A.; Sommer, W.; Marion, N.; Stevens, E. D.; Cavallo, L.; Nolan, S. P. *Organometallics* **2004**, *23*, 1629-1635.

93. Jensen, T. R.; Schaller, C. P.; Hillmyer, M. A.; Tolman, W. B. *J. Organomet. Chem.* **2005**, *690*, 5881-5891.

94. Lee, Y.; Li, B.; Hoveyda, A. H. *J. Am. Chem. Soc.* **2009**, *131*, 11625-11633.

95. (a) van Rensburg, H.; Tooze, R. P.; Foster, D. F.; Slawin, A. M. Z. *Inorg. Chem.* **2004**, *43*, 2468-2470; (b) McGuinness, D. S.; Cavell, K. J.; Skelton, B. W.; White, A. H. *Organometallics* **1999**, *18*, 1596-1605; (c) McGuinness, D. S.; Saendig, N.; Yates, B. F.; Cavell, K. J. *J. Am. Chem. Soc.* **2001**, *123*, 4029-4040.

96. Brindley, J. C.; Caldwell, J. M.; Meakins, G. D.; Plackett, S. J.; Price, S. J. *J. Chem. Soc., Perkin Trans. 1* **1987**, 1153-1158.

97. Herwig, W.; Zeiss, H. *J. Org. Chem.* **1958**, *23*, 1404.

98. Otwinowski, Z.; Minor, W. Processing of X-ray Diffraction Data Collected in Oscillation Mode; Academic Press: London, **1997**, 276, (Macromolecular Crystallography, Part A), 307−326.

99. Blessing, R. *Acta Crystallogr., Sect. A* **1995**, *51*, 33-38.

100. Palatinus, L.; Chapuis, G. *J. Appl. Crystallogr.* **2007**, *40*, 786-790.

101. Sheldrick, G. *Acta Crystallogr., Sect. A* **1990**, *46*, 467-473.

102. Altomare, A.; Cascarano, G.; Giacovazzo, C.; Guagliardi, A.; Burla, M. C.; Polidori, G.; Camalli, M. *J. Appl. Crystallogr.* **1994**, *27*, 435.

103. Sheldrick, G. *Acta Crystallogr., Sect. A* **2008**, *64*, 112-122.

104. Nobbs, J. D.; Tomov, A. K.; Cariou, R.; Gibson, V. C.; White, A. J. P.; Britovsek, G. J. P. *Dalton Trans.* **2012**, *41*, 5949-5964.

105. (a) Muñoz, S. B.; Foster, W. K.; Lin, H.-J.; Margarit, C. G.; Dickie, D. A.; Smith, J. M. *Inorg. Chem.* **2012**, *51*, 12660-12668; (b) Gusev, D. G. *Organometallics* **2009**, *28*, 6458-6461.

106. Back, O.; Henry-Ellinger, M.; Martin, C. D.; Martin, D.; Bertrand, G. *Angew. Chem. Int. Ed.* **2013**, *52*, 2939-2943.

107. Korotkikh, N. I.; Raenko, G. F.; Pekhtereva, T. M.; Shvaika, O. P.; Cowley, A. H.; Jones, J. N. *Russ. J. Org. Chem.* **2006**, *42*, 1822-1833.

108. Güizado-Rodríguez, M.; Ariza-Castolo, A.; Merino, G.; Vela, A.; Noth, H.; Bakhmutov, V. I.; Contreras, R. *J. Am. Chem. Soc.* **2001**, *123*, 9144-9152.

109. Al Thagfi, J.; Lavoie, G. G. *Organometallics* **2012**, *31*, 7351-7358.

110. (a) Gibson, V. C.; Mastroianni, S.; Newton, C.; Redshaw, C.; Solan, G. A.; White, A. J. P.; Williams, D. J. *J. Chem. Soc., Dalton Trans.* **2000**, 1969-1971; (b) Conde-Guadano, S.; Danopoulos, A. A.; Pattacini, R.; Hanton, M.; Tooze, R. P. *Organometallics* **2012**, *31*, 1643-1652.

111. Reiff, W. M.; Erickson, N. E.; Baker, W. A. *Inorg. Chem.* **1969**, *8*, 2019-2021.

112. Edwards, D. A.; Edwards, S. D.; Martin, W. R.; Pringle, T. J.; Thornton, P. *Polyhedron* **1992**, *11*, 1569-1573.

113. APEX2, SAINT and SADABS; Bruker AXS Inc., Madison, WI, **2007**.

114. Dolomanov, O. V.; Bourhis, L. J.; Gildea, R. J.; Howard, J. A. K.; Puschmann, H. *J. Appl. Crystallogr.* **2009**, *42*, 339-341.

115. (a) Díez-González, S.; Marion, N.; Nolan, S. P. *Chem. Rev.* **2009**, *109*, 3612-3676; (b) Poyatos, M.; Mata, J. A.; Peris, E. *Chem. Rev.* **2009**, *109*, 3677-3707; (c) Schaper, L.-A.; Hock, S. J.; Herrmann, W. A.; Kühn, F. E. *Angew. Chem. Int. Ed.* **2013**, *52*, 270-289.

116. Huang, J.; Schanz, H.-J.; Stevens, E. D.; Nolan, S. P. *Organometallics* **1999**, *18*, 2370-2375.

117. Hillier, A. C.; Sommer, W. J.; Yong, B. S.; Petersen, J. L.; Cavallo, L.; Nolan, S. P. *Organometallics* **2003**, *22*, 4322-4326.

118. Tolman, C. A. *Chem. Rev.* **1977**, *77*, 313-348.

119. Chianese, A. R.; Li, X.; Janzen, M. C.; Faller, J. W.; Crabtree, R. H. *Organometallics* **2003**, *22*, 1663-1667.

120. Dorta, R.; Stevens, E. D.; Scott, N. M.; Costabile, C.; Cavallo, L.; Hoff, C. D.; Nolan, S. P. *J. Am. Chem. Soc.* **2005**, *127*, 2485-2495.

121. (a) Herrmann, W. A.; Schütz, J.; Frey, G. D.; Herdtweck, E. *Organometallics* **2006**, *25*, 2437-2448; (b) Viciano, M.; Mas-Marzá, E.; Sanaú, M.; Peris, E. *Organometallics* **2006**, *25*, 3063-3069; (c) Scott, N. M.; Nolan, S. P. *Eur. J. Inorg. Chem.* **2005**, 1815-1828; (d) Präsang, C.; Donnadieu, B.; Bertrand, G. *J. Am. Chem. Soc.* **2005**, *127*, 10182-10183.

122. Huynh, H. V.; Han, Y.; Jothibasu, R.; Yang, J. A. *Organometallics* **2009**, *28*, 5395-5404.

123. Liske, A.; Verlinden, K.; Buhl, H.; Schaper, K.; Ganter, C. *Organometallics* **2013**, *32*, 5269-5272.

124. Eric de S. Gil, C. H. A., Núsia L. Barbosa, Rodolpho C. Braga and Sílvia H. P. Serrano *J. Braz. Chem. Soc.* **2012**, *23* 565-572.

125. Bianchini, C.; Mantovani, G.; Meli, A.; Migliacci, F.; Zanobini, F.; Laschi, F.; Sommazzi, A. *Eur. J. Inorg. Chem.* **2003**, 1620-1631.

126. Gibson, V. C.; Long, N. J.; Oxford, P. J.; White, A. J. P.; Williams, D. J. *Organometallics* **2006**, *25*, 1932-1939.

127. (a) Becke, A. D. *J. Chem. Phys.* **1993**, *98*, 5648-5652; (b) Godbout, N.; Salahub, D. R.; Andzelm, J.; Wimmer, E. *Can. J. Chem.* **1992**, *70*, 560-571; (c) Lee, C.; Yang, W.; Parr, R. G. *Phys. Rev. B* **1988**, *37*, 785-789.

128. Al Thagfi, J.; Lavoie, G. G. *Can. J. Chem.* **2014**, DOI:10.1139/cjc-2014-0022.

129. Buhl, H.; Ganter, C. *Chem. Commun.* **2013**, *49*, 5417-5419.

130. Martin, D.; Lassauque, N.; Donnadieu, B.; Bertrand, G. *Angew. Chem.* **2012**, *124*, 6276-6279.

131. Chermette, H. *Coord. Chem. Rev.* **1998**, *178–180*, 699-721.

132. (a) Schäfer, A.; Horn, H.; Ahlrichs, R. *J. Chem. Phys.* **1992**, *97*, 2571-2577; (b) Schäfer, A.; Huber, C.; Ahlrichs, R. *J. Chem. Phys.* **1994**, *100*, 5829-5835.

133. Guerard, F.; Lee, Y.-S.; Tripier, R.; Szajek, L. P.; Deschamps, J. R.; Brechbiel, M. W. *Chem. Commun.* **2013**, *49*, 1002-1004.

134. Liu, Y.; Sun, X.; Gahungu, G.; Qu, X.; Wang, Y.; Wu, Z. *J. Mater. Chem. C* **2013**, *1*, 3700-3709.

135. (a) Gorelsky, S. I.; Lever, A. B. P. *J. Organomet. Chem.* **2001**, *635*, 187-196; (b) Gorelsky, S. I. AOMix: Program for Molecular Orbital Analysis; University of Ottawa, **2011**, http://www.sg-chem.net/.

136. (a) Dapprich, S.; Frenking, G. *J. Phys. Chem.* **1995**, *99*, 9352-9362; (b) Gorelsky, S. I.; Ghosh, S.; Solomon, E. I. *J. Am. Chem. Soc.* **2006**, *128*, 278-290.

137. Kausamo, A.; Tuononen, H. M.; Krahulic, K. E.; Roesler, R. *Inorg. Chem.* **2008**, *47*, 1145-1154.

138. Gritzner, G. K. *J. Pure Appl. Chem.* **1984**, *56*, 461−466.

139. Frisch, M. J.; Trucks, G. W.; Schlegel, H. B.; Scuseria, G. E.; Robb, M. A.; Cheeseman, J. R.; Montgomery, J., J. A.; Vreven, T.; Kudin, K. N.; Burant, J. C.; Millam, J. M.; Iyengar, S. S.; Tomasi, J.; Barone, V.; Mennucci, B.; Cossi, M.; Scalmani, G.; Rega, N.; Petersson, G. A.; Nakatsuji, H.; Hada, M.; Ehara, M.; Toyota, K.; Fukuda, R.; Hasegawa, J.; Ishida, M.; Nakajima, T.; Honda, Y.; Kitao, O.; Nakai, H.; Klene, M.; Li, X.; Knox, J. E.; Hratchian, H. P.; Cross, J. B.; Bakken, V.; Adamo, C.; Jaramillo, J.; Gomperts, R.; Stratmann, R. E.; Yazyev, O.; Austin, A. J.; Cammi, R.; Pomelli, C.; Ochterski, J. W.; Ayala, P. Y.; Morokuma, K.; Voth, G. A.; Salvador, P.; Dannenberg, J. J.; Zakrzewski, V. G.; Dapprich, S.; Daniels, A. D.; Strain, M. C.; Farkas, O.; Malick, D. K.; Rabuck, A. D.; Raghavachari, K.; Foresman, J. B.; Ortiz, J. V.; Cui, Q.; Baboul, A. G.; Clifford, S.; Cioslowski, J.; Stefanov, B. B.; Liu, G.; Liashenko, A.; Piskorz, P.; Komaromi, I.; Martin, R. L.; Fox, D. J.; Keith, T.; Al-Laham, M. A.; Peng, C. Y.; Nanayakkara, A.; Challacombe, M.; Gill, P. M. W.; Johnson, B.; Chen, W.; Wong, M. W.; Gonzalez, C.; Pople, J. A. *Gaussian 03*, *Revision B.04*; Gaussian, Inc., Wallingford, CT, **2004**.

140. Frisch, M. J.; Trucks, G. W.; Schlegel, H. B.; Scuseria, G. E.; Robb, M. A.; Cheeseman, J. R.; Scalmani, G.; Barone, V.; Mennucci, B.; Petersson, G. A.; Nakatsuji, H.; Caricato, M.; Li, X.; Hratchian, H. P.; Izmaylov, A. F.; Bloino, J.; Zheng, G.; Sonnenberg, J. L.; Hada, M.; Ehara, M.; Toyota, K.; Fukuda, R.; Hasegawa, J.; Ishida, M.; Nakajima, T.; Honda, Y.; Kitao, O.; Nakai, H.; Vreven, T.; Montgomery, J. A.; Jr.; Peralta, J. E.; Ogliaro, F.; Bearpark, M.; Heyd, J. J.; Brothers, E.; Kudin, K. N.; Staroverov, V. N.; Keith, T.; Kobayashi, R.; Normand, J.; Raghavachari, K.; Rendell, A.; Burant, J. C.; Iyengar, S. S.; Tomasi, J.; Cossi, M.; Rega, N.; Millam, J. M.; Klene, M.; Knox, J. E.; Cross, J. B.; Bakken, V.; Adamo, C.; Jaramillo, J.; Gomperts, R.; Stratmann, R. E.; Yazyev, O.; Austin, A. J.; Cammi, R.; Pomelli, C.; Ochterski, J. W.; Martin, R. L.; Morokuma, K.; Zakrzewski, V. G.; Voth, G. A.; Salvador, P.; Dannenberg, J. J.; Dapprich, S.; Daniels, A. D.; Farkas, O.; Foresman, J. B.; Ortiz, J. V.; Cioslowski, J.; Fox, D. J. *Gaussian 09, Revision C.01*; Gaussian, Inc., Wallingford, CT, **2010**.

141. Ik, R. D.; Keith, T.; Millam, J.; Eppinnett, K.; Hovell, L. W.; Gilliland, R. *GaussView 3*; Gaussian, Inc., Carnegie, PA, **2003**.

Appendices

Appendix A: X-ray crystal structure data

1,3-Bis[1-(2,6-dimethylphenylimino)ethyl]imidazolium chloride (2.7).

Table S1. Crystal data and structure refinement for k1074g (**2.7**).

Identification code	k1074g	
Empirical formula	C25 H30 Cl N5	
Formula weight	435.99	
Temperature	150(1) K	
Wavelength	0.71073 Å	
Crystal system	Triclinic	
Space group	P -1	
Unit cell dimensions	a = 11.2342(8) Å	α = 111.193(4)°.
	b = 11.2603(9) Å	β = 91.473(4)°.
	c = 11.4874(6) Å	γ = 115.376(3)°.
Volume	1195.68(14) $Å^3$	
Z	2	
Density (calculated)	1.211 Mg/m^3	
Absorption coefficient	0.181 mm^{-1}	
F(000)	464	
Crystal size	0.30 x 0.30 x 0.20 mm^3	
Theta range for data collection	2.60 to 27.48°.	
Index ranges	-14<=h<=14, -14<=k<=14, -13<=l<=14	
Reflections collected	10835	
Independent reflections	5385 [R(int) = 0.0742]	
Completeness to theta = 27.48°	98.0 %	
Absorption correction	Semi-empirical from equivalents	
Max. and min. transmission	1.088 and 0.517	
Refinement method	Full-matrix least-squares on F^2	
Data / restraints / parameters	5385 / 0 / 287	
Goodness-of-fit on F^2	0.994	
Final R indices [I>2sigma(I)]	R1 = 0.0626, wR2 = 0.1367	
R indices (all data)	R1 = 0.1416, wR2 = 0.1717	
Largest diff. peak and hole	0.333 and -0.340 e.$Å^{-3}$	

Table S2. Atomic coordinates (x 10^4) and equivalent isotropic displacement parameters ($Å^2$ x 10^3) for k1074g (**2.7**). U(eq) is defined as one third of the trace of the orthogonalized U^{ij} tensor.

	x	y	z	U(eq)
C(1)	7004(2)	1236(3)	2262(2)	26(1)
C(2)	8452(3)	2784(3)	4122(2)	30(1)
C(3)	7888(3)	1476(3)	4137(2)	31(1)
C(4)	8284(3)	3766(3)	2519(2)	25(1)
C(5)	7533(3)	3316(3)	1220(2)	34(1)
C(6)	6097(2)	-991(3)	2650(2)	26(1)
C(7)	4951(3)	-1691(3)	1542(2)	34(1)
C(8)	5589(3)	-2913(3)	3230(2)	27(1)
C(9)	4923(3)	-3074(3)	4216(2)	33(1)
C(10)	4162(3)	-4470(3)	4130(3)	41(1)
C(11)	4114(3)	-5645(3)	3131(3)	46(1)
C(12)	4813(3)	-5455(3)	2194(3)	40(1)
C(13)	5572(3)	-4079(3)	2218(2)	32(1)
C(14)	5068(3)	-1776(3)	5343(3)	46(1)
C(15)	6408(3)	-3868(3)	1234(3)	37(1)
C(16)	9690(3)	6224(3)	3025(2)	29(1)
C(17)	9293(3)	7268(3)	3646(2)	32(1)
C(18)	9844(3)	8529(5 3)	3436(3)	38(1)
C(19)	10799(3)	8763(3)	2692(3)	41(1)
C(20)	11207(3)	7735(3)	2124(3)	40(1)
C(21)	10658(3)	6427(3)	2272(2)	34(1)
C(22)	8341(3)	7069(3)	4533(3)	38(1)
C(23)	11121(3)	5323(3)	1671(3)	46(1)
C(1S)	10588(3)	1731(4)	1299(3)	48(1)
C(2S)	11440(3)	1969(4)	400(3)	51(1)
N(1)	7900(2)	2621(2)	2945(2)	25(1)
N(2)	6984(2)	516(2)	2971(2)	26(1)
N(3)	9198(2)	4977(2)	3303(2)	29(1)
N(4)	6411(2)	-1468(2)	3377(2)	28(1)
N(1S)	9915(3)	1525(4)	2006(3)	69(1)
Cl(1)	6252(1)	-619(1)	-992(1)	39(1)

Table S3. Bond lengths [Å] and angles [°] for k1074g (**2.7**).

C(1)-N(2)	1.335(3)
C(1)-N(1)	1.339(3)
C(2)-C(3)	1.338(4)
C(2)-N(1)	1.389(3)
C(3)-N(2)	1.392(3)
C(4)-N(3)	1.261(3)
C(4)-N(1)	1.441(3)
C(4)-C(5)	1.489(3)
C(6)-N(4)	1.258(3)
C(6)-N(2)	1.445(3)
C(6)-C(7)	1.490(3)
C(8)-C(9)	1.396(4)
C(8)-C(13)	1.397(4)
C(8)-N(4)	1.426(3)
C(9)-C(10)	1.394(4)
C(9)-C(14)	1.502(4)
C(10)-C(11)	1.381(4)
C(11)-C(12)	1.373(4)
C(12)-C(13)	1.401(4)
C(13)-C(15)	1.507(4)
C(16)-C(17)	1.396(4)
C(16)-C(21)	1.400(4)
C(16)-N(3)	1.431(3)
C(17)-C(18)	1.400(4)
C(17)-C(22)	1.500(4)
C(18)-C(19)	1.385(4)
C(19)-C(20)	1.378(4)
C(20)-C(21)	1.410(4)
C(21)-C(23)	1.499(4)
C(1S)-N(1S)	1.142(4)
C(1S)-C(2S)	1.443(5)
N(2)-C(1)-N(1)	107.3(2)
C(3)-C(2)-N(1)	107.0(2)
C(2)-C(3)-N(2)	107.2(2)
N(3)-C(4)-N(1)	114.9(2)
N(3)-C(4)-C(5)	130.8(2)
N(1)-C(4)-C(5)	114.3(2)
N(4)-C(6)-N(2)	114.2(2)
N(4)-C(6)-C(7)	131.5(2)
N(2)-C(6)-C(7)	114.3(2)

C(9)-C(8)-C(13)	122.5(2)
C(9)-C(8)-N(4)	116.2(2)
C(13)-C(8)-N(4)	120.9(2)
C(10)- C(9)-C(8)	117.6(3)
C(10)-C(9)-C(14)	121.8(3)
C(8)-C(9)-C(14)	120.6(3)
C(11)-C(10)-C(9)	121.0(3)
C(12)-C(11)-C(10)	120.3(3)
C(11)-C(12)-C(13)	121.2(3)
C(8)-C(13)-C(12)	117.3(3)
C(8)-C(13)-C(15)	121.7(2)
C(12)-C(13)-C(15)	120.9(3)
C(17)-C(16)-C(21)	122.8(2)
C(17)-C(16)-N(3)	117.6(2)
C(21)-C(16)-N(3)	119.2(3)
C(16)-C(17)-C(18)	117.6(3)
C(16)-C(17)-C(22)	121.4(2)
C(18)-C(17)-C(22)	121.0(3)
C(19)-C(18)-C(17)	121.1(3)
C(20)-C(19)-C(18)	120.1(3)
C(19)-C(20)-C(21)	121.2(3)
C(16)-C(21)-C(20)	117.1(3)
C(16)-C(21)-C(23)	121.8(2)
C(20)-C(21)-C(23)	121.0(3)
N(1S)-C(1S)-C(2S)	179.1(4)
C(1)-N(1)-C(2)	109.3(2)
C(1)-N(1)-C(4)	125.9(2)
C(2)-N(1)-C(4)	124.7(2)
C(1)-N(2)-C(3)	109.2(2)
C(1)-N(2)-C(6)	126.5(2)
C(3)-N(2)-C(6)	124.2(2)
C(4)-N(3)-C(16)	121.7(2)
C(6)-N(4)-C(8)	120.9(2)

Symmetry transformations used to generate equivalent atoms:

Table S4. Anisotropic displacement parameters ($Å^2$ x 10^3) for k1074g (**2.7**). The anisotropic displacement factor exponent takes the form: $-2\pi^2[h^2 a^{*2}U^{11} + ... + 2 h k a^* b^* U^{12}]$

	U^{11}	U^{22}	U^{33}	U^{23}	U^{13}	U^{12}
C(1)	26(1)	26(2)	26(1)	11(1)	6(1)	10(1)
C(2)	32(2)	27(2)	22(1)	6(1)	-3(1)	8(1)
C(3)	31(2)	26(2)	28(1)	11(1)	-2(1)	7(1)
C(4)	28(2)	24(2)	25(1)	11(1)	7(1)	13(1)
C(5)	42(2)	28(2)	27(1)	10(1)	1(1)	14(1)
C(6)	26(1)	22(2)	27(1)	8(1)	8(1)	11(1)
C(7)	30(2)	26(2)	38(2)	11(1)	-3(1)	9(1)
C(8)	28(2)	23(2)	31(1)	14(1)	1(1)	11(1)
C(9)	35(2)	35(2)	31(1)	17(1)	8(1)	16(1)
C(10)	41(2)	40(2)	44(2)	25(2)	10(1)	14(2)
C(11)	51(2)	30(2)	47(2)	21(2)	-5(2)	6(2)
C(12)	53(2)	27(2)	37(2)	10(1)	-2(1)	20(2)
C(13)	38(2)	29(2)	29(1)	10(1)	-1(1)	16(1)
C(14)	57(2)	48(2)	40(2)	21(2)	20(1)	28(2)
C(15)	41(2)	37(2)	36(2)	10(1)	6(1)	24(2)
C(16)	32(2)	21(2)	27(1)	9(1)	-1(1)	6(1)
C(17)	31(2)	27(2)	30(1)	11(1)	-2(1)	8(1)
C(18)	43(2)	27(2)	34(2)	9(1)	-5(1)	13(1)
C(19)	46(2)	27(2)	41(2)	18(1)	-1(1)	7(2)
C(20)	39(2)	38(2)	36(2)	19(2)	7(1)	9(2)
C(21)	34(2)	28(2)	30(1)	11(1)	4(1)	9(1)
C(22)	35(2)	36(2)	42(2)	14(1)	4(1)	15(1)
C(23)	46(2)	36(2)	52(2)	18(2)	21(2)	16(2)
C(1S)	45(2)	41(2)	52(2)	11(2)	6(2)	24(2)
C(2S)	54(2)	48(2)	48(2)	15(2)	9(2)	26(2)
N(1)	26(1)	20(1)	26(1)	10(1)	2(1)	6(1)
N(2)	26(1)	22(1)	26(1)	9(1)	3(1)	10(1)
N(3)	30(1)	22(1)	31(1)	12(1)	3(1)	8(1)
N(4)	33(1)	24(1)	27(1)	11(1)	6(1)	13(1)
N(1S)	61(2)	69(2)	74(2)	24(2)	28(2)	32(2)
Cl(1)	52(1)	34(1)	34(1)	13(1)	10(1)	24(1)

Table S5. Hydrogen coordinates (x 10^4) and isotropic displacement parameters ($Å^2$ x 10^3) for k1074g (**2.7**).

	x	y	z	U(eq)
H(1)	6479	837	1427	32
H(2)	9107	3658	4790	36
H(3)	8070	1246	4817	37
H(5A)	7822	4157	1015	51
H(5B)	6564	2902	1200	51
H(5C)	7720	2592	591	51
H(7A)	4356	-2682	1429	51
H(7B)	5300	-1704	767	51
H(7C)	4442	-1146	1701	51
H(10)	3668	-4616	4768	49
H(11)	3597	-6587	3092	56
H(12)	4781	-6270	1518	48
H(14A)	6026	-1077	5684	69
H(14B)	4678	-2072	6007	69
H(14C)	4594	-1332	5074	69
H(15A)	6090	-3462	750	56
H(15B)	6322	-4799	650	56
H(15C)	7356	-3204	1664	56
H(18)	9558	9237	3810	45
H(19)	11175	9634	2574	49
H(20)	11869	7911	1622	48
H(22A)	7490	6187	4070	58
H(22B)	8166	7899	4857	58
H(22C)	8743	6990	5250	58
H(23A)	11359	5036	2316	68
H(23B)	11913	5734	1326	68
H(23C)	10395	4476	977	68
H(2S1)	11943	1424	308	77
H(2S2)	12075	3000	714	77
H(2S3)	10881	1645	-431	77

1,3-Bis[(2,4,6-trimethylphenylimino)benzyl]imidazolium tetrafluoroborate (2.10).

Table S6. Crystal data and structure refinement for k09240 (**2.10**).

Identification code	k09240	
Empirical formula	C35 H35 B F4 N4	
Formula weight	598.48	
Temperature	150(1) K	
Wavelength	0.71073 Å	
Crystal system	Monoclinic	
Space group	P 21/m	
Unit cell dimensions	a = 7.1346(3) Å	a= 90°.
	b = 31.4177(11) Å	b= 113.5240(19)°.
	c = 7.5643(2) Å	g = 90°.
Volume	1554.65(9) $Å^3$	
Z	2	
Density (calculated)	1.278 Mg/m^3	
Absorption coefficient	0.092 mm^{-1}	
F(000)	628	
Crystal size	0.40 x 0.26 x 0.05 mm^3	
Theta range for data collection	2.59 to 27.49°.	
Index ranges	-9<=h<=9, -37<=k<=40, -7<=l<=9	
Reflections collected	11654	
Independent reflections	3575 [R(int) = 0.0593]	
Completeness to theta = 25.24°	99.3 %	
Absorption correction	Semi-empirical from equivalents	
Max. and min. transmission	0.996 and 0.751	
Refinement method	Full-matrix least-squares on F^2	
Data / restraints / parameters	3575 / 1 / 216	
Goodness-of-fit on F^2	1.046	
Final R indices [I>2sigma(I)]	R1 = 0.0629, wR2 = 0.1673	
R indices (all data)	R1 = 0.1133, wR2 = 0.1995	
Largest diff. peak and hole	0.305 and -0.407 e.$Å^{-3}$	

Table S7. Atomic coordinates (x 10^4) and equivalent isotropic displacement parameters ($Å^2$ x 10^3) For k09240 (**2.10**). U(eq) is defined as one third of the trace of the orthogonalized U^{ij} tensor.

	x	y	z	U(eq)
N(1)	1248(3)	2155(1)	2080(2)	30(1)
N(2)	720(3)	1433(1)	1642(3)	36(1)
C(1)	2331(5)	2500	2903(4)	30(1)
C(2)	-653(3)	2286(1)	715(3)	34(1)
C(3)	2010(3)	1724(1)	2490(3)	32(1)
C(4)	4178(3)	1692(1)	3866(3)	34(1)
C(5)	4642(4)	1475(1)	5595(3)	42(1)
C(6)	6656(4)	1470(1)	6948(3)	49(1)
C(7)	8159(4)	1677(1)	6587(3)	51(1)
C(8)	7702(4)	1885(1)	4853(4)	48(1)
C(9)	5712(3)	1891(1)	3481(3)	39(1)
C(10)	1381(4)	997(1)	1856(3)	37(1)
C(11)	2622(4)	840(1)	976(3)	40(1)
C(12)	3111(4)	407(1)	1172(3)	47(1)
C(13)	2384(4)	128(1)	2171(4)	53(1)
C(14)	1090(5)	294(1)	2956(4)	58(1)
C(15)	549(4)	723(1)	2818(3)	47(1)
C(16)	-851(5)	887(1)	3702(5)	67(1)
C(17)	2946(6)	-338(1)	2343(5)	72(1)
C(18)	3413(4)	1115(1)	-213(4)	50(1)
F(2)	5087(3)	2500	7661(4)	70(1)
F(3)	1694(4)	2500	6205(3)	71(1)
F(1)	3141(4)	2148(1)	8966(3)	98(1)
B(1)	3300(6)	2500	7953(5)	40(1)
F(1A)	2210(30)	2152(6)	6890(30)	82(7)
F(3A)	3580(50)	2500	9810(20)	114(11)

Table S8. Bond lengths [Å] and angles [°] for k09240 (**2.10**).

N(1)-C(1)	1.333(2)
N(1)-C(2)	1.399(3)
N(1)-C(3)	1.446(2)
N(2)-C(3)	1.273(3)
N(2)-C(10)	1.438(2)
C(1)-N(1)#1	1.333(2)
C(2)-C(2)#1	1.348(4)
C(3)-C(4)	1.484(3)
C(4)-C(9)	1.389(3)
C(4)-C(5)	1.392(3)
C(5)-C(6)	1.392(3)
C(6)-C(7)	1.371(4)
C(7)-C(8)	1.383(4)
C(8)-C(9)	1.385(3)
C(10)-C(11)	1.393(3)
C(10)-C(15)	1.403(3)
C(11)-C(12)	1.398(3)
C(11)-C(18)	1.510(3)
C(12)-C(13)	1.385(3)
C(13)-C(14)	1.383(4)
C(13)-C(17)	1.512(3)
C(14)-C(15)	1.394(3)
C(15)-C(16)	1.499(3)
F(2)-B(1)	1.378(4)
F(3)-F(1A)#1	1.201(19)
F(3)-F(1A)	1.201(19)
F(3)-B(1)	1.361(4)
F(1)-F(3A)	1.254(8)
F(1)-B(1)	1.376(3)
F(1)-F(1A)	1.443(19)
B(1)-F(3A)	1.342(11)
B(1)-F(1)#1	1.376(3)
B(1)-F(1A)	1.395(17)
B(1)-F(1A)#1	1.395(17)
F(3A)-F(1)#1	1.254(8)
C(1)-N(1)-C(2)	108.46(17)
C(1)-N(1)-C(3)	124.30(19)
C(2)-N(1)-C(3)	127.14(16)
C(3)-N(2)-C(10)	119.26(19)

N(1)-C(1)-N(1)#1	108.9(3)
C(2)#1-C(2)-N(1)	107.07(10)
N(2)-C(3)-N(1)	115.43(19)
N(2)-C(3)-C(4)	130.29(18)
N(1)-C(3)-C(4)	114.27(16)
C(9)-C(4)-C(5)	120.4(2)
C(9)-C(4)-C(3)	120.68(18)
C(5)-C(4)-C(3)	118.9(2)
C(4)-C(5)-C(6)	119.0(2)
C(7)-C(6)-C(5)	120.6(2)
C(6)-C(7)-C(8)	120.4(2)
C(7)-C(8)-C(9)	120.0(2)
C(8)-C(9)-C(4)	119.6(2)
C(11)-C(10)-C(15)	120.82(19)
C(11)-C(10)-N(2)	121.75(19)
C(15)-C(10)-N(2)	117.10(19)
C(10)-C(11)-C(12)	118.2(2)
C(10)-C(11)-C(18)	122.83(19)
C(12)-C(11)-C(18)	118.9(2)
C(13)-C(12)-C(11)	122.8(2)
C(14)-C(13)-C(12)	117.1(2)
C(14)-C(13)-C(17)	121.8(2)
C(12)-C(13)-C(17)	121.0(2)
C(13)-C(14)-C(15)	122.9(2)
C(14)-C(15)-C(10)	118.0(2)
C(14)-C(15)-C(16)	120.9(2)
C(10)-C(15)-C(16)	121.0(2)
F(1A)#1-F(3)-F(1A)	130.8(17)
F(1A)#1-F(3)-B(1)	65.6(9)
F(1A)-F(3)-B(1)	65.6(9)
F(3A)-F(1)-B(1)	61.2(5)
F(3A)-F(1)-F(1A)	117.5(9)
B(1)-F(1)-F(1A)	59.3(7)
F(3A)-B(1)-F(3)	137.2(14)
F(3A)-B(1)-F(1)#1	54.9(3)
F(3)-B(1)-F(1)#1	108.5(2)
F(3A)-B(1)-F(1)	54.9(3)
F(3)-B(1)-F(1)	108.5(2)
F(1)#1-B(1)-F(1)	107.0(3)
F(3A)-B(1)-F(2)	114.2(14)
F(3)-B(1)-F(2)	108.6(3)
F(1)#1-B(1)-F(2)	112.1(2)
F(1)-B(1)-F(2)	112.1(2)

F(3A)-B(1)-F(1A)	114.9(10)
F(3)-B(1)-F(1A)	51.7(8)
F(1)#1-B(1)-F(1A)	143.2(8)
F(1)-B(1)-F(1A)	62.8(8)
F(2)-B(1)-F(1A)	104.1(8)
F(3A)-B(1)-F(1A)#1	114.9(10)
F(3)-B(1)-F(1A)#1	51.7(8)
F(1)#1-B(1)-F(1A)#1	62.8(8)
F(1)-B(1)-F(1A)#1	143.2(8)
F(2)-B(1)-F(1A)#1	104.1(8)
F(1A)-B(1)-F(1A)#1	103.1(17)
F(3)-F(1A)-B(1)	62.7(9)
F(3)-F(1A)-F(1)	113.9(13)
B(1)-F(1A)-F(1)	58.0(7)
F(1)-F(3A)-F(1)#1	123.8(13)
F(1)-F(3A)-B(1)	63.9(5)
F(1)#1-F(3A)-B(1)	63.9(5)

Symmetry transformations used to generate equivalent atoms:
#1 x,-y+1/2,z

Table S9. Anisotropic displacement parameters ($Å^2 \times 10^3$) for k09240 (**2.10**). The anisotropic displacement factor exponent takes the form: $-2\pi^2[h^2 a^{*2}U^{11} + ... + 2 h k a^* b^* U^{12}]$

	U^{11}	U^{22}	U^{33}	U^{23}	U^{13}	U^{12}
N(1)	37(1)	22(1)	31(1)	0(1)	13(1)	0(1)
N(2)	42(1)	23(1)	43(1)	-2(1)	17(1)	1(1)
C(1)	36(2)	23(1)	31(1)	0	13(1)	0
C(2)	35(1)	28(1)	36(1)	-1(1)	11(1)	0(1)
C(3)	41(1)	23(1)	33(1)	2(1)	16(1)	2(1)
C(4)	40(1)	23(1)	36(1)	-2(1)	14(1)	3(1)
C(5)	52(2)	31(1)	38(1)	-1(1)	12(1)	2(1)
C(6)	62(2)	37(1)	36(1)	-1(1)	6(1)	12(1)
C(7)	42(2)	48(1)	48(1)	-14(1)	3(1)	15(1)
C(8)	40(1)	45(1)	58(1)	-12(1)	20(1)	1(1)
C(9)	40(1)	32(1)	45(1)	-3(1)	17(1)	3(1)
C(10)	46(1)	20(1)	42(1)	-2(1)	14(1)	1(1)
C(11)	47(1)	29(1)	42(1)	-2(1)	16(1)	3(1)
C(12)	59(2)	33(1)	53(1)	-3(1)	26(1)	8(1)
C(13)	76(2)	28(1)	61(2)	-1(1)	33(1)	4(1)
C(14)	88(2)	27(1)	76(2)	6(1)	50(2)	2(1)
C(15)	62(2)	27(1)	59(1)	-1(1)	33(1)	0(1)
C(16)	90(2)	38(1)	100(2)	4(1)	66(2)	3(1)
C(17)	109(3)	30(1)	94(2)	6(1)	59(2)	12(1)
C(18)	66(2)	38(1)	56(1)	2(1)	33(1)	9(1)
F(2)	39(1)	68(2)	97(2)	0	21(1)	0
F(3)	44(2)	121(3)	42(1)	0	10(1)	0
F(1)	137(2)	71(2)	90(2)	38(1)	50(2)	3(1)
B(1)	41(2)	37(2)	34(2)	0	9(2)	0

Table S10. Hydrogen coordinates (x 10^4) and isotropic displacement parameters (Å^2 x 10^3) for k09240 (**2.10**).

	x	y	z	U(eq)
H(1)	3659	2500	3912	36
H(2)	-1739	2106	-65	41
H(5A)	3600	1333	5847	50
H(6A)	6990	1323	8133	59
H(7A)	9523	1676	7532	61
H(8A)	8753	2024	4604	57
H(9A)	5397	2031	2283	46
H(12A)	3977	299	596	57
H(14A)	545	107	3619	70
H(16A)	-1664	652	3874	100
H(16B)	-1766	1102	2853	100
H(16C)	-40	1015	4958	100
H(17A)	3159	-428	1197	107
H(17B)	1837	-506	2450	107
H(17C)	4204	-383	3495	107
H(18A)	2380	1328	-914	75
H(18B)	3706	936	-1134	75
H(18C)	4668	1259	639	75

1,3-Bis[1-(2,6-dimethylphenylimino)ethyl]imidazol-2-ylidene copper(I) iodide (2.15).

Table S11. Crystal data and structure refinement for k1022 (**2.15**).

Identification code	k1022	
Empirical formula	C48 H56 Cl4 Cu2 I2 N8	
Formula weight	1267.69	
Temperature	150(1) K	
Wavelength	0.71073 Å	
Crystal system	Triclinic	
Space group	P -1	
Unit cell dimensions	a = 9.3771(2) Å	a= 87.1930(15)°.
	b = 10.1743(3) Å	b= 73.0400(13)°.
	c = 14.8030(4) Å	g = 80.1890(13)°.
Volume	1331.11(6) $Å^3$	
Z	1	
Density (calculated)	1.581 Mg/m^3	
Absorption coefficient	2.199 mm^{-1}	
F(000)	632	
Crystal size	0.24 x 0.12 x 0.10 mm^3	
Theta range for data collection	2.81 to 27.49°.	
Index ranges	-11<=h<=12, -13<=k<=13, -19<=l<=19	
Reflections collected	12467	
Independent reflections	6014 [R(int) = 0.0402]	
Completeness to theta = 25.24°	99.5 %	
Absorption correction	Semi-empirical from equivalents	
Max. and min. transmission	0.813 and 0.698	
Refinement method	Full-matrix least-squares on F^2	
Data / restraints / parameters	6014 / 0 / 295	
Goodness-of-fit on F^2	1.058	
Final R indices [I>2sigma(I)]	R1 = 0.0466, wR2 = 0.1081	
R indices (all data)	R1 = 0.0736, wR2 = 0.1272	
Largest diff. peak and hole	1.966 and -1.403 e.$Å^{-3}$	

Table S12. Atomic coordinates (x 10^4) and equivalent isotropic displacement parameters ($Å^2$ x 10^3) for k1022 (**2.15**). U(eq) is defined as one third of the trace of the orthogonalized U^{ij} tensor.

	x	y	z	U(eq)
I(1)	8335(1)	3706(1)	816(1)	35(1)
Cu(1)	10964(1)	4520(1)	475(1)	27(1)
N(1)	12879(4)	3235(4)	1520(2)	24(1)
N(2)	11320(4)	4648(4)	2502(2)	26(1)
N(3)	12943(4)	2798(3)	12(2)	24(1)
N(4)	9605(5)	5627(4)	3814(3)	34(1)
C(1)	11696(5)	4263(4)	1583(3)	24(1)
C(2)	13235(5)	3016(5)	2375(3)	32(1)
C(3)	12249(5)	3883(5)	2992(3)	33(1)
C(4)	13602(4)	2541(4)	643(3)	25(1)
C(5)	15026(5)	1603(5)	613(3)	34(1)
C(6)	10087(5)	5673(4)	2924(3)	28(1)
C(7)	9582(5)	6677(5)	2273(3)	36(1)
C(8)	8384(6)	6602(5)	4309(3)	34(1)
C(9)	8699(6)	7657(5)	4755(3)	40(1)
C(10)	7482(7)	8543(5)	5291(4)	47(1)
C(11)	6021(7)	8394(6)	5389(4)	51(2)
C(12)	5724(6)	7351(6)	4950(4)	46(1)
C(13)	6901(6)	6438(5)	4395(3)	42(1)
C(14)	10307(7)	7786(6)	4645(4)	53(2)
C(15)	6569(6)	5324(6)	3893(4)	54(2)
C(16)	13640(5)	2260(4)	-921(3)	28(1)
C(17)	14862(5)	2786(5)	-1526(3)	34(1)
C(18)	15433(6)	2304(6)	-2454(4)	46(1)
C(19)	14833(7)	1328(6)	-2752(4)	51(2)
C(20)	13642(6)	822(5)	-2153(4)	46(1)
C(21)	12998(5)	1277(5)	-1222(4)	34(1)
C(22)	15535(5)	3852(5)	-1211(4)	40(1)
C(23)	11676(5)	746(5)	-569(4)	45(1)
Cl(1)	11533(3)	121(2)	2262(2)	86(1)
Cl(2)	8424(2)	937(2)	3412(1)	88(1)
C(1S)	10008(8)	1442(8)	2610(6)	82(2)

Table S13. Bond lengths [Å] and angles [°] for k1022 (**2.15**).

I(1)-Cu(1)#1	2.5838(6)
I(1)-Cu(1)	2.6357(6)
Cu(1)-C(1)	1.945(4)
Cu(1)-N(3)	2.292(3)
Cu(1)-I(1)#1	2.5838(6)
Cu(1)-Cu(1)#1	2.6357(10)
N(1)-C(1)	1.374(5)
N(1)-C(2)	1.398(5)
N(1)-C(4)	1.435(5)
N(2)-C(1)	1.362(5)
N(2)-C(3)	1.404(5)
N(2)-C(6)	1.430(6)
N(3)-C(4)	1.257(5)
N(3)-C(16)	1.435(5)
N(4)-C(6)	1.263(6)
N(4)-C(8)	1.423(6)
C(2)-C(3)	1.333(7)
C(4)-C(5)	1.494(6)
C(6)-C(7)	1.484(6)
C(8)-C(13)	1.397(7)
C(8)-C(9)	1.402(7)
C(9)-C(10)	1.392(7)
C(9)-C(14)	1.497(8)
C(10)-C(11)	1.369(8)
C(11)-C(12)	1.379(8)
C(12)-C(13)	1.397(7)
C(13)-C(15)	1.508(8)
C(16)-C(21)	1.402(6)
C(16)-C(17)	1.402(7)
C(17)-C(18)	1.401(7)
C(17)-C(22)	1.499(7)
C(18)-C(19)	1.369(8)
C(19)-C(20)	1.368(8)
C(20)-C(21)	1.401(7)
C(21)-C(23)	1.497(7)
Cl(1)-C(1S)	1.761(8)
Cl(2)-C(1S)	1.747(7)
Cu(1)#1-I(1)-Cu(1)	60.65(2)
C(1)-Cu(1)-N(3)	77.86(15)

C(1)-Cu(1)-I(1)#1	124.85(12)
N(3)-Cu(1)-I(1)#1	102.89(9)
C(1)-Cu(1)-Cu(1)#1	155.29(13)
N(3)-Cu(1)-Cu(1)#1	126.19(9)
I(1)#1-Cu(1)-Cu(1)#1	60.65(2)
C(1)-Cu(1)-I(1)	110.38(12)
N(3)-Cu(1)-I(1)	111.83(9)
I(1)#1-Cu(1)-I(1)	119.35(2)
Cu(1)#1-Cu(1)-I(1)	58.70(2)
C(1)-N(1)-C(2)	112.1(4)
C(1)-N(1)-C(4)	120.1(3)
C(2)-N(1)-C(4)	127.9(4)
C(1)-N(2)-C(3)	111.9(4)
C(1)-N(2)-C(6)	123.8(4)
C(3)-N(2)-C(6)	124.2(4)
C(4)-N(3)-C(16)	120.2(3)
C(4)-N(3)-Cu(1)	110.5(3)
C(16)-N(3)-Cu(1)	127.7(3)
C(6)-N(4)-C(8)	119.9(4)
N(2)-C(1)-N(1)	102.7(3)
N(2)-C(1)-Cu(1)	141.3(3)
N(1)-C(1)-Cu(1)	115.3(3)
C(3)-C(2)-N(1)	106.4(4)
C(2)-C(3)-N(2)	106.9(4)
N(3)-C(4)-N(1)	115.6(4)
N(3)-C(4)-C(5)	129.2(4)
N(1)-C(4)-C(5)	115.2(4)
N(4)-C(6)-N(2)	115.1(4)
N(4)-C(6)-C(7)	128.4(4)
N(2)-C(6)-C(7)	116.4(4)
C(13)-C(8)-C(9)	121.5(5)
C(13)-C(8)-N(4)	119.5(4)
C(9)-C(8)-N(4)	118.9(5)
C(10)-C(9)-C(8)	117.9(5)
C(10)-C(9)-C(14)	122.6(5)
C(8)-C(9)-C(14)	119.5(5)
C(11)-C(10)-C(9)	121.5(5)
C(10)-C(11)-C(12)	120.2(5)
C(11)-C(12)-C(13)	120.8(5)
C(8)-C(13)-C(12)	118.2(5)
C(8)-C(13)-C(15)	121.3(5)
C(12)-C(13)-C(15)	120.5(5)
C(21)-C(16)-C(17)	121.8(4)

C(21)-C(16)-N(3)	118.2(4)
C(17)-C(16)-N(3)	119.8(4)
C(18)-C(17)-C(16)	118.0(5)
C(18)-C(17)-C(22)	120.1(5)
C(16)-C(17)-C(22)	121.9(4)
C(19)-C(18)-C(17)	120.8(5)
C(20)-C(19)-C(18)	120.6(5)
C(19)-C(20)-C(21)	121.5(5)
C(20)-C(21)-C(16)	117.3(5)
C(20)-C(21)-C(23)	121.8(5)
C(16)-C(21)-C(23)	121.0(4)
Cl(2)-C(1S)-Cl(1)	112.5(4)

Symmetry transformations used to generate equivalent atoms:
#1 -x+2,-y+1,-z

Table S14. Anisotropic displacement parameters ($Å^2$ x 10^3) for k1022 (**2.15**). The anisotropic displacement factor exponent takes the form: $-2\pi^2[h^2 a^{*2}U^{11} + ... + 2 h k a^* b^* U^{12}]$

	U^{11}	U^{22}	U^{33}	U^{23}	U^{13}	U^{12}
I(1)	29(1)	37(1)	42(1)	13(1)	-13(1)	-11(1)
Cu(1)	26(1)	30(1)	28(1)	3(1)	-11(1)	-3(1)
N(1)	26(2)	23(2)	27(2)	1(1)	-12(2)	-1(1)
N(2)	31(2)	22(2)	24(2)	3(2)	-9(2)	-4(2)
N(3)	18(2)	21(2)	32(2)	0(2)	-6(2)	-3(1)
N(4)	42(2)	32(2)	25(2)	1(2)	-5(2)	-6(2)
C(1)	26(2)	24(2)	23(2)	2(2)	-6(2)	-7(2)
C(2)	35(2)	33(3)	29(2)	7(2)	-15(2)	-3(2)
C(3)	43(3)	28(3)	31(2)	8(2)	-17(2)	-6(2)
C(4)	23(2)	17(2)	36(2)	1(2)	-11(2)	-4(2)
C(5)	35(2)	26(2)	43(3)	-4(2)	-19(2)	3(2)
C(6)	32(2)	23(2)	28(2)	1(2)	-7(2)	-5(2)
C(7)	38(3)	34(3)	30(2)	-1(2)	-6(2)	6(2)
C(8)	48(3)	28(3)	21(2)	2(2)	-5(2)	0(2)
C(9)	62(3)	32(3)	24(2)	6(2)	-11(2)	-8(2)
C(10)	76(4)	30(3)	29(3)	0(2)	-9(3)	-1(3)
C(11)	62(4)	38(3)	34(3)	2(2)	4(3)	9(3)
C(12)	45(3)	44(3)	41(3)	0(2)	0(2)	-2(2)
C(13)	51(3)	36(3)	30(2)	0(2)	-1(2)	-6(2)
C(14)	64(4)	52(4)	44(3)	-11(3)	-15(3)	-11(3)
C(15)	46(3)	52(4)	54(3)	-7(3)	4(3)	-13(3)
C(16)	24(2)	26(2)	34(2)	-4(2)	-13(2)	1(2)
C(17)	29(2)	33(3)	38(3)	-5(2)	-11(2)	3(2)
C(18)	45(3)	51(4)	31(3)	-2(2)	-2(2)	4(3)
C(19)	63(4)	50(4)	34(3)	-15(3)	-15(3)	14(3)
C(20)	54(3)	33(3)	59(3)	-20(3)	-36(3)	11(2)
C(21)	34(2)	23(2)	50(3)	-7(2)	-23(2)	5(2)
C(22)	29(2)	45(3)	46(3)	3(2)	-6(2)	-12(2)
C(23)	35(3)	30(3)	75(4)	-11(3)	-24(3)	-3(2)
Cl(1)	99(1)	63(1)	100(1)	28(1)	-31(1)	-28(1)
Cl(2)	92(1)	124(2)	72(1)	11(1)	-35(1)	-68(1)
C(1S)	76(5)	75(5)	111(6)	54(5)	-47(5)	-34(4)

Table S15. Hydrogen coordinates (x 10^4) and isotropic displacement parameters (Å^2 x 10^3) for k1022 (**2.15**).

	x	y	z	U(eq)
H(2A)	14024	2375	2493	38
H(3A)	12186	3968	3639	39
H(5A)	15465	1211	-19	51
H(5B)	14801	893	1079	51
H(5C)	15746	2091	761	51
H(7A)	8890	7424	2639	55
H(7B)	9061	6265	1903	55
H(7C)	10462	7004	1845	55
H(10A)	7670	9268	5597	57
H(11A)	5209	9011	5760	61
H(12A)	4706	7252	5025	56
H(14A)	10335	8500	5057	80
H(14B)	10799	7999	3987	80
H(14C)	10840	6943	4820	80
H(15A)	7132	4473	4033	80
H(15B)	6876	5484	3210	80
H(15C)	5484	5290	4108	80
H(18A)	16246	2659	-2882	55
H(19A)	15247	999	-3380	61
H(20A)	13242	145	-2374	55
H(22A)	14730	4479	-793	61
H(22B)	16066	4331	-1763	61
H(22C)	16250	3443	-869	61
H(23A)	11936	385	-1	67
H(23B)	11417	38	-888	67
H(23C)	10809	1468	-390	67
H(1SA)	10327	2154	2901	99
H(1SB)	9730	1822	2044	99

1,3-Bis[(2,4,6-trimethylphenylimino)benzyl]imidazol-2-ylidene copper(I) iodide (2.16).

Table S16. Crystal data and structure refinement for k1021twin (**2.16**).

Identification code	k1021twin	
Empirical formula	C35 H34 Cu I N4	
Formula weight	701.10	
Temperature	150(2) K	
Wavelength	0.71073 Å	
Crystal system	Triclinic	
Space group	P -1	
Unit cell dimensions	a = 7.6786(3) Å	a= 77.56(3)°.
	b = 12.9696(9) Å	b= 80.64(3)°.
	c = 17.1766(12) Å	g = 78.56(3)°.
Volume	1624.3(3) $Å^3$	
Z	2	
Density (calculated)	1.433 Mg/m^3	
Absorption coefficient	1.651 mm^{-1}	
F(000)	708	
Crystal size	0.16 x 0.08 x 0.06 mm^3	
Theta range for data collection	2.67 to 27.43°.	
Index ranges	-9<=h<=9, -16<=k<=16, -19<=l<=22	
Reflections collected	14666	
Independent reflections	7231 [R(int) = 0.081]	
Completeness to theta = 25.24°	99 %	
Absorption correction	Semi-empirical from equivalents	
Max. and min. transmission	0.912 and 0.711	
Refinement method	Full-matrix least-squares on F^2	
Data / restraints / parameters	7231 / 0 / 376	
Goodness-of-fit on F^2	1.000	
Final R indices [I>2sigma(I)]	R1 = 0.0606, wR2 = 0.1330	
R indices (all data)	R1 = 0.1333, wR2 = 0.1722	
Largest diff. peak and hole	1.305 and -1.043 e.$Å^{-3}$	

Table S17. Atomic coordinates (x 10^4) and equivalent isotropic displacement parameters ($Å^2$ x 10^3) for k1021twin (**2.16**). U(eq) is defined as one third of the trace of the orthogonalized U^{ij} tensor.

	x	y	z	U(eq)
I(1)	8442(1)	5855(1)	1903(1)	52(1)
Cu(1)	5289(1)	6106(1)	2350(1)	32(1)
N(1)	1744(6)	7272(4)	2879(3)	28(1)
N(2)	2145(5)	5641(4)	3498(3)	27(1)
N(3)	1049(6)	9095(4)	2535(3)	35(1)
N(4)	2346(6)	4116(4)	4448(3)	29(1)
C(1)	2916(7)	6343(5)	2884(3)	29(1)
C(2)	297(7)	7172(5)	3492(3)	33(1)
C(3)	556(7)	6147(5)	3876(3)	34(1)
C(4)	1927(7)	8252(5)	2307(3)	28(1)
C(5)	3004(7)	8108(4)	1531(3)	28(1)
C(6)	4314(7)	8756(5)	1190(4)	32(1)
C(7)	5312(8)	8616(5)	458(4)	39(2)
C(8)	5028(7)	7875(5)	57(4)	38(2)
C(9)	3767(7)	7218(5)	398(4)	36(2)
C(10)	2759(7)	7340(5)	1124(4)	32(1)
C(11)	2847(6)	4523(4)	3724(3)	28(1)
C(12)	3950(6)	4013(4)	3071(3)	28(1)
C(13)	3429(7)	4248(5)	2299(3)	30(1)
C(14)	4460(7)	3781(5)	1698(4)	38(2)
C(15)	6030(8)	3072(5)	1839(4)	39(2)
C(16)	6562(7)	2832(5)	2609(4)	38(2)
C(17)	5529(7)	3299(5)	3220(4)	33(1)
C(18)	2661(7)	2987(4)	4745(3)	29(1)
C(19)	1552(7)	2342(5)	4565(4)	35(1)
C(20)	1715(7)	1283(5)	4965(4)	37(2)
C(21)	2935(8)	836(5)	5512(4)	37(2)
C(22)	4009(7)	1493(5)	5670(4)	37(2)
C(23)	3889(7)	2555(5)	5307(3)	33(1)
C(24)	148(8)	2822(6)	4013(4)	46(2)
C(25)	2990(9)	-318(5)	5964(4)	54(2)
C(26)	5025(8)	3272(5)	5509(4)	47(2)
C(27)	943(7)	10124(5)	2010(4)	33(1)
C(28)	-95(7)	10376(5)	1369(4)	36(2)
C(29)	-239(7)	11410(5)	920(4)	34(1)
C(30)	537(7)	12194(5)	1092(4)	36(2)

C(31)	1508(7)	11919(5)	1737(4)	36(2)
C(32)	1737(7)	10895(5)	2200(3)	34(1)
C(33)	-1077(8)	9576(5)	1188(5)	54(2)
C(34)	344(8)	13315(5)	591(4)	48(2)
C(35)	2832(9)	10612(5)	2895(4)	50(2)

Table S18. Bond lengths [Å] and angles [°] for k1021twin (**2.16**).

I(1)-Cu(1)	2.3969(8)
Cu(1)-C(1)	1.901(5)
N(1)-C(1)	1.353(7)
N(1)-C(2)	1.407(7)
N(1)-C(4)	1.445(7)
N(2)-C(1)	1.375(7)
N(2)-C(3)	1.396(7)
N(2)-C(11)	1.435(7)
N(3)-C(4)	1.269(7)
N(3)-C(27)	1.436(7)
N(4)-C(11)	1.271(7)
N(4)-C(18)	1.429(7)
C(2)-C(3)	1.343(8)
C(4)-C(5)	1.477(8)
C(5)-C(10)	1.390(8)
C(5)-C(6)	1.412(7)
C(6)-C(7)	1.390(9)
C(7)-C(8)	1.365(9)
C(8)-C(9)	1.391(8)
C(9)-C(10)	1.380(8)
C(11)-C(12)	1.484(8)
C(12)-C(17)	1.396(7)
C(12)-C(13)	1.399(8)
C(13)-C(14)	1.369(9)
C(14)-C(15)	1.384(8)
C(15)-C(16)	1.399(9)
C(16)-C(17)	1.383(8)
C(18)-C(23)	1.411(7)
C(18)-C(19)	1.414(8)
C(19)-C(20)	1.388(8)
C(19)-C(24)	1.504(8)
C(20)-C(21)	1.390(8)
C(21)-C(22)	1.390(8)
C(21)-C(25)	1.527(8)
C(22)-C(23)	1.376(8)
C(23)-C(26)	1.518(8)
C(27)-C(32)	1.388(8)
C(27)-C(28)	1.407(8)
C(28)-C(29)	1.388(8)
C(28)-C(33)	1.505(8)

C(29)-C(30)	1.380(8)
C(30)-C(31)	1.379(8)
C(30)-C(34)	1.514(8)
C(31)-C(32)	1.388(8)
C(32)-C(35)	1.510(8)
C(1)-Cu(1)-I(1)	169.35(17)
C(1)-N(1)-C(2)	112.0(4)
C(1)-N(1)-C(4)	124.5(5)
C(2)-N(1)-C(4)	123.5(5)
C(1)-N(2)-C(3)	111.5(5)
C(1)-N(2)-C(11)	125.0(5)
C(3)-N(2)-C(11)	123.5(4)
C(4)-N(3)-C(27)	121.7(5)
C(11)-N(4)-C(18)	122.2(5)
N(1)-C(1)-N(2)	103.4(4)
N(1)-C(1)-Cu(1)	129.0(4)
N(2)-C(1)-Cu(1)	126.3(4)
C(3)-C(2)-N(1)	106.3(5)
C(2)-C(3)-N(2)	106.8(5)
N(3)-C(4)-N(1)	114.6(5)
N(3)-C(4)-C(5)	130.2(5)
N(1)-C(4)-C(5)	115.1(5)
C(10)-C(5)-C(6)	118.8(5)
C(10)-C(5)-C(4)	121.3(5)
C(6)-C(5)-C(4)	120.0(5)
C(7)-C(6)-C(5)	119.4(6)
C(8)-C(7)-C(6)	121.1(6)
C(7)-C(8)-C(9)	119.7(6)
C(10)-C(9)-C(8)	120.2(6)
C(9)-C(10)-C(5)	120.7(5)
N(4)-C(11)-N(2)	114.1(5)
N(4)-C(11)-C(12)	130.3(5)
N(2)-C(11)-C(12)	115.5(5)
C(17)-C(12)-C(13)	119.4(5)
C(17)-C(12)-C(11)	120.1(5)
C(13)-C(12)-C(11)	120.5(5)
C(14)-C(13)-C(12)	120.2(5)
C(13)-C(14)-C(15)	120.9(6)
C(14)-C(15)-C(16)	119.3(6)
C(17)-C(16)-C(15)	120.3(5)
C(16)-C(17)-C(12)	119.9(5)
C(23)-C(18)-C(19)	120.5(5)

C(23)-C(18)-N(4)	119.4(5)
C(19)-C(18)-N(4)	119.4(5)
C(20)-C(19)-C(18)	117.6(5)
C(20)-C(19)-C(24)	121.8(5)
C(18)-C(19)-C(24)	120.4(5)
C(19)-C(20)-C(21)	123.0(5)
C(22)-C(21)-C(20)	117.9(5)
C(22)-C(21)-C(25)	121.4(5)
C(20)-C(21)-C(25)	120.6(6)
C(23)-C(22)-C(21)	122.1(5)
C(22)-C(23)-C(18)	119.0(5)
C(22)-C(23)-C(26)	121.4(5)
C(18)-C(23)-C(26)	119.5(5)
C(32)-C(27)-C(28)	120.9(5)
C(32)-C(27)-N(3)	118.1(5)
C(28)-C(27)-N(3)	120.7(5)
C(29)-C(28)-C(27)	117.6(5)
C(29)-C(28)-C(33)	120.6(5)
C(27)-C(28)-C(33)	121.8(5)
C(30)-C(29)-C(28)	123.0(5)
C(31)-C(30)-C(29)	117.5(5)
C(31)-C(30)-C(34)	121.0(6)
C(29)-C(30)-C(34)	121.5(6)
C(30)-C(31)-C(32)	122.5(6)
C(31)-C(32)-C(27)	118.5(5)
C(31)-C(32)-C(35)	121.3(5)
C(27)-C(32)-C(35)	120.2(5)

Symmetry transformations used to generate equivalent atoms:

Table S19. Anisotropic displacement parameters ($Å^2$ x 10^3) for k1021twin (**2.16**). The anisotropic displacement factor exponent takes the form: $-2\pi^2$[h^2 $a^{*2}U^{11}$ + ... + 2 h k a* b* U^{12}]

	U^{11}	U^{22}	U^{33}	U^{23}	U^{13}	U^{12}
I(1)	26(1)	64(1)	61(1)	-11(1)	2(1)	-7(1)
Cu(1)	26(1)	35(1)	34(1)	-5(1)	2(1)	-3(1)
N(1)	32(2)	28(3)	22(3)	-8(2)	1(2)	-1(2)
N(2)	24(2)	28(3)	24(3)	-3(2)	1(2)	-1(2)
N(3)	33(3)	33(3)	34(3)	-3(2)	-1(2)	-2(2)
N(4)	31(2)	26(3)	29(3)	-4(2)	-2(2)	-3(2)
C(1)	34(3)	25(3)	25(3)	-5(3)	0(2)	-4(2)
C(2)	29(3)	32(4)	33(4)	-9(3)	10(2)	-4(2)
C(3)	36(3)	34(4)	24(3)	-4(3)	10(2)	-1(2)
C(4)	24(3)	32(4)	24(3)	-1(3)	-3(2)	-4(2)
C(5)	28(3)	26(3)	26(3)	-1(3)	-2(2)	-1(2)
C(6)	30(3)	30(3)	36(4)	-3(3)	-3(2)	-8(2)
C(7)	35(3)	42(4)	38(4)	-5(3)	2(3)	-9(3)
C(8)	33(3)	47(4)	30(4)	-10(3)	4(3)	2(3)
C(9)	33(3)	37(4)	36(4)	-7(3)	-6(3)	-2(3)
C(10)	24(3)	34(4)	34(4)	0(3)	-4(2)	-1(2)
C(11)	25(3)	23(3)	34(4)	-3(3)	-4(2)	-2(2)
C(12)	24(3)	28(3)	30(3)	-2(3)	-1(2)	-4(2)
C(13)	30(3)	28(3)	32(4)	-5(3)	-6(2)	-5(2)
C(14)	36(3)	39(4)	40(4)	-9(3)	-7(3)	-4(3)
C(15)	39(3)	36(4)	40(4)	-14(3)	8(3)	-3(3)
C(16)	32(3)	36(4)	38(4)	0(3)	0(3)	4(3)
C(17)	29(3)	33(4)	32(4)	1(3)	-2(2)	-4(2)
C(18)	35(3)	26(3)	25(3)	-4(3)	0(2)	-1(2)
C(19)	39(3)	30(4)	32(4)	-2(3)	2(2)	-7(3)
C(20)	37(3)	39(4)	37(4)	-11(3)	2(3)	-10(3)
C(21)	39(3)	33(4)	33(4)	-7(3)	1(3)	3(3)
C(22)	38(3)	37(4)	29(4)	2(3)	-7(3)	1(3)
C(23)	33(3)	39(4)	29(3)	-9(3)	0(2)	-5(3)
C(24)	47(4)	54(5)	38(4)	-2(3)	-12(3)	-9(3)
C(25)	66(4)	32(4)	55(5)	7(4)	-6(4)	-3(3)
C(26)	49(4)	47(4)	46(4)	-4(3)	-11(3)	-11(3)
C(27)	30(3)	32(4)	34(4)	-9(3)	1(2)	0(2)
C(28)	28(3)	39(4)	42(4)	-14(3)	0(3)	-1(3)
C(29)	29(3)	35(4)	36(4)	-8(3)	-4(2)	2(3)
C(30)	30(3)	30(4)	41(4)	-4(3)	7(3)	2(2)

C(31)	38(3)	28(4)	41(4)	-7(3)	-5(3)	-1(3)
C(32)	32(3)	41(4)	29(3)	-11(3)	-3(2)	0(3)
C(33)	43(4)	44(4)	79(6)	-20(4)	-23(4)	1(3)
C(34)	48(4)	35(4)	55(5)	4(3)	-11(3)	0(3)
C(35)	61(4)	40(4)	54(5)	-17(4)	-18(3)	-2(3)

Table S20. Hydrogen coordinates (x 10^4) and isotropic displacement parameters (Å^2 x 10^3) for k1021twin (**2.16**).

	x	y	z	U(eq)
H(2A)	-669	7721	3611	39
H(3A)	-198	5827	4319	40
H(6A)	4511	9283	1458	39
H(7A)	6208	9044	232	47
H(8A)	5689	7808	-453	46
H(9A)	3599	6684	129	43
H(10A)	1888	6895	1349	39
H(13A)	2356	4733	2193	36
H(14A)	4092	3945	1177	46
H(15A)	6738	2752	1418	47
H(16A)	7637	2346	2711	46
H(17A)	5894	3133	3742	40
H(20A)	958	845	4861	45
H(22A)	4854	1199	6041	44
H(24A)	-588	2286	4009	69
H(24B)	730	3050	3468	69
H(24C)	-614	3443	4203	69
H(25A)	4233	-649	6033	81
H(25B)	2496	-723	5657	81
H(25C)	2278	-324	6493	81
H(26A)	5966	2831	5817	71
H(26B)	4269	3773	5828	71
H(26C)	5574	3674	5010	71
H(29A)	-902	11585	475	41
H(31A)	2040	12450	1869	44
H(33A)	-1919	9942	804	81
H(33B)	-1736	9243	1686	81
H(33C)	-214	9023	957	81
H(34A)	1283	13676	678	73
H(34B)	-834	13719	749	73
H(34C)	459	13274	21	73
H(35A)	2169	10224	3366	75
H(35B)	3068	11270	3021	75
H(35C)	3970	10160	2748	75

1,3-Bis[1-(2,6-dimethylphenylimino)ethyl]imidazol-2-ylidene iron(II) chloride (2.17).

Table S21. Crystal data and structure refinement for k10109 (**2.17**).

Identification code	k10109	
Empirical formula	C25 H30 Cl6 Fe N4	
Formula weight	655.08	
Temperature	150(1) K	
Wavelength	0.71073 Å	
Crystal system	Monoclinic	
Space group	P 21/c	
Unit cell dimensions	a = 9.0305(3) Å	α= 90°.
	b = 14.7984(3) Å	β= 94.628(2)°.
	c = 23.3313(8) Å	γ = 90°.
Volume	3107.76(16) Å3	
Z	4	
Density (calculated)	1.400 Mg/m^3	
Absorption coefficient	1.022 mm^{-1}	
F(000)	1344	
Crystal size	0.29 x 0.25 x 0.11 mm^3	
Theta range for data collection	2.65 to 27.48°.	
Index ranges	-11<=h<=11, -19<=k<=19, -29<=l<=30	
Reflections collected	21778	
Independent reflections	7091 [R(int) = 0.0569]	
Completeness to theta = 27.48°	99.4 %	
Absorption correction	Semi-empirical from equivalents	
Max. and min. transmission	0.933 and 0.756	
Refinement method	Full-matrix least-squares on F2	
Data / restraints / parameters	7091 / 0 / 331	
Goodness-of-fit on F^2	1.030	
Final R indices [I>2sigma(I)]	R1 = 0.0552, wR2 = 0.1351	
R indices (all data)	R1 = 0.1132, wR2 = 0.1671	
Largest diff. peak and hole	0.887 and -0.561 e.$Å^{-3}$	

Table S22. Atomic coordinates (x 10^4) and equivalent isotropic displacement parameters ($Å^2$ x 10^3) for k10109 (**2.17**). U(eq) is defined as one third of the trace of the orthogonalized U^{ij} tensor.

	x	y	z	U(eq)
Fe(1)	5280(1)	1258(1)	2482(1)	28(1)
Cl(2)	7740(1)	1221(1)	2404(1)	39(1)
Cl(1)	3979(1)	2517(1)	2261(1)	43(1)
ClS4	9790(1)	8126(1)	1300(1)	72(1)
ClS3	8630(2)	6308(1)	1425(1)	91(1)
ClS1	327(1)	3357(1)	1691(1)	69(1)
ClS2	1568(2)	4754(1)	997(1)	82(1)
N(3)	4069(3)	96(2)	2154(1)	26(1)
N(1)	4104(3)	-235(2)	3103(1)	27(1)
N(2)	4957(3)	583(2)	3808(1)	29(1)
N(4)	5507(3)	1243(2)	4686(1)	32(1)
C(20)	1766(5)	175(2)	758(2)	45(1)
C(8)	5987(4)	1959(2)	5065(1)	36(1)
C(13)	4879(5)	2455(2)	5313(2)	46(1)
C(1)	4783(4)	576(2)	3228(1)	27(1)
C(21)	2167(4)	276(2)	1342(2)	34(1)
C(5)	2725(4)	-1272(2)	2425(2)	36(1)
C(10)	7872(6)	2762(3)	5642(2)	57(1)
C(4)	3644(3)	-454(2)	2524(1)	28(1)
C(3)	4396(4)	-203(2)	4046(2)	35(1)
C(23)	1122(4)	696(3)	1731(2)	45(1)
C(9)	7488(5)	2088(2)	5232(2)	44(1)
C(16)	3578(4)	-32(2)	1548(1)	29(1)
C(11)	6788(7)	3260(3)	5882(2)	63(1)
C(6)	5549(4)	1327(2)	4153(1)	29(1)
C(2)	3868(4)	-718(2)	3603(1)	34(1)
C(17)	4571(4)	-425(2)	1188(2)	34(1)
C(19)	2717(5)	-216(2)	397(2)	49(1)
C(2S)	9171(5)	7310(3)	1780(2)	61(1)
C(7)	6103(4)	2109(2)	3824(2)	39(1)
C(18)	4106(5)	-516(2)	610(2)	43(1)
C(14)	8669(5)	1522(3)	4989(2)	57(1)
C(22)	6083(4)	-739(2)	1430(2)	43(1)
C(15)	3262(5)	2296(3)	5140(2)	67(1)
C(12)	5337(7)	3113(2)	5721(2)	59(1)
C(1S)	1692(6)	4207(3)	1655(2)	77(2)

Table S23. Bond lengths [Å] and angles [°] for k10109 (**2.17**).

Fe(1)-C(1)	2.091(3)
Fe(1)-N(3)	2.145(3)
Fe(1)-Cl(1)	2.2404(9)
Fe(1)-Cl(2)	2.2442(10)
ClS4-C(2S)	1.767(5)
ClS3-C(2S)	1.749(5)
ClS1-C(1S)	1.767(5)
ClS2-C(1S)	1.732(5)
N(3)-C(4)	1.269(4)
N(3)-C(16)	1.458(4)
N(1)-C(1)	1.369(4)
N(1)-C(2)	1.398(4)
N(1)-C(4)	1.419(4)
N(2)-C(1)	1.350(4)
N(2)-C(3)	1.401(4)
N(2)-C(6)	1.440(4)
N(4)-C(6)	1.256(4)
N(4)-C(8)	1.425(4)
C(20)-C(19)	1.378(6)
C(20)-C(21)	1.391(5)
C(8)-C(9)	1.393(5)
C(8)-C(13)	1.403(5)
C(13)-C(12)	1.401(6)
C(13)-C(15)	1.501(6)
C(21)-C(16)	1.401(5)
C(21)-C(23)	1.496(5)
C(5)-C(4)	1.475(4)
C(10)-C(11)	1.380(6)
C(10)-C(9)	1.406(5)
C(3)-C(2)	1.340(5)
C(9)-C(14)	1.503(6)
C(16)-C(17)	1.403(5)
C(11)-C(12)	1.352(7)
C(6)-C(7)	1.496(4)
C(17)-C(18)	1.387(5)
C(17)-C(22)	1.508(5)
C(19)-C(18)	1.385(6)
C(1)-Fe(1)-N(3)	76.90(11)
C(1)-Fe(1)-Cl(1)	116.67(9)
N(3)-Fe(1)-Cl(1)	109.95(7)

C(1)-Fe(1)-Cl(2)	109.62(9)
N(3)-Fe(1)-Cl(2)	115.57(7)
Cl(1)-Fe(1)-Cl(2)	120.37(4)
C(4)-N(3)-C(16)	119.4(3)
C(4)-N(3)-Fe(1)	116.4(2)
C(16)-N(3)-Fe(1)	123.85(18)
C(1)-N(1)-C(2)	111.5(3)
C(1)-N(1)-C(4)	119.6(2)
C(2)-N(1)-C(4)	128.7(3)
C(1)-N(2)-C(3)	111.9(3)
C(1)-N(2)-C(6)	125.0(3)
C(3)-N(2)-C(6)	122.9(3)
C(6)-N(4)-C(8)	120.6(3)
C(19)-C(20)-C(21)	121.2(4)
C(9)-C(8)-C(13)	121.5(3)
C(9)-C(8)-N(4)	121.1(3)
C(13)-C(8)-N(4)	117.0(3)
C(12)-C(13)-C(8)	117.5(4)
C(12)-C(13)-C(15)	121.3(4)
C(8)-C(13)-C(15)	121.2(3)
N(2)-C(1)-N(1)	103.5(3)
N(2)-C(1)-Fe(1)	144.6(2)
N(1)-C(1)-Fe(1)	111.7(2)
C(20)-C(21)-C(16)	117.4(3)
C(20)-C(21)-C(23)	120.8(3)
C(16)-C(21)-C(23)	121.9(3)
C(11)-C(10)-C(9)	120.7(4)
N(3)-C(4)-N(1)	114.9(3)
N(3)-C(4)-C(5)	128.1(3)
N(1)-C(4)-C(5)	117.1(3)
C(2)-C(3)-N(2)	106.6(3)
C(8)-C(9)-C(10)	118.0(4)
C(8)-C(9)-C(14)	121.4(3)
C(10)-C(9)-C(14)	120.6(4)
C(21)-C(16)-C(17)	122.4(3)
C(21)-C(16)-N(3)	119.1(3)
C(17)-C(16)-N(3)	118.3(3)
C(12)-C(11)-C(10)	120.3(4)
N(4)-C(6)-N(2)	116.0(3)
N(4)-C(6)-C(7)	128.5(3)
N(2)-C(6)-C(7)	115.5(3)
C(3)-C(2)-N(1)	106.4(3)
C(18)-C(17)-C(16)	117.7(3)

C(18)-C(17)-C(22)	121.8(3)
C(16)-C(17)-C(22)	120.5(3)
C(20)-C(19)-C(18)	120.4(4)
ClS3-C(2S)-ClS4	111.8(3)
C(19)-C(18)-C(17)	120.8(3)
C(11)-C(12)-C(13)	121.9(4)
ClS2-C(1S)-ClS1	112.2(3)

Symmetry transformations used to generate equivalent atoms:

Table S24. Anisotropic displacement parameters ($Å^2$ x 10^3) for k10109 (**2.17**). The anisotropic displacement factor exponent takes the form: $-2\pi^2[h^2a^{*2}U^{11} + ... + 2 h k a^* b^* U^{12}]$

	U11	U22	U33	U23	U13	U12
Fe(1)	36(1)	26(1)	23(1)	2(1)	2(1)	-2(1)
Cl(2)	36(1)	46(1)	35(1)	1(1)	4(1)	-2(1)
Cl(1)	48(1)	34(1)	47(1)	7(1)	1(1)	6(1)
ClS4	57(1)	76(1)	79(1)	1(1)	-10(1)	2(1)
ClS3	79(1)	103(1)	94(1)	-25(1)	21(1)	-39(1)
ClS1	57(1)	73(1)	79(1)	8(1)	10(1)	-10(1)
ClS2	78(1)	80(1)	86(1)	17(1)	1(1)	-19(1)
N(3)	30(2)	27(1)	21(2)	-3(1)	4(1)	5(1)
N(1)	36(2)	25(1)	21(2)	2(1)	4(1)	0(1)
N(2)	36(2)	26(1)	24(2)	1(1)	2(1)	-2(1)
N(4)	47(2)	27(1)	23(2)	0(1)	3(1)	-2(1)
C(20)	50(2)	45(2)	37(2)	0(2)	-10(2)	-1(2)
C(8)	65(3)	26(2)	16(2)	7(1)	2(2)	-5(2)
C(13)	76(3)	32(2)	30(2)	5(2)	11(2)	3(2)
C(1)	30(2)	27(2)	23(2)	-2(1)	2(1)	3(1)
C(21)	35(2)	34(2)	32(2)	2(2)	1(2)	-2(1)
C(5)	45(2)	31(2)	30(2)	-3(1)	1(2)	-4(2)
C(10)	87(3)	47(2)	34(2)	1(2)	-16(2)	-21(2)
C(4)	30(2)	25(2)	28(2)	0(1)	4(2)	2(1)
C(3)	49(2)	27(2)	29(2)	7(2)	5(2)	-4(2)
C(23)	37(2)	52(2)	45(2)	-2(2)	-1(2)	5(2)
C(9)	71(3)	35(2)	25(2)	2(2)	-3(2)	-8(2)
C(16)	42(2)	23(2)	22(2)	0(1)	6(2)	-5(1)
C(11)	130(5)	33(2)	25(2)	-7(2)	-1(3)	-11(3)
C(6)	38(2)	25(2)	23(2)	0(1)	0(2)	2(1)
C(2)	46(2)	26(2)	28(2)	3(1)	1(2)	-8(1)
C(17)	45(2)	26(2)	32(2)	-1(2)	5(2)	-1(1)
C(19)	79(3)	42(2)	23(2)	0(2)	-6(2)	-9(2)
C(2S)	48(3)	77(3)	58(3)	-8(2)	-2(2)	6(2)
C(7)	64(3)	26(2)	26(2)	1(1)	2(2)	-7(2)
C(18)	68(3)	31(2)	31(2)	-6(2)	16(2)	-5(2)
C(14)	55(3)	68(3)	44(3)	-3(2)	-11(2)	-5(2)
C(22)	52(2)	38(2)	39(2)	-2(2)	14(2)	1(2)
C(15)	77(4)	64(3)	61(3)	-12(2)	19(3)	14(2)
C(12)	121(4)	28(2)	29(2)	-1(2)	15(3)	3(2)
C(1S)	77(3)	50(3)	96(4)	17(3)	-32(3)	-14(2)

Table S25. Hydrogen coordinates (x 10^4) and isotropic displacement parameters ($Å^2$ x 10^3) for k10109 (**2.17**).

	x	y	z	U(eq)
H(20)	838	376	608	54
H(5A)	3177	-1767	2640	53
H(5B)	2650	-1419	2022	53
H(5C)	1751	-1163	2547	53
H(10)	8868	2874	5753	69
H(3)	4390	-340	4435	42
H(23A)	1589	1208	1922	68
H(23B)	867	260	2012	68
H(23C)	237	887	1508	68
H(11)	7058	3700	6156	76
H(2)	3431	-1285	3624	40
H(19)	2424	-279	7	58
H(2S1)	9964	7182	2074	73
H(2S2)	8338	7553	1967	73
H(7A)	5334	2310	3545	58
H(7B)	6954	1926	3632	58
H(7C)	6377	2594	4085	58
H(18)	4736	-783	362	51
H(14A)	8454	894	5043	85
H(14B)	9618	1665	5183	85
H(14C)	8689	1645	4586	85
H(22A)	5971	-1187	1721	64
H(22B)	6633	-235	1595	64
H(22C)	6608	-997	1128	64
H(15A)	2670	2608	5401	100
H(15B)	3055	1661	5151	100
H(15C)	3028	2519	4757	100
H(12)	4622	3458	5886	71
H(1S1)	1579	4645	1958	92
H(1S2)	2669	3936	1722	92

1,3-Bis[1-(2,6-dimethylphenylimino)ethyl]imidazol-2-ylidene cobalt(II) chloride (2.18).

Table S26. Crystal data and structure refinement for k10110 (**2.18**).

Identification code	k10110	
Empirical formula	C25 H30 Cl6 Co N4	
Formula weight	658.16	
Temperature	150(1) K	
Wavelength	0.71073 Å	
Crystal system	Monoclinic	
Space group	P 21/c	
Unit cell dimensions	a = 9.0052(3) Å	α= 90°.
	b = 14.7348(3) Å	β= 94.6970(10)°.
	c = 23.3276(7) Å	γ = 90°.
Volume	3084.94(15) Å^3	
Z	4	
Density (calculated)	1.417 Mg/m^3	
Absorption coefficient	1.097 mm^{-1}	
F(000)	1348	
Crystal size	0.25 x 0.24 x 0.20 mm^3	
Theta range for data collection	2.66 to 27.49°.	
Index ranges	-11<=h<=11, -17<=k<=19, -30<=l<=30	
Reflections collected	20424	
Independent reflections	7033 [R(int) = 0.0391]	
Completeness to theta = 27.49°	99.3 %	
Absorption correction	Semi-empirical from equivalents	
Max. and min. transmission	0.864 and 0.806	
Refinement method	Full-matrix least-squares on F^2	
Data / restraints / parameters	7033 / 0 / 325	
Goodness-of-fit on F^2	1.055	
Final R indices [I>2sigma(I)]	R1 = 0.0567, wR2 = 0.1465	
R indices (all data)	R1 = 0.0972, wR2 = 0.1736	
Largest diff. peak and hole	0.769 and -0.624 e.Å^{-3}	

Table S27. Atomic coordinates (x 10^4) and equivalent isotropic displacement parameters ($Å^2$ x 10^3) for k10110 (**2.18**). U(eq) is defined as one third of the trace of the orthogonalized U^{ij} tensor.

	x	y	z	U(eq)
Co(1)	9776(1)	1203(1)	2507(1)	26(1)
Cl(2)	7329(1)	1227(1)	2595(1)	35(1)
Cl(1)	10975(1)	2494(1)	2720(1)	39(1)
Cl(3S)	4760(2)	3109(1)	1305(1)	68(1)
Cl(4S)	6591(2)	9731(1)	1001(1)	74(1)
Cl(5S)	5347(2)	8342(1)	1701(1)	64(1)
Cl(2S)	3649(2)	1270(1)	1433(1)	85(1)
N(4)	9494(4)	1241(2)	320(1)	30(1)
N(3)	10945(3)	87(2)	2850(1)	25(1)
N(1)	10903(3)	-256(2)	1896(1)	25(1)
N(2)	10049(3)	569(2)	1191(1)	27(1)
C(12)	7116(7)	2761(3)	-633(2)	55(1)
C(18)	13265(5)	183(3)	4243(2)	44(1)
C(11)	8191(8)	3262(3)	-878(2)	63(2)
C(8)	9019(5)	1961(2)	-62(2)	34(1)
C(17)	12851(4)	277(3)	3658(2)	34(1)
C(13)	7490(5)	2091(3)	-222(2)	41(1)
C(3)	10610(5)	-220(2)	958(2)	32(1)
C(9)	10117(6)	2461(3)	-307(2)	43(1)
C(1)	10223(4)	558(2)	1771(1)	26(1)
C(6)	9442(4)	1321(2)	853(2)	27(1)
C(4)	11364(4)	-472(2)	2479(1)	25(1)
C(1S)	4179(6)	2278(3)	1785(2)	56(1)
C(5)	12305(4)	-1286(2)	2582(2)	33(1)
C(7)	8898(5)	2098(2)	1190(2)	36(1)
C(22)	13894(5)	706(3)	3264(2)	44(1)
C(21)	10442(5)	-425(2)	3814(2)	33(1)
C(2)	11143(4)	-737(3)	1397(2)	33(1)
C(16)	11441(4)	-34(2)	3455(1)	28(1)
C(20)	10915(5)	-507(3)	4396(2)	42(1)
C(15)	6321(6)	1518(3)	23(2)	55(1)
C(2S)	6729(6)	9188(4)	1668(2)	66(2)
C(19)	12302(6)	-208(3)	4605(2)	48(1)
C(23)	8933(5)	-743(3)	3578(2)	41(1)
C(10)	9660(7)	3113(3)	-719(2)	55(1)
C(14)	11720(6)	2303(4)	-140(2)	63(1)

Table S28. Bond lengths [Å] and angles [°] for k10110 (**2.18**).

Co(1)-C(1)	2.030(3)
Co(1)-N(3)	2.077(3)
Co(1)-Cl(1)	2.2239(10)
Co(1)-Cl(2)	2.2293(11)
Cl(3S)-C(1S)	1.768(5)
Cl(4S)-C(2S)	1.745(5)
Cl(5S)-C(2S)	1.768(5)
Cl(2S)-C(1S)	1.745(5)
N(4)-C(6)	1.253(4)
N(4)-C(8)	1.428(5)
N(3)-C(4)	1.273(4)
N(3)-C(16)	1.455(4)
N(1)-C(1)	1.367(4)
N(1)-C(2)	1.394(4)
N(1)-C(4)	1.426(4)
N(2)-C(1)	1.350(4)
N(2)-C(3)	1.395(4)
N(2)-C(6)	1.443(4)
C(12)-C(11)	1.378(8)
C(12)-C(13)	1.397(6)
C(18)-C(19)	1.384(6)
C(18)-C(17)	1.392(5)
C(11)-C(10)	1.362(8)
C(8)-C(9)	1.393(6)
C(8)-C(13)	1.410(6)
C(17)-C(16)	1.396(5)
C(17)-C(22)	1.506(6)
C(13)-C(15)	1.499(6)
C(3)-C(2)	1.335(5)
C(9)-C(10)	1.397(6)
C(9)-C(14)	1.482(7)
C(6)-C(7)	1.495(5)
C(4)-C(5)	1.477(5)
C(21)-C(20)	1.394(5)
C(21)-C(16)	1.403(5)
C(21)-C(23)	1.499(6)
C(20)-C(19)	1.376(6)
C(1)-Co(1)-N(3)	79.99(12)
C(1)-Co(1)-Cl(1)	117.57(10)
N(3)-Co(1)-Cl(1)	111.64(9)

C(1)-Co(1)-Cl(2)	110.61(11)
N(3)-Co(1)-Cl(2)	116.81(8)
Cl(1)-Co(1)-Cl(2)	115.52(4)
C(6)-N(4)-C(8)	121.0(3)
C(4)-N(3)-C(16)	119.6(3)
C(4)-N(3)-Co(1)	114.8(2)
C(16)-N(3)-Co(1)	125.2(2)
C(1)-N(1)-C(2)	111.5(3)
C(1)-N(1)-C(4)	119.3(3)
C(2)-N(1)-C(4)	129.1(3)
C(1)-N(2)-C(3)	111.4(3)
C(1)-N(2)-C(6)	124.4(3)
C(3)-N(2)-C(6)	124.1(3)
C(11)-C(12)-C(13)	121.6(5)
C(19)-C(18)-C(17)	120.5(4)
C(10)-C(11)-C(12)	120.0(4)
C(9)-C(8)-C(13)	122.0(4)
C(9)-C(8)-N(4)	117.6(4)
C(13)-C(8)-N(4)	120.2(4)
C(18)-C(17)-C(16)	117.7(4)
C(18)-C(17)-C(22)	120.6(4)
C(16)-C(17)-C(22)	121.7(3)
C(12)-C(13)-C(8)	116.9(4)
C(12)-C(13)-C(15)	121.5(4)
C(8)-C(13)-C(15)	121.5(4)
C(2)-C(3)-N(2)	107.1(3)
C(8)-C(9)-C(10)	117.9(5)
C(8)-C(9)-C(14)	121.2(4)
C(10)-C(9)-C(14)	121.0(5)
N(2)-C(1)-N(1)	103.7(3)
N(2)-C(1)-Co(1)	145.8(3)
N(1)-C(1)-Co(1)	110.3(2)
N(4)-C(6)-N(2)	115.3(3)
N(4)-C(6)-C(7)	129.4(3)
N(2)-C(6)-C(7)	115.2(3)
N(3)-C(4)-N(1)	115.2(3)
N(3)-C(4)-C(5)	127.8(3)
N(1)-C(4)-C(5)	117.0(3)
Cl(2S)-C(1S)-Cl(3S)	112.1(3)
C(20)-C(21)-C(16)	117.3(4)
C(20)-C(21)-C(23)	121.7(4)
C(16)-C(21)-C(23)	121.0(3)
C(3)-C(2)-N(1)	106.3(3)

C(17)-C(16)-C(21)	122.8(3)
C(17)-C(16)-N(3)	119.2(3)
C(21)-C(16)-N(3)	118.0(3)
C(19)-C(20)-C(21)	120.9(4)
Cl(4S)-C(2S)-Cl(5S)	111.3(3)
C(20)-C(19)-C(18)	120.9(4)
C(11)-C(10)-C(9)	121.5(5)

Symmetry transformations used to generate equivalent atoms:

Table S29. Anisotropic displacement parameters ($Å^2 \times 10^3$) for k10110 (**2.18**). The anisotropic displacement factor exponent takes the form: $-2\pi^2[h^2a^{*2}U^{11} + ... + 2 h k a^* b^* U^{12}]$

	U11	U22	U33	U23	U13	U12
Co(1)	33(1)	25(1)	20(1)	-2(1)	2(1)	3(1)
Cl(2)	33(1)	41(1)	32(1)	0(1)	4(1)	2(1)
Cl(1)	43(1)	33(1)	41(1)	-7(1)	0(1)	-4(1)
Cl(3S)	55(1)	73(1)	73(1)	1(1)	-12(1)	1(1)
Cl(4S)	70(1)	74(1)	77(1)	16(1)	1(1)	-15(1)
Cl(5S)	54(1)	66(1)	73(1)	6(1)	10(1)	-9(1)
Cl(2S)	73(1)	95(1)	89(1)	-28(1)	21(1)	-35(1)
N(4)	45(2)	27(2)	19(2)	-1(1)	3(1)	2(1)
N(3)	28(2)	26(2)	21(1)	3(1)	2(1)	-2(1)
N(1)	31(2)	25(2)	19(1)	-2(1)	1(1)	2(1)
N(2)	36(2)	25(2)	19(1)	-2(1)	1(1)	3(1)
C(12)	87(4)	45(3)	30(2)	-1(2)	-14(2)	17(3)
C(18)	52(3)	44(2)	34(2)	-1(2)	-10(2)	4(2)
C(11)	130(5)	33(2)	25(2)	6(2)	-1(3)	10(3)
C(8)	58(3)	26(2)	18(2)	-4(1)	1(2)	3(2)
C(17)	36(2)	35(2)	31(2)	1(2)	-2(2)	2(2)
C(13)	60(3)	36(2)	24(2)	-2(2)	-3(2)	4(2)
C(3)	47(2)	25(2)	24(2)	-5(1)	4(2)	1(2)
C(9)	71(3)	34(2)	26(2)	-7(2)	10(2)	-4(2)
C(1)	31(2)	27(2)	21(2)	1(1)	1(1)	-1(2)
C(6)	33(2)	25(2)	23(2)	-1(1)	0(2)	-1(1)
C(4)	27(2)	23(2)	25(2)	2(1)	0(1)	-3(1)
C(1S)	46(3)	70(3)	51(3)	-9(2)	1(2)	6(2)
C(5)	41(2)	28(2)	28(2)	0(1)	2(2)	4(2)
C(7)	60(3)	25(2)	22(2)	0(1)	3(2)	11(2)
C(22)	33(2)	56(3)	41(2)	3(2)	-3(2)	-5(2)
C(21)	49(2)	24(2)	26(2)	2(1)	7(2)	2(2)
C(2)	45(2)	29(2)	24(2)	-5(2)	2(2)	6(2)
C(16)	37(2)	25(2)	22(2)	0(1)	2(2)	3(2)
C(20)	67(3)	34(2)	25(2)	5(2)	13(2)	4(2)
C(15)	55(3)	59(3)	48(3)	1(2)	-10(2)	3(2)
C(2S)	62(3)	49(3)	82(4)	14(3)	-25(3)	-9(3)
C(19)	78(3)	42(2)	22(2)	2(2)	-9(2)	7(2)
C(23)	51(3)	33(2)	41(2)	4(2)	15(2)	-6(2)
C(10)	111(5)	30(2)	26(2)	1(2)	16(3)	-3(3)
C(14)	75(4)	59(3)	59(3)	8(2)	20(3)	-10(3)

Table S30. Hydrogen coordinates (x 10^4) and isotropic displacement parameters ($Å^2$ x 10^3) for k10110 (**2.18**).

	x	y	z	U(eq)
H(12)	6117	2872	-743	66
H(18)	14196	385	4392	53
H(11)	7914	3702	-1152	75
H(3)	10613	-359	569	39
H(1S1)	4987	2154	2075	67
H(1S2)	3346	2512	1978	67
H(5A)	12418	-1586	2223	49
H(5B)	11843	-1691	2836	49
H(5C)	13267	-1109	2753	49
H(7A)	9003	1952	1592	53
H(7B)	7868	2211	1073	53
H(7C)	9474	2630	1122	53
H(22A)	13430	716	2879	66
H(22B)	14799	360	3274	66
H(22C)	14117	1315	3389	66
H(2)	11585	-1305	1375	40
H(20)	10284	-767	4646	50
H(15A)	6788	1102	299	83
H(15B)	5785	1184	-280	83
H(15C)	5643	1901	209	83
H(2S1)	6622	9632	1968	79
H(2S2)	7707	8913	1734	79
H(19)	12597	-270	4994	58
H(23A)	8823	-644	3170	61
H(23B)	8179	-409	3757	61
H(23C)	8829	-1378	3657	61
H(10)	10376	3453	-888	66
H(14A)	12308	2706	-353	95
H(14B)	11968	1686	-223	95
H(14C)	11922	2415	264	95

1,3-Bis[(2,4,6-trimethylphenylimino)benzyl]imidazol-2-ylidene chromium(III) chloride (2.20).

Table S31. Crystal data and structure refinement for k10187 (**2.20**).

Identification code	k10187	
Empirical formula	C43 H50 Cl3 Cr N4 O2	
Formula weight	813.22	
Temperature	150(1) K	
Wavelength	0.71073 Å	
Crystal system	Triclinic	
Space group	P-1	
Unit cell dimensions	a = 15.3436(8) Å	α= 64.999(2)°.
	b = 17.5786(10) Å	β= 82.728(3)°.
	c = 17.7453(10) Å	γ = 73.661(3)°.
Volume	4162.4(4) $Å^3$	
Z	4	
Density (calculated)	1.298 Mg/m^3	
Absorption coefficient	0.508 mm^{-1}	
F(000)	1708	
Crystal size	0.22 x 0.12 x 0.12 mm^3	
Theta range for data collection	2.64 to 27.62°.	
Index ranges	-19<=h<=19, -21<=k<=22, -23<=l<=23	
Reflections collected	46693	
Independent reflections	18755 [R(int) = 0.0886]	
Completeness to theta = 27.62°	97.0 %	
Absorption correction	Semi-empirical from equivalents	
Max. and min. transmission	0.9416 and 0.8965	
Refinement method	Full-matrix least-squares on F^2	
Data / restraints / parameters	18755 / 33 / 977	
Goodness-of-fit on F^2	1.013	
Final R indices [I>2sigma(I)]	R1 = 0.0707, wR2 = 0.1558	
R indices (all data)	R1 = 0.1774, wR2 = 0.2005	
Largest diff. peak and hole	0.479 and -0.436 e.$Å^{-3}$	

Table S32. Atomic coordinates (x 10^4) and equivalent isotropic displacement parameters ($Å^2$ x10^3) for k10187 (**2.20**). U(eq) is defined as one third of the trace of the orthogonalized U^{ij} tensor.

	x	y	z	U(eq)
Cr(1A)	2009(1)	9502(1)	1806(1)	40(1)
Cl(1A)	1873(1)	10908(1)	1614(1)	50(1)
Cl(3A)	3547(1)	9254(1)	1591(1)	51(1)
Cl(2A)	432(1)	9712(1)	1979(1)	47(1)
O(1A)	2141(2)	9048(2)	3088(2)	50(1)
N(1A)	1582(2)	9021(2)	562(2)	37(1)
N(2A)	1386(2)	10398(2)	-100(2)	37(1)
N(3A)	2101(2)	8230(2)	1885(2)	39(1)
N(4A)	701(2)	11847(2)	-574(2)	45(1)
C(1A)	1724(3)	9734(3)	615(2)	38(1)
C(2A)	1132(3)	9254(3)	-174(2)	40(1)
C(3A)	1016(3)	10105(3)	-584(3)	41(1)
C(4A)	1869(3)	8206(3)	1214(3)	39(1)
C(5A)	1948(3)	7421(3)	1067(3)	39(1)
C(6A)	1643(3)	6731(3)	1650(3)	45(1)
C(7A)	1805(3)	5973(3)	1530(3)	50(1)
C(8A)	2253(3)	5910(3)	830(3)	53(1)
C(9A)	2539(3)	6608(3)	236(3)	52(1)
C(10A)	2383(3)	7372(3)	340(3)	44(1)
C(11A)	2527(3)	7424(3)	2562(3)	43(1)
C(12A)	2033(3)	7121(3)	3305(3)	50(1)
C(13A)	2474(4)	6379(3)	3956(3)	63(1)
C(14A)	3365(4)	5940(3)	3892(3)	65(2)
C(15A)	3823(3)	6248(3)	3151(4)	62(2)
C(16A)	3421(3)	6991(3)	2467(3)	48(1)
C(17A)	1058(3)	7543(3)	3399(3)	58(1)
C(18A)	3821(4)	5115(4)	4630(4)	94(2)
C(19A)	3958(3)	7239(3)	1672(3)	58(1)
C(20A)	1456(3)	11284(3)	-392(2)	39(1)
C(21A)	2405(3)	11366(3)	-493(3)	43(1)
C(22A)	3106(3)	10726(3)	-632(3)	49(1)
C(23A)	3992(3)	10790(3)	-734(3)	60(1)
C(24A)	4198(3)	11480(4)	-691(3)	66(2)
C(25A)	3508(3)	12119(3)	-554(3)	63(1)
C(26A)	2622(3)	12068(3)	-461(3)	51(1)
C(27A)	615(3)	12764(3)	-949(3)	45(1)
C(28A)	795(3)	13178(3)	-1786(3)	54(1)

C(29A)	600(3)	14090(3)	-2135(3)	61(1)
C(30A)	246(3)	14567(3)	-1670(4)	62(1)
C(31A)	70(3)	14126(3)	-841(4)	59(1)
C(32A)	229(3)	13223(3)	-454(3)	49(1)
C(33A)	1171(4)	12674(3)	-2313(3)	70(2)
C(34A)	-5(4)	15554(3)	-2077(4)	85(2)
C(35A)	-14(3)	12761(3)	430(3)	60(1)
C(36A)	2968(3)	8567(3)	3578(3)	63(1)
C(37A)	2618(6)	8362(5)	4454(3)	73(4)
C(38A)	1898(4)	9174(4)	4377(3)	104(2)
C(36C)	2968(3)	8567(3)	3578(3)	63(1)
C(37C)	2900(5)	8967(12)	4189(9)	96(7)
C(38C)	1898(4)	9174(4)	4377(3)	104(2)
C(39A)	1500(3)	9488(3)	3545(3)	75(2)
Cr(1B)	6444(1)	1341(1)	2702(1)	42(1)
Cl(1B)	6217(1)	2777(1)	1855(1)	55(1)
Cl(2B)	6808(1)	987(1)	1547(1)	52(1)
Cl(3B)	5994(1)	1642(1)	3856(1)	57(1)
O(1B)	7810(2)	1189(2)	2854(2)	45(1)
N(1B)	5222(2)	337(2)	2806(2)	45(1)
N(2B)	4469(2)	1621(2)	2069(2)	49(1)
N(3B)	6546(2)	-33(2)	3464(2)	42(1)
N(4B)	3981(2)	2803(2)	877(2)	48(1)
C(1B)	5217(3)	1198(3)	2541(3)	44(1)
C(2B)	4508(3)	248(3)	2460(3)	56(1)
C(3B)	4040(3)	1046(3)	2004(3)	53(1)
C(4B)	5926(3)	-313(3)	3321(3)	44(1)
C(5B)	5866(3)	-1213(3)	3584(3)	48(1)
C(6B)	5465(4)	-1658(3)	4309(3)	66(1)
C(7B)	5362(4)	-2467(4)	4483(4)	76(2)
C(8B)	5622(4)	-2836(3)	3926(4)	73(2)
C(9B)	6014(5)	-2392(4)	3184(4)	97(2)
C(10B)	6139(4)	-1585(4)	3017(4)	83(2)
C(11B)	7246(3)	-625(3)	4073(3)	49(1)
C(12B)	7080(3)	-774(3)	4903(3)	55(1)
C(13B)	7818(4)	-1265(3)	5453(3)	71(2)
C(14B)	8661(4)	-1607(4)	5210(4)	75(2)
C(15B)	8788(4)	-1457(3)	4370(4)	72(2)
C(16B)	8099(3)	-973(3)	3793(3)	55(1)
C(17B)	6173(4)	-442(4)	5234(3)	71(2)
C(18B)	9423(4)	-2140(4)	5836(5)	116(3)
C(19B)	8259(4)	-862(3)	2904(3)	70(2)
C(20B)	4122(3)	2559(3)	1635(3)	45(1)

C(21B)	3935(3)	3040(3)	2175(3)	48(1)
C(22B)	3640(3)	2657(4)	2991(3)	68(2)
C(23B)	3421(4)	3116(4)	3493(4)	83(2)
C(24B)	3514(4)	3949(4)	3181(4)	82(2)
C(25B)	3812(3)	4334(3)	2388(3)	63(1)
C(26B)	4017(3)	3886(3)	1880(3)	54(1)
C(27B)	3509(3)	3660(3)	346(3)	47(1)
C(28B)	2557(3)	3858(3)	346(3)	49(1)
C(29B)	2111(3)	4647(3)	-279(3)	54(1)
C(30B)	2570(3)	5212(3)	-858(3)	51(1)
C(31B)	3515(3)	5001(3)	-830(3)	51(1)
C(32B)	4001(3)	4203(3)	-229(3)	48(1)
C(33B)	2040(3)	3262(3)	977(3)	62(1)
C(34B)	2059(3)	6064(3)	-1511(3)	64(1)
C(35B)	4998(3)	3966(3)	-221(3)	50(1)
C(36B)	8453(3)	1458(3)	2165(3)	50(1)
C(37B)	9244(3)	1530(3)	2541(3)	55(1)
C(38B)	9199(3)	903(3)	3444(3)	55(1)
C(39B)	8195(3)	1076(3)	3612(3)	53(1)
O(1S)	8845(8)	4934(7)	5177(8)	271(5)
C(1S)	8887(8)	4999(7)	5960(6)	195(5)
C(2S)	9007(9)	5881(8)	5743(8)	197(5)
C(3S)	8611(12)	6420(5)	4891(7)	230(7)
C(4S)	8426(13)	5806(9)	4602(8)	311(12)
O(2S)	3845(9)	5751(12)	6648(8)	322(7)
C(5S)	3039(14)	6321(6)	6163(7)	223(8)
C(6S)	2331(6)	5833(15)	6348(10)	327(16)
C(7S)	2749(13)	4949(11)	6977(11)	291(12)
C(8S)	3750(11)	4877(9)	6888(10)	223(9)

Table S33. Bond lengths [Å] and angles [°] for k10187 (**2.20**).

Cr(1A)-C(1A)	2.057(4)
Cr(1A)-O(1A)	2.084(3)
Cr(1A)-N(3A)	2.144(3)
Cr(1A)-Cl(3A)	2.2890(12)
Cr(1A)-Cl(1A)	2.2986(13)
Cr(1A)-Cl(2A)	2.3420(12)
O(1A)-C(39A)	1.459(4)
O(1A)-C(36A)	1.461(3)
N(1A)-C(1A)	1.375(5)
N(1A)-C(4A)	1.399(5)
N(1A)-C(2A)	1.402(5)
N(2A)-C(1A)	1.347(5)
N(2A)-C(3A)	1.409(5)
N(2A)-C(20A)	1.451(5)
N(3A)-C(4A)	1.305(5)
N(3A)-C(11A)	1.456(5)
N(4A)-C(20A)	1.267(5)
N(4A)-C(27A)	1.435(6)
C(2A)-C(3A)	1.327(6)
C(4A)-C(5A)	1.480(6)
C(5A)-C(6A)	1.378(6)
C(5A)-C(10A)	1.400(6)
C(6A)-C(7A)	1.386(6)
C(7A)-C(8A)	1.374(6)
C(8A)-C(9A)	1.379(7)
C(9A)-C(10A)	1.383(6)
C(11A)-C(16A)	1.398(6)
C(11A)-C(12A)	1.405(6)
C(12A)-C(13A)	1.386(6)
C(12A)-C(17A)	1.495(6)
C(13A)-C(14A)	1.386(7)
C(14A)-C(15A)	1.376(8)
C(14A)-C(18A)	1.537(7)
C(15A)-C(16A)	1.399(6)
C(16A)-C(19A)	1.499(7)
C(20A)-C(21A)	1.484(6)
C(21A)-C(26A)	1.392(6)
C(21A)-C(22A)	1.403(6)
C(22A)-C(23A)	1.379(6)
C(23A)-C(24A)	1.371(7)

C(24A)-C(25A)	1.392(6)
C(25A)-C(26A)	1.372(6)
C(27A)-C(28A)	1.381(6)
C(27A)-C(32A)	1.405(6)
C(28A)-C(29A)	1.408(7)
C(28A)-C(33A)	1.505(6)
C(29A)-C(30A)	1.376(7)
C(30A)-C(31A)	1.376(7)
C(30A)-C(34A)	1.521(7)
C(31A)-C(32A)	1.398(7)
C(32A)-C(35A)	1.485(7)
C(36A)-C(37A)	1.502(4)
C(37A)-C(38A)	1.504(4)
C(38A)-C(39A)	1.485(4)
Cr(1B)-C(1B)	2.038(4)
Cr(1B)-O(1B)	2.075(3)
Cr(1B)-N(3B)	2.183(4)
Cr(1B)-Cl(1B)	2.2773(14)
Cr(1B)-Cl(3B)	2.3027(13)
Cr(1B)-Cl(2B)	2.3432(12)
O(1B)-C(39B)	1.452(5)
O(1B)-C(36B)	1.468(5)
N(1B)-C(1B)	1.379(5)
N(1B)-C(2B)	1.397(5)
N(1B)-C(4B)	1.406(5)
N(2B)-C(1B)	1.345(5)
N(2B)-C(3B)	1.399(5)
N(2B)-C(20B)	1.461(5)
N(3B)-C(4B)	1.282(5)
N(3B)-C(11B)	1.455(5)
N(4B)-C(20B)	1.255(5)
N(4B)-C(27B)	1.428(5)
C(2B)-C(3B)	1.326(6)
C(4B)-C(5B)	1.476(6)
C(5B)-C(6B)	1.365(7)
C(5B)-C(10B)	1.383(7)
C(6B)-C(7B)	1.374(7)
C(7B)-C(8B)	1.362(8)
C(8B)-C(9B)	1.378(9)
C(9B)-C(10B)	1.385(8)
C(11B)-C(12B)	1.385(6)
C(11B)-C(16B)	1.405(6)
C(12B)-C(13B)	1.413(6)

C(12B)-C(17B)	1.500(7)
C(13B)-C(14B)	1.364(8)
C(14B)-C(15B)	1.398(8)
C(14B)-C(18B)	1.520(7)
C(15B)-C(16B)	1.387(6)
C(16B)-C(19B)	1.502(7)
C(20B)-C(21B)	1.483(6)
C(21B)-C(26B)	1.389(6)
C(21B)-C(22B)	1.391(7)
C(22B)-C(23B)	1.392(7)
C(23B)-C(24B)	1.372(8)
C(24B)-C(25B)	1.362(8)
C(25B)-C(26B)	1.386(6)
C(27B)-C(32B)	1.382(7)
C(27B)-C(28B)	1.403(6)
C(28B)-C(29B)	1.407(6)
C(28B)-C(33B)	1.494(7)
C(29B)-C(30B)	1.373(7)
C(30B)-C(31B)	1.394(6)
C(30B)-C(34B)	1.518(6)
C(31B)-C(32B)	1.418(6)
C(32B)-C(35B)	1.470(6)
C(36B)-C(37B)	1.516(6)
C(37B)-C(38B)	1.520(7)
C(38B)-C(39B)	1.501(6)
O(1S)-C(4S)	1.448(5)
O(1S)-C(1S)	1.452(5)
C(1S)-C(2S)	1.490(5)
C(2S)-C(3S)	1.501(5)
C(3S)-C(4S)	1.479(5)
O(2S)-C(5S)	1.454(5)
O(2S)-C(8S)	1.456(5)
C(5S)-C(6S)	1.491(5)
C(6S)-C(7S)	1.492(5)
C(7S)-C(8S)	1.498(5)
C(1A)-Cr(1A)-O(1A)	167.01(15)
C(1A)-Cr(1A)-N(3A)	76.95(15)
O(1A)-Cr(1A)-N(3A)	92.34(12)
C(1A)-Cr(1A)-Cl(3A)	94.42(12)
O(1A)-Cr(1A)-Cl(3A)	92.61(8)
N(3A)-Cr(1A)-Cl(3A)	88.56(9)
C(1A)-Cr(1A)-Cl(1A)	98.46(12)
O(1A)-Cr(1A)-Cl(1A)	92.17(9)

N(3A)-Cr(1A)-Cl(1A)	175.39(9)
Cl(3A)-Cr(1A)-Cl(1A)	92.18(5)
C(1A)-Cr(1A)-Cl(2A)	82.98(11)
O(1A)-Cr(1A)-Cl(2A)	89.55(8)
N(3A)-Cr(1A)-Cl(2A)	88.80(9)
Cl(3A)-Cr(1A)-Cl(2A)	176.65(5)
Cl(1A)-Cr(1A)-Cl(2A)	90.29(4)
C(39A)-O(1A)-C(36A)	108.3(3)
C(39A)-O(1A)-Cr(1A)	119.6(2)
C(36A)-O(1A)-Cr(1A)	127.7(2)
C(1A)-N(1A)-C(4A)	118.9(3)
C(1A)-N(1A)-C(2A)	111.2(3)
C(4A)-N(1A)-C(2A)	129.9(3)
C(1A)-N(2A)-C(3A)	110.8(3)
C(1A)-N(2A)-C(20A)	126.1(3)
C(3A)-N(2A)-C(20A)	122.9(3)
C(4A)-N(3A)-C(11A)	119.3(3)
C(4A)-N(3A)-Cr(1A)	115.3(3)
C(11A)-N(3A)-Cr(1A)	124.6(2)
C(20A)-N(4A)-C(27A)	123.6(4)
N(2A)-C(1A)-N(1A)	104.1(3)
N(2A)-C(1A)-Cr(1A)	140.3(3)
N(1A)-C(1A)-Cr(1A)	112.4(3)
C(3A)-C(2A)-N(1A)	106.1(3)
C(2A)-C(3A)-N(2A)	107.7(3)
N(3A)-C(4A)-N(1A)	114.4(3)
N(3A)-C(4A)-C(5A)	126.7(4)
N(1A)-C(4A)-C(5A)	118.7(3)
C(6A)-C(5A)-C(10A)	120.2(4)
C(6A)-C(5A)-C(4A)	121.0(4)
C(10A)-C(5A)-C(4A)	118.7(4)
C(5A)-C(6A)-C(7A)	119.6(4)
C(8A)-C(7A)-C(6A)	120.6(5)
C(7A)-C(8A)-C(9A)	119.9(4)
C(8A)-C(9A)-C(10A)	120.6(5)
C(9A)-C(10A)-C(5A)	119.1(5)
C(16A)-C(11A)-C(12A)	122.0(4)
C(16A)-C(11A)-N(3A)	119.3(4)
C(12A)-C(11A)-N(3A)	118.7(4)
C(13A)-C(12A)-C(11A)	117.4(4)
C(13A)-C(12A)-C(17A)	119.8(5)
C(11A)-C(12A)-C(17A)	122.7(4)
C(14A)-C(13A)-C(12A)	122.3(5)

C(15A)-C(14A)-C(13A)	118.6(5)
C(15A)-C(14A)-C(18A)	121.0(5)
C(13A)-C(14A)-C(18A)	120.4(6)
C(14A)-C(15A)-C(16A)	122.2(5)
C(11A)-C(16A)-C(15A)	117.3(5)
C(11A)-C(16A)-C(19A)	124.6(4)
C(15A)-C(16A)-C(19A)	118.0(4)
N(4A)-C(20A)-N(2A)	114.0(4)
N(4A)-C(20A)-C(21A)	131.9(4)
N(2A)-C(20A)-C(21A)	113.8(3)
C(26A)-C(21A)-C(22A)	118.6(4)
C(26A)-C(21A)-C(20A)	121.7(4)
C(22A)-C(21A)-C(20A)	119.7(4)
C(23A)-C(22A)-C(21A)	120.8(4)
C(24A)-C(23A)-C(22A)	119.9(4)
C(23A)-C(24A)-C(25A)	119.7(5)
C(26A)-C(25A)-C(24A)	120.9(5)
C(25A)-C(26A)-C(21A)	120.0(4)
C(28A)-C(27A)-C(32A)	122.3(4)
C(28A)-C(27A)-N(4A)	120.5(4)
C(32A)-C(27A)-N(4A)	116.6(4)
C(27A)-C(28A)-C(29A)	117.7(4)
C(27A)-C(28A)-C(33A)	121.4(4)
C(29A)-C(28A)-C(33A)	121.0(5)
C(30A)-C(29A)-C(28A)	122.2(5)
C(31A)-C(30A)-C(29A)	117.9(5)
C(31A)-C(30A)-C(34A)	121.2(5)
C(29A)-C(30A)-C(34A)	120.7(5)
C(30A)-C(31A)-C(32A)	123.2(5)
C(31A)-C(32A)-C(27A)	116.6(5)
C(31A)-C(32A)-C(35A)	122.5(4)
C(27A)-C(32A)-C(35A)	120.9(4)
O(1A)-C(36A)-C(37A)	102.6(4)
C(36A)-C(37A)-C(38A)	103.1(4)
C(39A)-C(38A)-C(37A)	104.1(4)
O(1A)-C(39A)-C(38A)	106.8(3)
C(1B)-Cr(1B)-O(1B)	165.86(15)
C(1B)-Cr(1B)-N(3B)	76.85(15)
O(1B)-Cr(1B)-N(3B)	92.05(12)
C(1B)-Cr(1B)-Cl(1B)	97.93(13)
O(1B)-Cr(1B)-Cl(1B)	92.94(9)
N(3B)-Cr(1B)-Cl(1B)	174.67(10)
C(1B)-Cr(1B)-Cl(3B)	94.81(12)

O(1B)-Cr(1B)-Cl(3B)	93.88(8)
N(3B)-Cr(1B)-Cl(3B)	89.87(9)
Cl(1B)-Cr(1B)-Cl(3B)	91.66(5)
C(1B)-Cr(1B)-Cl(2B)	81.11(12)
O(1B)-Cr(1B)-Cl(2B)	89.84(8)
N(3B)-Cr(1B)-Cl(2B)	87.76(9)
Cl(1B)-Cr(1B)-Cl(2B)	90.38(5)
Cl(3B)-Cr(1B)-Cl(2B)	175.66(6)
C(39B)-O(1B)-C(36B)	108.7(3)
C(39B)-O(1B)-Cr(1B)	124.2(3)
C(36B)-O(1B)-Cr(1B)	124.3(2)
C(1B)-N(1B)-C(2B)	111.3(3)
C(1B)-N(1B)-C(4B)	119.6(3)
C(2B)-N(1B)-C(4B)	129.0(4)
C(1B)-N(2B)-C(3B)	111.7(4)
C(1B)-N(2B)-C(20B)	127.0(4)
C(3B)-N(2B)-C(20B)	121.3(3)
C(4B)-N(3B)-C(11B)	120.0(4)
C(4B)-N(3B)-Cr(1B)	113.8(3)
C(11B)-N(3B)-Cr(1B)	126.2(3)
C(20B)-N(4B)-C(27B)	124.4(4)
N(2B)-C(1B)-N(1B)	103.2(4)
N(2B)-C(1B)-Cr(1B)	141.3(3)
N(1B)-C(1B)-Cr(1B)	112.0(3)
C(3B)-C(2B)-N(1B)	106.4(4)
C(2B)-C(3B)-N(2B)	107.3(4)
N(3B)-C(4B)-N(1B)	114.7(4)
N(3B)-C(4B)-C(5B)	129.5(4)
N(1B)-C(4B)-C(5B)	115.7(4)
C(6B)-C(5B)-C(10B)	118.3(5)
C(6B)-C(5B)-C(4B)	123.9(4)
C(10B)-C(5B)-C(4B)	117.4(5)
C(5B)-C(6B)-C(7B)	120.9(5)
C(8B)-C(7B)-C(6B)	121.2(6)
C(7B)-C(8B)-C(9B)	118.8(5)
C(8B)-C(9B)-C(10B)	120.0(6)
C(5B)-C(10B)-C(9B)	120.7(6)
C(12B)-C(11B)-C(16B)	121.7(4)
C(12B)-C(11B)-N(3B)	119.2(4)
C(16B)-C(11B)-N(3B)	118.9(4)
C(11B)-C(12B)-C(13B)	116.9(5)
C(11B)-C(12B)-C(17B)	123.6(4)
C(13B)-C(12B)-C(17B)	119.5(5)

C(14B)-C(13B)-C(12B)	123.6(5)
C(13B)-C(14B)-C(15B)	117.3(5)
C(13B)-C(14B)-C(18B)	121.0(6)
C(15B)-C(14B)-C(18B)	121.8(6)
C(16B)-C(15B)-C(14B)	122.4(5)
C(15B)-C(16B)-C(11B)	118.1(5)
C(15B)-C(16B)-C(19B)	120.3(5)
C(11B)-C(16B)-C(19B)	121.6(4)
N(4B)-C(20B)-N(2B)	113.4(4)
N(4B)-C(20B)-C(21B)	131.7(4)
N(2B)-C(20B)-C(21B)	114.7(4)
C(26B)-C(21B)-C(22B)	118.4(4)
C(26B)-C(21B)-C(20B)	121.5(4)
C(22B)-C(21B)-C(20B)	120.0(5)
C(21B)-C(22B)-C(23B)	120.6(6)
C(24B)-C(23B)-C(22B)	119.4(6)
C(25B)-C(24B)-C(23B)	121.0(5)
C(24B)-C(25B)-C(26B)	119.9(5)
C(25B)-C(26B)-C(21B)	120.7(5)
C(32B)-C(27B)-C(28B)	122.8(4)
C(32B)-C(27B)-N(4B)	118.8(4)
C(28B)-C(27B)-N(4B)	117.6(4)
C(27B)-C(28B)-C(29B)	116.7(5)
C(27B)-C(28B)-C(33B)	121.8(4)
C(29B)-C(28B)-C(33B)	121.5(4)
C(30B)-C(29B)-C(28B)	122.6(4)
C(29B)-C(30B)-C(31B)	119.2(4)
C(29B)-C(30B)-C(34B)	120.7(4)
C(31B)-C(30B)-C(34B)	120.1(5)
C(30B)-C(31B)-C(32B)	120.6(5)
C(27B)-C(32B)-C(31B)	118.1(4)
C(27B)-C(32B)-C(35B)	121.3(4)
C(31B)-C(32B)-C(35B)	120.6(5)
O(1B)-C(36B)-C(37B)	105.7(3)
C(36B)-C(37B)-C(38B)	102.1(4)
C(39B)-C(38B)-C(37B)	102.0(3)
O(1B)-C(39B)-C(38B)	104.0(3)
C(4S)-O(1S)-C(1S)	105.0(7)
O(1S)-C(1S)-C(2S)	106.4(5)
C(1S)-C(2S)-C(3S)	104.9(5)
C(4S)-C(3S)-C(2S)	106.0(5)
O(1S)-C(4S)-C(3S)	108.1(5)
C(5S)-O(2S)-C(8S)	104.9(6)

O(2S)-C(5S)-C(6S)	109.2(5)
C(5S)-C(6S)-C(7S)	105.0(5)
C(6S)-C(7S)-C(8S)	104.5(6)
O(2S)-C(8S)-C(7S)	105.7(5)

Symmetry transformations used to generate equivalent atoms:

Table S34. Anisotropic displacement parameters ($Å^2$ x 10^3) for k10187 (**2.20**). The anisotropic displacement factor exponent takes the form: $-2\pi^2[h^2a^{*2}U^{11} + ... + 2 h k a^* b^* U^{12}]$

	U^{11}	U^{22}	U^{33}	U^{23}	U^{13}	U^{12}
Cr(1A)	38(1)	46(1)	40(1)	-21(1)	-5(1)	-9(1)
Cl(1A)	48(1)	50(1)	58(1)	-28(1)	-6(1)	-11(1)
Cl(3A)	39(1)	60(1)	61(1)	-31(1)	-1(1)	-13(1)
Cl(2A)	38(1)	59(1)	49(1)	-29(1)	-2(1)	-10(1)
O(1A)	49(2)	59(2)	45(2)	-27(2)	-7(2)	-7(2)
N(1A)	38(2)	42(2)	37(2)	-19(2)	4(2)	-15(2)
N(2A)	33(2)	43(2)	37(2)	-18(2)	1(2)	-13(2)
N(3A)	36(2)	42(2)	40(2)	-16(2)	-1(2)	-10(2)
N(4A)	41(2)	50(2)	44(2)	-21(2)	-2(2)	-6(2)
C(1A)	33(2)	44(3)	37(3)	-16(2)	3(2)	-11(2)
C(2A)	38(2)	51(3)	36(2)	-22(2)	-1(2)	-14(2)
C(3A)	37(2)	54(3)	37(2)	-21(2)	-3(2)	-12(2)
C(4A)	32(2)	45(3)	41(3)	-20(2)	2(2)	-9(2)
C(5A)	37(2)	41(3)	42(3)	-19(2)	-2(2)	-11(2)
C(6A)	43(2)	51(3)	47(3)	-23(2)	-2(2)	-12(2)
C(7A)	51(3)	49(3)	51(3)	-14(2)	-6(2)	-23(2)
C(8A)	56(3)	53(3)	58(3)	-31(3)	-8(3)	-11(2)
C(9A)	44(3)	61(3)	57(3)	-35(3)	-4(2)	-5(2)
C(10A)	43(2)	49(3)	44(3)	-23(2)	2(2)	-12(2)
C(11A)	47(3)	44(3)	40(3)	-18(2)	-8(2)	-11(2)
C(12A)	58(3)	51(3)	43(3)	-19(2)	-4(2)	-16(2)
C(13A)	77(4)	61(3)	44(3)	-14(3)	-1(3)	-22(3)
C(14A)	78(4)	54(3)	56(4)	-15(3)	-22(3)	-10(3)
C(15A)	57(3)	61(3)	74(4)	-35(3)	-20(3)	-1(3)
C(16A)	46(3)	50(3)	52(3)	-24(2)	-8(2)	-11(2)
C(17A)	59(3)	68(3)	44(3)	-21(3)	8(2)	-19(3)
C(18A)	110(5)	72(4)	73(4)	-9(3)	-29(4)	-5(4)
C(19A)	42(3)	59(3)	75(4)	-37(3)	-2(3)	-2(2)
C(20A)	44(2)	45(3)	28(2)	-15(2)	4(2)	-14(2)
C(21A)	42(2)	45(3)	41(3)	-17(2)	0(2)	-11(2)
C(22A)	48(3)	50(3)	48(3)	-19(2)	5(2)	-13(2)
C(23A)	44(3)	65(3)	68(4)	-31(3)	9(2)	-9(2)
C(24A)	42(3)	86(4)	74(4)	-35(3)	5(3)	-22(3)
C(25A)	55(3)	74(4)	77(4)	-40(3)	12(3)	-34(3)
C(26A)	48(3)	55(3)	58(3)	-32(3)	5(2)	-14(2)
C(27A)	35(2)	47(3)	52(3)	-20(2)	-5(2)	-7(2)
C(28A)	51(3)	55(3)	53(3)	-22(3)	1(2)	-9(2)

C(29A)	56(3)	50(3)	60(3)	-9(3)	-4(3)	-5(2)
C(30A)	47(3)	52(3)	81(4)	-23(3)	-9(3)	-7(2)
C(31A)	44(3)	61(4)	82(4)	-42(3)	-8(3)	-3(2)
C(32A)	35(2)	53(3)	62(3)	-28(3)	-6(2)	-6(2)
C(33A)	88(4)	58(3)	48(3)	-14(3)	-1(3)	-5(3)
C(34A)	77(4)	54(4)	116(5)	-26(4)	-5(4)	-15(3)
C(35A)	49(3)	70(3)	66(4)	-36(3)	5(3)	-14(2)
C(36A)	59(3)	74(4)	55(3)	-22(3)	-21(3)	-14(3)
C(37A)	85(8)	84(8)	45(6)	-22(6)	-22(6)	-12(6)
C(38A)	101(5)	153(7)	73(4)	-68(5)	-11(4)	-13(5)
C(36C)	59(3)	74(4)	55(3)	-22(3)	-21(3)	-14(3)
C(37C)	107(13)	124(16)	75(11)	-44(11)	-23(9)	-40(11)
C(38C)	101(5)	153(7)	73(4)	-68(5)	-11(4)	-13(5)
C(39A)	89(4)	83(4)	49(3)	-37(3)	1(3)	-2(3)
Cr(1B)	42(1)	45(1)	41(1)	-18(1)	2(1)	-14(1)
Cl(1B)	49(1)	47(1)	64(1)	-16(1)	-1(1)	-14(1)
Cl(2B)	60(1)	61(1)	42(1)	-24(1)	7(1)	-24(1)
Cl(3B)	55(1)	72(1)	53(1)	-34(1)	8(1)	-18(1)
O(1B)	43(2)	57(2)	39(2)	-22(2)	4(1)	-17(1)
N(1B)	45(2)	41(2)	48(2)	-17(2)	0(2)	-13(2)
N(2B)	46(2)	46(2)	54(2)	-16(2)	-6(2)	-15(2)
N(3B)	39(2)	44(2)	43(2)	-18(2)	4(2)	-11(2)
N(4B)	49(2)	44(2)	49(2)	-17(2)	-6(2)	-12(2)
C(1B)	44(3)	47(3)	40(3)	-16(2)	4(2)	-13(2)
C(2B)	54(3)	53(3)	62(3)	-18(3)	-5(3)	-23(2)
C(3B)	48(3)	49(3)	59(3)	-12(3)	-8(2)	-21(2)
C(4B)	42(2)	49(3)	38(3)	-16(2)	6(2)	-11(2)
C(5B)	49(3)	43(3)	50(3)	-17(2)	2(2)	-13(2)
C(6B)	87(4)	54(3)	52(3)	-15(3)	20(3)	-30(3)
C(7B)	98(4)	55(4)	60(4)	-4(3)	2(3)	-32(3)
C(8B)	92(4)	40(3)	75(4)	-3(3)	-13(3)	-25(3)
C(9B)	147(6)	72(4)	92(5)	-45(4)	19(5)	-46(4)
C(10B)	122(5)	64(4)	68(4)	-26(3)	28(4)	-44(4)
C(11B)	48(3)	43(3)	50(3)	-11(2)	-3(2)	-15(2)
C(12B)	55(3)	56(3)	49(3)	-13(2)	2(2)	-20(2)
C(13B)	88(4)	67(4)	56(3)	-14(3)	-12(3)	-30(3)
C(14B)	62(4)	62(4)	87(5)	-13(3)	-18(3)	-17(3)
C(15B)	53(3)	54(3)	100(5)	-22(3)	-3(3)	-14(3)
C(16B)	49(3)	44(3)	64(3)	-15(3)	2(3)	-15(2)
C(17B)	76(4)	83(4)	41(3)	-13(3)	7(3)	-23(3)
C(18B)	100(5)	93(5)	137(7)	-11(4)	-68(5)	-25(4)
C(19B)	68(3)	62(3)	82(4)	-39(3)	16(3)	-11(3)
C(20B)	35(2)	46(3)	53(3)	-19(2)	1(2)	-12(2)

C(21B)	45(3)	47(3)	47(3)	-14(2)	-4(2)	-9(2)
C(22B)	70(3)	61(3)	61(4)	-21(3)	11(3)	-12(3)
C(23B)	103(5)	76(4)	57(4)	-29(3)	19(3)	-8(4)
C(24B)	103(5)	76(5)	57(4)	-35(3)	-3(3)	3(4)
C(25B)	72(3)	59(3)	61(4)	-30(3)	-4(3)	-13(3)
C(26B)	56(3)	56(3)	51(3)	-21(3)	-2(2)	-16(2)
C(27B)	47(3)	48(3)	53(3)	-27(2)	-6(2)	-9(2)
C(28B)	53(3)	49(3)	50(3)	-24(2)	-8(2)	-11(2)
C(29B)	46(3)	61(3)	68(3)	-38(3)	-3(3)	-13(2)
C(30B)	59(3)	49(3)	49(3)	-24(2)	-7(2)	-11(2)
C(31B)	49(3)	58(3)	49(3)	-27(3)	0(2)	-13(2)
C(32B)	57(3)	47(3)	50(3)	-24(2)	0(2)	-20(2)
C(33B)	59(3)	66(3)	61(3)	-24(3)	-7(3)	-18(3)
C(34B)	66(3)	56(3)	60(3)	-18(3)	-17(3)	-4(3)
C(35B)	50(3)	48(3)	48(3)	-20(2)	2(2)	-8(2)
C(36B)	45(3)	58(3)	45(3)	-19(2)	5(2)	-17(2)
C(37B)	44(3)	57(3)	62(3)	-21(3)	3(2)	-18(2)
C(38B)	46(3)	62(3)	59(3)	-25(3)	-3(2)	-14(2)
C(39B)	57(3)	68(3)	43(3)	-29(3)	-2(2)	-18(2)
O(1S)	329(14)	336(16)	229(11)	-138(12)	56(10)	-192(12)
C(1S)	220(13)	256(17)	152(11)	-101(11)	9(9)	-99(11)
C(2S)	262(14)	156(10)	213(15)	-97(10)	-22(11)	-69(10)
C(3S)	400(20)	166(12)	148(12)	-84(10)	1(13)	-81(13)
C(4S)	480(30)	210(17)	170(15)	30(14)	-65(17)	-128(19)
O(2S)	343(18)	410(20)	210(12)	-126(14)	-28(11)	-74(15)
C(5S)	283(18)	198(12)	188(14)	-125(11)	-79(15)	46(14)
C(6S)	209(15)	660(50)	184(18)	-260(30)	96(13)	-130(20)
C(7S)	310(20)	490(30)	300(30)	-320(30)	144(18)	-260(20)
C(8S)	249(16)	172(12)	292(19)	-157(14)	-133(15)	38(11)

Table S35. Hydrogen coordinates (x 10^4) and isotropic displacement parameters ($Å^2$ x 10^3) for k10187 (**2.20**).

	x	y	z	U(eq)
H(2AA)	947	8879	-345	48
H(3AA)	733	10454	-1109	49
H(6AA)	1324	6774	2131	54
H(7AA)	1603	5493	1936	61
H(8AA)	2365	5387	754	63
H(9AA)	2847	6563	-249	62
H(10B)	2569	7856	-75	53
H(13B)	2154	6165	4465	75
H(15B)	4432	5945	3103	75
H(17D)	731	7711	2890	87
H(17E)	1016	8060	3497	87
H(17F)	787	7135	3870	87
H(18D)	4377	4806	4437	141
H(18E)	3404	4738	4868	141
H(18F)	3974	5274	5054	141
H(19D)	3703	7850	1313	87
H(19E)	3930	6875	1387	87
H(19F)	4592	7153	1795	87
H(22B)	2968	10243	-657	59
H(23B)	4460	10355	-834	71
H(24B)	4809	11523	-755	79
H(25B)	3653	12597	-525	75
H(26B)	2157	12513	-375	61
H(29B)	717	14386	-2711	74
H(31B)	-171	14451	-515	71
H(33D)	839	12232	-2190	106
H(33E)	1816	12392	-2190	106
H(33F)	1102	13070	-2902	106
H(34D)	368	15750	-2578	128
H(34E)	102	15778	-1687	128
H(34F)	-648	15768	-2230	128
H(35D)	-217	13176	690	90
H(35E)	518	12312	724	90
H(35F)	-504	12492	460	90
H(36C)	3407	8927	3437	75
H(36D)	3261	8031	3492	75
H(37C)	3107	8246	4832	88
H(37D)	2358	7854	4661	88

H(38C)	1432	9044	4820	125
H(38D)	2166	9609	4409	125
H(36E)	3515	8637	3221	75
H(36F)	2990	7942	3868	75
H(37E)	3123	9499	3941	115
H(37F)	3251	8553	4697	115
H(38E)	1710	8651	4780	125
H(38F)	1724	9628	4596	125
H(39C)	906	9351	3601	90
H(39D)	1408	10125	3250	90
H(2BA)	4383	-279	2536	67
H(3BA)	3512	1199	1691	64
H(6BA)	5254	-1404	4698	79
H(7BA)	5105	-2775	5002	91
H(8BA)	5534	-3390	4046	88
H(9BA)	6198	-2639	2788	117
H(10A)	6415	-1285	2507	100
H(13A)	7721	-1362	6022	85
H(15A)	9367	-1696	4188	87
H(17A)	5834	84	4792	107
H(17B)	6261	-308	5698	107
H(17C)	5831	-886	5430	107
H(18A)	9347	-1927	6275	174
H(18B)	10009	-2088	5554	174
H(18C)	9404	-2750	6082	174
H(19A)	8901	-1115	2822	105
H(19B)	8100	-242	2536	105
H(19C)	7881	-1155	2772	105
H(22A)	3588	2076	3207	81
H(23A)	3208	2856	4046	100
H(24A)	3369	4262	3524	98
H(25A)	3879	4909	2183	75
H(26A)	4216	4160	1324	65
H(29A)	1467	4794	-302	65
H(31A)	3837	5397	-1218	61
H(33A)	2250	2687	964	93
H(33B)	1391	3493	849	93
H(33C)	2140	3215	1532	93
H(34A)	1602	6383	-1238	96
H(34B)	1757	5948	-1891	96
H(34C)	2486	6413	-1825	96
H(35A)	5228	3361	-153	75
H(35B)	5206	4034	241	75

H(35C)	5227	4346	-747	75
H(36A)	8166	2023	1723	60
H(36B)	8659	1021	1923	60
H(37A)	9165	2128	2489	66
H(37B)	9827	1350	2276	66
H(38A)	9464	294	3517	66
H(38B)	9517	1032	3811	66
H(39A)	8043	581	4095	64
H(39B)	7970	1607	3721	64
H(1SA)	9405	4547	6294	235
H(1SB)	8320	4925	6285	235
H(2SA)	9658	5863	5739	236
H(2SB)	8681	6117	6147	236
H(3SA)	8043	6851	4914	276
H(3SB)	9046	6733	4511	276
H(4SA)	7763	5886	4583	373
H(4SB)	8680	5911	4036	373
H(5SA)	3194	6532	5563	267
H(5SB)	2807	6830	6306	267
H(6SA)	2173	5802	5840	393
H(6SB)	1774	6114	6575	393
H(7SA)	2599	4497	6861	350
H(7SB)	2536	4889	7545	350
H(8SA)	4061	4476	7421	268
H(8SB)	4015	4660	6456	268

1,3-Bis[1-(2,6-dimethylphenylimino)ethyl]imidazol-2-ylidene palladium(II) allyl chloride (2.21).

Table S36. Crystal data and structure refinement for k11117 (**2.21**).

Identification code	k11117	
Empirical formula	C26 H31 Cl N4 Pd	
Formula weight	541.40	
Temperature	150(2) K	
Wavelength	0.71073 Å	
Crystal system	Triclinic	
Space group	P -1	
Unit cell dimensions	a = 10.6548(5) Å	a= 83.055(2)°.
	b = 11.1978(5) Å	b= 74.138(2)°.
	c = 11.2184(6) Å	g = 76.188(3)°.
Volume	1248.06(10) $Å^3$	
Z	2	
Density (calculated)	1.441 Mg/m^3	
Absorption coefficient	0.871 mm^{-1}	
F(000)	556	
Crystal size	0.24 x 0.10 x 0.06 mm^3	
Theta range for data collection	2.58 to 27.57°.	
Index ranges	-13<=h<=13, -14<=k<=14, -14<=l<=14	
Reflections collected	20251	
Independent reflections	5670 [R(int) = 0.0890]	
Completeness to theta = 27.57°	97.9 %	
Absorption correction	Semi-empirical from equivalents	
Max. and min. transmission	0.952 and 0.768	
Refinement method	Full-matrix least-squares on F^2	
Data / restraints / parameters	5670 / 0 / 300	
Goodness-of-fit on F^2	1.056	
Final R indices [I>2sigma(I)]	R1 = 0.0592, wR2 = 0.1323	
R indices (all data)	R1 = 0.1138, wR2 = 0.1633	
Extinction coefficient	0.0061(13)	
Largest diff. peak and hole	2.093 and -1.669 e.$Å^{-3}$	

Table S37. Atomic coordinates (x 10^4) and equivalent isotropic displacement parameters ($Å^2$ x 10^3) for k11117 (**2.21**). U(eq) is defined as one third of the trace of the orthogonalized U^{ij} tensor.

	x	y	z	U(eq)
Pd(1)	9377(1)	7785(1)	1781(1)	29(1)
Cl(1)	9546(2)	7841(2)	-372(1)	51(1)
N(4)	13998(4)	6775(4)	-192(4)	30(1)
N(1)	12237(4)	6193(4)	1212(4)	29(1)
N(2)	10817(4)	5110(4)	2146(4)	29(1)
C(13)	7250(7)	5607(6)	5207(7)	54(2)
C(1)	10902(5)	6284(5)	1705(5)	27(1)
N(3)	9651(4)	4065(4)	3769(4)	30(1)
C(11)	8735(6)	2240(5)	4464(5)	29(1)
C(15)	12200(6)	8449(5)	801(6)	38(1)
C(8)	6440(6)	3640(6)	5931(5)	44(2)
C(25)	7858(7)	8679(6)	3261(6)	46(2)
C(16)	14735(5)	7620(4)	-957(5)	26(1)
C(107)	14646(5)	7836(5)	-2187(5)	35(1)
C(26)	9047(6)	8132(6)	3666(5)	40(2)
C(7)	7408(6)	4250(5)	5201(5)	35(1)
C(20)	15426(6)	8582(6)	-2960(6)	47(2)
C(14)	12881(5)	7148(5)	543(5)	26(1)
C(17)	15611(5)	8085(5)	-518(5)	34(1)
C(10)	7732(6)	1688(5)	5213(5)	37(1)
C(18)	16380(6)	8829(5)	-1351(7)	46(2)
C(19)	16282(7)	9083(5)	-2548(7)	51(2)
C(12)	9985(6)	1504(5)	3676(5)	35(1)
C(2)	12958(6)	4978(5)	1320(6)	40(2)
C(9)	6595(6)	2386(6)	5938(5)	40(1)
C(6)	8565(5)	3528(5)	4443(5)	32(1)
C(22)	13741(7)	7251(7)	-2633(6)	53(2)
C(4)	9599(5)	4700(5)	2770(5)	30(1)
C(24)	7906(6)	9498(6)	2212(6)	46(2)
C(23)	15763(7)	7772(7)	787(6)	55(2)
C(3)	12058(6)	4317(5)	1907(6)	40(2)
C(5)	8546(6)	4987(6)	2084(6)	42(2)

Table S38. Bond lengths [Å] and angles [°] for k11117 (**2.21**).

Pd(1)-C(1)	2.031(5)
Pd(1)-C(26)	2.115(6)
Pd(1)-C(25)	2.130(6)
Pd(1)-C(24)	2.178(6)
Pd(1)-Cl(1)	2.3671(16)
N(4)-C(14)	1.257(6)
N(4)-C(16)	1.428(6)
N(1)-C(1)	1.362(6)
N(1)-C(2)	1.404(7)
N(1)-C(14)	1.432(6)
N(2)-C(1)	1.362(6)
N(2)-C(3)	1.383(7)
N(2)-C(4)	1.448(6)
C(13)-C(7)	1.490(8)
N(3)-C(4)	1.260(7)
N(3)-C(6)	1.419(6)
C(11)-C(10)	1.389(7)
C(11)-C(6)	1.408(8)
C(11)-C(12)	1.498(8)
C(15)-C(14)	1.488(7)
C(8)-C(9)	1.373(9)
C(8)-C(7)	1.393(8)
C(25)-C(24)	1.399(9)
C(25)-C(26)	1.436(9)
C(16)-C(17)	1.390(8)
C(16)-C(107)	1.396(8)
C(107)-C(20)	1.380(8)
C(107)-C(22)	1.501(9)
C(7)-C(6)	1.419(8)
C(20)-C(19)	1.377(10)
C(17)-C(18)	1.399(8)
C(17)-C(23)	1.507(9)
C(10)-C(9)	1.380(8)
C(18)-C(19)	1.365(10)
C(2)-C(3)	1.333(7)
C(4)-C(5)	1.481(8)
C(1)-Pd(1)-C(26)	98.0(2)
C(1)-Pd(1)-C(25)	133.7(2)
C(26)-Pd(1)-C(25)	39.6(2)

C(1)-Pd(1)-C(24)	166.7(2)
C(26)-Pd(1)-C(24)	70.0(2)
C(25)-Pd(1)-C(24)	37.9(2)
C(1)-Pd(1)-Cl(1)	92.89(16)
C(26)-Pd(1)-Cl(1)	167.98(18)
C(25)-Pd(1)-Cl(1)	131.6(2)
C(24)-Pd(1)-Cl(1)	98.54(18)
C(14)-N(4)-C(16)	121.2(4)
C(1)-N(1)-C(2)	111.6(4)
C(1)-N(1)-C(14)	126.9(4)
C(2)-N(1)-C(14)	121.2(4)
C(1)-N(2)-C(3)	111.6(4)
C(1)-N(2)-C(4)	125.7(4)
C(3)-N(2)-C(4)	122.6(4)
N(1)-C(1)-N(2)	103.2(4)
N(1)-C(1)-Pd(1)	129.3(4)
N(2)-C(1)-Pd(1)	127.4(4)
C(4)-N(3)-C(6)	120.6(5)
C(10)-C(11)-C(6)	118.9(5)
C(10)-C(11)-C(12)	121.8(5)
C(6)-C(11)-C(12)	119.3(5)
C(9)-C(8)-C(7)	121.8(6)
C(24)-C(25)-C(26)	120.7(6)
C(24)-C(25)-Pd(1)	73.0(3)
C(26)-C(25)-Pd(1)	69.7(3)
C(17)-C(16)-C(107)	122.3(5)
C(17)-C(16)-N(4)	120.2(5)
C(107)-C(16)-N(4)	117.1(5)
C(20)-C(107)-C(16)	117.6(6)
C(20)-C(107)-C(22)	122.2(6)
C(16)-C(107)-C(22)	120.1(5)
C(25)-C(26)-Pd(1)	70.8(3)
C(8)-C(7)-C(6)	117.5(5)
C(8)-C(7)-C(13)	121.8(5)
C(6)-C(7)-C(13)	120.7(5)
C(19)-C(20)-C(107)	121.6(6)
N(4)-C(14)-N(1)	114.8(4)
N(4)-C(14)-C(15)	127.1(5)
N(1)-C(14)-C(15)	118.1(4)
C(16)-C(17)-C(18)	117.2(6)
C(16)-C(17)-C(23)	121.7(5)
C(18)-C(17)-C(23)	121.1(6)
C(9)-C(10)-C(11)	120.7(5)

C(19)-C(18)-C(17)	121.5(6)
C(18)-C(19)-C(20)	119.8(6)
C(3)-C(2)-N(1)	105.9(5)
C(8)-C(9)-C(10)	120.4(5)
C(11)-C(6)-N(3)	118.2(5)
C(11)-C(6)-C(7)	120.7(5)
N(3)-C(6)-C(7)	120.6(5)
N(3)-C(4)-N(2)	114.1(5)
N(3)-C(4)-C(5)	130.2(5)
N(2)-C(4)-C(5)	115.5(5)
C(25)-C(24)-Pd(1)	69.2(3)
C(2)-C(3)-N(2)	107.6(5)

Symmetry transformations used to generate equivalent atoms:

Table S39. Anisotropic displacement parameters ($Å^2$ x 10^3) for k11117 (**2.21**). The anisotropic displacement factor exponent takes the form: $-2\pi^2$[$h^2a^{*2}U^{11}$ + ... + 2 h k a* b* U^{12}]

	U^{11}	U^{22}	U^{33}	U^{23}	U^{13}	U^{12}
Pd(1)	26(1)	25(1)	32(1)	-3(1)	-4(1)	-2(1)
Cl(1)	55(1)	66(1)	30(1)	-2(1)	-11(1)	-6(1)
N(4)	27(2)	21(2)	37(3)	4(2)	-2(2)	-7(2)
N(1)	24(2)	20(2)	37(3)	5(2)	-2(2)	-5(2)
N(2)	23(2)	16(2)	40(3)	2(2)	5(2)	-4(2)
C(13)	46(4)	40(4)	62(5)	-13(3)	7(3)	-5(3)
C(1)	19(3)	24(3)	33(3)	-1(2)	-2(2)	-1(2)
N(3)	23(2)	27(2)	37(3)	-2(2)	1(2)	-7(2)
C(11)	37(3)	32(3)	19(3)	8(2)	-9(2)	-10(2)
C(15)	31(3)	23(3)	50(4)	-4(3)	7(3)	-8(2)
C(8)	37(3)	55(4)	31(3)	-5(3)	9(3)	-13(3)
C(25)	43(4)	39(4)	44(4)	-20(3)	9(3)	-4(3)
C(16)	20(3)	16(2)	35(3)	-2(2)	4(2)	-1(2)
C(107)	26(3)	36(3)	36(3)	-2(3)	-5(2)	3(2)
C(26)	42(4)	45(4)	33(3)	-20(3)	1(3)	-12(3)
C(7)	33(3)	29(3)	36(3)	-2(2)	-2(3)	-3(2)
C(20)	40(4)	41(4)	38(4)	7(3)	7(3)	9(3)
C(14)	20(3)	24(3)	31(3)	3(2)	-4(2)	-3(2)
C(17)	27(3)	33(3)	40(3)	-7(3)	-1(2)	-8(2)
C(10)	46(4)	33(3)	33(3)	12(3)	-10(3)	-17(3)
C(18)	24(3)	33(3)	79(5)	-16(3)	2(3)	-13(3)
C(19)	41(4)	26(3)	64(5)	11(3)	16(3)	-4(3)
C(12)	41(3)	31(3)	28(3)	-1(2)	-2(3)	-6(3)
C(2)	23(3)	22(3)	63(4)	5(3)	4(3)	-1(2)
C(9)	36(3)	49(4)	31(3)	7(3)	2(3)	-20(3)
C(6)	30(3)	31(3)	34(3)	0(2)	-4(2)	-11(2)
C(22)	47(4)	72(5)	37(4)	-6(3)	-16(3)	-2(4)
C(4)	26(3)	20(3)	36(3)	-5(2)	5(2)	-4(2)
C(24)	46(4)	28(3)	50(4)	-5(3)	-9(3)	15(3)
C(23)	46(4)	77(5)	46(4)	-16(4)	-8(3)	-18(4)
C(3)	31(3)	17(3)	57(4)	8(3)	6(3)	0(2)
C(5)	36(3)	38(3)	49(4)	4(3)	-4(3)	-13(3)

Table S40. Hydrogen coordinates (x 10^4) and isotropic displacement parameters (Å^2 x 10^3) for k11117(**2.21**).

	x	y	z	U(eq)
H(13A)	7143	5993	4398	80
H(13B)	8043	5785	5369	80
H(13C)	6458	5937	5858	80
H(15A)	12842	8981	484	57
H(15B)	11842	8519	1699	57
H(15C)	11467	8704	392	57
H(6)	5650	4104	6438	53
H(10A)	8999	7414	4272	48
H(10B)	9542	8707	3841	48
H(12)	15372	8755	-3797	56
H(15)	7830	821	5225	44
H(16)	16983	9167	-1078	55
H(17)	16801	9602	-3094	62
H(12A)	10070	630	3952	53
H(12B)	10760	1786	3755	53
H(12C)	9943	1613	2807	53
H(19)	13896	4686	1033	48
H(20)	5916	1997	6445	48
H(22A)	13859	7438	-3528	79
H(22B)	12810	7578	-2198	79
H(22C)	13962	6357	-2463	79
H(24A)	8255	10240	2221	55
H(24B)	7135	9658	1839	55
H(23A)	15008	8262	1366	82
H(23B)	16599	7956	844	82
H(23C)	15783	6894	1000	82
H(26)	12237	3457	2123	48
H(5A)	7733	4752	2612	63
H(5B)	8855	4526	1331	63
H(5C)	8354	5872	1855	63
H(70)	7150(70)	8230(60)	3580(60)	60(20)

1,3-Bis[1-(2,6-dimethylphenylimino)ethyl]imidazol-2-ylidene zinc(II) chloride (2.23).

Table S41. Crystal data and structure refinement for k1053 (**2.23**).

Identification code	k1053	
Empirical formula	C25 H30 Cl6 N4 Zn	
Formula weight	664.60	
Temperature	150(1) K	
Wavelength	0.71073 Å	
Crystal system	Monoclinic	
Space group	P 21/c	
Unit cell dimensions	a = 9.0015(4) Å	a= 90°.
	b = 14.7205(7) Å	b= 94.816(2)°.
	c = 23.4112(8) Å	g = 90°.
Volume	3091.2(2) $Å^3$	
Z	4	
Density (calculated)	1.428 Mg/m^3	
Absorption coefficient	1.334 mm^{-1}	
F(000)	1360	
Crystal size	0.10 x 0.10 x 0.08 mm^3	
Theta range for data collection	2.66 to 27.47°.	
Index ranges	-11<=h<=11, -17<=k<=19, -30<=l<=30	
Reflections collected	19183	
Independent reflections	7045 [R(int) = 0.0726]	
Completeness to theta = 27.47°	99.4 %	
Absorption correction	Semi-empirical from equivalents	
Max. and min. transmission	0.909 and 0.740	
Refinement method	Full-matrix least-squares on F^2	
Data / restraints / parameters	7045 / 0 / 331	
Goodness-of-fit on F^2	1.017	
Final R indices [I>2sigma(I)]	R1 = 0.0603, wR2 = 0.1408	
R indices (all data)	R1 = 0.1487, wR2 = 0.1809	
Largest diff. peak and hole	0.785 and -0.728 e.$Å^{-3}$	

Table S42. Atomic coordinates (x 10^4) and equivalent isotropic displacement parameters ($Å^2$ x 10^3) for k1053 (**2.23**). U(eq) is defined as one third of the trace of the orthogonalized U^{ij} tensor.

	x	y	z	U(eq)
Zn(1)	4732(1)	8760(1)	2483(1)	32(1)
Cl(1)	5981(1)	7508(1)	2737(1)	44(1)
Cl(2)	2310(1)	8759(1)	2606(1)	40(1)
N(1)	5895(4)	10243(2)	1894(1)	28(1)
N(2)	5034(4)	9424(2)	1187(1)	31(1)
N(3)	5919(4)	9911(2)	2843(1)	30(1)
N(4)	4469(4)	8768(2)	312(1)	35(1)
C(1)	5213(5)	9432(3)	1763(2)	30(1)
C(2)	6141(5)	10737(3)	1398(2)	37(1)
C(3)	5604(5)	10219(3)	955(2)	37(1)
C(4)	6352(5)	10465(3)	2474(2)	31(1)
C(5)	7298(5)	11267(3)	2576(2)	38(1)
C(6)	6407(5)	10041(3)	3448(2)	32(1)
C(7)	7828(5)	9726(3)	3653(2)	39(1)
C(8)	8238(6)	9825(3)	4239(2)	45(1)
C(9)	7281(7)	10214(4)	4600(2)	52(1)
C(10)	5883(6)	10505(3)	4384(2)	46(1)
C(11)	5409(6)	10423(3)	3804(2)	38(1)
C(12)	8885(5)	9301(4)	3265(2)	48(1)
C(13)	3890(5)	10739(3)	3565(2)	46(1)
C(14)	4432(5)	8675(3)	847(2)	32(1)
C(15)	3885(6)	7897(3)	1181(2)	40(1)
C(16)	3971(6)	8042(3)	-67(2)	40(1)
C(17)	2462(7)	7921(3)	-225(2)	49(1)
C(18)	2059(8)	7254(4)	-633(2)	61(2)
C(19)	3109(10)	6748(4)	-877(2)	71(2)
C(20)	4582(9)	6887(4)	-722(2)	66(2)
C(21)	5084(7)	7546(3)	-314(2)	50(1)
C(22)	1288(6)	8502(4)	20(2)	64(2)
C(23)	6685(7)	7697(4)	-147(2)	68(2)
C(1S)	-820(6)	7727(4)	1786(2)	60(2)
Cl(3)	-224(2)	6891(1)	1304(1)	74(1)
Cl(4)	-1365(2)	8722(1)	1432(1)	93(1)
C(2S)	-1715(7)	9201(4)	-1678(3)	78(2)
Cl(5)	-1591(2)	9734(1)	-1014(1)	90(1)
Cl(6)	-337(2)	8345(1)	-1709(1)	77(1)

Table S43. Bond lengths [Å] and angles [°] for k1053 (**2.23**).

Zn(1)-C(1)	2.031(4)
Zn(1)-N(3)	2.139(3)
Zn(1)-Cl(1)	2.2152(13)
Zn(1)-Cl(2)	2.2234(13)
N(1)-C(1)	1.365(5)
N(1)-C(2)	1.403(5)
N(1)-C(4)	1.424(5)
N(2)-C(1)	1.345(5)
N(2)-C(3)	1.404(5)
N(2)-C(14)	1.439(5)
N(3)-C(4)	1.273(5)
N(3)-C(6)	1.459(5)
N(4)-C(14)	1.263(5)
N(4)-C(16)	1.437(6)
C(2)-C(3)	1.346(6)
C(4)-C(5)	1.463(6)
C(6)-C(11)	1.393(6)
C(6)-C(7)	1.407(6)
C(7)-C(8)	1.399(6)
C(7)-C(12)	1.506(6)
C(8)-C(9)	1.381(7)
C(9)-C(10)	1.384(7)
C(10)-C(11)	1.395(6)
C(11)-C(13)	1.507(7)
C(14)-C(15)	1.493(6)
C(16)-C(17)	1.389(7)
C(16)-C(21)	1.402(7)
C(17)-C(18)	1.396(7)
C(17)-C(22)	1.510(8)
C(18)-C(19)	1.366(9)
C(19)-C(20)	1.360(9)
C(20)-C(21)	1.409(8)
C(21)-C(23)	1.478(8)
C(1S)-Cl(4)	1.734(6)
C(1S)-Cl(3)	1.783(6)
C(2S)-Cl(5)	1.738(6)
C(2S)-Cl(6)	1.773(6)
C(1)-Zn(1)-N(3)	78.91(15)
C(1)-Zn(1)-Cl(1)	119.31(13)

N(3)-Zn(1)-Cl(1)	109.16(10)
C(1)-Zn(1)-Cl(2)	112.79(12)
N(3)-Zn(1)-Cl(2)	114.35(10)
Cl(1)-Zn(1)-Cl(2)	116.46(5)
C(1)-N(1)-C(2)	111.5(3)
C(1)-N(1)-C(4)	120.3(3)
C(2)-N(1)-C(4)	128.1(4)
C(1)-N(2)-C(3)	111.3(3)
C(1)-N(2)-C(14)	124.7(4)
C(3)-N(2)-C(14)	123.9(3)
C(4)-N(3)-C(6)	119.4(4)
C(4)-N(3)-Zn(1)	114.2(3)
C(6)-N(3)-Zn(1)	125.9(3)
C(14)-N(4)-C(16)	120.0(4)
N(2)-C(1)-N(1)	104.3(3)
N(2)-C(1)-Zn(1)	144.3(3)
N(1)-C(1)-Zn(1)	111.2(3)
C(3)-C(2)-N(1)	105.8(4)
C(2)-C(3)-N(2)	107.1(4)
N(3)-C(4)-N(1)	114.8(4)
N(3)-C(4)-C(5)	127.9(4)
N(1)-C(4)-C(5)	117.2(4)
C(11)-C(6)-C(7)	122.8(4)
C(11)-C(6)-N(3)	118.5(4)
C(7)-C(6)-N(3)	118.6(4)
C(8)-C(7)-C(6)	117.2(4)
C(8)-C(7)-C(12)	120.5(4)
C(6)-C(7)-C(12)	122.2(4)
C(9)-C(8)-C(7)	121.2(5)
C(8)-C(9)-C(10)	119.9(4)
C(9)-C(10)-C(11)	121.6(5)
C(6)-C(11)-C(10)	117.2(4)
C(6)-C(11)-C(13)	120.9(4)
C(10)-C(11)-C(13)	121.9(4)
N(4)-C(14)-N(2)	115.2(4)
N(4)-C(14)-C(15)	129.7(4)
N(2)-C(14)-C(15)	115.1(4)
C(17)-C(16)-C(21)	122.7(5)
C(17)-C(16)-N(4)	120.4(5)
C(21)-C(16)-N(4)	116.4(5)
C(16)-C(17)-C(18)	117.7(5)
C(16)-C(17)-C(22)	121.8(5)
C(18)-C(17)-C(22)	120.5(5)

C(19)-C(18)-C(17)	121.4(6)
C(20)-C(19)-C(18)	120.0(6)
C(19)-C(20)-C(21)	122.3(6)
C(16)-C(21)-C(20)	115.9(6)
C(16)-C(21)-C(23)	121.8(5)
C(20)-C(21)-C(23)	122.2(6)
Cl(4)-C(1S)-Cl(3)	111.6(3)
Cl(5)-C(2S)-Cl(6)	111.3(3)

Symmetry transformations used to generate equivalent atoms:

Table S44. Anisotropic displacement parameters (Å^{2}x 10^3) for k1053 (**2.23**). The anisotropic displacement factor exponent takes the form: $-2\pi^2$[h^2 $a^{*2}U^{11}$ + ... + 2 h k a* b* U^{12}]

	U^{11}	U^{22}	U^{33}	U^{23}	U^{13}	U^{12}
Zn(1)	44(1)	28(1)	25(1)	1(1)	6(1)	-3(1)
Cl(1)	51(1)	35(1)	47(1)	7(1)	4(1)	5(1)
Cl(2)	42(1)	43(1)	36(1)	1(1)	8(1)	-2(1)
N(1)	37(2)	25(2)	24(2)	1(2)	6(2)	2(2)
N(2)	44(2)	27(2)	23(2)	1(2)	6(2)	-3(2)
N(3)	36(2)	29(2)	26(2)	-7(2)	4(2)	1(2)
N(4)	54(3)	32(2)	19(2)	0(2)	5(2)	-4(2)
C(1)	30(3)	30(2)	30(2)	-1(2)	7(2)	1(2)
C(2)	51(3)	29(3)	31(2)	4(2)	6(2)	-6(2)
C(3)	54(3)	25(2)	30(2)	5(2)	5(2)	-3(2)
C(4)	38(3)	25(2)	31(2)	-1(2)	5(2)	3(2)
C(5)	47(3)	29(3)	36(3)	-4(2)	1(2)	1(2)
C(6)	48(3)	23(2)	27(2)	0(2)	8(2)	-4(2)
C(7)	41(3)	37(3)	39(3)	2(2)	2(2)	-4(2)
C(8)	48(3)	47(3)	38(3)	2(2)	-8(2)	-8(3)
C(9)	77(4)	47(3)	31(3)	-1(2)	-6(3)	-5(3)
C(10)	77(4)	33(3)	30(3)	-6(2)	22(3)	-2(3)
C(11)	52(3)	27(3)	38(3)	0(2)	11(2)	3(2)
C(12)	47(3)	57(3)	40(3)	-4(3)	3(2)	5(3)
C(13)	53(3)	43(3)	46(3)	-6(2)	18(2)	1(3)
C(14)	37(3)	21(2)	38(3)	0(2)	3(2)	2(2)
C(15)	65(4)	28(3)	27(2)	-2(2)	5(2)	-11(2)
C(16)	71(4)	29(3)	21(2)	7(2)	6(2)	-9(3)
C(17)	73(4)	39(3)	33(3)	4(2)	2(3)	-10(3)
C(18)	93(5)	50(4)	35(3)	-2(3)	-14(3)	-17(3)
C(19)	143(7)	47(4)	23(3)	-5(3)	-1(4)	-20(4)
C(20)	136(7)	33(3)	33(3)	-2(3)	19(3)	7(4)
C(21)	90(5)	34(3)	30(3)	6(2)	16(3)	-1(3)
C(22)	64(4)	73(4)	52(3)	-1(3)	-16(3)	-10(3)
C(23)	82(5)	63(4)	62(4)	-8(3)	24(3)	10(4)
C(1S)	52(4)	73(4)	55(3)	6(3)	4(3)	0(3)
Cl(3)	61(1)	77(1)	82(1)	1(1)	-8(1)	-2(1)
Cl(4)	84(1)	104(2)	96(1)	29(1)	27(1)	39(1)
C(2S)	79(5)	53(4)	96(5)	-14(4)	-30(4)	11(3)
Cl(5)	87(1)	92(1)	91(1)	-17(1)	5(1)	20(1)
Cl(6)	65(1)	76(1)	90(1)	-7(1)	14(1)	10(1)

Table S45. Hydrogen coordinates (x 10^4) and isotropic displacement parameters ($Å^2$ x 10^3) for k1053 (**2.23**).

	x	y	z	U(eq)
H(2A)	6594	11319	1380	44
H(3A)	5609	10363	560	44
H(5A)	7460	11380	2988	56
H(5B)	6808	11795	2387	56
H(5C)	8259	11163	2419	56
H(8A)	9191	9621	4392	54
H(9A)	7582	10281	4997	63
H(10A)	5231	10767	4637	55
H(12A)	9750	9055	3496	72
H(12B)	9216	9762	3001	72
H(12C)	8375	8810	3044	72
H(13A)	3351	10993	3875	70
H(13B)	3330	10224	3391	70
H(13C)	4000	11206	3273	70
H(15A)	3549	7407	918	60
H(15B)	3052	8099	1393	60
H(15C)	4695	7675	1451	60
H(18A)	1033	7149	-742	73
H(19A)	2811	6300	-1155	86
H(20A)	5297	6526	-894	80
H(22A)	1572	9143	0	96
H(22B)	1201	8333	420	96
H(22C)	327	8408	-202	96
H(23A)	7282	7319	-385	102
H(23B)	6906	7534	257	102
H(23C)	6928	8339	-201	102
H(1SA)	-1667	7484	1983	72
H(1SB)	4	7861	2081	72
H(2SA)	-1589	9658	-1981	94
H(2SB)	-2716	8926	-1753	94

1,3-Bis[(2,4,6-trimethylphenylimino)benzyl]benzimidazole-2-*N*,*N*-bis(trimethylsilyl)amine (3.7)

Table S46. Crystal data and structure refinement for jameel_0m (**3.7**).

Identification code	jameel_0m	
Empirical formula	C54 H64 N5 Si2	
Formula weight	839.28	
Temperature	293(2) K	
Wavelength	0.71073 Å	
Crystal system	Monoclinic	
Space group	P 1 21/n 1	
Unit cell dimensions	a = 9.4484(15) Å	a= 90°.
	b = 38.540(6) Å	b= 107.325(3)°.
	c = 13.913(2) Å	g = 90°.
Volume	4836.3(13) $Å^3$	
Z	4	
Density (calculated)	1.153 Mg/m^3	
Absorption coefficient	0.114 mm^{-1}	
F(000)	1804	
Crystal size	0.755 x 0.362 x 0.216 mm^3	
Theta range for data collection	1.86 to 26.83°.	
Index ranges	-12<=h<=7, -44<=k<=48, -16<=l<=17	
Reflections collected	50103	
Independent reflections	10267 [R(int) = 0.0612]	
Completeness to theta = 26.83°	99.1 %	
Absorption correction	Numerical	
Max. and min. transmission	0.8799 and 0.6129	
Refinement method	Full-matrix least-squares on F^2	
Data / restraints / parameters	10267 / 0 / 562	
Goodness-of-fit on F^2	1.042	
Final R indices [I>2sigma(I)]	R1 = 0.0588, wR2 = 0.1483	
R indices (all data)	R1 = 0.0861, wR2 = 0.1643	
Largest diff. peak and hole	0.594 and -0.553 e.$Å^{-3}$	

Table S47. Atomic coordinates (x 10^4) and equivalent isotropic displacement parameters (Å^2 x 10^3) for jameel_0m (**3.7**). U(eq) is defined as one third of the trace of the orthogonalized U^{ij} tensor.

	x	y	z	U(eq)
Si(1)	5979(1)	5467(1)	8400(1)	21(1)
Si(2)	9241(1)	5672(1)	8835(1)	21(1)
N(1)	7384(2)	5787(1)	8712(1)	18(1)
N(2)	7968(2)	6257(1)	9974(1)	17(1)
N(3)	7290(2)	6412(1)	8317(1)	19(1)
N(4)	6502(2)	5946(1)	10696(1)	19(1)
N(5)	7117(2)	6563(1)	6686(1)	20(1)
C(2)	8490(2)	6620(1)	8829(2)	18(1)
C(37)	5433(3)	6985(1)	5597(2)	24(1)
C(32)	6260(2)	6678(1)	5708(2)	20(1)
C(8)	7564(2)	6166(1)	10824(2)	18(1)
C(7)	8897(2)	6534(1)	9852(2)	17(1)
C(15)	5893(2)	5868(1)	11493(2)	20(1)
C(5)	10805(2)	6965(1)	10166(2)	22(1)
C(16)	6509(3)	5619(1)	12230(2)	22(1)
C(20)	4539(3)	6029(1)	11452(2)	22(1)
C(1)	7024(2)	6133(1)	8979(2)	17(1)
C(18)	4455(3)	5703(1)	12932(2)	26(1)
C(9)	8377(2)	6338(1)	11792(2)	21(1)
C(17)	5776(3)	5545(1)	12946(2)	24(1)
C(10)	9741(3)	6212(1)	12389(2)	29(1)
C(31)	4044(3)	6209(1)	6216(2)	31(1)
C(38)	5418(3)	7207(1)	6490(2)	29(1)
C(25)	6465(2)	6449(1)	7310(2)	18(1)
C(3)	9216(2)	6878(1)	8467(2)	21(1)
C(26)	4830(2)	6388(1)	7076(2)	20(1)
C(6)	10071(2)	6705(1)	10530(2)	20(1)
C(42)	5693(3)	5326(1)	7066(2)	35(1)
C(27)	4071(3)	6538(1)	7687(2)	24(1)
C(23)	3697(3)	5621(1)	13725(2)	36(1)
C(45)	10166(3)	5988(1)	8217(3)	47(1)
C(4)	10382(2)	7052(1)	9160(2)	22(1)
C(33)	6373(3)	6492(1)	4866(2)	25(1)
C(13)	8585(3)	6807(1)	12964(2)	49(1)
C(41)	4156(2)	5629(1)	8476(2)	26(1)
C(22)	3852(3)	6293(1)	10645(2)	29(1)

C(19)	3849(3)	5944(1)	12172(2)	25(1)
C(3S)	3752(3)	7600(1)	7(2)	32(1)
C(14)	7801(3)	6635(1)	12092(2)	34(1)
C(36)	4627(3)	7087(1)	4624(2)	28(1)
C(6S)	6685(3)	7397(1)	624(3)	62(1)
C(8S)	4981(4)	314(1)	9517(3)	54(1)
C(29)	1760(3)	6346(1)	6558(2)	47(1)
C(39)	7325(3)	6173(1)	4990(2)	33(1)
C(30)	2504(3)	6188(1)	5965(2)	45(1)
C(28)	2540(3)	6518(1)	7426(2)	36(1)
C(34)	5552(3)	6609(1)	3913(2)	30(1)
C(35)	4658(3)	6901(1)	3778(2)	32(1)
C(24)	7903(3)	5424(1)	12263(2)	29(1)
C(11)	10520(3)	6389(1)	13252(2)	37(1)
C(12)	9944(3)	6685(1)	13537(2)	45(1)
C(43)	6463(3)	5090(1)	9281(2)	34(1)
C(44)	10356(3)	5639(1)	10182(2)	47(1)
C(2S)	4711(4)	7754(1)	828(2)	45(1)
C(9S)	6220(4)	102(1)	9728(3)	52(1)
C(40)	3760(4)	7018(1)	2734(2)	48(1)
C(7S)	3765(4)	210(1)	9789(3)	51(1)
C(5S)	5729(3)	7249(1)	-196(3)	63(1)
C(46)	9340(3)	5249(1)	8216(3)	46(1)
C(1S)	6183(4)	7653(1)	1135(3)	68(1)
C(4S)	4253(3)	7349(1)	-508(3)	54(1)

Table S48. Bond lengths [Å] and angles [°] for jameel_0m (**3.7**).

Si(1)-N(1)	1.769(2)
Si(1)-C(41)	1.865(2)
Si(1)-C(43)	1.866(3)
Si(1)-C(42)	1.874(3)
Si(2)-N(1)	1.7674(19)
Si(2)-C(45)	1.851(3)
Si(2)-C(46)	1.859(3)
Si(2)-C(44)	1.861(3)
N(1)-C(1)	1.451(3)
N(2)-C(8)	1.391(3)
N(2)-C(7)	1.425(3)
N(2)-C(1)	1.486(3)
N(3)-C(25)	1.393(3)
N(3)-C(2)	1.397(3)
N(3)-C(1)	1.487(3)
N(4)-C(8)	1.284(3)
N(4)-C(15)	1.426(3)
N(5)-C(25)	1.281(3)
N(5)-C(32)	1.431(3)
C(2)-C(3)	1.386(3)
C(2)-C(7)	1.398(3)
C(37)-C(36)	1.398(3)
C(37)-C(32)	1.399(3)
C(37)-C(38)	1.514(4)
C(32)-C(33)	1.405(3)
C(8)-C(9)	1.492(3)
C(7)-C(6)	1.389(3)
C(15)-C(16)	1.398(3)
C(15)-C(20)	1.409(3)
C(5)-C(4)	1.378(3)
C(5)-C(6)	1.396(3)
C(16)-C(17)	1.401(3)
C(16)-C(24)	1.506(3)
C(20)-C(19)	1.387(3)
C(20)-C(22)	1.511(4)
C(18)-C(17)	1.385(4)
C(18)-C(19)	1.394(4)
C(18)-C(23)	1.517(3)
C(9)-C(14)	1.383(4)
C(9)-C(10)	1.396(3)

C(10)-C(11)	1.386(4)
C(31)-C(26)	1.387(3)
C(31)-C(30)	1.394(4)
C(25)-C(26)	1.500(3)
C(3)-C(4)	1.401(3)
C(26)-C(27)	1.391(3)
C(27)-C(28)	1.384(3)
C(33)-C(34)	1.396(3)
C(33)-C(39)	1.503(4)
C(13)-C(12)	1.377(5)
C(13)-C(14)	1.388(4)
C(3S)-C(2S)	1.364(4)
C(3S)-C(4S)	1.369(4)
C(36)-C(35)	1.385(4)
C(6S)-C(5S)	1.353(5)
C(6S)-C(1S)	1.379(6)
C(8S)-C(7S)	1.371(5)
C(8S)-C(9S)	1.384(5)
C(29)-C(30)	1.375(5)
C(29)-C(28)	1.383(5)
C(34)-C(35)	1.386(4)
C(35)-C(40)	1.517(4)
C(11)-C(12)	1.375(5)
C(2S)-C(1S)	1.385(5)
C(9S)-C(7S)#1	1.378(5)
C(7S)-C(9S)#1	1.378(5)
C(5S)-C(4S)	1.386(4)
N(1)-Si(1)-C(41)	113.00(11)
N(1)-Si(1)-C(43)	111.22(11)
C(41)-Si(1)-C(43)	105.82(12)
N(1)-Si(1)-C(42)	108.72(11)
C(41)-Si(1)-C(42)	106.86(13)
C(43)-Si(1)-C(42)	111.14(14)
N(1)-Si(2)-C(45)	112.53(11)
N(1)-Si(2)-C(46)	111.05(12)
C(45)-Si(2)-C(46)	105.38(15)
N(1)-Si(2)-C(44)	111.28(11)
C(45)-Si(2)-C(44)	107.96(17)
C(46)-Si(2)-C(44)	108.38(16)
C(1)-N(1)-Si(2)	120.38(14)
C(1)-N(1)-Si(1)	119.18(14)
Si(2)-N(1)-Si(1)	120.04(11)

C(8)-N(2)-C(7)	128.77(19)
C(8)-N(2)-C(1)	118.03(18)
C(7)-N(2)-C(1)	110.53(17)
C(25)-N(3)-C(2)	125.43(19)
C(25)-N(3)-C(1)	123.45(18)
C(2)-N(3)-C(1)	111.08(18)
C(8)-N(4)-C(15)	120.8(2)
C(25)-N(5)-C(32)	119.95(19)
C(3)-C(2)-N(3)	129.8(2)
C(3)-C(2)-C(7)	121.5(2)
N(3)-C(2)-C(7)	108.69(19)
C(36)-C(37)-C(32)	118.1(2)
C(36)-C(37)-C(38)	120.0(2)
C(32)-C(37)-C(38)	122.0(2)
C(37)-C(32)-C(33)	121.2(2)
C(37)-C(32)-N(5)	120.4(2)
C(33)-C(32)-N(5)	118.2(2)
N(4)-C(8)-N(2)	116.7(2)
N(4)-C(8)-C(9)	126.1(2)
N(2)-C(8)-C(9)	117.19(19)
C(6)-C(7)-C(2)	120.2(2)
C(6)-C(7)-N(2)	132.0(2)
C(2)-C(7)-N(2)	107.77(19)
C(16)-C(15)-C(20)	120.5(2)
C(16)-C(15)-N(4)	122.7(2)
C(20)-C(15)-N(4)	116.5(2)
C(4)-C(5)-C(6)	121.3(2)
C(15)-C(16)-C(17)	118.4(2)
C(15)-C(16)-C(24)	122.3(2)
C(17)-C(16)-C(24)	119.4(2)
C(19)-C(20)-C(15)	118.8(2)
C(19)-C(20)-C(22)	120.4(2)
C(15)-C(20)-C(22)	120.8(2)
N(1)-C(1)-N(2)	114.49(18)
N(1)-C(1)-N(3)	114.28(18)
N(2)-C(1)-N(3)	100.27(17)
C(17)-C(18)-C(19)	117.9(2)
C(17)-C(18)-C(23)	121.1(2)
C(19)-C(18)-C(23)	121.0(2)
C(14)-C(9)-C(10)	119.0(2)
C(14)-C(9)-C(8)	119.8(2)
C(10)-C(9)-C(8)	121.2(2)
C(18)-C(17)-C(16)	122.3(2)

C(11)-C(10)-C(9)	120.1(3)
C(26)-C(31)-C(30)	119.7(3)
N(5)-C(25)-N(3)	118.6(2)
N(5)-C(25)-C(26)	125.4(2)
N(3)-C(25)-C(26)	115.65(19)
C(2)-C(3)-C(4)	117.9(2)
C(31)-C(26)-C(27)	119.4(2)
C(31)-C(26)-C(25)	121.2(2)
C(27)-C(26)-C(25)	119.1(2)
C(7)-C(6)-C(5)	118.3(2)
C(28)-C(27)-C(26)	120.4(3)
C(5)-C(4)-C(3)	120.8(2)
C(34)-C(33)-C(32)	118.0(2)
C(34)-C(33)-C(39)	121.2(2)
C(32)-C(33)-C(39)	120.9(2)
C(12)-C(13)-C(14)	120.4(3)
C(20)-C(19)-C(18)	122.1(2)
C(2S)-C(3S)-C(4S)	119.9(3)
C(9)-C(14)-C(13)	120.2(3)
C(35)-C(36)-C(37)	122.2(3)
C(5S)-C(6S)-C(1S)	119.4(3)
C(7S)-C(8S)-C(9S)	119.8(4)
C(30)-C(29)-C(28)	120.1(2)
C(29)-C(30)-C(31)	120.4(3)
C(29)-C(28)-C(27)	120.0(3)
C(35)-C(34)-C(33)	122.3(2)
C(36)-C(35)-C(34)	118.1(2)
C(36)-C(35)-C(40)	120.8(3)
C(34)-C(35)-C(40)	121.1(3)
C(12)-C(11)-C(10)	120.3(3)
C(11)-C(12)-C(13)	119.8(3)
C(3S)-C(2S)-C(1S)	119.4(3)
C(7S)#1-C(9S)-C(8S)	120.2(3)
C(8S)-C(7S)-C(9S)#1	120.0(3)
C(6S)-C(5S)-C(4S)	120.2(3)
C(6S)-C(1S)-C(2S)	120.7(3)
C(3S)-C(4S)-C(5S)	120.4(3)

Symmetry transformations used to generate equivalent atoms:
#1 -x+1,-y,-z+2

Table S49. Anisotropic displacement parameters ($Å^2 \times 10^3$) for jameel_0m (**3.7**). The anisotropic displacement factor exponent takes the form: $-2\pi^2[h^2a^{*2}U^{11} + ... + 2 h k a^* b^* U^{12}]$

	U^{11}	U^{22}	U^{33}	U^{23}	U^{13}	U^{12}
Si(1)	22(1)	17(1)	26(1)	0(1)	9(1)	-3(1)
Si(2)	20(1)	22(1)	25(1)	3(1)	10(1)	2(1)
N(1)	19(1)	17(1)	19(1)	-1(1)	7(1)	-1(1)
N(2)	18(1)	17(1)	15(1)	0(1)	4(1)	-3(1)
N(3)	19(1)	20(1)	14(1)	2(1)	2(1)	-5(1)
N(4)	20(1)	21(1)	19(1)	1(1)	8(1)	-1(1)
N(5)	21(1)	23(1)	14(1)	0(1)	4(1)	-2(1)
C(2)	16(1)	18(1)	19(1)	0(1)	4(1)	0(1)
C(37)	24(1)	25(1)	21(1)	3(1)	6(1)	-6(1)
C(32)	20(1)	23(1)	16(1)	3(1)	4(1)	-6(1)
C(8)	19(1)	18(1)	17(1)	3(1)	6(1)	6(1)
C(7)	17(1)	14(1)	19(1)	1(1)	7(1)	2(1)
C(15)	21(1)	21(1)	19(1)	-4(1)	8(1)	-4(1)
C(5)	19(1)	22(1)	23(1)	-3(1)	3(1)	-3(1)
C(16)	24(1)	22(1)	21(1)	-3(1)	9(1)	-3(1)
C(20)	22(1)	22(1)	24(1)	-5(1)	8(1)	-3(1)
C(1)	18(1)	18(1)	14(1)	2(1)	5(1)	-3(1)
C(18)	32(1)	28(1)	21(1)	-6(1)	14(1)	-11(1)
C(9)	24(1)	24(1)	17(1)	2(1)	9(1)	-5(1)
C(17)	32(1)	21(1)	19(1)	-1(1)	9(1)	-7(1)
C(10)	32(1)	29(2)	22(1)	6(1)	3(1)	-1(1)
C(31)	35(1)	36(2)	18(1)	4(1)	4(1)	-17(1)
C(38)	35(1)	24(1)	27(1)	1(1)	7(1)	0(1)
C(25)	21(1)	16(1)	17(1)	-1(1)	4(1)	-1(1)
C(3)	21(1)	21(1)	19(1)	3(1)	5(1)	-2(1)
C(26)	20(1)	19(1)	17(1)	6(1)	2(1)	-3(1)
C(6)	20(1)	22(1)	16(1)	0(1)	3(1)	1(1)
C(42)	40(2)	31(2)	33(2)	-11(1)	12(1)	-9(1)
C(27)	23(1)	23(1)	28(1)	7(1)	7(1)	1(1)
C(23)	43(2)	41(2)	34(2)	-6(1)	25(1)	-9(1)
C(45)	33(2)	41(2)	77(2)	24(2)	34(2)	13(1)
C(4)	22(1)	20(1)	26(1)	2(1)	8(1)	-4(1)
C(33)	23(1)	33(2)	18(1)	-3(1)	7(1)	-9(1)
C(13)	42(2)	59(2)	47(2)	-32(2)	17(1)	-6(2)
C(41)	20(1)	24(1)	31(1)	2(1)	7(1)	-5(1)

C(22)	23(1)	33(2)	33(2)	2(1)	11(1)	7(1)
C(19)	23(1)	29(1)	29(1)	-8(1)	14(1)	-4(1)
C(3S)	27(1)	32(2)	38(2)	3(1)	10(1)	-4(1)
C(14)	25(1)	44(2)	35(2)	-16(1)	10(1)	-2(1)
C(36)	28(1)	26(1)	25(1)	7(1)	2(1)	-5(1)
C(6S)	26(2)	38(2)	105(3)	0(2)	-7(2)	-4(1)
C(8S)	64(2)	55(2)	45(2)	-4(2)	19(2)	0(2)
C(29)	19(1)	71(2)	44(2)	35(2)	0(1)	-10(1)
C(39)	30(1)	41(2)	28(1)	-12(1)	7(1)	0(1)
C(30)	37(2)	64(2)	24(2)	15(1)	-5(1)	-30(2)
C(28)	25(1)	42(2)	45(2)	22(1)	15(1)	7(1)
C(34)	34(1)	39(2)	15(1)	-2(1)	6(1)	-13(1)
C(35)	31(1)	39(2)	20(1)	8(1)	-1(1)	-13(1)
C(24)	33(1)	30(2)	28(1)	8(1)	12(1)	6(1)
C(11)	38(2)	49(2)	20(1)	5(1)	-1(1)	-7(1)
C(12)	47(2)	64(2)	24(2)	-17(2)	11(1)	-20(2)
C(43)	30(1)	26(2)	49(2)	12(1)	17(1)	3(1)
C(44)	34(2)	65(2)	38(2)	1(2)	3(1)	28(2)
C(2S)	50(2)	52(2)	35(2)	-8(2)	14(1)	-6(2)
C(9S)	46(2)	72(3)	43(2)	-12(2)	21(2)	-10(2)
C(40)	57(2)	53(2)	23(2)	11(1)	-5(1)	-11(2)
C(7S)	45(2)	68(3)	40(2)	-10(2)	11(2)	10(2)
C(5S)	31(2)	44(2)	107(3)	-30(2)	8(2)	1(2)
C(46)	38(2)	42(2)	68(2)	-17(2)	28(2)	-1(1)
C(1S)	56(2)	66(3)	60(2)	-10(2)	-18(2)	-12(2)
C(4S)	32(2)	51(2)	68(2)	-26(2)	-1(2)	0(1)

Table S50. Hydrogen coordinates (x 10^4) and isotropic displacement parameters (Å^2 x 10^3) for jameel_0m (**3.7**).

	x	y	z	U(eq)
H(5)	11594	7081	10610	26
H(17)	6193	5384	13449	29
H(10)	10128	6009	12207	35
H(31)	4543	6104	5810	37
H(38A)	6019	7101	7099	44
H(38B)	4419	7229	6518	44
H(38C)	5805	7433	6420	44
H(3)	8937	6934	7786	25
H(6)	10361	6648	11210	24
H(42A)	6610	5240	6995	52
H(42B)	5363	5520	6624	52
H(42C)	4958	5146	6896	52
H(27)	4595	6651	8275	29
H(23A)	4269	5452	14186	54
H(23B)	2724	5531	13406	54
H(23C)	3619	5829	14086	54
H(45A)	10156	6213	8509	70
H(45B)	9649	5997	7510	70
H(45C)	11172	5917	8313	70
H(4)	10877	7229	8938	26
H(13)	8189	7006	13162	58
H(41A)	3849	5824	8034	38
H(41B)	4250	5698	9155	38
H(41C)	3430	5448	8279	38
H(22A)	4472	6322	10215	44
H(22B)	3758	6511	10953	44
H(22C)	2889	6214	10253	44
H(19)	2954	6050	12146	31
H(3S)	2759	7665	-202	39
H(14)	6884	6719	11708	41
H(36)	4050	7286	4541	33
H(6S)	7672	7327	840	75
H(8S)	4974	525	9193	65
H(29)	730	6336	6377	56
H(39A)	7802	6133	5693	50
H(39B)	8063	6206	4650	50

H(39C)	6718	5977	4707	50
H(30)	1977	6067	5392	54
H(28)	2037	6622	7832	44
H(34)	5607	6486	3349	35
H(24A)	8141	5265	12821	44
H(24B)	8704	5585	12339	44
H(24C)	7753	5296	11648	44
H(11)	11438	6306	13640	45
H(12)	10472	6804	14115	54
H(43A)	7398	4996	9272	50
H(43B)	5708	4916	9074	50
H(43C)	6530	5166	9950	50
H(44A)	9899	5476	10518	71
H(44B)	10406	5863	10496	71
H(44C)	11340	5562	10227	71
H(2S)	4379	7926	1177	54
H(40A)	3914	6860	2242	72
H(40B)	4070	7246	2608	72
H(40C)	2727	7022	2691	72
H(5S)	6062	7079	-552	76
H(46A)	8877	5073	8507	69
H(46B)	10359	5189	8313	69
H(46C)	8834	5267	7508	69
H(1S)	6841	7758	1693	82
H(4S)	3600	7245	-1070	65
H(1)	5940(30)	6135(6)	8980(17)	13(6)
H(9S)	2920(40)	359(9)	9630(30)	52(10)
H(7S)	7090(40)	175(10)	9530(30)	63(11)

1-borontrifluoride-3-(2,4,6-Trimethylphenylimino)benzyl) benzimidazole (3.8).

Table S51. Crystal data and structure refinement for k11112 (**3.8**).

Identification code	k11112	
Empirical formula	C26 H24 B F3 N3	
Formula weight	446.30	
Temperature	150(1) K	
Wavelength	0.71073 Å	
Crystal system	Monoclinic	
Space group	P 21/a	
Unit cell dimensions	a = 7.7142(3) Å	a= 90°.
	b = 35.7493(11) Å	b= 108.744(2)°.
	c = 8.6726(3) Å	g = 90°.
Volume	2264.86(14) $Å^3$	
Z	4	
Density (calculated)	1.309 Mg/m^3	
Absorption coefficient	0.094 mm^{-1}	
F(000)	932	
Crystal size	0.16 x 0.14 x 0.12 mm^3	
Theta range for data collection	2.73 to 25.29°.	
Index ranges	-9<=h<=9, -42<=k<=42, -10<=l<=10	
Reflections collected	11467	
Independent reflections	4049 [R(int) = 0.0582]	
Completeness to theta = 25.29°	98.1 %	
Absorption correction	Semi-empirical from equivalents	
Max. and min. transmission	0.989 and 0.870	
Refinement method	Full-matrix least-squares on F^2	
Data / restraints / parameters	4049 / 0 / 314	
Goodness-of-fit on F^2	1.022	
Final R indices [I>2sigma(I)]	R1 = 0.0518, wR2 = 0.1230	
R indices (all data)	R1 = 0.1121, wR2 = 0.1580	
Extinction coefficient	0.008(2)	
Largest diff. peak and hole	0.222 and -0.214 e.$Å^{-3}$	

Table S52. Atomic coordinates (x 10^4) and equivalent isotropic displacement parameters ($Å^2$ x 10^3) for k11112 (**3.8**). U(eq) is defined as one third of the trace of the orthogonalized U^{ij} tensor.

	x	y	z	U(eq)
F(3)	717(2)	7186(1)	3341(2)	53(1)
F(2)	3480(2)	7007(1)	3192(2)	59(1)
F(1)	870(3)	6794(1)	1326(2)	60(1)
N(2)	1604(3)	8033(1)	464(2)	35(1)
N(1)	1668(3)	7441(1)	1207(2)	38(1)
N(3)	1124(3)	8604(1)	-812(3)	37(1)
C(10)	2901(4)	8516(1)	3516(3)	42(1)
C(9)	1418(4)	8584(1)	2128(3)	35(1)
C(17)	-761(4)	9542(1)	-2137(3)	40(1)
C(16)	-663(4)	9159(1)	-1838(3)	38(1)
C(14)	-55(4)	8793(1)	2238(3)	45(1)
C(15)	1010(4)	9003(1)	-931(3)	35(1)
C(2S)	9292(4)	5337(1)	4312(4)	52(1)
C(12)	1421(5)	8863(1)	5103(4)	57(1)
C(22)	643(4)	10185(1)	-1957(4)	49(1)
C(18)	779(4)	9771(1)	-1579(3)	38(1)
C(20)	2592(4)	9221(1)	-368(3)	35(1)
C(19)	2418(4)	9604(1)	-711(3)	39(1)
C(1)	1457(4)	7789(1)	1606(3)	36(1)
C(8)	1375(4)	8430(1)	521(3)	35(1)
C(3S)	8861(4)	5203(1)	5619(4)	52(1)
C(3)	2225(4)	7159(1)	-1283(3)	45(1)
C(1S)	10436(4)	5136(1)	3690(4)	52(1)
C(4)	2460(4)	7256(1)	-2727(3)	49(1)
C(11)	2896(5)	8657(1)	5004(3)	50(1)
C(2)	1961(4)	7449(1)	-308(3)	37(1)
C(5)	2417(4)	7629(1)	-3217(3)	50(1)
C(6)	2155(4)	7920(1)	-2269(3)	44(1)
C(7)	1927(4)	7822(1)	-797(3)	35(1)
C(21)	4429(4)	9051(1)	491(3)	47(1)
C(13)	-52(5)	8927(1)	3726(4)	53(1)
C(23)	-2330(4)	8915(1)	-2530(4)	53(1)
B(1)	1695(5)	7087(1)	2319(4)	43(1)

Table S53. Bond lengths [Å] and angles [°] for k11112 (**3.8**).

F(3)-B(1)	1.382(4)
F(2)-B(1)	1.372(4)
F(1)-B(1)	1.375(3)
N(2)-C(1)	1.353(3)
N(2)-C(7)	1.415(3)
N(2)-C(8)	1.434(3)
N(1)-C(1)	1.313(3)
N(1)-C(2)	1.403(3)
N(1)-B(1)	1.588(4)
N(3)-C(8)	1.271(3)
N(3)-C(15)	1.430(3)
C(10)-C(11)	1.387(4)
C(10)-C(9)	1.389(4)
C(9)-C(14)	1.390(4)
C(9)-C(8)	1.488(3)
C(17)-C(16)	1.391(3)
C(17)-C(18)	1.394(4)
C(16)-C(15)	1.395(4)
C(16)-C(23)	1.510(4)
C(14)-C(13)	1.376(4)
C(15)-C(20)	1.398(3)
C(2S)-C(3S)	1.368(4)
C(2S)-C(1S)	1.376(4)
C(12)-C(13)	1.378(4)
C(12)-C(11)	1.380(4)
C(22)-C(18)	1.515(3)
C(18)-C(19)	1.381(4)
C(20)-C(19)	1.397(3)
C(20)-C(21)	1.502(4)
C(3S)-C(1S)#1	1.383(4)
C(3)-C(4)	1.367(4)
C(3)-C(2)	1.394(3)
C(1S)-C(3S)#1	1.383(4)
C(4)-C(5)	1.398(4)
C(2)-C(7)	1.398(3)
C(5)-C(6)	1.379(3)
C(6)-C(7)	1.388(3)
C(1)-N(2)-C(7)	107.4(2)
C(1)-N(2)-C(8)	125.0(2)

C(7)-N(2)-C(8)	127.5(2)
C(1)-N(1)-C(2)	107.4(2)
C(1)-N(1)-B(1)	124.9(2)
C(2)-N(1)-B(1)	127.6(2)
C(8)-N(3)-C(15)	122.7(2)
C(11)-C(10)-C(9)	119.7(3)
C(10)-C(9)-C(14)	119.9(3)
C(10)-C(9)-C(8)	120.8(2)
C(14)-C(9)-C(8)	119.3(2)
C(16)-C(17)-C(18)	121.5(3)
C(17)-C(16)-C(15)	119.0(3)
C(17)-C(16)-C(23)	120.4(3)
C(15)-C(16)-C(23)	120.5(2)
C(13)-C(14)-C(9)	119.8(3)
C(16)-C(15)-C(20)	121.2(2)
C(16)-C(15)-N(3)	117.7(2)
C(20)-C(15)-N(3)	120.4(2)
C(3S)-C(2S)-C(1S)	119.9(3)
C(13)-C(12)-C(11)	120.1(3)
C(19)-C(18)-C(17)	117.7(2)
C(19)-C(18)-C(22)	121.9(2)
C(17)-C(18)-C(22)	120.4(3)
C(19)-C(20)-C(15)	117.4(2)
C(19)-C(20)-C(21)	120.9(2)
C(15)-C(20)-C(21)	121.7(2)
C(18)-C(19)-C(20)	123.1(2)
N(1)-C(1)-N(2)	111.8(2)
N(3)-C(8)-N(2)	115.8(2)
N(3)-C(8)-C(9)	128.6(2)
N(2)-C(8)-C(9)	115.5(2)
C(2S)-C(3S)-C(1S)#1	120.1(3)
C(4)-C(3)-C(2)	117.0(2)
C(2S)-C(1S)-C(3S)#1	120.0(3)
C(3)-C(4)-C(5)	121.6(3)
C(12)-C(11)-C(10)	120.0(3)
C(3)-C(2)-C(7)	121.3(2)
C(3)-C(2)-N(1)	130.7(2)
C(7)-C(2)-N(1)	108.0(2)
C(6)-C(5)-C(4)	122.1(3)
C(5)-C(6)-C(7)	116.5(2)
C(6)-C(7)-C(2)	121.5(2)
C(6)-C(7)-N(2)	133.1(2)
C(2)-C(7)-N(2)	105.4(2)

C(14)-C(13)-C(12)	120.4(3)
F(2)-B(1)-F(1)	111.5(2)
F(2)-B(1)-F(3)	111.0(3)
F(1)-B(1)-F(3)	111.0(3)
F(2)-B(1)-N(1)	108.5(2)
F(1)-B(1)-N(1)	108.3(2)
F(3)-B(1)-N(1)	106.4(2)

Symmetry transformations used to generate equivalent atoms:
#1 -x+2,-y+1,-z+1

Table S54. Anisotropic displacement parameters ($Å^2$x 10^3) for k11112 (**3.8**). The anisotropic displacement factor exponent takes the form: $-2\pi^2[h^2a^{*2}U^{11} + ... + 2 h k a^* b^* U^{12}]$

	U^{11}	U^{22}	U^{33}	U^{23}	U^{13}	U^{12}
F(3)	66(1)	40(1)	56(1)	5(1)	25(1)	-2(1)
F(2)	52(1)	51(1)	70(1)	23(1)	12(1)	6(1)
F(1)	82(1)	34(1)	59(1)	-4(1)	17(1)	-11(1)
N(2)	42(2)	25(1)	36(1)	-1(1)	11(1)	2(1)
N(1)	43(2)	27(1)	40(1)	-1(1)	9(1)	-1(1)
N(3)	43(2)	28(1)	39(1)	1(1)	11(1)	3(1)
C(10)	50(2)	36(2)	42(2)	-1(1)	18(2)	-5(1)
C(9)	46(2)	25(1)	37(2)	1(1)	16(1)	-3(1)
C(17)	37(2)	38(2)	42(2)	7(1)	12(1)	4(1)
C(16)	39(2)	33(2)	42(2)	0(1)	11(1)	1(1)
C(14)	57(2)	32(2)	51(2)	5(1)	25(2)	5(1)
C(15)	43(2)	28(1)	35(1)	1(1)	15(1)	-1(1)
C(2S)	59(2)	42(2)	53(2)	0(2)	14(2)	-2(2)
C(12)	91(3)	42(2)	48(2)	-7(2)	37(2)	-12(2)
C(22)	54(2)	32(2)	64(2)	5(1)	25(2)	4(1)
C(18)	47(2)	29(1)	43(2)	5(1)	22(1)	1(1)
C(20)	39(2)	31(1)	37(1)	-1(1)	16(1)	1(1)
C(19)	45(2)	31(2)	43(2)	1(1)	17(1)	-5(1)
C(1)	41(2)	31(2)	36(2)	2(1)	10(1)	0(1)
C(8)	39(2)	25(1)	40(2)	2(1)	12(1)	-1(1)
C(3S)	55(2)	55(2)	48(2)	-5(2)	21(2)	4(2)
C(3)	51(2)	32(2)	45(2)	-2(1)	6(1)	5(1)
C(1S)	56(2)	55(2)	46(2)	4(2)	18(2)	-2(2)
C(4)	61(2)	38(2)	44(2)	-8(1)	11(2)	8(2)
C(11)	61(2)	50(2)	41(2)	-3(1)	17(2)	-16(2)
C(2)	41(2)	32(2)	34(2)	1(1)	6(1)	3(1)
C(5)	65(2)	45(2)	40(2)	-2(1)	15(2)	10(2)
C(6)	56(2)	34(2)	40(2)	1(1)	11(1)	4(1)
C(7)	40(2)	29(1)	35(1)	-3(1)	10(1)	2(1)
C(21)	42(2)	40(2)	56(2)	1(1)	14(2)	0(1)
C(13)	76(2)	32(2)	65(2)	7(2)	43(2)	7(2)
C(23)	49(2)	43(2)	60(2)	6(1)	7(2)	-3(2)
B(1)	51(2)	31(2)	45(2)	1(2)	12(2)	-2(2)

Table S55. Hydrogen coordinates (x 10^4) and isotropic displacement parameters ($Å^2$ x 10^3) for k11112 (**3.8**).

	x	y	z	U(eq)
H(4)	3891	8376	3447	50
H(6)	-1880	9648	-2721	48
H(8)	-1041	8842	1309	54
H(3S)	8813	5565	3844	63
H(11)	1422	8958	6101	68
H(12A)	1728	10309	-1287	73
H(12B)	-407	10287	-1740	73
H(12C)	520	10223	-3084	73
H(15)	3455	9754	-336	46
H(19)	2241	6910	-965	54
H(21)	2653	7069	-3400	59
H(22)	3887	8613	5935	61
H(24)	2570	7684	-4215	60
H(25)	2133	8168	-2598	53
H(27A)	5376	9224	478	70
H(27B)	4566	8825	-52	70
H(27C)	4519	8996	1598	70
H(28)	-1051	9063	3803	63
H(29A)	-3316	9063	-3218	80
H(29B)	-2685	8811	-1656	80
H(29C)	-2048	8716	-3155	80
H(1)	1170(40)	7863(7)	2560(30)	48(8)
H(2S)	8110(40)	5341(7)	6080(30)	48(8)
H(1S)	10840(40)	5218(8)	2750(30)	57(8)

1,3-Bis[1-(2,6-dimethylphenylimino)ethyl]-4,5,6-trihydropyrimidin-2-ylidene chromium(III) chloride (4.6).

Table S56. Crystal data and structure refinement for d12130 (**4.6**).

Identification code	d12130	
Empirical formula	C49 H62 Cl8 N8 Cr2	
Formula weight	1150.67	
Temperature/K	146.98	
Crystal system	monoclinic	
Space group	P21/n	
	a = 12.7925(4) Å	α = 90.00°.
	b = 15.2069(5) Å	β = 108.8331(17)°.
	c = 14.7165(5) Å	γ = 90.00°
Volume	2709.59(15) Å^3	
Z	2	
Density (calculated)	1.410 mg/mm^3	
Absorption coefficient	7.259 mm^{-1}	
F(000)	1192.0	
Crystal size	0.09 × 0.09 × 0.02 mm	
Theta range for data collection	7.98 to 132.92°	
Index ranges	$-15 \le h \le 12$, $-13 \le k \le 17$, $-17 \le l \le 17$	
Reflections collected	17786	
Independent reflections	4658[R(int) = 0.0377]	
Data/restraints/parameters	4658/3/320	
Goodness-of-fit on F^2	1.048	
Final R indexes [I>=2σ (I)]	R1 = 0.0414, wR2 = 0.1087	
Final R indexes [all data]	R1 = 0.0465, wR2 = 0.1130	
Largest diff. peak and hole	0.84 and -1.16 e.Å^{-3}	

Table S57. Fractional atomic coordinates (×10^4) and equivalent isotropic displacement parameters ($Å^2$ ×10^3) for d12130 (**4.6**). Ueq is defined as 1/3 of the trace of the orthogonalised U^{ij} tensor.

	x	y	z	U(eq)
Cr1	3281.6(3)	1970.4(3)	6941.0(3)	18.29(14)
Cl2	2592.5(5)	1006.9(4)	5655.5(4)	24.91(17)
Cl3	3294.8(6)	3133.7(5)	5895.7(5)	29.06(18)
Cl1	3310.2(6)	947.6(5)	8094.9(5)	28.56(18)
N1	5016.5(19)	3109.3(15)	8058.4(17)	24.8(5)
N2	3265.8(18)	3521.9(15)	8056.9(16)	24.0(5)
N3	5020.7(19)	1813.8(15)	7261.8(17)	24.1(5)
N4	1900.1(17)	2576.3(15)	7212.0(15)	20.6(5)
C1	3935(2)	2956.3(18)	7831.7(19)	22.4(6)
C2	5526(3)	3961(2)	8457(2)	35.8(7)
C3A	4895(4)	4376(3)	9001(4)	33.7(15)
C3B	4580(8)	4632(7)	8326(9)	32(4)
C4	3644(3)	4392(2)	8492(3)	40.3(8)
C5	5601(2)	2440(2)	7767(2)	26.4(6)
C6	6824(2)	2525(2)	8067(2)	38.4(8)
C7	5574(2)	1068.4(19)	7002(2)	26.1(6)
C8	5637(2)	1044(2)	6074(2)	28.7(7)
C9	6113(2)	307(2)	5802(2)	34.2(7)
C10	6512(2)	-375(2)	6439(2)	38.7(8)
C11	6479(2)	-320(2)	7361(2)	38.3(8)
C12	6029(2)	409(2)	7679(2)	31.4(7)
C13	5229(3)	1791(2)	5380(2)	36.9(7)
C14	6086(3)	461(2)	8714(2)	42.4(8)
C15	2143(2)	3278.7(18)	7727.4(19)	23.4(6)
C16	1359(3)	3858(2)	8009(2)	34.2(7)
C17	777(2)	2255.2(19)	6928(2)	26.2(6)
C18	400(3)	1795(2)	7584(3)	36.9(8)
C19	-678(3)	1484(3)	7261(3)	55(1)
C20	-1357(3)	1634(3)	6348(4)	60.6(12)
C21	-988(3)	2116(3)	5724(3)	50.1(10)
C22	88(2)	2440(2)	5998(2)	34.2(7)
C23	1086(3)	1656(3)	8615(3)	47.7(9)
C24	471(3)	2985(3)	5323(2)	43.8(9)
Cl4	5551(13)	4547(17)	5782(16)	84.8(19)
C1S	5437(8)	5350(5)	4899(7)	59(2)
Cl4A	4169(13)	5449(18)	4055(17)	84.8(19)

Table S58. Anisotropic displacement parameters (Å^2 ×10^3) for d12130 (**4.6**). The anisotropic displacement factor exponent takes the form: $-2\pi^2[h^2a^*2U^{11}+...+2hka\times b\times U^{12}]$

	U^{11}	U^{22}	U^{33}	U^{23}	U^{13}	U^{12}
Cr1	17.6(2)	17.1(2)	19.1(2)	-2.52(16)	4.38(17)	-0.55(17)
Cl2	26.8(3)	25.3(4)	21.0(3)	-4.8(2)	5.5(3)	-5.6(3)
Cl3	31.7(4)	25.8(4)	31.0(4)	5.4(3)	12.1(3)	-0.3(3)
Cl1	32.9(4)	26.1(4)	24.3(3)	4.0(3)	5.9(3)	1.1(3)
N1	22.5(12)	21.7(13)	26.3(12)	-6.1(10)	2.6(10)	-2.4(9)
N2	25.1(12)	19.1(12)	24.8(12)	-4.5(9)	3.9(10)	2.5(10)
N3	20.1(11)	25.6(13)	25.8(12)	-4.8(10)	6.2(10)	1.1(10)
N4	19.8(11)	20.6(12)	20.9(11)	0.5(9)	6.0(9)	1.4(9)
C1	24.5(14)	20.8(14)	19.9(13)	-0.3(11)	4.4(11)	0.2(11)
C2	31.7(16)	26.3(17)	40.1(17)	-12.7(14)	-1.4(13)	-6.4(13)
C3A	31(3)	26(3)	37(3)	-11(2)	3(2)	-4.6(19)
C3B	28(6)	27(6)	37(8)	-10(5)	5(5)	-8(4)
C4	37.8(18)	22.7(16)	50(2)	-17.3(14)	-0.7(15)	2.5(14)
C5	22.8(14)	27.9(16)	26.9(14)	-3.5(12)	5.6(11)	-0.2(12)
C6	20.5(15)	39.5(19)	50(2)	-13.8(15)	4.0(14)	-4.4(13)
C7	14.5(13)	28.7(16)	33.1(15)	-9.6(12)	4.8(11)	-1.6(11)
C8	17.3(13)	32.4(17)	37.2(16)	-10.3(13)	10.0(12)	-4.7(12)
C9	20.1(14)	42.6(19)	40.9(17)	-15.2(15)	11.4(13)	-1.9(13)
C10	23.6(15)	40.5(19)	51(2)	-15.7(16)	10.3(14)	6.3(14)
C11	23.6(15)	37.5(19)	47.4(19)	-5.0(15)	2.5(14)	9.0(13)
C12	18.6(14)	35.6(18)	35.6(16)	-6.7(13)	2.8(12)	4.1(12)
C13	38.3(18)	39.4(19)	40.3(17)	-2.4(15)	22.9(15)	-2.6(15)
C14	38.2(18)	46(2)	36.6(18)	0.0(15)	2.7(14)	16.1(16)
C15	28.0(15)	19.3(14)	23.0(13)	3.8(11)	8.5(11)	4.3(11)
C16	33.8(16)	27.8(17)	43.1(18)	-3.6(14)	15.3(14)	5.4(13)
C17	22.8(14)	22.9(15)	35.4(16)	-3.2(12)	12.9(12)	1.2(11)
C18	33.2(17)	32.0(17)	54(2)	0.1(15)	25.6(16)	1.5(14)
C19	43(2)	49(2)	86(3)	2(2)	38(2)	-5.3(18)
C20	26.3(18)	69(3)	91(3)	-18(2)	24(2)	-14.8(18)
C21	24.6(17)	66(3)	54(2)	-17.1(19)	5.3(16)	0.8(17)
C22	22.9(15)	41.2(18)	37.3(17)	-6.2(14)	7.9(13)	3.4(13)
C23	54(2)	53(2)	47(2)	15.8(17)	32.2(18)	7.2(18)
C24	32.7(17)	61(2)	30.7(17)	6.7(16)	1.0(14)	7.4(16)
Cl4	102(7)	79.3(10)	77(6)	1(4)	34(5)	3(5)
C1S	85(6)	37(4)	82(6)	-19(4)	65(5)	-28(4)
Cl4A	102(7)	79.3(10)	77(6)	1(4)	34(5)	3(5)

Table S59. Bond lengths [Å] and angles [°] for d12130 (**4.6**).

Cr1 Cl2	2.3293(7)
Cr1 Cl3	2.3479(8)
Cr1 Cl1	2.2945(8)
Cr1 N3	2.133(2)
Cr1 N4	2.142(2)
Cr1 C1	1.989(3)
N1 C1	1.335(4)
N1 C2	1.483(4)
N1 C5	1.409(4)
N2 C1	1.329(4)
N2 C4	1.481(4)
N2 C15	1.409(4)
N3 C5	1.286(4)
N3 C7	1.451(4)
N4 C15	1.289(4)
N4 C17	1.446(4)
C2 C3A	1.453(6)
C2 C3B	1.547(11)
C3A C4	1.532(6)
C3B C4	1.347(11)
C5 C6	1.488(4)
C7 C8	1.395(4)
C7 C12	1.401(4)
C8 C9	1.395(4)
C8 C13	1.504(5)
C9 C10	1.382(5)
C10 C11	1.374(5)
C11 C12	1.396(4)
C12 C14	1.503(4)
C15 C16	1.490(4)
C17 C18	1.398(4)
C17 C22	1.397(4)
C18 C19	1.389(5)
C18 C23	1.503(5)
C19 C20	1.362(6)
C20 C21	1.373(6)
C21 C22	1.394(5)
C22 C24	1.492(5)
Cl4 C1S	1.754(10)
Cl4 C1S1	1.34(2)
Cl4 Cl4A1	0.36(3)

C1S Cl41	1.34(2)
C1S C1S1	1.640(13)
C1S Cl4A1	1.90(2)
C1S Cl4A	1.702(9)
Cl4A Cl41	0.36(3)
Cl4A C1S1	1.90(2)
Cl2 Cr1 Cl3	91.30(3)
Cl1 Cr1 Cl2	94.94(3)
Cl1 Cr1 Cl3	173.67(3)
N3 Cr1 Cl2	101.75(7)
N3 Cr1 Cl3	90.09(7)
N3 Cr1 Cl1	89.67(7)
N3 Cr1 N4	150.59(9)
N4 Cr1 Cl2	107.65(6)
N4 Cr1 Cl3	88.78(6)
N4 Cr1 Cl1	88.33(6)
C1 Cr1 Cl2	167.85(8)
C1 Cr1 Cl3	76.91(8)
C1 Cr1 Cl1	96.90(8)
C1 Cr1 N3	75.65(10)
C1 Cr1 N4	75.49(10)
C1 N1 C2	122.6(2)
C1 N1 C5	114.0(2)
C5 N1 C2	122.9(2)
C1 N2 C4	122.6(2)
C1 N2 C15	114.3(2)
C15 N2 C4	122.5(2)
C5 N3 Cr1	114.28(18)
C5 N3 C7	119.4(2)
C7 N3 Cr1	126.27(17)
C15 N4 Cr1	114.20(18)
C15 N4 C17	118.6(2)
C17 N4 Cr1	127.14(17)
N1 C1 Cr1	118.5(2)
N2 C1 Cr1	119.0(2)
N2 C1 N1	121.6(2)
N1 C2 C3B	107.5(4)
C3A C2 N1	110.2(3)
C3A C2 C3B	39.7(5)
C2 C3A C4	114.5(4)
C4 C3B C2	120.3(8)
N2 C4 C3A	110.0(3)
C3B C4 N2	110.4(5)

C3B C4 C3A	40.9(5)
N1 C5 C6	117.2(3)
N3 C5 N1	116.5(2)
N3 C5 C6	126.3(3)
C8 C7 N3	117.7(3)
C8 C7 C12	122.4(3)
C12 C7 N3	119.9(3)
C7 C8 C13	121.9(3)
C9 C8 C7	118.1(3)
C9 C8 C13	120.0(3)
C10 C9 C8	120.5(3)
C11 C10 C9	120.2(3)
C10 C11 C12	121.8(3)
C7 C12 C14	123.7(3)
C11 C12 C7	116.8(3)
C11 C12 C14	119.4(3)
N2 C15 C16	116.9(2)
N4 C15 N2	116.4(2)
N4 C15 C16	126.7(3)
C18 C17 N4	120.1(3)
C22 C17 N4	118.0(3)
C22 C17 C18	121.9(3)
C17 C18 C23	123.3(3)
C19 C18 C17	117.4(3)
C19 C18 C23	119.3(3)
C20 C19 C18	121.9(4)
C19 C20 C21	120.0(3)
C20 C21 C22	121.1(4)
C17 C22 C24	121.7(3)
C21 C22 C17	117.6(3)
C21 C22 C24	120.7(3)
C1S1 Cl4 C1S	62.2(6)
Cl4A1 Cl4 C1S1	170(5)
Cl4A1 Cl4 C1S	108(4)
Cl41 C1S Cl4	117.8(6)
Cl41 C1S C1S1	71.2(8)
Cl41 C1S Cl4A1	128.2(11)
Cl4 C1S Cl4A1	10.4(8)
Cl41 C1S Cl4A	2.1(10)
C1S1 C1S Cl4	46.5(8)
C1S1 C1S Cl4A1	57.0(6)
C1S1 C1S Cl4A	69.2(9)
Cl4A C1S Cl4	115.7(7)

Cl4A C1S Cl4A1	126.1(5)
Cl41 Cl4A C1S1	62(4)
Cl41 Cl4A C1S	8(4)
C1S Cl4A C1S1	53.9(6)

11-X,1-Y,1-Z

Table S60. Hydrogen atom coordinates (Å × 10^4) and isotropic displacement parameters (Å^2 × 10^3) for d12130 (**4.6**).

	x	y	z	U(eq)
H2AA	6294	3862	8879	43
H2AB	5549	4353	7927	43
H2BC	6032	4163	8113	43
H2BD	5955	3896	9146	43
H3AA	5157	4989	9148	40
H3AB	5045	4062	9620	40
H3BA	4890	5139	8748	38
H3BB	4367	4849	7657	38
H4AA	3261	4539	8959	48
H4AB	3460	4849	7986	48
H4BC	3062	4836	8216	48
H4BD	3779	4364	9193	48
H6A	7019	3044	7760	58
H6B	7138	1999	7871	58
H6C	7121	2590	8766	58
H9	6164	275	5173	41
H10	6809	-884	6240	46
H11	6769	-790	7794	46
H13A	4441	1886	5273	55
H13B	5341	1647	4769	55
H13C	5640	2327	5646	55
H14A	6696	849	9063	64
H14B	6211	-128	8999	64
H14C	5390	697	8754	64
H16A	615	3606	7773	51
H16B	1354	4443	7728	51
H16C	1593	3907	8710	51
H19	-950	1159	7688	66
H20	-2087	1404	6144	73
H21	-1474	2230	5095	60
H23A	1755	2017	8767	71
H23B	1293	1035	8719	71
H23C	658	1826	9032	71
H24A	758	3547	5629	66
H24B	-149	3094	4737	66
H24C	1057	2672	5161	66
H1SA	5959	5209	4576	71
H1SB	5644	5907	5211	71

Appendix B: DFT data for the optimized structures

1,3-Bis[1-(2,6-dimethylphenylimino)ethyl]imidazolium chloride (2.7).

Table S61. Atomic coordinates and relative energy of the optimized structure of **2.7** using the B3LYP/DGDZVP level of calculation.

Charge = 0, Multiplicity = 1
Gas phase energy: −1571.97621104 hartree

Optimized atomic coordinates:

Center Number	Atomic Number	Coordinates (Angstroms) X	Y	Z
1	6	-0.000030	0.089914	0.588075
2	1	0.000012	1.005449	1.224550
3	6	0.677679	-1.400006	-0.940217
4	1	1.399032	-1.958149	-1.515315
5	6	-0.677832	-1.399961	-0.940224
6	1	-1.399213	-1.958059	-1.515330
7	6	2.466917	-0.126813	0.303029
8	6	2.683294	0.744877	1.502909
9	1	3.749617	0.935442	1.625222
10	1	2.305596	0.248642	2.404333
11	1	2.138442	1.697381	1.416859
12	6	-2.466985	-0.126512	0.302886
13	6	-2.683216	0.746181	1.502062
14	1	-3.749541	0.936658	1.624491
15	1	-2.138561	1.698696	1.414985
16	1	-2.305151	0.250891	2.403842
17	6	-4.703672	-0.393511	-0.381884
18	6	-5.511447	-1.395554	0.194713
19	6	-6.895900	-1.188140	0.241648
20	1	-7.530002	-1.950134	0.689944
21	6	-7.467652	-0.026101	-0.281820
22	1	-8.544244	0.118913	-0.241878
23	6	-6.650845	0.943530	-0.867603
24	1	-7.095354	1.843739	-1.286438
25	6	-5.260069	0.780771	-0.932022
26	6	-4.892729	-2.657732	0.751922
27	1	-4.223479	-3.127548	0.022320

28	1	-5.664072	-3.383030	1.024499
29	1	-4.295656	-2.458034	1.650401
30	6	-4.386828	1.828126	-1.587232
31	1	-3.758533	2.358546	-0.862165
32	1	-4.998899	2.576969	-2.096564
33	1	-3.713429	1.380402	-2.326343
34	6	4.703540	-0.393428	-0.382050
35	6	5.511291	-1.395979	0.193702
36	6	6.895753	-1.188664	0.240770
37	1	7.529834	-1.951055	0.688423
38	6	7.467540	-0.026218	-0.281756
39	1	8.544140	0.118718	-0.241725
40	6	6.650758	0.943924	-0.866727
41	1	7.095296	1.844454	-1.284845
42	6	5.259974	0.781279	-0.931244
43	6	4.892536	-2.658596	0.749880
44	1	4.295368	-2.459607	1.648453
45	1	5.663863	-3.384093	1.021975
46	1	4.223374	-3.127866	0.019846
47	6	4.386754	1.829220	-1.585547
48	1	3.712976	1.382086	-2.324667
49	1	4.998828	2.578203	-2.094670
50	1	3.758845	2.359378	-0.859951
51	7	1.086010	-0.468024	0.017972
52	7	-1.086107	-0.467924	0.017935
53	7	3.306049	-0.632723	-0.502792
54	7	-3.306197	-0.632994	-0.502496
55	17	0.000567	3.057119	1.470340

Table S62. Comparison of the optimized bond lengths using the B3LYP/DGDZVP level of calculation with X-ray structural parameters for **2.7**.

X-ray data				B3LYP/DGDZVP	
Number	Atom 1	Atom 2	Length (Å)	Length (Å)	Δ (Å)
1	C1	N1	1.339(3)	1.3475	-0.009
2	C1	N2	1.335(3)	1.3475	-0.013
3	C2	C3	1.338(4)	1.3555	-0.018
4	C2	N1	1.389(3)	1.3977	-0.009
5	C3	N2	1.392(3)	1.3977	-0.006
6	C4	C5	1.489(3)	1.4988	-0.010
7	C4	N1	1.441(3)	1.4507	-0.010
8	C4	N3	1.261(3)	1.2686	-0.008
9	C6	C7	1.490(3)	1.4988	-0.009
10	C6	N2	1.445(3)	1.4507	-0.006
11	C6	N4	1.258(3)	1.2686	-0.011
12	C8	C9	1.396(4)	1.4103	-0.014
13	C8	C13	1.397(4)	1.4111	-0.014
14	C8	N4	1.426(3)	1.4230	0.003
15	C9	C10	1.394(4)	1.4007	-0.007
16	C9	C14	1.502(4)	1.5120	-0.010
17	C10	C11	1.381(4)	1.3968	-0.016
18	C11	C12	1.373(4)	1.3966	-0.024
19	C12	C13	1.401(4)	1.4017	-0.001
20	C13	C15	1.507(4)	1.5129	-0.006
21	C16	C17	1.396(4)	1.4104	-0.014
22	C16	C21	1.400(4)	1.4111	-0.011
23	C16	N3	1.431(3)	1.4230	0.008
24	C17	C18	1.400(4)	1.4007	-0.001
25	C17	C22	1.500(4)	1.5121	-0.012
26	C18	C19	1.385(4)	1.3969	-0.012
27	C19	C20	1.378(4)	1.3965	-0.019
28	C20	C21	1.410(4)	1.4018	0.008
29	C21	C23	1.499(4)	1.5128	-0.014

Table S63. Comparison of the optimized bond angles using the B3LYP/DGDZVP level of calculation with X-ray structural parameters for **2.7**.

x-ray data					B3LYP/DGDZVP	
Number	Atom1	Atom2	Atom3	Angle (deg.)	Angle (deg.)	Δ (deg.)
1	N1	C1	N2	107.3(2)	107.42	-0.1
2	C3	C2	N1	107.0(2)	107.03	0.0
3	C2	C3	N2	107.2(2)	107.23	0.0
4	C5	C4	N1	114.3(2)	114.32	0.0
5	C5	C4	N3	130.8(2)	130.83	0.0
6	N1	C4	N3	114.9(2)	114.93	0.0
7	C7	C6	N2	114.3(2)	114.32	0.0
8	C7	C6	N4	131.5(2)	131.53	0.0
9	N2	C6	N4	114.2(2)	114.22	0.0
10	C9	C8	C13	122.5(2)	122.53	0.0
11	C9	C8	N4	116.2(2)	116.23	0.0
12	C13	C8	N4	120.9(2)	121.03	-0.1
13	C8	C9	C10	117.6(3)	117.63	0.0
14	C8	C9	C14	120.6(3)	120.63	0.0
15	C10	C9	C14	121.8(3)	121.83	0.0
16	C9	C10	C11	121.0(3)	121.13	-0.1
17	C10	C11	C12	120.3(3)	120.23	0.1
18	C11	C12	C13	121.2(3)	121.13	0.1
19	C8	C13	C12	117.3(3)	117.43	-0.1
20	C8	C13	C15	121.7(2)	121.73	0.0
21	C12	C13	C15	120.9(3)	120.83	0.1
22	C17	C16	C21	122.8(2)	122.83	0.0
23	C17	C16	N3	117.6(2)	117.63	0.0
24	C21	C16	N3	119.2(3)	119.23	0.0
25	C16	C17	C18	117.6(3)	117.53	0.1
26	C16	C17	C22	121.4(2)	121.53	-0.1
27	C18	C17	C22	121.0(3)	121.03	0.0
28	C17	C18	C19	121.1(3)	121.23	-0.1
29	C18	C19	C20	120.1(3)	120.13	0.0
30	C19	C20	C21	121.2(3)	121.23	0.0

31	C16	C21	C20	117.1(3)	117.13	0.0
32	C16	C21	C23	121.8(2)	121.83	0.0
33	C20	C21	C23	121.0(3)	121.03	0.0

1,3-Bis[1-(2,6-dimethylphenylimino)ethyl]imidazol-2-ylidene (1.55).

Table S64. Atomic coordinates and relative energy of the optimized structure of **1.55** using the B3LYP/DGDZVP level of calculation.

Charge = 0, Multiplicity = 1
Gas phase energy: −1111.1723647 hartree

Optimized atomic coordinates:

Center Number	Atomic Number	Coordinates (Angstroms) X	Y	Z
1	6	-0.000021	-0.000152	0.811332
2	6	0.674738	-0.000791	-1.406194
3	1	1.393074	-0.001051	-2.210828
4	6	-0.674632	-0.001011	-1.406222
5	1	-1.392877	-0.001315	-2.210921
6	6	2.423890	0.000016	0.375932
7	6	2.638014	0.000334	1.868088
8	1	3.706385	0.001126	2.087144
9	1	2.165774	-0.874869	2.321596
10	1	2.164397	0.874819	2.321508
11	6	-2.423826	-0.000303	0.375931
12	6	-2.637976	0.000210	1.868094
13	1	-2.165926	0.875747	2.321157
14	1	-2.164322	-0.873989	2.322023
15	1	-3.706366	-0.000568	2.087047
16	6	-4.699794	-0.000043	-0.255369
17	6	-5.389006	1.229634	-0.173968
18	6	-6.777189	1.207656	0.015473
19	1	-7.316193	2.150684	0.082122
20	6	-7.474012	0.000710	0.113838
21	1	-8.551683	0.001017	0.257431
22	6	-6.777876	-1.206610	0.015296
23	1	-7.317394	-2.149355	0.081801
24	6	-5.389708	-1.229329	-0.174192
25	6	-4.641299	2.538396	-0.294911
26	1	-3.971917	2.707697	0.557553
27	1	-5.335935	3.381735	-0.341241
28	1	-4.016650	2.556469	-1.194909
29	6	-4.642648	-2.538452	-0.295162

30	1	-4.017174	-2.556385	-1.194581
31	1	-5.337703	-3.381388	-0.342534
32	1	-3.974128	-2.708521	0.557837
33	6	4.699760	-0.000006	-0.255495
34	6	5.389502	-1.229386	-0.173821
35	6	6.777639	-1.206849	0.015745
36	1	7.316987	-2.149662	0.082618
37	6	7.473985	0.000390	0.113939
38	1	8.551646	0.000546	0.257602
39	6	6.777376	1.207416	0.015126
40	1	7.316517	2.150383	0.081498
41	6	5.389224	1.229563	-0.174453
42	6	4.642223	-2.538433	-0.294430
43	1	5.337127	-3.381499	-0.341610
44	1	4.016754	-2.556503	-1.193860
45	1	3.973656	-2.708179	0.558595
46	6	4.641700	2.538406	-0.295725
47	1	4.015818	2.555708	-1.194879
48	1	5.336465	3.381536	-0.343845
49	1	3.973497	2.708708	0.557478
50	7	1.066402	-0.000311	-0.053717
51	7	-1.066419	-0.000541	-0.053699
52	7	3.311384	-0.000226	-0.539078
53	7	-3.311399	-0.000504	-0.539066

1,3-Bis[1-(2,6-dimethylphenylimino)ethyl]benzimidazol-2-ylidene (1.56).

Table S65. Atomic coordinates and relative energy of the optimized structure of **1.56** using the B3LYP/DGDZVP level of calculation.

Charge = 0, Multiplicity = 1
Gas phase energy: −1264.8286896 hartree

Optimized atomic coordinates

Center Number	Atomic Number	Coordinates (Angstroms) X	Y	Z
1	6	0.000295	-0.990551	0.005037
2	6	0.702517	1.219688	-0.037297
3	6	-0.702793	1.219441	-0.036730
4	6	2.410471	-0.663654	0.002897
5	6	2.529235	-2.168621	0.032581
6	1	3.583319	-2.448877	0.038596
7	1	2.032871	-2.611919	-0.833962
8	1	2.031890	-2.577762	0.915225
9	6	-2.410027	-0.664502	0.004657
10	6	-2.528259	-2.169404	0.039832
11	1	-2.024025	-2.576050	0.919643
12	1	-2.038447	-2.614990	-0.829345
13	1	-3.582201	-2.449883	0.054150
14	6	-4.730572	-0.212709	0.005714
15	6	-5.406773	-0.304312	1.242300
16	6	-6.777687	-0.593819	1.235971
17	1	-7.305860	-0.668755	2.184487
18	6	-7.471406	-0.780822	0.037752
19	1	-8.535816	-1.001878	0.050161
20	6	-6.789763	-0.671503	-1.176848
21	1	-7.327580	-0.806879	-2.113173
22	6	-5.418872	-0.383751	-1.215597
23	6	-4.664065	-0.090221	2.542006
24	1	-3.934390	-0.887063	2.731922
25	1	-5.356700	-0.069074	3.388020
26	1	-4.105506	0.852193	2.530466
27	6	-4.689367	-0.254136	-2.533827
28	1	-4.126668	0.684380	-2.586704
29	1	-5.391155	-0.281666	-3.372065

30	1	-3.965645	-1.065148	-2.682242
31	6	4.730754	-0.211426	0.006974
32	6	5.420601	-0.374254	-1.214589
33	6	6.791094	-0.663878	-1.176020
34	1	7.330061	-0.793110	-2.112557
35	6	7.470949	-0.782481	0.038724
36	1	8.535107	-1.004767	0.051031
37	6	6.775883	-0.602768	1.237260
38	1	7.302792	-0.684412	2.185936
39	6	5.405235	-0.311876	1.243783
40	6	4.692778	-0.235726	-2.532838
41	1	5.396675	-0.245392	-3.369719
42	1	4.120052	0.697147	-2.575284
43	1	3.978259	-1.052747	-2.692953
44	6	4.660960	-0.106964	2.544099
45	1	4.087595	0.826382	2.531718
46	1	5.354256	-0.073727	3.389202
47	1	3.944385	-0.915210	2.736285
48	7	1.083200	-0.149427	-0.011549
49	7	-1.082957	-0.149783	-0.010331
50	7	3.368570	0.178000	-0.009919
51	7	-3.368443	0.176693	-0.011641
52	6	-1.429380	2.413257	-0.058869
53	1	-2.510078	2.402375	-0.058660
54	6	-0.702206	3.607972	-0.081451
55	1	-1.239749	4.552668	-0.099215
56	6	0.701085	3.608201	-0.081899
57	1	1.238315	4.553065	-0.099930
58	6	1.428690	2.413710	-0.059809
59	1	2.509391	2.403357	-0.059828

1,3-Bis[1-(2,6-dimethylphenylimino)ethyl]-4,5,6-trihydropyrimidin-2-ylidene (1.57).

Table S66. Atomic coordinates and relative energy of the optimized structure of **1.57** using the B3LYP/DGDZVP level of calculation.

Charge = 0, Multiplicity = 1
Gas phase energy: −1151.700997 hartree

Optimized atomic coordinates

Center Number	Atomic Number	Coordinates (Angstroms) X	Y	Z
1	6	0.000008	-0.136486	-0.160488
2	6	2.379417	-0.056666	-0.142888
3	6	-2.379411	-0.056491	-0.142791
4	7	3.452600	-0.158637	0.546931
5	6	4.739237	0.081749	0.012949
6	6	5.487391	-0.995602	-0.512964
7	6	5.305549	1.372194	0.118157
8	6	6.795367	-0.755234	-0.953521
9	6	6.616711	1.570478	-0.333844
10	6	7.362900	0.518881	-0.871910
11	1	7.375622	-1.580482	-1.361919
12	1	7.057380	2.562776	-0.258292
13	1	8.380345	0.688627	-1.215550
14	6	2.297142	0.331839	-1.600481
15	1	1.722210	1.252281	-1.723895
16	1	1.775814	-0.434730	-2.177739
17	1	3.305322	0.472006	-1.993424
18	6	4.509615	2.511698	0.713255
19	1	5.137158	3.397076	0.849595
20	1	4.088614	2.233762	1.685882
21	1	3.665623	2.799403	0.074034
22	6	4.885136	-2.380373	-0.592451
23	1	4.474890	-2.689812	0.375402
24	1	4.060881	-2.427766	-1.314865
25	1	5.634808	-3.115663	-0.898362
26	7	1.152834	-0.331355	0.528645
27	7	-1.152820	-0.331287	0.528690
28	6	1.249298	-0.756151	1.948058
29	1	2.153862	-1.351547	2.066214

30	1	1.366042	0.132070	2.580319
31	6	0.000064	-1.540652	2.320496
32	1	0.000053	-1.749837	3.394786
33	1	0.000173	-2.504999	1.798781
34	6	-1.249319	-0.756396	1.948015
35	1	-1.366433	0.131656	2.580440
36	1	-2.153723	-1.352078	2.065946
37	6	-2.297130	0.332578	-1.600231
38	1	-1.721358	1.252518	-1.723385
39	1	-1.776654	-0.434261	-2.177915
40	1	-3.305272	0.473783	-1.992890
41	7	-3.452610	-0.158836	0.546976
42	6	-4.739258	0.081508	0.012950
43	6	-5.306181	1.371568	0.119647
44	6	-5.486769	-0.995519	-0.514488
45	6	-6.617312	1.569832	-0.332435
46	6	-6.794758	-0.755189	-0.955072
47	6	-7.362886	0.518558	-0.872007
48	1	-7.058459	2.561832	-0.255769
49	1	-7.374539	-1.580188	-1.364647
50	1	-8.380318	0.688275	-1.215701
51	6	-4.510893	2.510652	0.716389
52	1	-4.090708	2.231910	1.689146
53	1	-3.666355	2.798964	0.078171
54	1	-5.138648	3.395843	0.852946
55	6	-4.883907	-2.379936	-0.595585
56	1	-4.060097	-2.426299	-1.318578
57	1	-4.472900	-2.690052	0.371721
58	1	-5.633426	-3.115301	-0.901694

1,3-Bis[1-(2,6-dimethylphenylimino)ethyl]imidazol-2-ylidene iron(II) chloride (2.17).

Table S67. Atomic coordinates and relative energy of the optimized structure of **2.17** (quintet) using the UB3LYP/TZVP level of calculation.

Charge = 0, Multiplicity = 5

Gas phase energy: −3295.8193606 hartree

Optimized atomic coordinates:

Center Number	Atomic Number	Coordinates (Angstroms) X	Y	Z
1	6	-0.058922	-0.404893	-0.475122
2	6	-0.055261	-1.698140	-2.360739
3	1	0.359514	-2.258116	-3.178026
4	6	-1.337608	-1.476750	-2.024725
5	1	-2.261688	-1.787773	-2.474145
6	6	2.140884	-0.950266	-1.345002
7	6	2.890211	-1.668774	-2.423522
8	1	3.959112	-1.537298	-2.282118
9	1	2.613557	-1.281598	-3.406614
10	1	2.659743	-2.736261	-2.404596
11	6	-2.523679	-0.221081	-0.219575
12	6	-2.334257	0.575132	1.031627
13	1	-1.767284	1.487096	0.832875
14	1	-1.770092	0.006025	1.773221
15	1	-3.307547	0.837661	1.439415
16	6	-4.873626	-0.166223	-0.312382
17	6	-5.437893	1.042284	-0.753953
18	6	-6.731228	1.356562	-0.338634
19	1	-7.175933	2.288001	-0.669583
20	6	-7.452153	0.498078	0.480967
21	1	-8.456166	0.758307	0.792252
22	6	-6.881792	-0.699116	0.893470
23	1	-7.444419	-1.376057	1.526065
24	6	-5.592075	-1.056338	0.502547
25	6	-4.668220	1.971295	-1.656352
26	1	-3.819195	2.431283	-1.142771
27	1	-5.308701	2.776908	-2.015324

28	1	-4.267586	1.440132	-2.523265
29	6	-4.982417	-2.361972	0.941285
30	1	-4.599083	-2.926614	0.087600
31	1	-5.720278	-2.977664	1.455495
32	1	-4.142977	-2.211139	1.625998
33	6	4.047526	-0.101197	-0.239128
34	6	4.655896	1.019186	-0.826671
35	6	6.022149	1.203905	-0.614909
36	1	6.508159	2.065516	-1.057021
37	6	6.756542	0.313014	0.155804
38	1	7.815023	0.477795	0.315222
39	6	6.129858	-0.785390	0.728281
40	1	6.700356	-1.478258	1.335396
41	6	4.765660	-1.015073	0.547651
42	6	3.866072	1.996570	-1.657460
43	1	4.491459	2.840387	-1.948039
44	1	3.004104	2.383468	-1.109869
45	1	3.490012	1.537226	-2.577332
46	6	4.096635	-2.205016	1.184857
47	1	3.254646	-1.905167	1.812235
48	1	4.806459	-2.750754	1.806066
49	1	3.711702	-2.905603	0.437077
50	17	0.966168	2.841439	0.723791
51	17	1.049319	-0.616710	2.918663
52	26	1.104023	0.606524	1.019461
53	7	0.722133	-1.034248	-1.403727
54	7	-1.320194	-0.685705	-0.869686
55	7	2.630713	-0.270885	-0.388391
56	7	-3.597592	-0.549488	-0.793596

Table S68. Atomic coordinates and relative energy of the optimized structure of **2.17** (triplet) using the UB3LYP/TZVP level of calculation.

Charge = 0, Multiplicity = 3
Gas phase energy: −3295.7879637 hartree

Optimized atomic coordinates:

Center Number	Atomic Number	Coordinates (Angstroms) X	Y	Z
1	6	0.068937	-0.110559	-0.566611
2	6	0.003390	-0.381135	-2.844628
3	1	0.388769	-0.499294	-3.840305
4	6	-1.260836	-0.334632	-2.401101
5	1	-2.201625	-0.398619	-2.913614
6	6	2.213193	-0.207897	-1.615086
7	6	3.009970	-0.339962	-2.872562
8	1	4.071670	-0.285585	-2.648005
9	1	2.755457	0.459291	-3.572500
10	1	2.800388	-1.294034	-3.362000
11	6	-2.428938	-0.068011	-0.227741
12	6	-2.273003	0.061196	1.251557
13	1	-1.716166	0.965503	1.505497
14	1	-1.715894	-0.784942	1.658260
15	1	-3.257313	0.102901	1.712079
16	6	-4.780733	-0.014323	-0.310061
17	6	-5.377153	1.248366	-0.151615
18	6	-6.678116	1.307313	0.346462
19	1	-7.146535	2.276419	0.474958
20	6	-7.377563	0.152098	0.670326
21	1	-8.388076	0.217001	1.054303
22	6	-6.776571	-1.087225	0.492138
23	1	-7.321464	-1.992027	0.736134
24	6	-5.478529	-1.195070	-0.004771
25	6	-4.632898	2.505639	-0.519399
26	1	-3.771307	2.678667	0.131116
27	1	-5.285069	3.375350	-0.439431
28	1	-4.253112	2.455611	-1.543060
29	6	-4.837675	-2.542535	-0.211401

30	1	-4.449976	-2.643944	-1.228273
31	1	-5.557838	-3.342245	-0.037781
32	1	-3.995023	-2.703187	0.466905
33	6	4.050226	0.003900	-0.124456
34	6	4.684302	1.257185	-0.101425
35	6	6.032425	1.300250	0.254372
36	1	6.536006	2.259299	0.281372
37	6	6.727071	0.143168	0.579030
38	1	7.771463	0.198132	0.860606
39	6	6.079080	-1.084045	0.547963
40	1	6.619461	-1.987615	0.804310
41	6	4.731847	-1.181005	0.199146
42	6	3.943934	2.521691	-0.451655
43	1	4.574889	3.392231	-0.273709
44	1	3.031617	2.632956	0.136990
45	1	3.651876	2.540885	-1.506529
46	6	4.042488	-2.520228	0.170724
47	1	3.142990	-2.526011	0.789062
48	1	4.712762	-3.299288	0.533282
49	1	3.737479	-2.797532	-0.843281
50	17	0.697528	2.242339	1.540860
51	17	0.764249	-1.881967	2.038704
52	26	1.040164	0.088695	0.995119
53	7	0.823047	-0.242725	-1.718710
54	7	-1.222560	-0.169464	-1.006983
55	7	2.649476	-0.058348	-0.419476
56	7	-3.498394	-0.106233	-0.900162

Table S69. Comparison of the optimized bond lengths (quintet multiplicity) using the UB3LYP/TZVP level of calculation with X–ray data for **2.17**.

X-ray				UB3LYP/TZVP (quintet multiplicity)	
Number	Atom1	Atom2	Length (Å)	Length (Å)	Δ (Å)
1	C1	Fe1	2.091(3)	2.14690	-0.056
2	C1	N1	1.369(4)	1.36691	0.002
3	C1	N2	1.350(4)	1.35105	-0.001
4	C2	C3	1.340(5)	1.34400	-0.004
5	C2	N1	1.398(4)	1.40034	-0.002
6	C3	N2	1.401(4)	1.40006	0.001
7	C4	C5	1.475(4)	1.49698	-0.022
8	C4	N1	1.419(4)	1.42245	-0.004
9	C4	N3	1.269(4)	1.27145	-0.003
10	C6	C7	1.496(4)	1.49511	0.001
11	C6	N2	1.440(4)	1.44461	-0.005
12	C6	N4	1.256(4)	1.26121	-0.005
13	C8	C9	1.393(5)	1.40449	-0.012
14	C8	C13	1.403(5)	1.40495	-0.002
15	C8	N4	1.425(4)	1.41659	0.008
16	C9	C10	1.406(5)	1.39420	0.012
17	C9	C14	1.503(6)	1.50627	-0.003
18	C10	C11	1.380(6)	1.38879	-0.009
19	C11	C12	1.352(7)	1.38869	-0.037
20	C12	C13	1.401(6)	1.39427	0.007
21	C13	C15	1.501(6)	1.50658	-0.006
22	C16	C17	1.403(5)	1.40353	-0.001
23	C16	C21	1.401(5)	1.40377	-0.003
24	C16	N3	1.458(4)	1.43472	0.023
25	C17	C18	1.387(5)	1.39514	-0.008
26	C17	C22	1.508(5)	1.50652	0.002
27	C18	C19	1.385(6)	1.38815	-0.003
28	C19	C20	1.378(6)	1.38817	-0.010
29	C20	C21	1.391(5)	1.39485	-0.004

30	C21	C23	1.496(5)	1.50642	-0.010
31	Cl2	Fe1	2.2442(10)	2.25970	-0.016
32	Cl1	Fe1	2.2404(9)	2.25860	-0.018
33	Fe1	N3	2.145(3)	2.25448	-0.110

Table S70. Comparison of the optimized bond angles (quintet multiplicity) using the UB3LYP/TZVP level of calculation with X–ray data for **2.17**.

X-ray					UB3LYP/TZVP (quintet multiplicity)	
Number	Atom1	Atom2	Atom3	Angle (deg.)	Angle (deg.)	Δ (deg.)
1	Fe1	C1	N1	111.7(2)	112.3535	-0.7
2	Fe1	C1	N2	144.6(2)	143.7955	0.8
3	N1	C1	N2	103.5(3)	103.8474	-0.4
4	C3	C2	N1	106.4(3)	106.3034	0.1
5	C2	C3	N2	106.6(3)	106.706	-0.1
6	C5	C4	N1	117.1(3)	116.179	0.9
7	C5	C4	N3	128.1(3)	127.278	0.8
8	N1	C4	N3	114.9(3)	116.5423	-1.6
9	C7	C6	N2	115.5(3)	116.2535	-0.8
10	C7	C6	N4	128.5(3)	128.8614	-0.4
11	N2	C6	N4	116.0(3)	114.8851	1.1
12	C9	C8	C13	121.5(3)	121.4712	0.0
13	C9	C8	N4	121.1(3)	119.1055	2.0
14	C13	C8	N4	117.0(3)	119.1921	-2.2
15	C8	C9	C10	118.0(4)	118.2625	-0.3
16	C8	C9	C14	121.4(3)	120.7512	0.7
17	C10	C9	C14	120.6(4)	120.9863	-0.4
18	C9	C10	C11	120.7(4)	121.1647	-0.5
19	C10	C11	C12	120.3(4)	119.6701	0.6
20	C11	C12	C13	121.9(4)	121.1994	0.7
21	C8	C13	C12	117.5(4)	118.2178	-0.7
22	C8	C13	C15	121.2(3)	120.8967	0.3
23	C12	C13	C15	121.3(4)	120.8851	0.4
24	C17	C16	C21	122.4(3)	122.1784	0.2
25	C17	C16	N3	118.3(3)	119.1163	-0.8
26	C21	C16	N3	119.1(3)	118.6086	0.5
27	C16	C17	C18	117.7(3)	117.7553	-0.1
28	C16	C17	C22	120.5(3)	121.6131	-1.1
29	C18	C17	C22	121.8(3)	120.6314	1.2

30	C17	C18	C19	120.8(3)	121.2192	-0.4
31	C18	C19	C20	120.4(4)	119.8644	0.5
32	C19	C20	C21	121.2(4)	121.164	0.0
33	C16	C21	C20	117.4(3)	117.817	-0.4
34	C16	C21	C23	121.9(3)	121.4285	0.5
35	C20	C21	C23	120.8(3)	120.7544	0.1
36	C1	Fe1	Cl2	109.62(9)	108.4793	1.1
37	C1	Fe1	Cl1	116.67(9)	109.997	6.7
38	C1	Fe1	N3	76.90(11)	75.44807	1.5
39	Cl2	Fe1	Cl1	120.37(4)	130.1053	-9.7
40	Cl2	Fe1	N3	115.57(7)	109.3029	6.3
41	Cl1	Fe1	N3	109.95(7)	110.1627	-0.2
42	C1	N1	C2	111.5(3)	111.4288	0.1
43	C1	N1	C4	119.6(2)	120.9766	-1.4
44	C2	N1	C4	128.7(3)	127.5828	1.1
45	C1	N2	C3	111.9(3)	111.7143	0.2
46	C1	N2	C6	125.0(3)	125.4119	-0.4
47	C3	N2	C6	122.9(3)	122.8626	0.04
48	C4	N3	C16	119.4(3)	121.4606	-2.1
49	C4	N3	Fe1	116.4(2)	114.6394	1.8
50	C16	N3	Fe1	123.85(18)	123.899	-0.1
51	C6	N4	C8	120.6(3)	122.8166	-2.2

1,3-Bis[1-(2,6-dimethylphenylimino)ethyl]benzimidazol-2-ylidene] iron(II) chloride (3.13).

Table S71. Atomic coordinates and relative energy of the optimized structure of **3.13** (quintet) using the UB3LYP/TZVP level of calculation.

Charge = 0, Multiplicity = 5
Gas phase energy: −3449.5078042 hartree

Optimized atomic coordinates:

Center Number	Atomic Number	Coordinates (Angstroms) X	Y	Z
1	6	-0.052642	0.346261	0.019500
2	6	-0.024881	2.642023	-0.041643
3	6	1.300096	2.184645	-0.026777
4	6	-2.250148	1.343035	-0.026068
5	6	-3.072903	2.591997	-0.061786
6	1	-4.126312	2.327890	-0.067521
7	1	-2.852258	3.174734	-0.957128
8	1	-2.871012	3.212589	0.812294
9	6	2.359537	-0.132919	0.033896
10	6	2.054736	-1.595455	0.118475
11	1	1.483299	-1.931058	-0.749217
12	1	1.462855	-1.827502	1.005520
13	1	2.992571	-2.144446	0.160014
14	6	4.705266	-0.331766	-0.016448
15	6	5.269341	-0.729625	-1.240406
16	6	6.506594	-1.372186	-1.219034
17	1	6.949266	-1.687360	-2.156896
18	6	7.174909	-1.607128	-0.024641
19	1	8.135825	-2.106422	-0.027660
20	6	6.607121	-1.193234	1.173217
21	1	7.128159	-1.368847	2.107363
22	6	5.372741	-0.545796	1.201302
23	6	4.557446	-0.468360	-2.542345
24	1	3.642245	-1.059931	-2.634087
25	1	5.197537	-0.722061	-3.387318
26	1	4.269187	0.581693	-2.634494
27	6	4.766714	-0.091563	2.503568
28	1	4.486724	0.964151	2.465358

29	1	5.470972	-0.229038	3.324088
30	1	3.860241	-0.651978	2.749609
31	6	-4.129013	-0.094871	-0.016834
32	6	-4.773599	-0.285055	-1.249349
33	6	-6.132847	-0.598388	-1.232049
34	1	-6.645480	-0.752562	-2.174145
35	6	-6.827028	-0.722738	-0.036460
36	1	-7.880136	-0.975412	-0.043815
37	6	-6.166678	-0.527578	1.168789
38	1	-6.705834	-0.626431	2.103472
39	6	-4.808233	-0.212377	1.206219
40	6	-4.033031	-0.155419	-2.554776
41	1	-4.687805	-0.408491	-3.388311
42	1	-3.163784	-0.815252	-2.591656
43	1	-3.674829	0.865842	-2.719594
44	6	-4.105378	-0.006827	2.522757
45	1	-3.243623	-0.669364	2.626182
46	1	-4.786756	-0.203054	3.350244
47	1	-3.742997	1.020014	2.634835
48	17	-1.084895	-2.492877	-1.953649
49	17	-1.152293	-2.370492	2.130132
50	26	-1.223714	-1.467144	0.057543
51	7	-0.829015	1.475718	-0.014359
52	7	1.229232	0.767789	0.012401
53	7	-2.715602	0.157145	-0.006182
54	7	3.498341	0.408942	-0.019063
55	6	2.372711	3.071430	-0.045724
56	1	3.382693	2.701348	-0.037848
57	6	2.085098	4.429477	-0.078153
58	1	2.900965	5.140504	-0.093559
59	6	0.768586	4.888992	-0.091766
60	1	0.570733	5.952923	-0.116779
61	6	-0.304038	4.006464	-0.073588
62	1	-1.307268	4.395145	-0.084095

1,3-Bis[1-(2,6-dimethylphenylimino)ethyl]-4,5,6-trihydropyrimidin-2-ylidene chromium(III) chloride (4.6).

Table S72. Atomic coordinates and relative energy of the optimized structure of **4.6** (quintet) using the UB3LYP/TZVP level of calculation.

Charge = 0, Multiplicity = 5

Gas phase energy: −3336.3527014 hartree

Optimized atomic coordinates:

Center Number	Atomic Number	Coordinates (Angstroms) X	Y	Z
1	6	-0.009351	1.029623	-0.141368
2	6	2.295917	1.441980	-0.652106
3	7	2.580507	0.288887	-0.182054
4	6	3.916875	-0.232577	-0.210068
5	6	4.278983	-1.080934	-1.269763
6	6	4.802113	0.058664	0.840553
7	6	5.557863	-1.637234	-1.257364
8	6	6.068802	-0.526129	0.808787
9	6	6.447997	-1.368588	-0.226775
10	1	5.849714	-2.295737	-2.066908
11	1	6.760581	-0.316320	1.616108
12	1	7.433741	-1.817320	-0.228926
13	6	3.309280	2.369509	-1.264190
14	1	3.459018	3.253895	-0.641332
15	1	2.999897	2.706009	-2.253928
16	1	4.260548	1.852972	-1.351049
17	6	4.415967	0.972144	1.974676
18	1	5.197075	0.980937	2.734670
19	1	3.483429	0.657174	2.445804
20	1	4.280688	2.004978	1.636955
21	6	3.324442	-1.383277	-2.395013
22	1	2.393537	-1.816862	-2.023963
23	1	3.062530	-0.482454	-2.959088
24	1	3.773395	-2.088119	-3.094718

25	7	0.944108	1.885185	-0.631696
26	7	-1.288742	1.375972	-0.294162
27	6	0.653183	3.224090	-1.201834
28	1	1.420787	3.921030	-0.875486
29	1	0.687104	3.169017	-2.293604
30	6	-0.708770	3.696544	-0.742726
31	1	-0.982187	4.601559	-1.286929
32	1	-0.685393	3.944116	0.321353
33	6	-1.725286	2.606794	-0.997897
34	1	-1.832818	2.395063	-2.063827
35	1	-2.709650	2.868218	-0.625259
36	26	0.926085	-0.740128	0.730213
37	17	1.107959	-0.433467	2.978336
38	17	0.342380	-2.616196	-0.410507
39	6	-2.367997	0.488299	0.101883
40	6	-2.150447	-0.457122	1.241771
41	1	-1.694484	-1.387654	0.897140
42	1	-1.508081	-0.033791	2.011274
43	1	-3.120568	-0.707982	1.668915
44	7	-3.442915	0.648938	-0.544624
45	6	-4.606803	-0.115380	-0.294301
46	6	-4.782286	-1.345726	-0.951837
47	6	-5.616353	0.427245	0.519225
48	6	-5.976547	-2.036347	-0.748935
49	6	-6.790729	-0.302249	0.697453
50	6	-6.974679	-1.528488	0.072276
51	1	-6.121443	-2.986920	-1.249326
52	1	-7.570815	0.104715	1.330700
53	1	-7.894139	-2.081833	0.217937
54	6	-5.433703	1.766763	1.184194
55	1	-4.630065	1.751768	1.926320
56	1	-5.179863	2.538707	0.452652
57	1	-6.347503	2.071051	1.694872
58	6	-3.719592	-1.897919	-1.866444
59	1	-3.421369	-1.158994	-2.614516
60	1	-2.813635	-2.189705	-1.329077
61	1	-4.087975	-2.780912	-2.388814
